

**Palacky University in Olomouc  
Faculty of Medicine and Dentistry**



**Identification and Characterization of Molecular  
Basis of Cancer Cell Drug Resistance  
Mechanisms towards Aurora Kinase Inhibitors  
CYC116 and ZM447439**

**PhD Thesis**

Madhu Kollareddy, MSc

**Supervising Department**



Institute of Molecular and Translational Medicine  
Laboratory of Experimental Medicine, Faculty of Medicine and  
Dentistry, Palacky University and Faculty Hospital in Olomouc

**Supervisor**

*MUDr. Marián Hajdúch, PhD*

**Olomouc 2013**

I declare that the work in this thesis was done by myself and was carried out in the Institute of Molecular and Translational Medicine, Laboratory of Experimental Medicine, Department of Pediatrics, Faculty of Medicine, Palacky University and Faculty Hospital in Olomouc, under the supervision of the head of the Institute of Molecular and Translational Medicine, **Marian Hajduch**, Associate Prof., MD, PhD.

## Acknowledgments

This PhD thesis was supported by grants awarded by the *Czech Ministry of Education* [MSM6198959216 and LC07017] and by a grant from Iceland, Liechtenstein and Norway through the EEA Financial Mechanism (CZ0099). The infrastructural part of this project (**Institute of Molecular and Translational Medicine**) was supported by the Operational Programme Research and Development for Innovations (**project CZ.1.05/2.1.00/01.0030**). This work was also supported by grant number **GAČR 303/09/H048**.

Foremost, I would like to express my sincere gratitude to my PhD mentor, *Associate Prof., Marian Hajduch, MD, PhD*, for inspiring me with his immense knowledge and for guidance to make this wonderful piece of work. I thank him heart fully for giving me the opportunities to participate and present in three successive AACR 2010, 2011 and 2012 conferences. I and my family will never forget for his support and kind nature during the most difficult situations we gone through. My wife Sailaja, would like to use this opportunity to dedicate her life to '*Marian*'.

I would like to express my heartfelt thanks to *Dr. Daniella Zheleva* for her continuous support and guidance throughout the study. Her extraordinary scientific knowledge in the related field helped me to complete this doctoral study in a meaningful way. I would also like to thank Daniella for showing this PhD opportunity.

I am very thankful to *Cancer Research Foundation, Olomouc* for financially assisting my stay in Neredin Kolej, Olomouc.

This is a wonderful time to express my in-depth gratitude to a great scientist, great husband, great father and great son, *Dr. Petr Dzubak*, who helped me and my family right from the time we landed in Prague airport. Petr fully supported me to settle in the lab and in Olomouc. His practical and technical guidance throughout my study has been very useful.

I would like to thank my former supervisor *Dr. Gary Griffiths* (UK) for his kind support.

I cannot thank enough to *Michaela Spenerova, Jana Furstova, Lal and Marie Rakova* for being very kind to my family during critical times.

I owe my due respect, gratitude and indebtedness to *Dr. Josef Srovnal* for his kind assistance during the microarray gene expression studies. I would like to thank him for supporting me during the difficult times.

Heartfelt thanks to *Dr. Jirka Drabek and Zuzana Cibulkova* for their kind moral support during my stay in Olomouc.

Sincere thanks to *Anna Janostakova* for her great helping hand and support she provided for my family.

I greatly appreciate the kind support of *Gabriel Rylova* and *Jiri Rehulka* during my grave situations.

I would like to thank my friends Rohit, Sachin, Arjun, Anand, Sudheer, Murali, Sekhar Shankri, Lenka Lachnitova, Jiri Houda, Andrea Benedikova, Khushboo, Tomas Novotny, Vladka, Dusan, Renata, Ivo, Vera, Jiri Vecerka, Sylwia, and Jana Stranska for their support.

I would like to thank doctors of Faculty of Medicine, Olomouc, Iavana Oborna, Jan Gregar, Martin Stasek, Vlastimil Prochazka, Vitezslav Kolek and Vladimir Mihal and all the nurses for helping us to overcome difficult situations.

I would like to express my sincere thanks to everyone who helped me during doctoral study.

I would like to thank my parents *Narasa Reddy* and *Himavathi* for their continuous support. I also thank my sister **Madhuri** for the support.

Last, but not the least, I would like to dedicate this work to my son *Sai Sujith* and to my wife *Sailaja*. I would like to take this opportunity to thank my wife for the support throughout the study.

Olomouc

June, 2013

.....

Madhu Kollareddy, MSc

# CONTENT

<b>1. INTRODUCTION</b> .....	6
<b>1.1 Drug Induced Resistance</b> .....	6
<b>1.2 Drug Resistance Mechanisms</b> .....	7
<b>1.2.1 ABC (ATP-binding Cassette) family members mediated drug efflux</b> ....	7
<b>1.2.2 Increased DNA repair activity</b> .....	7
<b>1.2.3 Modulation of p53 activity</b> .....	8
<b>1.2.4 Amplification of drug target</b> .....	9
<b>1.2.5 Upregulation of antiapoptotic genes</b> .....	10
<b>1.2.6 Drug target mutations</b> .....	11
<b>1.2.7 Activation of alternative survival pathways</b> .....	12
<b>1.3 Methods to Study Drug Resistance</b> .....	13
<b>1.4 Clinical Implications of Drug Resistance</b> .....	16
<b>1.5 Strategies to Overcome Drug Resistance</b> .....	17
<b>1.6 Targeting Cell Cycle in Cancer</b> .....	20
<b>1.6.1 Cell cycle</b> .....	20
<b>1.6.2 Cell cycle regulation</b> .....	20
<b>1.6.3 Cell cycle &amp; cancer</b> .....	24
<b>1.6.4 Targeting cyclin dependent kinases</b> .....	26
<b>1.6.5 Targeting polo-like kinases</b> .....	27
<b>1.7 Aurora Kinases and their Biology</b> .....	27
<b>1.7.1 Aurora A pathway</b> .....	28
<b>1.7.2 Aurora B pathway</b> .....	29
<b>1.7.3 Aurora kinases and Cancer</b> .....	30
<b>1.8 Aurora Kinase Inhibitors</b> .....	32
<b>1.8.1 CYC116, a novel pan-Aurora kinase inhibitor</b> .....	32
<b>1.8.2 Mechanism of action</b> .....	33
<b>1.8.3 ZM447439 characteristics and mode of action</b> .....	34
<b>1.9 Molecularly Targeted Therapy in Cancer</b> .....	36
<b>1.10 Clinically Valid Anticancer Targets and Respective Targeted Drugs</b> .....	38
<b>1.10.1 Bcr-Abl &amp; Imatinib, Dasatanib, Nilotinib</b> .....	38
<b>1.10.2 B-Raf (V600E) &amp; PLX4032</b> .....	39
<b>1.10.3 EGFR &amp; Gefitinib, Erlotinib</b> .....	39
<b>1.10.4 EGFR &amp; Lapatinib, Herceptin</b> .....	41
<b>1.10.5 VEGFR/PDGFR/Raf/c-KIT &amp; Sorafenib, Sunitinib</b> .....	42
<b>1.10.6 ALK &amp; Crizotinib</b> .....	43
<b>1.11 Investigational Targeted Drugs</b> .....	45
<b>1.11.1 PARP &amp; Olaparib</b> .....	45
<b>1.11.2 c-Met &amp; Foretinib (GSK1363089, XL880</b> .....	46

<b>2. AIMS OF THE STUDY.....</b>	<b>47</b>
<b>3. EXPERIMENTAL PART &amp; SURVEY OF RESULTS.....</b>	<b>48</b>
<b>3.1 Thesis background.....</b>	<b>48</b>
<b>3.1.1 Resistance mechanisms towards Aurora kinase inhibitors.....</b>	<b>48</b>
<b>3.1.2 Proteome analysis of CYC116 and ZM447439 resistant clones and identification of candidate proteins that may potentially mediate resistance.....</b>	<b>49</b>
<b>3.2 Kollareddy M, Dzubak P, Zheleva D, Hajduch M (2008) Aurora Kinases: structure, functions, and their association with cancer. Biomedical Papers; 152;27-33.....</b>	<b>51</b>
<b>3.3 Kollareddy M, Zheleva D, Dzubak P, Brahmshatriya PS, Lepsik M, Hajduch M (2012) Aurora kinase inhibitors: Progress towards the clinic. Investigational New Drugs 30;2411- 2432.....</b>	<b>58</b>
<b>3.4 Kollareddy M, Zheleva D, Dzubak P, Srovnal J, Radova L, Dolezal D, Koudelakova V, Brahmshatriya PS, Lepsik M, Hobza P, Hajduch M. (2012) Identification and characterization of molecular basis of cancer cell drug resistance to CYC116 and an experimental Aurora inhibitor, ZM447439 (under submission for publication).....</b>	<b>80</b>
<b>3.5 Hrabakova R, Kollareddy M, Tyleckova J, Halada P, Hajduch M, Gadher SJ, Kovarova H (2013) Cancer cell resistance to Aurora kinase inhibitors: Identification of novel targets for cancer therapy. Journal of Proteome Research 12; 455-469.....</b>	<b>127</b>
<b>4. SUMMARY OF THE THESIS.....</b>	<b>142</b>
<b>5. REFERENCES.....</b>	<b>145</b>
<b>6. BIBLIOGRAPHY.....</b>	<b>152</b>

# 1. INTRODUCTION

## 1.1. Drug Induced Resistance

Drug induced resistance in cancers is one of the major obstacles in successful chemotherapy. Drug induced resistance is frequently observed in clinical oncology and can significantly limit the clinical response to subsequent chemotherapy. Cancer patients respond significantly to selected anticancer agents during initial treatment. However during the long-term treatment, most of the cancers acquire resistance to the drug used for treatment, thereby the patients display little or no response. Cancer cell undergo continuous somatic genetic changes in order to escape natural defense mechanisms and drug-induced death. Continuous use of chemotherapy induces selection pressure on tumor cells, hence a sub-population evolve that are resistant to the agent. Emergence of an acquired drug resistance process can be comparable to Darwin's evolutionary theory at cellular level. **Acquired resistance** of a cancer cell population can lead to "**Multidrug resistance phenomenon**". Cancer cell resistant to one drug can display cross-resistance to numerous drugs, which have different structures and mode of actions. Emergence of multidrug resistance results in more aggressive disease and significantly reduces survival rates. Multidrug resistance is induced by upregulation of drug transporters, (**Borst et al., 2000**) antiapoptotic proteins, (**Huang et al., 1997**) and by many other mechanisms. Recently microRNAs were shown to involve in multidrug resistance (**Kovalchuk et al., 2008**). Multidrug resistance is multifactorial and that various cellular pathways are concomitantly involved in the clinical drug resistance. Delineation of cancer cellular pathways that determine the fate of response to a particular drug is important to understand and overcome drug resistance.

In contrary to acquired drug resistance, a sub-population of cancer cells inherently possesses resistance to wide variety of drugs. This is called "**Intrinsic Resistance**". Approximately in 50% of all cancers, resistance to chemotherapy already exists prior to drug treatment (**Pinedo, 2007**). For example, doxorubicin induces p53 dependent apoptosis in breast cancer patients. Aas et al. reported that specific mutations in p53 correlated to doxorubicin primary and early relapse in breast cancer patients (**Aas et al., 1997**). Growing evidence suggests association between intrinsic resistance and the presence of **cancer stem cells** in the tumor population. Cancer stem cells have been shown to constitutively express drug transporters, DNA repair genes, and are resistant to apoptosis (**Lou et al., 2007**). Presence of tumor stem cells may provide a source for disease recurrence and metastasis.

Drug induced resistance is a key issue for clinical development and resistance mechanism are very complex. Further, due to huge amount of heterogeneity among cancer cells, cancer patients acquire different types of resistance mechanisms to a particular drug. Hence resistance mechanisms vary from patient to patient. Many drug resistance mechanisms towards various anticancer drugs have been consistently reported. In the following sections, important resistance mechanisms that are frequently encountered in clinical oncology, methods to determine drug resistance, clinical implications of drug resistance, and strategies to circumvent drug resistance are described.

## 1.2 Drug Resistance Mechanisms

### 1.2.1 ABC (ATP-binding Cassette) family members mediated drug efflux

ABC family (ATP-binding cassette) family of drug transporters was consistently shown to pump many anticancer drugs out of the cell (drug efflux) in an ATP dependent manner. They are naturally involved in the transport of wide variety of substrates including xenobiotics, lipids, and sterols.

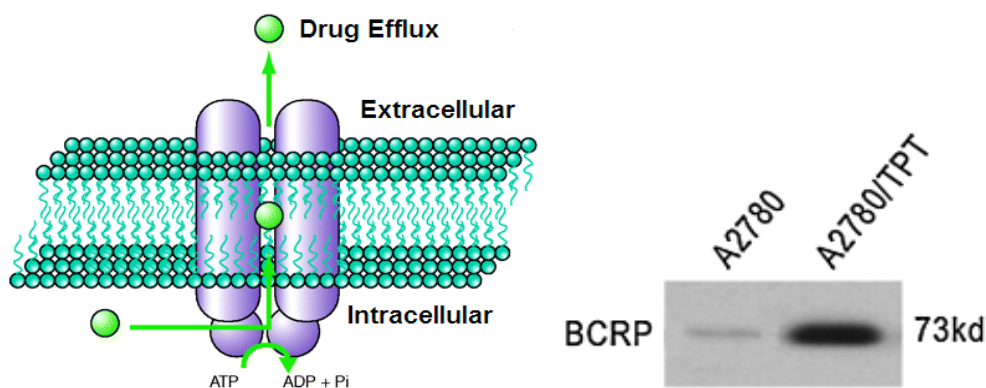


**Figure 1.** Schematic diagram of ABC family mediated drug efflux (left) (from Vanja et al., 2007). Up-regulation of ABCG2 in A2780/Topotecan resistant cell line (right) (from Jia et al., 2005).

ABC transporter proteins generally have two substrate-specific membrane-spanning domains, which creates a tunnel for passage of the substrates. Towards cytoplasm it contains two substrate-binding cytosolic nucleotide binding domains, which contain the site for ATP hydrolysis (Figure 18). Topotecan (Topoisomerase I inhibitor) is well known anticancer drug used in the treatment of ovarian cancer. Initially some ovarian cancers respond significantly to this agent; however patients develop resistance during long-term treatment. To study the *in vitro* tumor cell resistance mechanism to Topotecan, Jia et al. established topotecan resistant A2780 (ovarian carcinoma) by step wise increasing concentrations. The established cell line is 25 fold resistant to topotecan and showed high induction of ABCG2/BCRP protein (ATP-binding cassette sub-family G member 2/Breast cancer resistance protein) (Jia et al., 2005) (Figure 1). Knock-down of BCRP restored sensitivity to topotecan, suggesting its upregulation expression is enough to confer resistance to topotecan. Similarly ABCB1/PgP (ATP-binding cassette sub-family B member 1/permease-glycoprotein) and ABCC1/MRP1 (ATP-binding cassette sub-family C member 1/multidrug resistance-associated protein 1) are involved in paclitaxel and etoposide efflux respectively.

### 1.2.2 Increased DNA repair activity

Cisplatin is very efficient drug in the treatment of ovarian, lung, head and neck, and other carcinomas. Cisplatin cross links DNA strands, thereby forming DNA adducts (Figure 2). The resulting damage activates DNA repair pathways. However cisplatin induces irreversible DNA damage, such that the cells cannot repair this form of severe DNA damage. Cisplatin induces cell death by apoptosis. Increased DNA repair activity in cisplatin resistant cells is a significant disadvantage in the clinic. Upregulation of ERCC1 (excision repair cross-

complementing rodent repair deficiency, complementation group 1), which is a key candidate in the repair of cisplatin-induced DNA adducts,

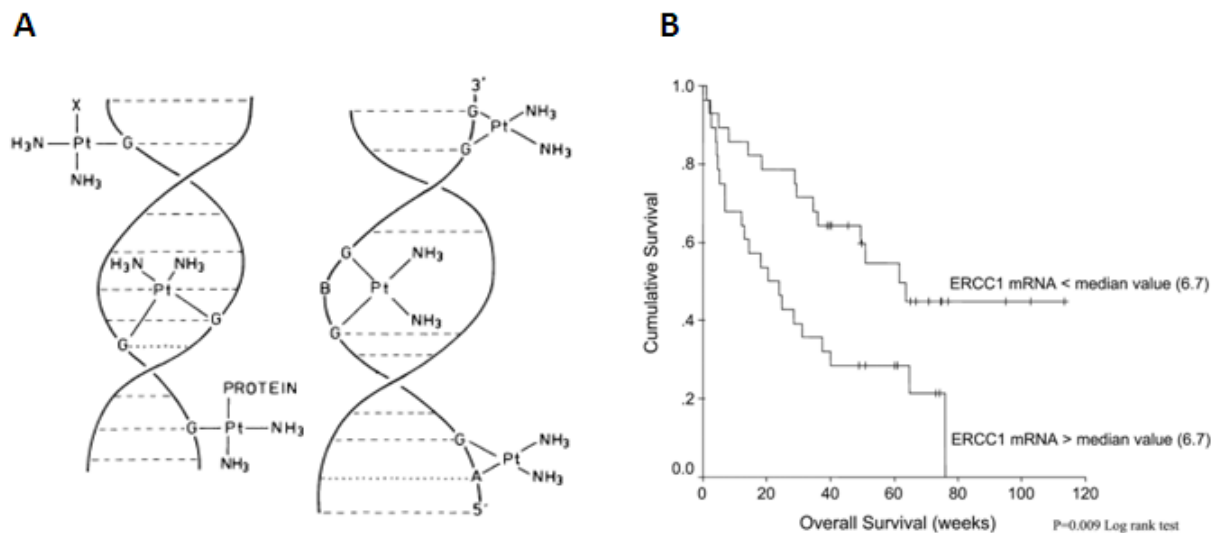


**Figure 2.** A. Various types of DNA adducts induced by Cisplatin (from Reddijk J). B. Kaplan-Meier survival curved in patients with low ERCC1 and high ERCC1 (from Lord et al., 2002)

confers resistance. Lord et al. showed correlation between the expression (Lord et al., 2002) (Figure 2). 65.3 weeks of overall median survival was reported in low ERCC1 expressing patients, compared to 20.4% weeks in high ERCC1 expressing patients.

### 1.2.3 Modulation of p53 activity

p53 is a well known and extensively characterized tumor suppressor gene. It is the key candidate in the regulation of apoptosis induced by various kinds of stimuli. It is also involved in G1 check point cell cycle regulation and maintenance of genomic stability. Many anticancer drugs exert their action by inducing DNA damage, which in turn activates p53 apoptotic pathway, eventually leading to cell death. Hence p53 is very important in suppressing tumor cell formation and progression and also in achieving successful chemotherapy. However roughly 50% of the cancers have defects in p53 pathway, due to p53 point mutations and deletions. Restoration of wild type p53 activity is a worldwide current interest of research. Many mutations were consistently reported across the p53 gene, some are highly significant and accepted in relation to causing drug resistance.

Aas et al. reported specific p53 point mutations and their link to primary resistance to doxorubicin therapy and early relapse (Aas et al., 1996). In their study 18% of patients had p53 mutations, of which four have experienced progressive disease during doxorubicin therapy. Different mutations across the p53 gene lead to the different responses to doxorubicin therapy. Four patients with progressive disease had mutations in L2 and L3 domains, which are crucial in making DNA contact (Table 1). All patients with progressive disease contained either point mutation or deletion or non-sense mutation in L3 domain. Overall survival of patients with p53 mutations in L2/L3 domains was poor when compared to wild type p53.



**Table 1.** Type of abnormalities of p53 in doxorubicin resistant relapsed patients (from Aas et al., 1996)

Type of p53 Mutation	Affecting	Response
Arginine249Glycine	L3 domain	Progressive disease
Arginine248Glutamine	L3 domain	Progressive disease
Glutamine204stop codon	L3 domain	Progressive disease
Deletion 14 bp codon 217-221	L3 domain	Progressive disease

Another study by Wong et al. reported R273H mutation and its association with doxorubicin resistance in *in vitro* established A431 (epidermoid carcinoma) squamous cancer cell line (Wong et al., 2007). In fact this specific mutation was also reported by Aas et al. in cancer patients. One can appreciate the incidence of identical mutations reported for p53 both at *in vitro* conditions and in the clinic, further supporting the reliability of *in vitro* models in drug resistance studies. R273 mutation induced p53 gain of drug resistance function in doxorubicin resistant cell line. Downregulation of procaspase-3 was identified by western blotting in this resistant cell line, which corresponded to the upregulation of mutated p53 (Figure 3). Inhibition of R273H p53 expression by antisense approach restored the levels of procaspase-3 and undergone subsequent apoptosis like parent cells.

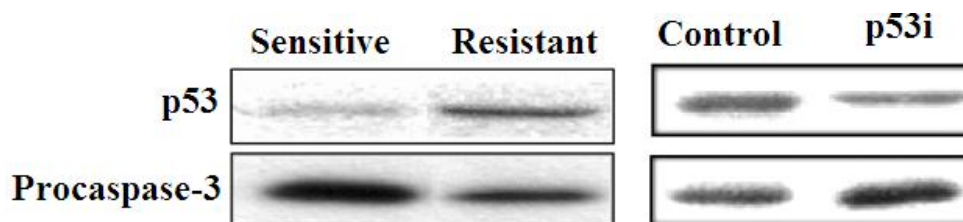


**Figure 3.** Levels of p53 and procaspase-3 in doxorubicin sensitive and resistant cell lines (left). Induction of procaspase-3 after mutated p53 downregulation (right) (from Wong et al. 2007).

#### 1.2.4 Amplification of drug target

Often amplification of drug target gene itself mediates resistance to a particular drug. Since the amplification of the gene increases the stoichiometric ratio of target to drug proportions, the target continues to exert its enzymatic activity (Figure 4). This mode of drug resistance can be exemplified by classical DHFR (dihydrofolate reductase) amplification in methotrexate resistant tumor cell lines. Methotrexate is the first generation anticancer drug used in the treatment of leukemias, lymphomas, osteocarcinomas and many other cancers. Methotrexate binds and inhibits DHFR, which is a key for tetrahydrofolate synthesis. Folate

is essential for purine and thymidine synthesis. Hence methotrexate indirectly inhibits DNA replication. Amplification of DHFR gene was reported in methotrexate

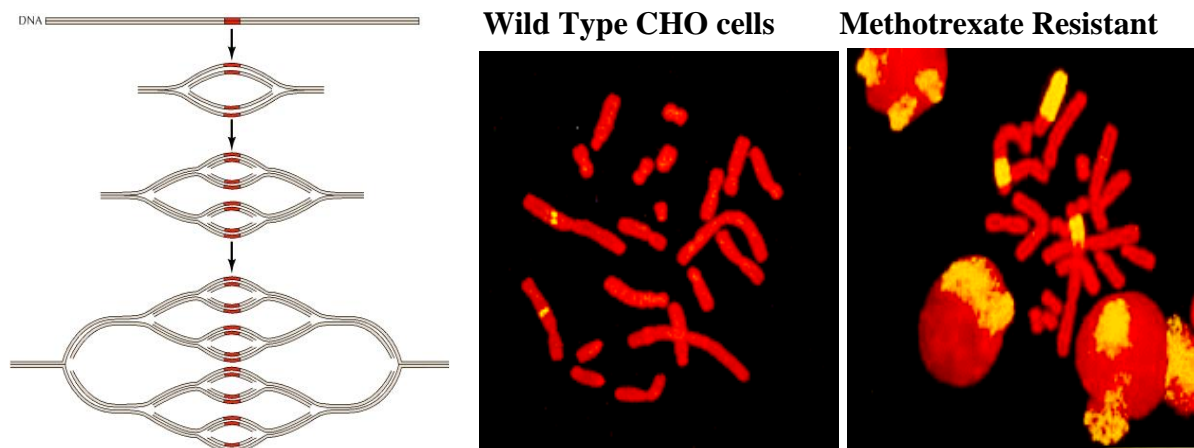


**Figure 4.** Schematic diagram of gene amplification by repeated replication (left) (from Cooper GM, The Cell). FISH (fluorescence in situ hybridization) staining of DHFR gene amplification in methotrexate resistant CHO cells (Chinese hamster ovary) vs. wild type cells. Staining can be noticed both at intrachromosomal and extrachromosomal (double minutes) levels (right).

resistant acute lymphoblastic leukemia patients (**Goker et al., 1995**). At the time of diagnosis patients have normal gene copy number, however the relapse of the disease correlated to increased DHFR gene copy number. Gene amplification was confirmed by southern blot analysis. In this study 31% of the patients showed gene amplification and associated relapse.

### 1.2.5 Upregulation of antiapoptotic genes

Apoptosis is a tightly regulated process executed by many genes. It is the balance between pro-apoptotic (**BAD**: BCL2-associated agonist of cell death, **BAX**: BCL2-associated X protein) and anti-apoptotic (**Bcl-2**: B-cell lymphoma 2, **Bcl-xL**: B-cell lymphoma-extra large, **Bcl-w**; Bcl-2 (B-cell leukemia 2) family member) genes products that dictates the cell fate. Upregulation of Bcl-2 induces apoptotic resistance to many anticancer drugs. Release of cytochrome c into the cytoplasm is an essential and upstream even of apoptotic program.

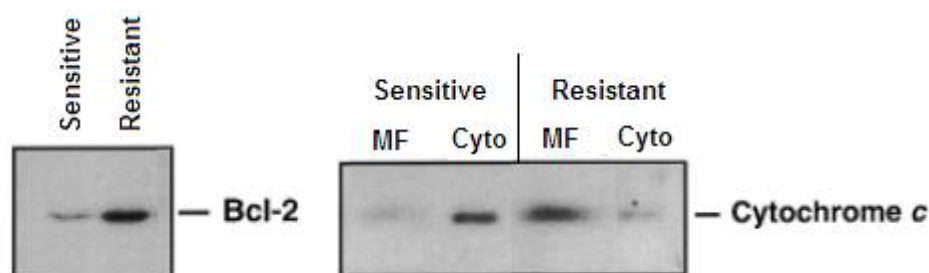


**Figure 5.** Levels of Bcl-2 in etoposide resistant and resistant small cell lung cancer cell line derived from patient (left). Levels of cytochrome c in membrane fractions (MF) and cytoplasm (Cyto) after drug treatment in sensitive and resistant cell lines (right) (from Sartorius et al., 2002).

Release of cytochrome c is negatively regulated by Bcl-2. Sartorius et al. established three etoposide (Topoisomerase II inhibitor) resistant lung cancer cell lines from sensitive tumor biopsies. All resistant clones showed significant upregulation of Bcl-2 and this corresponded to the inhibition of cytochrome c release into cytoplasm (Sartorius et al., 2002) (Figure 5). Inhibition of Bcl-2 expression by antisense approach restored the sensitivity to chemotherapy.

### 1.2.6 Drug target mutations

One can expect high frequency of target mutations, particularly in the case of targeted therapy. Continuous encounter of the target with the drug induces selection pressure and subsequent structural changes by mutations. Changes in the conformation of the target by selective mutations can inhibit or reduce the drug binding, thus resulting in the acquired resistance (Figure 6).

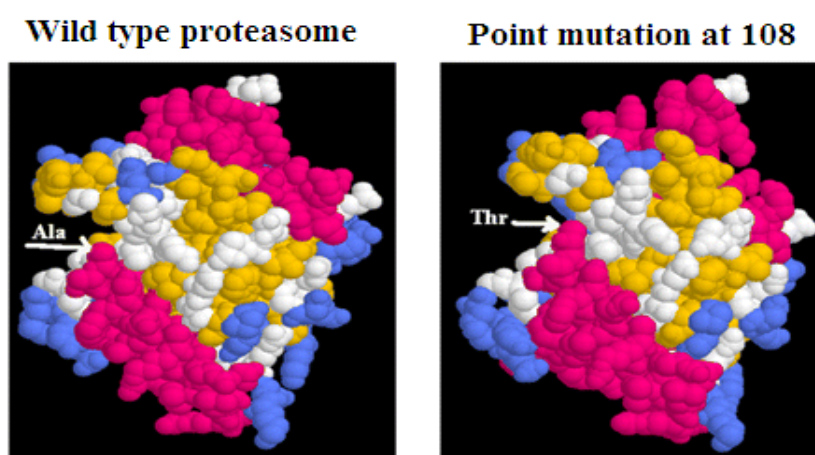


**Figure 6.** Structural model predicting the active site conformation change with one point mutation of proteasome subunit, rendering resistant to Bortezomib (from Lu et al., 2008).

This can be best exemplified by Bcr-Abl (T315I) and Imatinib story. The main driving event of chronic myelogenous leukemia is the fusion of Bcr and Abl genes, resulting in chimeric Bcr-Abl product. The deregulated tyrosine kinase Bcr-Abl constitutively drives cell proliferation, inhibits DNA repair and causes genomic instability. Imatinib is a highly selective Bcr-Abl inhibitor which is already a front line therapy for Bcr-Abl positive CML patients. Imatinib is referred to as a magic bullet, because it has cured many CML patients. Despite of the very high success, eventually CML patients develop resistance to imatinib by Bcr-Abl mutations. Particularly T315I gate keeper mutation was consistently reported in the clinic and it is the most aggressive mutation of all known Bcr-Abl mutations.

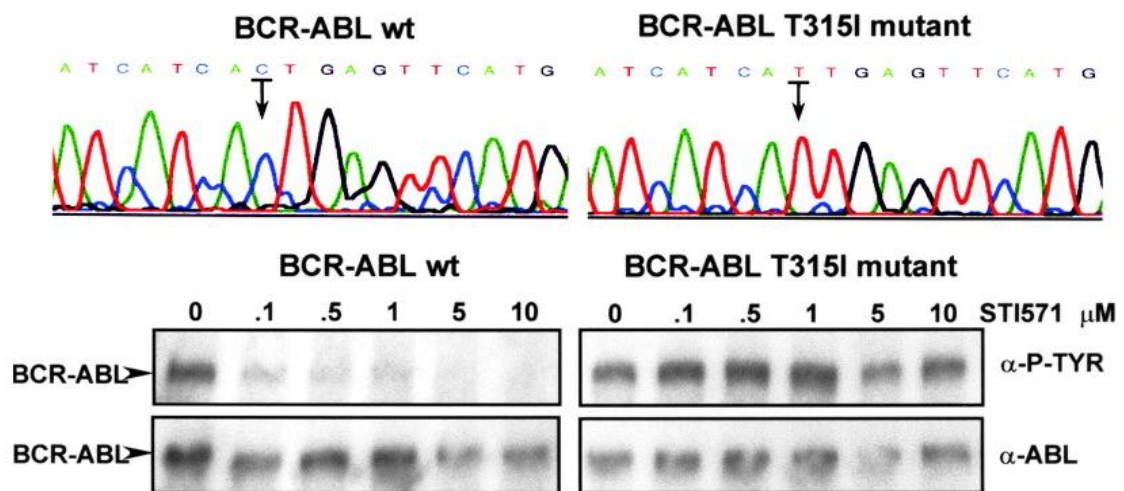


**Figure 7.** Wild type and mutated Bcr-Abl sequences (up). Imatinib was unable to inhibit tyrosine phosphorylation in T315I transfected cell line at even the highest concentrations tested (down) (from Gorre et al., 2001)

Gorre et al. sequenced Bcr-Abl DNA in nine patients, who relapsed during imatinib therapy. Six patients had point mutation (C→T) resulting in T315I gatekeeper residue alteration (**Gorre et al., 2001**) (Figure 7). This residue is located within the ATP binding site and activation loop, which are required for imatinib binding. The absence of oxygen atoms in isoleucine inhibits the formation of hydrogen bonding with the drug. To confirm the T315I relation to drug resistance, Gorre et al. transfected T315I Bcr-Abl in to wild type cells. Even the high concentrations of imatinib were unable to inhibit Bcr-Abl kinase activity in the transfected cell line.

### 1.2.7 Activation of alternative survival pathways

Cell signaling pathways are very complex and interlinked. Some genes involved in cell signaling pathways become oncogenic by several mechanisms including mutations, amplification, translocation, and viral infection. Many targeted drugs are available to specifically inhibit these oncogenic genes. However alternative pathways can reactivate and can confer resistance to a particular drug, where tumor cells no longer depend on original driving oncogene for uncontrolled cell division. PLX4032 is a highly specific inhibitor of mutated B-Raf (V600E) used in the treatment of malignant melanoma. 80% tumor response rate was reported, however patients acquire resistance within a few months. Surprisingly secondary mutations of B-Raf (V600E) did not arise both in relapsed patients and drug resistant melanoma cell lines.

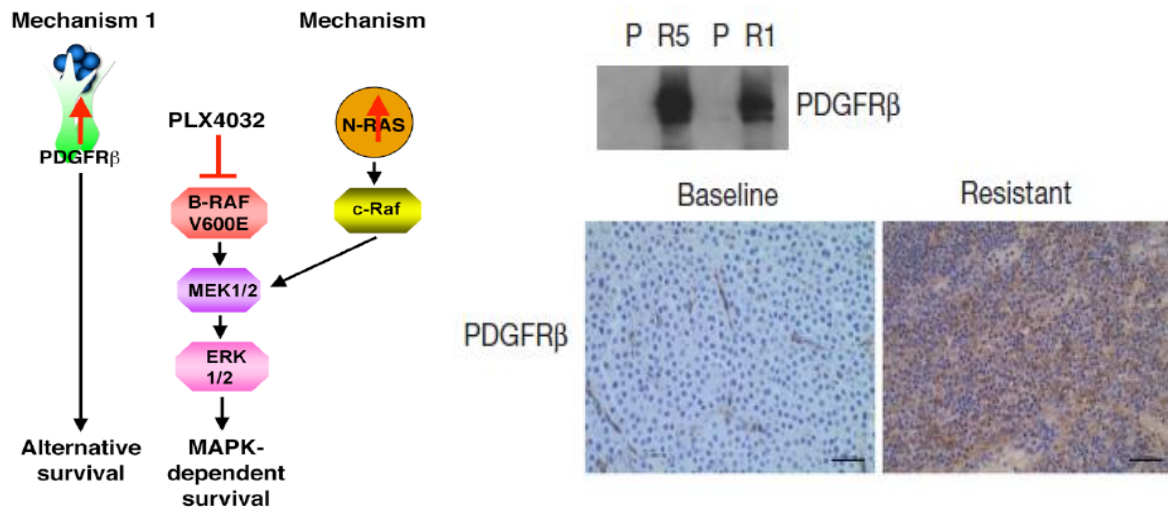


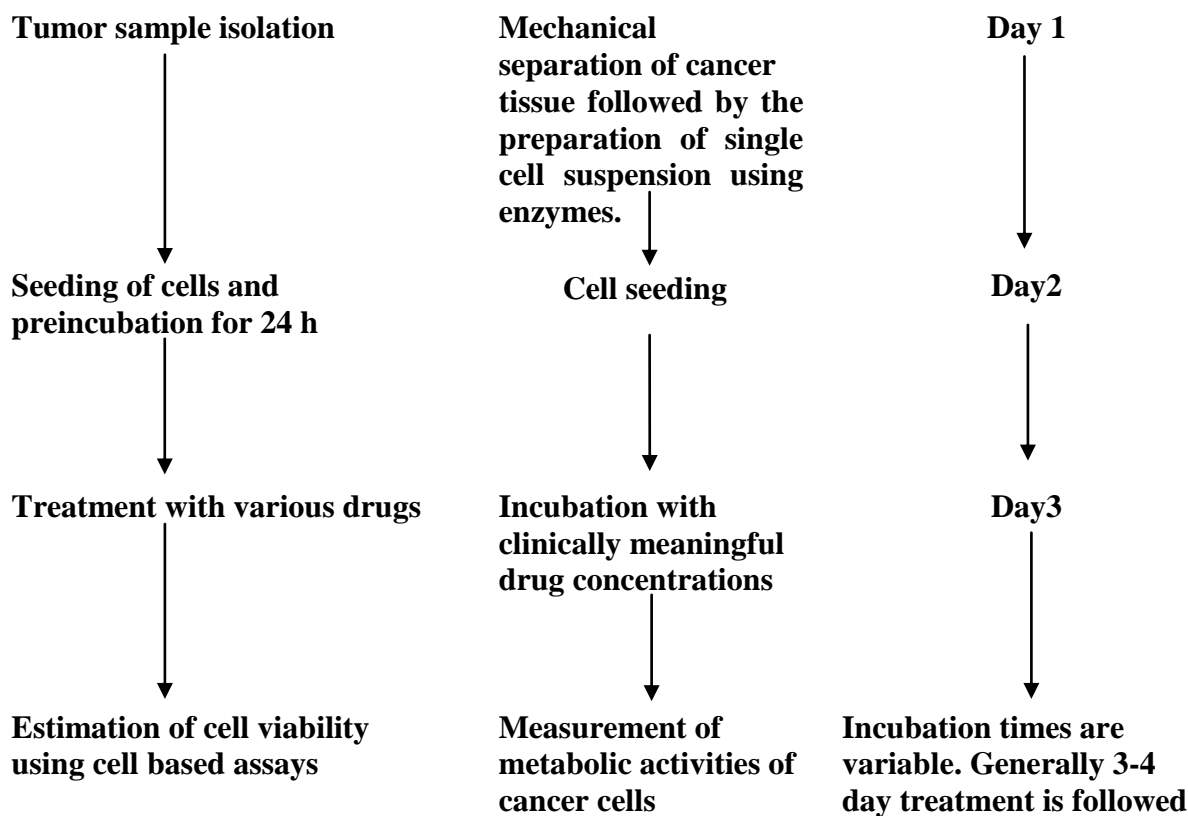
**Figure 8.** Schematic diagram showing alternative reactivation of cell signaling pathways (left). Overexpression of PDGFR $\beta$  in PLX4032 resistant cell lines (R5, R1) compared to parent cell lines (P) (right). Immunohistochemical staining of PDGFR $\beta$  in relapsed patient biopsy (right) (from Nazarian et al., 2010).

Instead, alternative survival pathways including PDGFR $\beta$  or N-RAS activated to bypass PLX4032 effects (Nazarian et al., 2010) (Figure 8). Two resistant melanoma cell lines established *in vitro* showed overexpression of enzymatically active PDGFR $\beta$  and this also correlates in relapsed tumor biopsies taken during clinical trials. On the other hand, one PLX4032 resistant clone harbored N-RAS (Q61K) mutation. Here also Q61K mutation matched under *in vivo* conditions at least in one patient. This patient continued to show progressive disease during PLX4032 treatment. Stable knockdown of PDGFR $\beta$  and N-RAS restored the sensitivity to PLX4032 in some resistant cell lines.

### 1.3 Methods to Study Drug Resistance

Despite the availability of valid biomarkers to predict response to a particular drug, at present resistance is usually detected during the course of chemotherapy after a long period of drug administration. Very few methods were currently available to study and predict drug resistance. In this section some of the important methods that are useful to diagnose resistance are described.

**Fresh tumor cells** (Fresh tumor cell culture tests) isolated from patients is a valuable source to test efficacy of drugs on tumor cell proliferation. However successful establishment and propagation of patient derived cancer cells are rate limiting factors, since the cancer cells in patients grow in completely different microenvironment compared to tissue culture flaks in the laboratory. Nonetheless, several labs were able to establish patient derived cancer cells using optimized protocols (Cree et al., 2010). Extensive description of protocols useful to establish primary tumor cells are currently available (Masters et al., 1991, Pfragner et al., 2004). The general procedure for culturing of primary tumor cells and drug testing is shown in the form of flow chart.



**Flow chart 1:** Showing schematic procedure for the isolation of tumor cells and subsequent drug testing.

Fresh tumor cell tests have been very useful in predicting the intrinsic drug resistance of primary tumors derived from a particular patient. The results from these tests are very useful to avoid unnecessary toxicity burden by eliminating ineffective drugs and to select drugs that might benefit cancer patients. However some questioned the validity of this method to diagnose drug resistance and also it lacks general recognition. Indeed none of the tests has been adopted so far in clinical routine practice. Nevertheless recent reports certify the value of such assays in the rapid detection of drug resistance which allows treatment modifications (Bosanquet et al., 2009).

A very promising technique has been recently developed to predict and identify drug resistant mechanisms, namely, **patient derived xenograft method (PDX)**. In this method newly diagnosed primary tumor is xenografted into the mice. A great advantage of this method is that, tumors never lose original architecture and heterogeneity and have similar microenvironment. Of all the models, PDX is clinically relevant to predict response and understand drug resistance mechanisms. This approach is very useful for the rapid assessment of tailored therapy. Dong et al. xenografted primary tumors into mice and have shown preserved original histopathologic architecture (Figure 9). They successfully used this model to quickly assess drug response within three weeks and to establish tailored therapy, thereby avoiding futile chemotherapy (Dong et al., 2010). By this approach they were able to select responders and non-responders to a particular drug regimen. Also the results they obtained were very close to those reported in clinical trials. Interestingly they also showed significant proportion of drug resistant population among responsive tumors, indicating that

heterogeneity was preserved unlike in vitro cell lines models and cancer cell line derived xenograft models. Tumor heterogeneity is the main reason for cancer relapse.

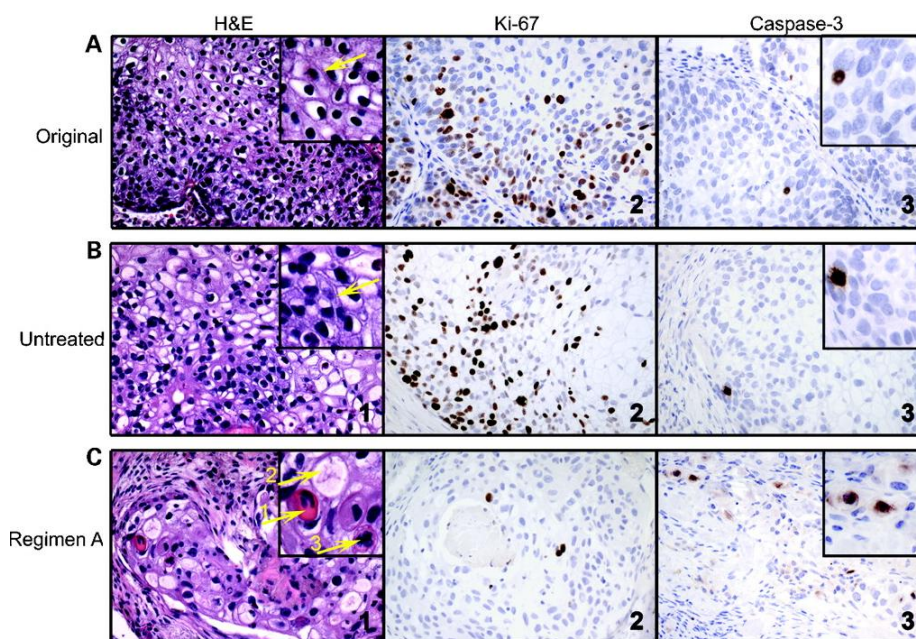


**Figure 9:** Tissue sections of original primary tumor (A), Untreated PDX (B), and treated PDX (C). Similar histopathological and morphological architecture can be noticed. PDX (squamous cell lung cancer) showed significant response to drug treatment regimens (from Dong et al., 2010).

Determination of **cancer biomarkers signatures** and their expression levels have been very useful in predicting response to anticancer drugs. Indeed a widely accepted field called predictive oncology deals with prediction of drug response and prognosis during the course of treatment. Few serum biomarkers expression levels which correlates to tumor response to therapy have already been in use in the clinic. Some of them include prostate-specific antigen (PSA-prostate cancer), CA 125 (ovarian cancer), and thyroglobulin (thyroid cancer). Tumor specific genes responsible for drug resistance can be studied using various methods including **immunohistochemistry, microarray based gene expression analysis, and proteomics.**

In the past diagnosis of drug resistance was difficult during the course of treatment. Now a day's **positron emission tomography (PET)** has been very useful in predicting tumor response to a particular anticancer drug based on metabolic activity of tumor. Dynamic imaging of cancer tissues can be determined by PET using radiopharmakon called 18-fluoro-deoxyglucose ( $^{18}\text{F}$ -FDG), which allows monitoring of tumor glycolysis rates (measure of metabolic activity of cancer cell) (**Larson et al., 2006**). PET is not only useful for diagnosis and staging of cancers, but also useful to evaluate drug response in early stages of chemotherapy (**Hicks et al. 2009**). Since the PET is superior to tumor size measurements it has already been proposed to replace the currently used RESIST (response evaluation criteria in solid tumors) by PERSIST (PET response criteria in solid tumors) (**Wahl et al., 2009**).

Since the 1980s, investigators have generated several drug resistant cancer sub-lines from well established immortalized cancer cell lines. These *in vitro* cell lines served as good models to identify and characterize drug resistance mechanisms. Majority of the drug resistance mechanisms including expression of MDR1 drug transporters, up-regulation of anti-apoptotic, and specific drug target mutations were identified using the cancer cell lines. Some of the *in vitro* determined drug resistance mechanisms correlated also in primary tumors, for example T315I Bcr-Abl gatekeeper imatinib induced mutations and overexpression of PgP in response to paclitaxel. There are two ways to select and establish drug resistant cell lines or colonies. Traditionally, cancer cells were exposed to gradual increasing concentrations of anticancer drug and selected at above lethal concentrations. This method is called prolonged, continuous, multistep selection. By this method the somatic genetic mutations accumulate gradually over the period of time. Calcagno et al. reported enrichment of cancer stem cells in MCF7/ADR (breast cancer cell line resistant to Adriamycin) cell line when selected by gradual increasing concentration (**Calcagno et al., 2010**). Single-step selection using lethal concentrations of drugs has also been used to select drug resistant colonies and to identify resistance mechanisms (**Girdler et al., 2008**). However, a debate surrounds on which method is more relevant clinically to study drug resistance. Cancer cell line derived xenograft models are also useful tools to determine drug sensitivity and resistance. This method to some extent helped to select specific cancers in the clinical trials that are likely to respond.

#### **1.4 Clinical Implications of Drug Resistance**

There are several clinical implications of drug resistance. Some of the important consequences were listed below.

- Drug resistance is a single most common cause for discontinuation of chemotherapy (**Hurley 2002**).
- Drug resistance is a complex problem in cancer chemotherapy, accounts for much useless treatment and has caused much hardship to patients.
- The main implication of drug resistance is the disease relapse where patient no longer responds to chemotherapy.
- Patients frequently develop multidrug resistance during the course of chemotherapy. Multidrug resistance is very complex and difficult to overcome.
- In some situations, drug resistance forces physicians to use higher doses of drug to overcome resistance, but at the cost patient life. Higher doses are extremely toxic to normal proliferating cells such as hematopoietic cells and immune cells. Compromising the immune system makes patients prone to microbial infections.
- Long-term cancer chemotherapy is very expensive, choosing the best alternative drug and switching to it, to overcome drug resistance is a huge financial burden.



## 1.5 Strategies to Overcome Clinical Drug Resistance

Attempts to overcome drug resistance by the use of different drug or combination of drugs are the most obvious approaches. However this strategy offers only temporary respite and eventually results in multidrug resistance. Therefore identification of molecular basis of resistance is crucial to determine genes that confer resistance. Targeting the genes that are responsible for drug resistance pathways with small molecular inhibitors can overcome drug resistance.

**Combination therapies** offer the potential for inhibiting multiple targets and cell signaling pathways simultaneously to kill cancer cells more effectively. Usage of combinational therapy can potentially overcome or even prevent the emergence of resistance. However the methods should be validated in preclinical and clinical studies before putting them work in the routine clinical use. Some of key issues that have to be considered while designing combination therapy include.

- Each drug should have its own anticancer activity with no cross-resistance.
- Evidence is required to show that both the drugs act synergistically.
- They should not have overlapping toxicities.

Some of the drug combinations that shown to be promising are described below.

It was shown that capecitabine/docetaxel therapy in anthracycline resistant cancer patients resulted in superior time to disease progression significantly compared to docetaxel alone (O'Shaughnessy et al., 2002). Median time to disease progression was 6.1 months in combination regimen when compared to 4.2 months with docetaxel alone. The survival curves significantly segregated and sustained over time (Figure 10). In combination arm 12 month survival rate was 57% compared to 47% in single agent arm. The response rate for combination and single arm regimens were 32% and 23%, respectively. Importantly the percentage of treatment related side effects were similar in both arms, which suggests that these drugs have no overlapping toxicities.

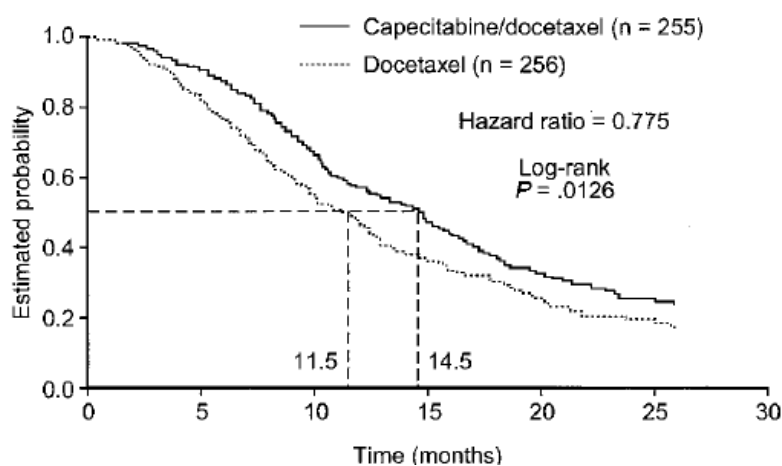


**Figure 10:** Comparison of overall survival between capecitabine/docetaxel combination and docetaxel alone. Clear early separation between the two regimens can be noticed (from O'Shaughnessy et al. 2002)

Several other rationally designed combinational therapies yielded significant survival advantage and were also effective in circumventing drug resistance. Important examples of effective combination regimens include trastuzumab and paclitaxel for breast cancer (**Slamon et al., 2001**), Gefitinib (EGFR inhibitor) and rapamycin (mTOR inhibitor) for malignant gliomas (**Doherty et al., 2006**), Sorafenib (VEGFR inhibitor) and gemcitabine for pancreatic cancer (**Siu et al., 2006**). Some of the routinely used and well known effective combinations include cyclophosphamide, doxorubicin, vincristine, dexamethasone, prednisone in the treatment of lymphoma and bleomycin, cisplatin, vinblastine, and etoposide in the treatment of testicular cancer.

Investigators also tried the **sequential treatment** with two different drugs and claimed that sequential approach is much effective in overcoming drug resistance and have less severe toxicities when compared to combination therapy. However the superior advantages of sequential therapy compared to combination is always under debate. In some clinical trials the efficacies of combination therapy and sequential therapy was compared. In one study, 303 patients with advanced breast cancer were initially randomized to either monotherapy or combination therapy. In single agent therapy patients received epirubicin until progression and then mitomycin C. In combination arm patients received first a combination of cyclophosphamide, epirubicin, and 5-FU, followed by mitomycin C and vinblastine. No significant differences in survival rates were reported in both arms. Further, quality of life and tolerability were more favorable for sequential therapy arm (**Joensuu et al., 1998**). Few other investigators reported similar results when they compared sequential and combination therapies.

One of the main reasons for multidrug resistance is the overexpression of ATP-binding cassette transporters. Pgp, MRP1, and BCRP have been shown to consistently overexpress in wide variety of drug resistant cancers. These genes have broad substrate specificity and can efflux wide variety of structurally distinct anticancer drugs. Several drugs that inhibit can inhibit drug transporters activity have been reported. However very limited success was achieved with these chemosensitizers when used in combination with anticancer drugs. First generation **MDR modulators** which include cyclosporine A, verapamil, and silybin derivatives were highly toxic and have poor modulatory activity and unpredictable interactions. Some of the second and third generation MDR activity modulators are listed in Table 2.

**Table 2:** 2<sup>nd</sup> and 3<sup>rd</sup> generation MDR modulators (**Borowski et al., 2005**)

<b>Modulator</b>	<b>Target</b>	<b>Status</b>
PSC833 – Valspodar (Cyclosporin Derivative)	PgP (MDR1)	Phase III
MS209 (quinoline derivative)	PgP MRP	Phase I/II
VX710 – Biricodar (pipeclinate derivative)	PgP MRP BCRP	Phase II
XR9576 – Tariquidar (anthranilamide derivative)	PgP MRP	Phase II/III
LY335979-Zosuquidar (disbenzosuberane derivative)	PgP	Phase III
GF120918-Elacridar (acridone carboxamide derivative)	PgP BCRP	Discontinued
R-101933-Laniquidar (bezazepine derivative)	PgP	II/III
ONT093 (diarylimidazole derivative)	PgP	Discontinued

Second generation MDR modulators (valsopodar, biricodar) had better tolerability; however they have unpredictable pharmacokinetic interactions and displayed non-specific interactions with other transporter proteins. Third generation modulators (tariquidar, zosuquidar, laniquidar) have favorable pharmacokinetic properties and displayed high potency and specificity towards PgP. Combination of anticancer drugs in combination of second generation modulators particularly valsopodar has resulted in the reversal of multidrug resistance in several cancers (**Thomas et al., 2003**). The preliminary results with the third generation modulators have been promising and may offer a new hope for drug resistant patients.

## 1.6 Targeting Cell Cycle in Cancer

### 1.6.1 Cell cycle

The cell cycle is a regulated process, culminating in cell growth and division into two daughter cells (Figure 11). Cell cycle is the original term used to describe the behaviour of cells as they grow and divide. The strict molecular events taking place during this cell cycle is responsible for accurate cell division.

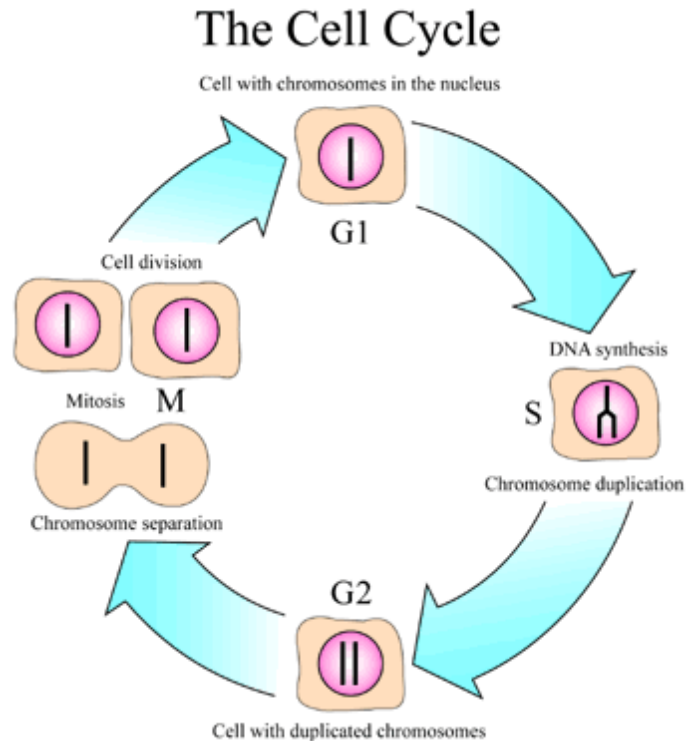


**Figure 11.** Simplified version of cell cycle

(Taken from: <http://nobelprize.org/medicine/laureates/2001/press.html>)

Control of the cell cycle is of prime importance in human disease, as cancer is a perturbation of normal cell cycle regulation. The cell cycle is driven by a sequence of enzymatic cascades that produce a linear sequence of discrete biochemical states of the cytoplasm. Each stage arises by destruction or inactivation of key enzymatic activities characteristic of the preceding state and expression or activation of a new cohort of activities. Biochemical pathways termed checkpoints control transitions between cell cycle stages. Check points modulate progression of cells through the cycle in response to external and internal signals (Nurse 2000).

### 1.6.2 Cell cycle regulation

The cell cycle consists of four main phases, **G1 phase**, **S phase**, **G2 phase**, and **M phase**. Biochemical points termed checkpoints control transitions between cell cycle stages to ensure the fidelity and progression into next stage. These check points ensure faithful inheritance of genetic material from parent cells to daughter cells, thus maintaining genomic stability.

**G1 phase** is considered as the longest and most variable of all phases of the cell cycle. G1 phase tightly regulates cell growth, accompanied by high rates of mRNA (messenger ribonucleic acid) synthesis and subsequently the protein synthesis. Healthy cells do not embark on a round of DNA replication and division until they reach an appropriate size. The smaller daughter cells need more time to grow before DNA replication size (**Lewin 1997**). Progression from this phase is controlled by two cell cycle regulated checkpoints.

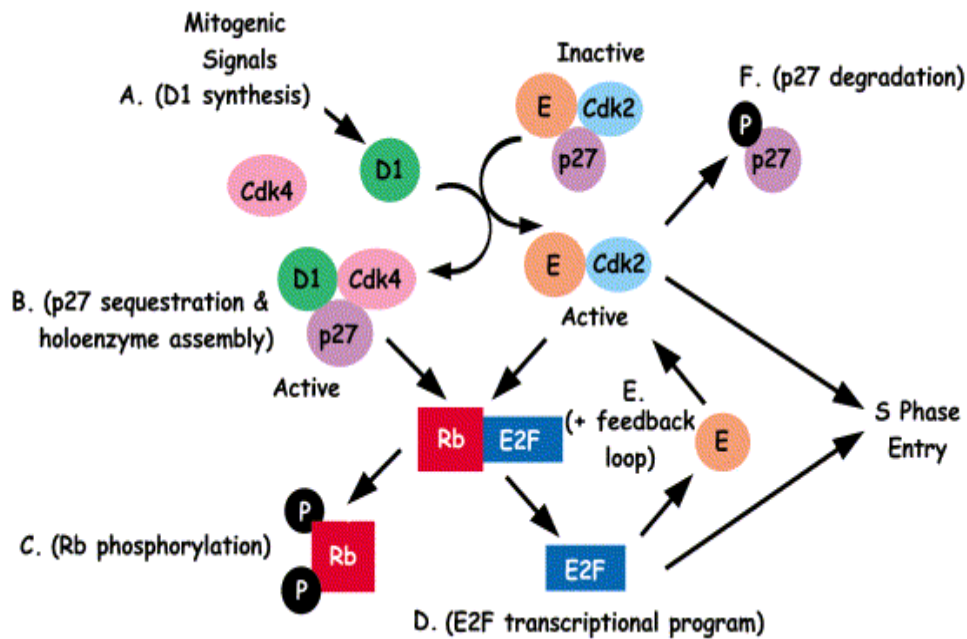


**Figure 12.** G1 cascade regulatory genes (from: Sherr, C.J. & McCormick, F. 2002)

Of all checkpoints, G1 phase is tightly regulated and once the cell passes the G1 Phase, then it is at the point of no return (Figure 12). pRB (retinoblastoma protein) and a family of essential transcription factors known as E2F are the main regulators of G1 check point (**from Sherr et al., 2002**).

Unphosphorylated pRB associates with E2F, thereby preventing the transcription of E2F responsive cell cycle progression genes (**Sherr et al., 2002**). Master regulator genes of the cell cycle, namely CDKs (cyclin dependent kinases) regulate the binding of pRB with E2F. CDK2 in association with cyclin A phosphorylates pRB, resulting in the dissociation of E2F (**Lundberg et al., 1998**). CDK activity in early G1 phase is in turn regulated by relative levels of D-type cyclins and the small inhibitory proteins including p27 and p21 (**Pietenpol et al., 2002**). Prolonged activation of G1 checkpoint leads to apoptotic cell death. p53 is the most characterized tumor suppressor protein, which is mainly involved in G1 checkpoint. p53 is a transcription factor, whose role in the G1 DNA damage checkpoint appears to regulate a set of target genes, including the p21, a CDK inhibitor. p53 is considered as guardian of genome and it maintains genomic stability. p53 induces cell death by stimulating transcription of number of genes involved in apoptosis, which include Bax (BCL2-associated X protein), CD95 (Fas/Apo1), and Apaf-1 (apoptotic peptidase activating factor 1) (**Anichini et al., 2005**). The main candidate genes namely caspases that are involved in the execution of apoptosis are induced by the p53. These are proteases having cysteine in their active site and cleave aspartate residues on the C-terminal side (**Bayascas et al., 2004**). Caspases are selective enzymes cleaving a very small subset of cellular proteins. Moreover cleavage of an

inhibitory chaperone by caspases is responsible for activation of the nuclease that destroys or beaks chromosomal DNA. During later stages of apoptosis the chromosomal DNA is cleaved by a nuclease. An initial cleavage of the chromosomes into fragments of roughly 50,000 bp is usually followed by further cleavage of the DNA between nucleosomes, producing a characteristic ladder of DNA fragments. The responsible nuclease is called CAD (Caspase – activated DNase) (**Bayacscas et al., 2004**).

**S-phase** is the DNA replication Phase, where the parent cells genetic material is duplicated before cell division. S-phase is induced by the combination of CDK-cyclin pairs, called as S-Phase promoting factors and a specialized kinase Cdc7p-Dbf4p (cell division cycle 7 homolog-activator of S-phase kinase) (**Sclafain 2002**). CDK2-cyclin E phosphorylates pRB, thereby further opening of the checkpoint gate, allowing E2F to function as a transcription factor, which induce the transcription of genes involved in DNA replication., E2F promotes transcription of cyclin A, Cdc25A (cell division cycle 25 homolog A), genes required for synthesis of DNA precursors, and origin binding proteins Cdc6p (cell division cycle 6 homolog) and ORC1 (origin recognition complex, subunit 1) (**Stillman et al., 1996**). Generally the bulk of attention in S-phase is on replication. However centrosome duplication also occurs in S-Phase. Many key proteins are involved in the duplication of centrosomes including Aurora A, CDK2-cylin E, and PLK1 (polo-like kinase 1) (**Lodish et al., 1995**). Finally with the completion of DNA replication and centrosome duplication, the cell is ready to divide however it must undergo one last checkpoint to ensure that the genome has been replicated correctly. All these controls, together with other ongoing preparations for mitosis are significant events of the G2 Phase (**Stillman et al., 1996**).

**G2 phase** - Once the replication and other important events of the S-Phase are completed, the cell is ready to divide. However one last series of checkpoints must ensure that the genome has replicated correctly and that no harmful DNA damage has occurred. These checks together with other important preparations for mitosis including high rate of cell growth and biosynthesis, are the principle events of the G2 Phase. G2 is defined as a gap between replication and the beginning of mitosis (**Lewin 1997**). A network of stimulatory and inhibitory protein kinases and phosphatases control entry into mitosis. This intricate and complex mechanism provides a number of ways to delay the G2/M transition until damaged DNA is repaired. G2 checkpoint is mainly governed by three components namely sensors, specific kinases, and effectors. If sensors detect damaged DNA, they activate protein kinases, which in turn transmit this information to effectors, which directly or indirectly block the cell cycle. Many factors of G2 checkpoints have been identified in genetic studies of yeast. After detecting the DNA damage, sensors transmit the signal to a family of very large protein kinases that resemble the lipid kinase phosphatidylinositol 3-kinase (**Djordjevic et al., 2002**). The main G2 checkpoint kinase is ATM (ataxia-telangiectasia mutated), encoded by the gene defective in human inherited disorders ataxia-telangiectasia (**Pauklin et al., 2005**). Another member of kinase family, ATR (ataxia-telangiectasia Rad3 related) also involved in G2 checkpoint control. If ATM/ATR receives signals from DNA damage, they phosphorylate at least two important substrates called p53 and a protein kinase CHK1 (checkpoint homolog) (**Ferrara et al., 2006**). CHK1 in turn phosphorylates Cdc25 inhibiting its action. ATM/ATR also targets p53, which is required to prolong the cell cycle arrest. p53 in turn regulates the expression of important proteins required for G2 checkpoint. p53

regulates the expression of p21, which inhibits CDK1-cyclinA. When the DNA damage is repaired, the check point regulations are turned-off. Inactivation of p53 triggers cell cycle progression into mitotic Phase.

**M-phase** is the mitotic phase, where the parent cell divides in two daughter cells. Mitosis is divided into five distinct Phases called prophase, prometaphase, metaphase, anaphase and telophase. During **prophase** the chromosomes condense and the change in the properties of the microtubules is accompanied by the separation of duplicated centrosomes, each of which nucleates the formation of one pole of the mitotic spindle (**Lewin 1997**). During **prometaphase** the nuclear envelope breaks down and chromosomes attach randomly to microtubules projecting from the two poles of the mitotic spindle. Once both kinetochores of a chromosome are attached to the opposite spindles, the chromosome slowly moves to a point midway to the poles. Once the chromosomes are properly attached to the spindles, the cell is said to be in **metaphase**. The chromatid arms unwind several times during metaphase. The later stage is known as **anaphase**, where the sister chromatids separate at their centromeres. The daughter chromosomes separate from each and move away towards one of the two spindle pole regions. Once the chromosomes approach spindle poles, the nuclear membrane reforms on the surface of the chromatin. This phase is called **telophase**. During this stage, a contractile ring of actin and myosin assembles as a circumferential belt in the cortex regions (central part of the cell) and constricts towards the equator of the cell. This process is called **cytokinesis**, which ultimately separates the two daughter cells (**Lewin 1997**).

Mitotic Phase has also various checkpoints; however metaphase checkpoint and spindle assembly checkpoints are main events that regulate proper segregation of chromosomes thus maintaining genomic stability. During prophase condensin plays a major role in chromosome condensation, which is activated by CDK1-CyclinB (**Hirano 2005**). The beginning of condensation correlates with H1 histone phosphorylation by CDK1-Cyclin B and H3 histone by Aurora kinase B (**Nigg 2001**). The initiation of mitotic spindle formation occurs during prophase. Prometaphase begins with the disassembly of nuclear envelope. Nuclear lamina breakdown occurs due to phosphorylation of lamins preferentially by CDK1-CyclinB. Recently Aurora A has been shown to have prominent role in nuclear envelope breakdown by recruiting D-Tacc (transforming, acidic coiled-coil containing protein),  $\gamma$ -tubulin, SPD-2, and ChToh (**Kollareddy et al., 2008**). At this stage the spindle searches and captures exposed chromosomes. The kinetochore tension-sensing mechanism involves a large kinesin, namely CENP-E (centromere protein) (**Garcia-Saez 2004**). Attainment of chromosomal bipolar attachments, which oscillates at equatorial position, marks the metaphase stage. A key checkpoint is involved prior to segregation, to ensure that all chromosomes are biattached and assembled at the metaphase plate. This is called metaphase checkpoint. In budding yeast and vertebrates the genetic analysis have revealed many protein kinases that operate during this checkpoint. Among them, Bub1p (budding uninhibited by benzimidazoles 1 homologue) and BubR1 have very prominent roles. As cells enter mitosis the BUB and MAD (mitotic arrest deficient) proteins bind to all kinetochores and produce activated Mad2p, which associate with APC/C cdc20 (anaphase promoting complex) and keeps it inactive (**Millband et al., 2002**). Aurora A and PLK1 also play a prominent role in

bipolar spindle assembly (**Kollareddy et al., 2008, Schmit et al., 2007**). Aurora B is one of the main components of chromosomal passenger complex, which regulates chromosomal bi-orientation, kinetochore-microtubule attachment, and cytokinesis. Inappropriate kinetochore and microtubule attachments including merotelic, syntelic, and monotelic are resolved by Aurora B (**Kollareddy et al., 2008**). Once bipolar attachments of all chromosomes were achieved, the inhibitory signals are removed and a Mad2p complex is extinguished, eventually APC/C cdc20 activates initiating anaphase onset. During anaphase the separation of sister chromatids takes place. Sister chromatids move to opposite pole during anaphase A and the poles move apart during anaphase B. Sudden drop in CDK1 activity initiates the transition from metaphase to anaphase. This starts eventually with cyclin A destruction at the onset of prometaphase. The transition is completed by APC/C-directed cleavage of several key proteins targets by proteasomes, including securin and cyclin B (**Schmit et al., 2007**). Sister chromatid separation is regulated by the chromosomes themselves, not by the mitotic spindle. However studies of budding yeast have identified three factors that regulate sister chromatid separation. A protein complex cohesin, a protease known as separase, and an inhibitor of protease known as securin are involved in the regulation of sister chromatid separation (**Horing et al., 2002**).

During telophase, the chromosomes recondense and the nuclear envelope reforms around the genetic material. The most dramatic change in cellular structure at this time is the constriction of the cleavage furrow and subsequent cytokinesis. The subunits of lamins disassembled in prophase are recycled to reform the nuclear envelope at the end of mitosis. B-type lamins are among the initial components of the nuclear envelope to target to the surface of the chromosomes (**Osouda et al., 2005**). Lamin A enters the reforming nucleus later during telophase, after the reassembly of nuclear pore complexes and reestablishment of nuclear import pathways. Transport of lamins through the nuclear pores appears to be an essential step in nuclear reassembly. Cytokinesis is the final stage of mitosis. The material within the parent cell is cleaved equally into two daughter cells through contraction of a ring of actin and myosin around the equator of the cell. The contractile ring is confirmed to a narrow band of cortex, which forms a cleavage furrow. The components of spindle required for cytokinesis include kinesins, INCENP (inner centromere protein), Aurora B, and survivin (**Schmit et al., 2007**). PLK1 regulates APC-targeted degradation through Emi1 (early mitotic inhibitor 1), which is necessary for mitotic exit (**Schmit et al., 2007**).

### **1.6.3 Cell cycle and cancer**

Abnormal cell division and associated high rates of uncontrolled proliferation is one of the main hall marks of cancer disease. Thus the connection between cell cycle and cancer is obvious. Several cell cycle regulators controlling the checkpoints and progression through the cell cycle are altered in tumors. Some of the key regulators of cell cycle checkpoints that are deregulated in cancer are described in above sections. Several activating mutations in proto-oncogenes and inactivating mutations in tumor suppressor genes have been reported in different types of cancers. Further altered expression of several cell cycle regulations in cancers have also been reported. CDKs are widely accepted as key regulators in progression of the cell cycle. Hence it is clear that altered expression of these kinases is responsible for abnormal cell cycle progression and eventually transformation. Amplification and



overexpression of CDKs have been consistently reported in several cancers. Wei et al. reported CDK4 amplification in osteosarcoma and associated pathology (Wei et al., 1999). CDK4 in complex with cyclin D1 regulates G1 to S transition by phosphorylation of pRB. Southern blotting revealed amplification of CDK4 from 8-14 copies in 9% of tumor samples including primary and metastatic tumors. CDK2 concurrently with cyclin E have been reported to be amplified in colorectal cancers and may have an important role in carcinogenesis (Kitahara et al., 1995). Eggers et al. reported overexpression of CDK5 in pancreatic ductal adenocarcinomas. Inhibition of CDK5 in pancreatic cancer cells either genetically or pharmacologically (Roscovitine) significantly decreased the migration and invasion (Eggers et al., 2011). CDK7 was also shown to be moderately elevated in several cancer cell lines compared to normal counterpart (Bartkova et al., 1996). CDK1 has been shown to overexpress in Barrett-associated esophageal adenocarcinoma cell lines. 96% of the high-grade dysplasias expressed abundant surface CDC2/CDK1. This study suggested that a role for CDK1 in carcinogenesis and thus can be used as histopathologic marker for dysplasia and potential drug for chemotherapy (Hansel et al., 2005).

Recently an important family of serine/threonine kinases, namely polo-like kinases (PLK1, PLK2, PLK3, and PLK4) gained much attention in the context of cell cycle and cancer. PLKs have multiple functions in mitosis including centrosome maturation, bipolar spindle formation, chromosome segregation, activation of CDC2 (cyclin dependent kinase 1), regulation of anaphase-promoting complex, and execution of cytokinesis (Takai et al., 2005). In fact some of their functions overlap with Aurora kinases (Lens et al., 2010). By reviewing the distinct functions of PLKs in mitosis, it is clearly obvious that their deregulation will cause genomic instability. Indeed aberrant expression of PLKs and associated transformation and progression has been consistently reported. PLKs are widely considered as oncogenes. Particularly PLK1 deregulation has been reported consistently in several cancers. Wolf et al. showed correlation between PLK1 elevated expression and associated worse prognosis. PLK1 was shown to be highly up-regulated at mRNA level in non-small cell lung cancer patients compared to controls. According to Kaplan Meier analysis, patients with low PLK1 expression survived significantly longer than with high expression (Wolf et al., 1997). The 5 year survival rates were 47.2% and 24.9%, respectively. PLK1 is a significant predictor for the survival and also an important target for intervention. PLK1 elevated expression has also been reported as a worst prognostic factor in several cancers including head and neck, esophageal, gastric, melanoma, breast, ovarian, endometrial, gliomas, and thyroid (Takai et al., 2005). On the other hand, PLK3 expression is negatively correlated with the development of certain cancers, particularly the lung cancers (Li et al., 1996).

As our study was mainly focused on Aurora kinase inhibition related resistance, the Aurora kinases role in cancers was described in a separate section.

Apart from the above described abnormalities of cell cycle regulated genes in cancer, several cell cycle gene alterations have been consistently reported including cyclins (D and E up-regulation), INK4 family (CDK4 and CDK6 inhibitors) (p16, 18, and 19 mutations or deletions), CIP/KIP family (p21 down-regulation: CDK2-cylin E and CDK 4-cylinD1 inhibitor) (Park et al., 2003). Among the tumor suppressor genes involved in the cell cycle

arrest, p53 is considered as the 'guardian of the genome'. p53 is primarily active in G1 DNA damage checkpoint. In response to DNA damage response, p53 induces cell cycle arrest via p21 (CDK inhibitor). Prolonged arrest in G1 Phase due to irreparable DNA damage activates p53 and subsequent apoptotic cell death. However in majority of the cancers, p53 is inactivated by variety of genetic alterations including mutations, dominant-negative mutations, and deletions. p53 mutations and deletions accounts for 50% of all human cancers. Hence p53 has gained significant attention in the clinic, efforts are being made to restore the wild-type p53 functions both using pharmacological and genetical approaches. R175H, R248W, R249S, R273H are considered as hot-spot mutations as they are very common in most of the human cancers (Willis et al., 2004). R175H and R273H are the most frequently reported gain-of-function mutation in several cancers, where the mutant protein promotes tumorigenesis. V143A and D281G have also been reported as gain-of-function mutations in few cases (Petitjean et al., 2007). Dominant negative p53 mutations have also reported several times in human cancers. In these cases a specific type of mutant protein interferes with wild type p53 through protein-protein interactions. R273H and R175H are frequent dominant negative mutations that have reported in several cancers (Willis et al., 2004). All these p53 mutations are very aggressive and confer resistance to variety of anticancer agents.

Apart from p53, number of genetic alterations have been reported for well known tumor suppressor genes including retinoblastoma gene, PTEN (phosphatase and tensin homolog), APC (adenomatous polyposis coli), BRCA1, BRCA2, and ATM etc.

#### **1.6.4 Targeting cyclin dependent kinases**

##### **CDK and Roscovitine**

As described in the above sections, altered expression of CDKs are associated with cancer progression. Hence blocking their activity with small molecule inhibitors would be beneficial for cancer treatment. Several CDK are already undergoing clinical trials. Roscovitine (Seliciclib), developed by Cyclacel has been evaluated for efficacy in a Phase II clinical study. It was shown to inhibit CDK2/cyclin E and CDK7/cyclin H with IC50 values of 0.1, 0.49  $\mu$ M, respectively. It inhibited proliferation of several cancer cell lines with an IC50 value range 7.9-30.2  $\mu$ M. Among all cell lines tested LoVo (colon cancer cell line) and MESSA/DX5 (uterine sarcoma cell line) cancer cell lines are highly sensitive. Moreover, roscovitine is less potent on normal human cells, indicating that it is suitable as an anticancer agent. Roscovitine significantly reduced tumor volumes by 48% in LoVo xenograft model compared to controls (McClue et al., 2002). In a Phase I study, 21 patients with malignant and refractory tumors were treated with 100, 200, and 800 mg b.i.d. At 800 mg dose limiting toxicities have been reported including grade 3 fatigue, grade 3 skin rashes, grade 3 hyponatraemia, and grade emesis. There were no major hematological toxicities. Objective responses were reported in this study. However one patient with metastatic ovarian cancer displayed disease stabilization (Benson et al., 2007). In another Phase I study 56 patients with advanced solid tumors or lymphomas received 218 cycles of roscovitine. The drug was administered in three schedules (schedule 1: twice daily for 5 consecutive days every three weeks, schedule 2: 10 consecutive days followed by 2 weeks off, schedules 3: three days every 2 weeks). Dose limiting toxicities at 1600 mg bid for schedule A include nausea,

vomiting, asthenia, and hypokalaemia. In schedule C, hypokalaemia and asthenia was reported at 1800 mg bid. Only one partial response was reported in patient with hepatocellular carcinoma. 6 patients displayed disease stabilization, which lasted for  $\geq 4$  months (**Le Tourneau et al., 2010**).

Several other CDK inhibitors in clinical trials include Alvocidib (flavopiridol: National cancer institute), PD 0332991 (Pfizer), SNS-032 (Sunesis), AT7519 (Astex), and AZD5438 (AstraZeneca) etc. Plenty of preclinical CDK inhibitors are being developed.

### **1.6.5 Targeting polo-like kinases**

#### **PLK1 and BI 6727**

BI 6727 discovered and developed by Boehringer Ingelheim is currently being evaluated in various phase II studies either as monotherapy and in combination with other approved anticancer drugs. It was shown to inhibit predominantly PLK1 with an IC<sub>50</sub> value 0.87 nM (**Rudolph D et al., 2009**). It also inhibits PLK2 and PLK3 with IC<sub>50</sub> values 5 and 56 nM, respectively. It was shown to inhibit proliferation of various cancer cell lines with an EC<sub>50</sub> (half maximal effective concentration) ranges 11-37 nM. Treatment of NCI-H640 (lung cancer cell line) at 100 nM for 24 h induced accumulation of mitotic cells displaying monopolar spindles, consistent with PLK1 inhibition phenotype. Flow cytometry analysis revealed accumulation of cells with 4N DNA content, suggesting a G<sub>2</sub>-M arrest. BI 6727 induced apoptosis as shown by the appearance of cleaved PARP, determined by western blotting analysis. In HCT116 xenograft model, a dose of 20 mg/kg administered on two consecutive days per week for 5 cycles resulted in tumor regression. Similar results were also obtained in NCI-H460 xenograft model. BI 6727 also suppressed tumor growth significantly in taxane-resistant colon cancer model. Overall, BI 6727 displayed promising efficacy in all xenograft models and was well tolerated at all doses administered either orally or intravenously (**Rudolph D et al., 2009**).

In a Phase I study, 65 patients with advanced solid tumors were enrolled for BI 6727 treatment and received a single 1 h infusion every 3 weeks. The established MTD (maximum tolerated dose) was 400 mg. Grade 3/4 neutropenia, grade 3 fatigue, grade 3 Anaemia, and grade 3/4 thrombocytopenia were reported as DLTs (dose limiting toxicities). Three patients exhibited partial response and stable disease was reported in 40% of patients (**Schoffski P et al., 2012**). Favorable pharmacokinetics for BI 6727 was reported in the study.

Other clinical trial Phase PLK inhibitors include ON-01910 (Oncova therapeutics), and GSK461364 (GlaxoSmithKline). Plenty of preclinical PLK inhibitors are being developed.

### **1.7 Aurora Kinases and their Biology**

Aurora kinases (A, B, & C) are mitotic serine/threonine kinases, mainly involved in the regulation of various mitotic events (my reference). Aurora A is primarily involved in the regulation of centrosome maturation and duplication, bipolar spindle assembly, and alignment of metaphase chromosomes (Figure 13). Aurora B is a chromosomal passenger protein involved in the regulation of chromosomal bi-orientation, the association between kinetochores and microtubules, and cytokinesis (Figure 14). Aurora C exhibits similar

functions to those assigned to Aurora B and is required for cytokinesis. Wild type Aurora C was also reported to rescue multinucleation induced by enzymatically inactive Aurora B, suggesting that Aurora C may complement the functions of Aurora B (Kollareddy et al., 2008).

One can easily relate the above mentioned roles of Aurora kinases and genomic stability. As Aurora kinases are essential for faithful chromosome segregation during mitosis, they are crucial in the maintenance of genomic stability. Abnormal Aurora expression or activity is directly associated with genomic instability, which induces aneuploidy. Aneuploidy is one of the hall marks of majority of the cancers and is the main driving force for cancer cell initiation and progression.

### 1.7.1 Aurora A pathway

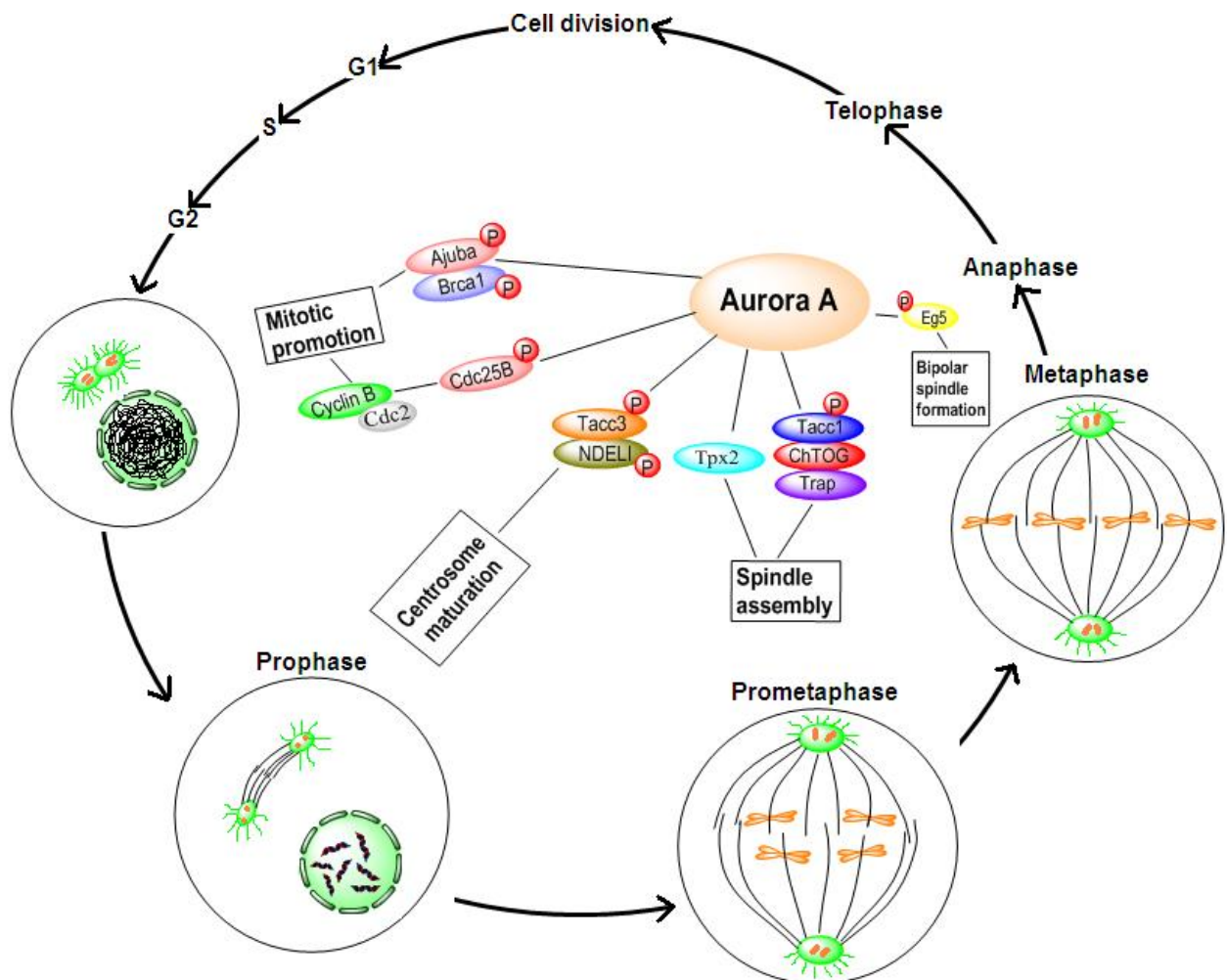


**Figure 13.** Aurora A Pathway

## 1.7.2 Aurora B pathway

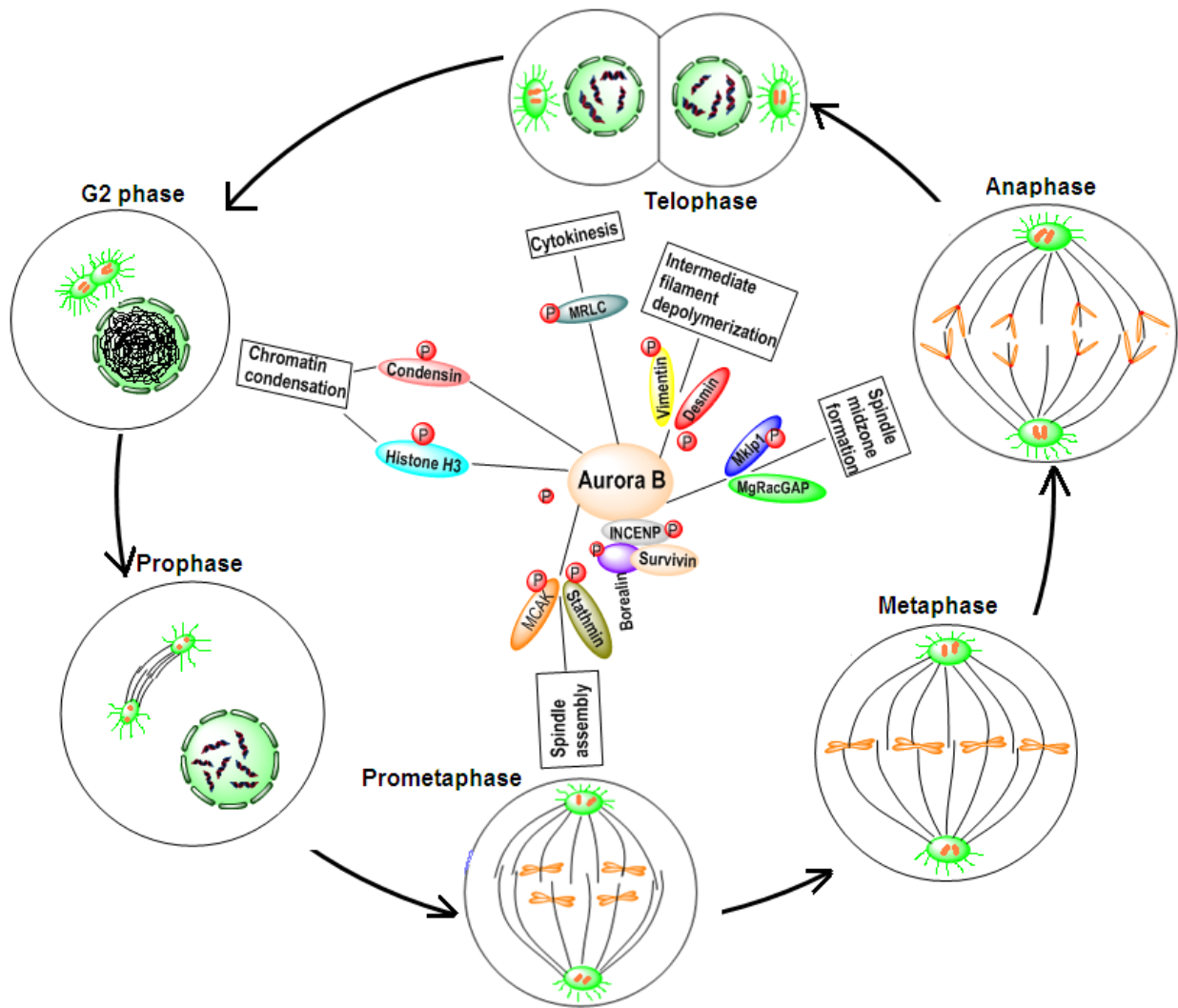
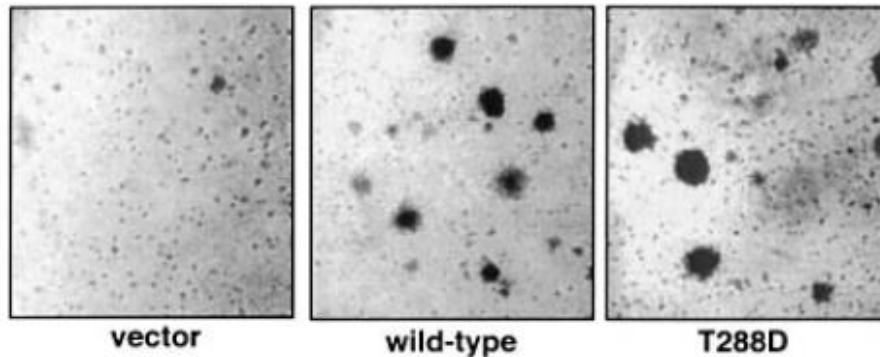


Figure 14. Aurora B pathway

### 1.7.3 Aurora kinases and cancer

Association of Aurora kinases overexpression or abnormal activity and transformation was reported by many previous studies. Bischoff et al. infected Rat1 (immortalized nontumorigenic rat fibroblast cell line) fibroblasts and NIH 3T3 cells (primary mouse embryo fibroblasts) with stably overexpressing Aurora A or mutant Aurora A (T288D) retrovirus (**Bischoff et al., 1998**). Both wild type and mutant Aurora constructs transformed the cells as evidenced by the formation of big colonies on soft agar (Figure 15)



**Figure 15.** Formation of Rat1 and NIH 3T3 transformed colonies on soft agar after stable overexpression of wild type or mutant Aurora A. (from Bischoff et al., 1998)

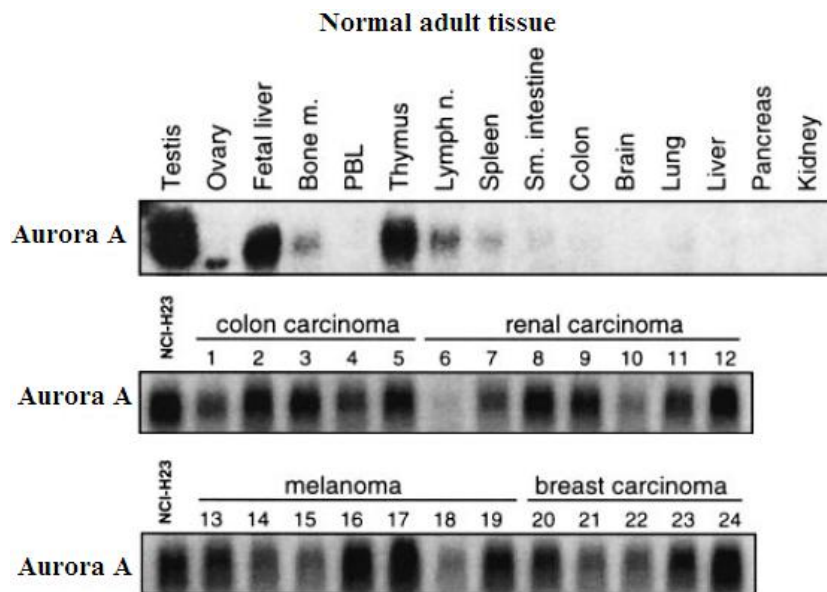


**Figure 16.** Expression levels of Aurora A in normal and cancer cells. (from Bischoff et al., 1998)

In the same study authors reported elevated expression of Aurora A in colon, renal, melanoma, and breast cancers, whereas its expression is primarily restricted to testis, fetal liver, thymus, and to some extent in ovary, lymph nodes, bone marrow, and spleen in normal tissue (Figure 16).

Aurora A maps adjacent to CYP24 gene (cytochrome 450, family 24) and RMC20C001 (minimal region of amplification) cosmid probe, located on chromosome 20. Both these

markers have been characterized for their existence in the 20q13 amplicon common to colon, bladder and breast cancers. Southern blot revealed amplification of Aurora A in 52% of colorectal tumors (**Bischoff et al., 1998**) (Figure 17). No amplification was observed in matched normal tissue. DNA amplification corresponded to increased RNA expression.

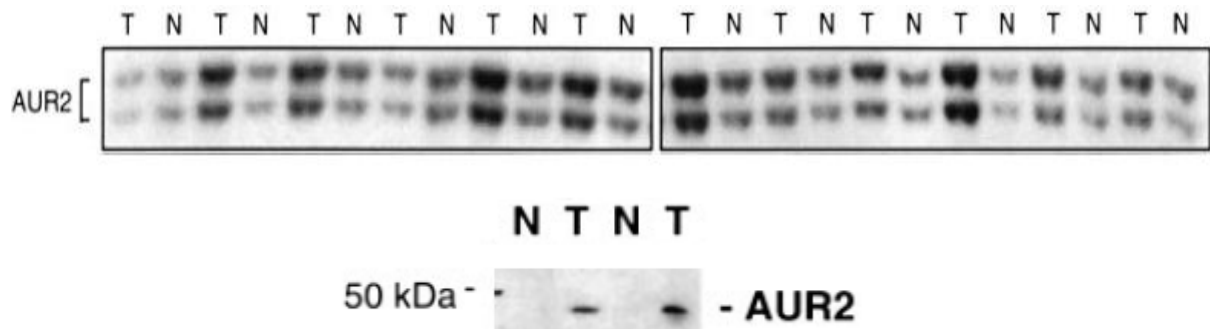


**Figure 17.** DNA amplification of Aurora A in colorectal cancer tissues, confirmed by southern blot. B. Western blotting analysis of Aurora A in colon cancer patients. Aur2 - Aurora A, T-Tumor, N- Normal matched tissue. (from Bischoff et al., 1998)

Western blotting analysis revealed elevated expression of Aurora A in two colorectal cancer patients (Figure 17). This study indicates the overexpression of Aurora A at protein level. They also showed increased expression of Aurora A in well known cancer cell lines.

Katayama et al. performed *in situ* mRNA hybridization, northern blotting, and western blotting to determine the levels of Aurora B in colorectal tumor biopsies.

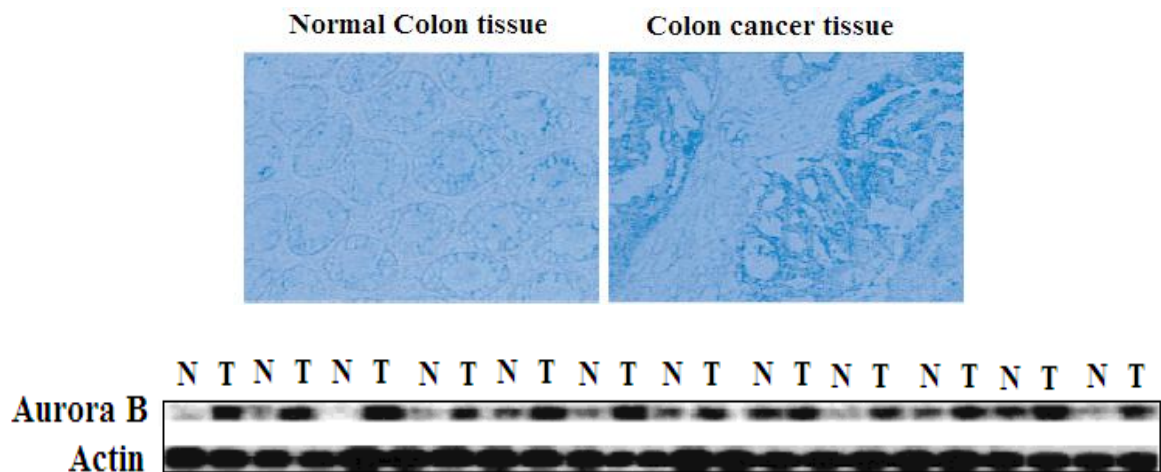


**Figure 18.** Aurora B mRNA messenger *in situ* staining. Western blotting of Aurora B in normal tissues and colorectal tissues obtained from the colorectal patients. N-Norma, T-Tumor. (from Katayama et al., 1999)

Aurora B was found to be overexpressed in most of the colorectal tumors (Figure 18). Aurora B overexpressions were increased as function of Dukes stage, which indicates that its expression is closely implicated progressive disease (**Katayama et al., 1999**). Apart from colorectal cancers, Aurora kinases overexpressions were reported in several types of cancers. Till date, oncogenic activity of Aurora C was not reported.

## 1.8 Aurora Kinase Inhibitors

The overexpression of Aurora kinases in various types of cancers formed a strong rationale for targeted therapy to develop small molecule inhibitors. Approximately 10 Aurora kinase inhibitors are already in clinical trials and many are being developed. Some Aurora kinase inhibitors displayed promising anticancer effects both in preclinical and clinical studies (Kollareddy et al., 2012). Since our project was mainly focused on identification of drug resistance mechanisms induced by CYC116 and ZM44739, we described CYC116 and ZM44739 characteristics in details in the following sections. Comprehensive information about other clinical and preclinical Aurora kinase inhibitors can be found in our previously published paper (see section 3.3).

### 1.8.1 CYC116, a novel pan-Aurora kinase inhibitor

CYC116, discovered and developed by **Cyclacel Pharmaceuticals**, is a pan-Aurora kinase inhibitor. Its chemical name is 4-methyl-5-(2-(4-morpholinophenylamino) pyrimidin-4-yl) thiazol-2-amine. It inhibits Aurora A, B, & C at 44 nM, 16 nM, and 65 nM IC<sub>50</sub> values respectively. It also inhibits some

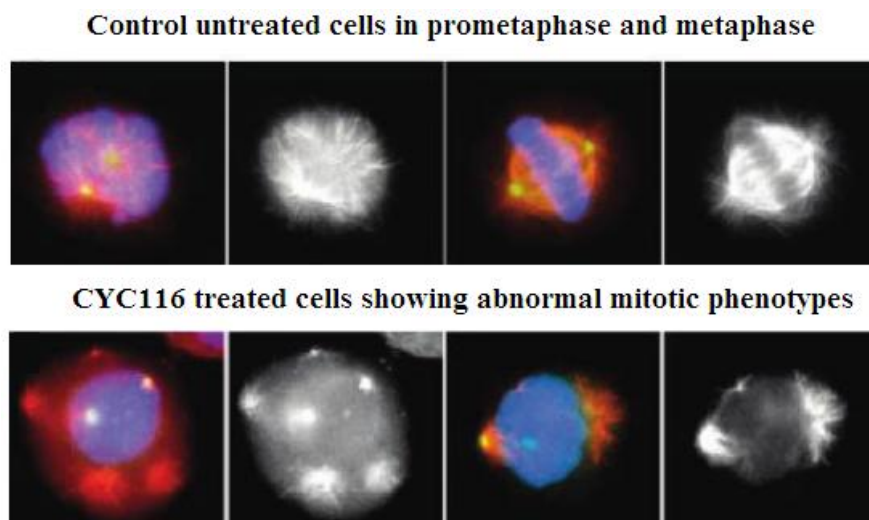


**Figure 19.** Mechanism of CYC116 action. Top panel represents control cells showing normal metaphase mitotic events. Bottom panel shows CYC116 treated cells with abnormal mitotic phenotypes including multiple acentrosomal microtubule-nucleating centers and misaligned chromosomes [Blue - DNA, Red -  $\alpha$ -tubulin, green- Centrosomal  $\gamma$ -tubulin, Black and white –  $\alpha$ -tubulin alone] (from Wang et al., 2010)

other oncogenic kinases including VEGFR2 and FLT-3. It showed promising anticancer activity in preclinical studies. CYC116 was discovered during cell-based screening of kinase-directed compound collection. A group of N-phenyl-4-(thiazol-5-yl) pyrimidin-2-amines were discovered, which inhibited histone H3 phosphorylation (ser10) and induced abnormal mitotic phenotypes (Wang et al., 2010) (Figure 19). Treatment of A549 cell line with CYC116 for 7 hrs resulted in G1 tetraploid cell (failed cytokinesis). However >4n cells appeared by 24 hrs.

*In vitro* ATP (adenosine triphosphate) competitive biochemical assay confirmed this compound as specific Aurora kinase inhibitor. Relatively at higher concentrations it also



inhibited other oncogenic kinases. It inhibits Aurora A, B, C, and VEGFR2 at 44 nM, 19 nM, 65 nM, and 69 nM IC50s respectively (**Griffiths et al., 2008**). The proliferations of various cancer cell lines with different genetic backgrounds were inhibited at 34-1370 nM IC50. CYC116 showed antitumor activity in various leukemia, solid xenograft and syngenic models. At 50 mg/kg, it reduced tumor weights and leukemia bone marrow infiltration significantly. In mice with P388D1 (mouse macrophage cell line) leukemia, it suppressed angiogenesis, decreased phosphorylation of histone H3, and induced accumulation of 4n and >4n DNA in cells (**Wang et al., 2010**). Moreover, tumor neovascularization was reduced significantly in a dose-dependent manner, possibly due to inhibition of VEGFR2 (**Hajduch et al 2008**). A Phase I trial in advanced solid tumors has been conducted to determine its MTD and evaluate its pharmacokinetic properties.

### 1.8.2 Mechanism of CYC116 action

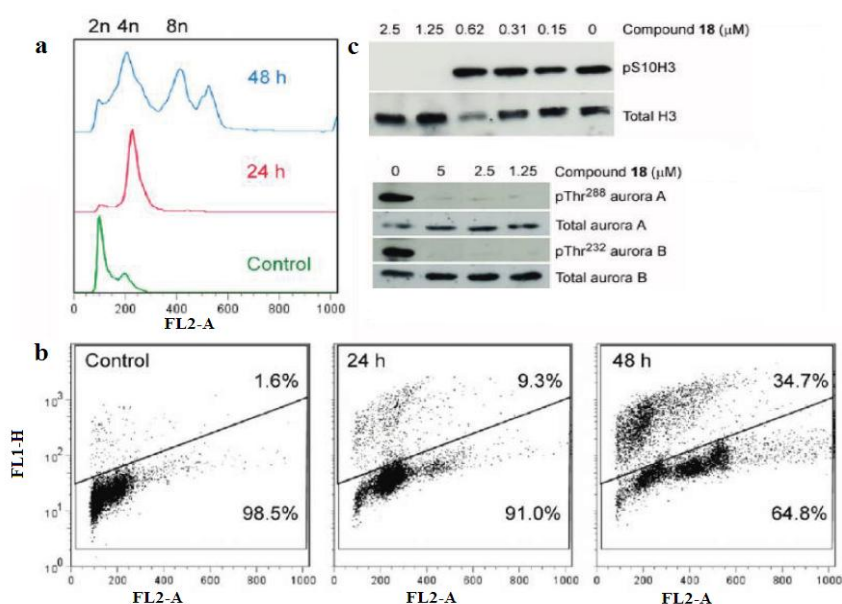


**Figure 20.** Mechanism of CYC116 action. a. Cell Cycle profile of SW620 after CYC116 treatment, b. >4n (polyploidy) corresponded to apoptosis as measured by TUNEL staining, c. Western blot of phospho histone H3 (biomarker for Aurora B inhibition) in HeLa cell line. c. Western blots showing inhibition of Aurora A and B autophosphorylation in A549 cell line. (from Wang et al., 2010).

CYC116 has broad-spectrum anticancer activity both in solid tumors and blood cancer cell lines. For the better understanding of CYC116 mode of action, it was tested on SW680 (colon cancer cell line) cell line (**Wang et al., 2010**). SW680 was treated with 1  $\mu$ M CYC116 for 24 and 48 h. By 24 h most of SW680 cells accumulated in G2/M, followed by >4n appearance by 48 hrs (Figure 20a).

This corresponded to the appearance of increased apoptotic TUNEL (terminal deoxynucleotidyl transferase dUTP nick end labeling) positive cells at 24 h and 48 h (Figure 20b). Clearly aneuploidy (abnormal number of chromosomes) induced by CYC116 activates G1 cell cycle check point and subsequent apoptosis. The specificity of CYC116 was tested on cellular level by looking at the biomarker level modulations. CYC116 specifically inhibited histone H3 phosphorylation (ser10) in HeLa (cervical cancer cell line) well below 1

$\mu\text{M}$  after 7 h (Figure 20c). It also inhibited autophosphorylation of both Aurora A and Aurora B in A549 cells at lower concentrations after 1 h treatment (Wang et al., 2010) (Figure 20c).

During *in vitro* studies CYC116 displayed significant selectivity and potency in several cancer cell lines. Compared to other compounds tested in the screening CYC116 has favorable biopharmaceutical and pharmacokinetics properties. However CYC116-induced resistance was not studied, despite of its successful transition into Phase I clinical study. Our study is mainly focused on identifying and understanding potential CYC116-induced resistance mechanisms in isogenic pairs HCT116 cells lines (colorectal cancer), one with p53<sup>+/+</sup> and other without p53<sup>-/-</sup>. Along with CYC116, we also used an experimental Aurora kinase inhibitor, ZM447439 (Ditchfield et al., 2003): (*N*-[4-[[6-Methoxy-7-[3-(4-morpholinyl)propoxy]-4-quinazolyl]amino]phenyl]benzamide) in order to compare the resistance mechanisms (Figure 21). It is more specific to Aurora B compared to Aurora A.

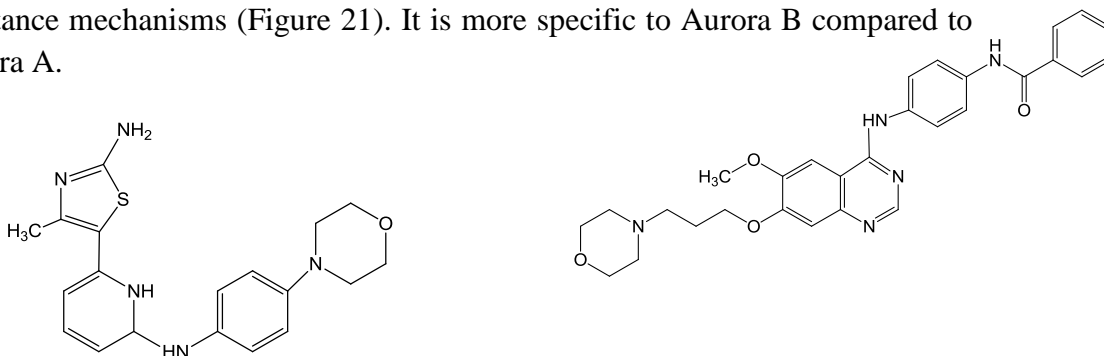


**Figure 21.** Structures of CYC116 and ZM447439

Like other molecularly targeted drugs, the emergence of cancer cell resistance to CYC116 in the clinic is possible. Drug-induced resistance studies in cell line models in parallel with preclinical development can be expected to yield significant information regarding the molecular basis of resistance. Drug resistance mechanisms towards several anticancer drugs have been reported consistently both in *in vitro* cell line models and in the clinic. These findings significantly contributed in understanding chemoresistance and helped in designing specific drug combinations regimens to overcome the resistance. Well known cancer cell resistance mechanisms that have been consistently reported towards some conventional anticancer drugs and contemporary targeted drugs are presented below.

### 1.8.3 ZM447439

ZM447439 ((4-(4-(*N*-benzoylamino)anilino)-6-methoxy-7-(3-(1-morpholino)propoxy)quinazoline), discovered and developed by AstraZeneca was the first Aurora family kinase inhibitor. Ditchfield et al. originally reported that ZM447439 inhibits Aurora A and Aurora B with IC<sub>50</sub> values of 110 nM and 130 nM, respectively (Ditchfield et al., 2003). However later it was reported that ZM447439 is 20-fold more selective to Aurora B compared to Aurora A. At 2  $\mu\text{M}$  concentration, ZM447439 inhibited cell division as evidenced by accumulation of cells with  $>4n$  DNA content (Figure 22). Its specificity towards Aurora B was evaluated by determining phosphorylation of histone H3 (Ser10).

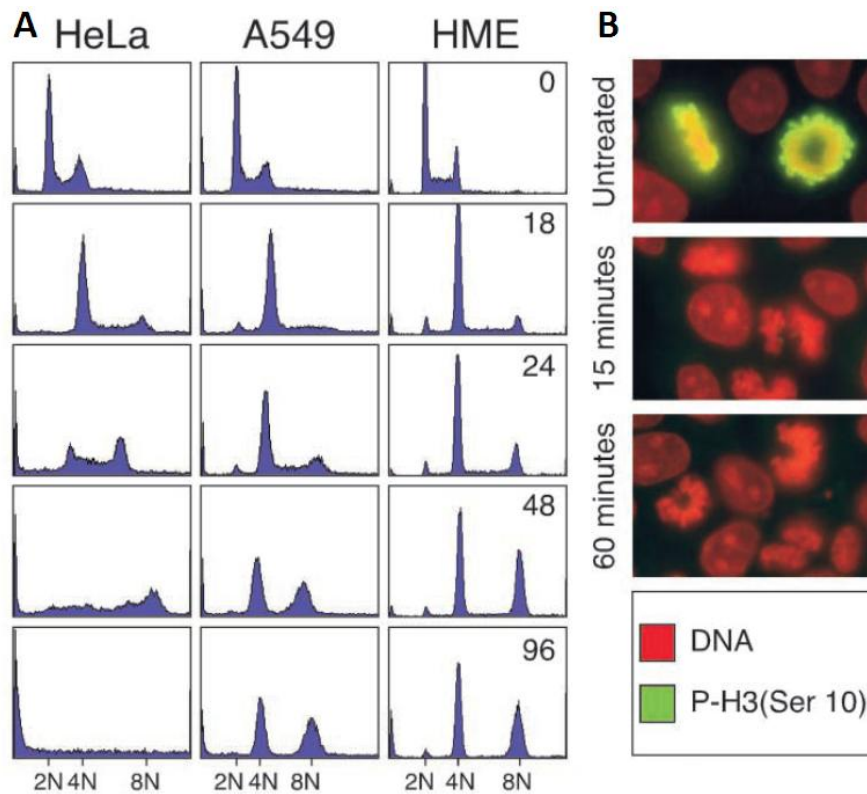
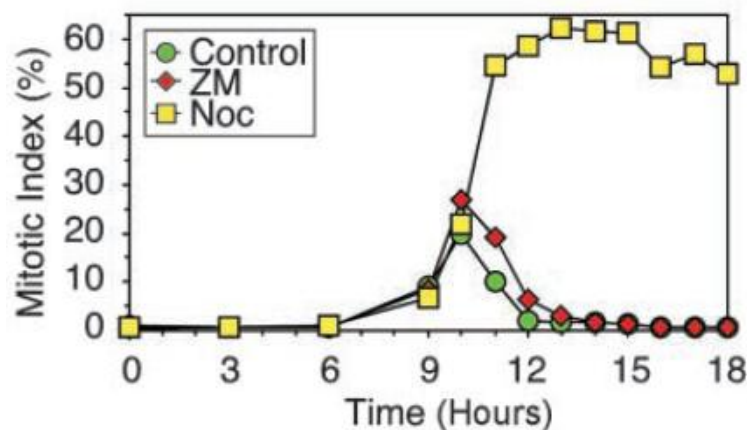


Figure 22. A, Cell cycle analysis: Treatment of HeLa, A549, and HME cell lines with ZM447439 induced accumulation of cells with  $>4n$  DNA content. B, Immunofluorescence: Treatment of cells with ZM447439 inhibited phosphorylation of histone H3 (green), DNA (red) (from Ditchfield et al., 2003).

Treatment of cancer cell lines with ZM447439 resulted in the inhibition of histone H3 phosphorylation. p53 proficient cells lost viability rapidly when compared to p53 deficient cells, indicating the presence of p53 dependent post mitotic checkpoint that occurs after failed cell division. ZM447439 inhibits chromosome alignment and segregation as evidenced by markedly reduced metaphase and anaphase spindles. ZM447439 was shown to compromise spindle checkpoint function as evidenced by the observation that cells treated with ZM447439 exit mitosis with normal kinetics despite the presence of misaligned chromosomes (Figure 23). Ditchfield et al. further showed that ZM447439 inhibited localization of BubR1, Mad2, and Cenp-E through inhibition of Aurora B but not Aurora A. Aurora B is essential to activate BubR1, Mad2, and Cenp-E (spindle checkpoint activating components) in response to misalignment of chromosomes.



**Figure 23.** ZM447439 cells exit mitosis similar to control cells despite the presence of misaligned chromosomes. Nocodazole was used as a positive control (from Ditchfield et al., 2003).

Similar effects of ZM447439 were reported in *Xenopus* egg extracts (Gadea et al., 2005). Some of the key points described by this authors include: ZM447439 induces premature chromosome decondensation, reduces the capability of microtubules to form half spindles, and inhibits spindle checkpoint integrity, but not its maintenance.

ZM447439 played a key role in assigning several functions regulated by Aurora kinases and other components of spindle check point. Some of important previously unknown functions of mitotic genes include: Aurora B kinase mediated regulation of the chromosome alignment and spindle checkpoint, and BubR1 mediated regulation of chromosome alignment.

ZM447439 has not been tested in clinical trials, as second generation Aurora inhibitors (AZD1152) developed by AstraZeneca were more potent and have better *in vivo* efficacy. ZM447439 has been extensively used as a model compound to study the biology of Aurora kinases and in their validation as targets for anti-cancer drug development.

Apart from the Aurora kinase inhibitors (targeted drugs), several targeted drugs specific to each cancer achieved high success rate in the clinic. Some of these targeted drugs are now being used routinely as first line treatment. Until now any of the Aurora kinase inhibitors did not get approved for clinical use. Like other targeted drugs, the Aurora kinase inhibitors might benefit cancer patients. Moreover some of the Aurora kinase inhibitors that have been tested in clinical trials displayed promising activity against drug resistant tumors (Kollareddy et al., 2012). In the below sections advantages of targeted chemotherapy compared to conventional chemotherapy are described. Few examples of approved targeted drugs mechanism of action and their efficacy are also described along with few investigational targeted drugs. Since these drugs are targeted against deregulated cancer cell signaling pathways, their actions on a particular oncogene was shown diagrammatically.

## 1.9 Molecularly Targeted Therapy in Cancer

Cancer can be effectively treatable or cured by surgery and radiation therapy if diagnosed at early stages. Once the cancer cells metastasize to distal organ sites, the disease becomes very aggressive and cannot be easily dealt with surgery and radiation therapy. The most

promising treatment for malignancies is chemotherapy, where the small molecule drugs can reach cancer sites and can kill the tumors by different mechanisms. The first generation anticancer drugs are highly toxic, due to the fact that they are not targeted specifically to tumor cells. Their action on normal body cells results in undesirable side effects, hence the dose-limiting toxicity issues are of high importance. Some of the drugs which do not come under targeted therapy category include taxol, vincristine, doxorubicin, gemcitabine, cisplatin, 5-Fluorouracil, Actinomycin-D, and many others (Table 3). These drugs were discovered and approved for routine use before completely understanding the molecular basis of cancer. The long-term benefits from the conventional anticancer drugs are not promising as the regression rates are significant. Focused research on biochemical pathways and evaluating differences between normal and transformed cells allowed to identify new cancer targets. This led to the discovery and development of new small molecule inhibitors that interfere with key molecular events that are responsible for transformation. Some of the targeted drugs which are already in the clinic have significant therapeutic window and less toxicity than conventional agents.

**Table 3.** Some examples of conventional anticancer drugs and comments

<b>Conventional drugs</b>	<b>Mode of action</b>	<b>Anticancer activity</b>	<b>Toxicities</b>
Taxol	Irreversible microtubule stabilization	Advanced ovarian and breast cancers	Myelotoxicity and peripheral neuropathy (Wiseman et al., 1998)
Vincristine	Inhibits microtubule assembly	Non-Hodgkins Lymphoma	Fatal Neuropathy (Tarlaci et al., 2008)
Doxorubicin	Inhibits Topoisomerase II and DNA(deoxyribonucleic acid) replication	Leukemia, bladder, lung, & breast cancers etc.	Cardiomyopathy (Chatterjee et al., 2010)
Gemcitabine	Inhibits DNA replication and ribonucleotide reductase	Non-small cell lung & pancreatic cancers	Severe pulmonary toxicity (Barlesi et al., 2004)
Cisplatin	Cross links DNA strands	[Lymphomas, and various solid tumors	Nephrotoxicity (Sheikh Hamad et al., 1997)
Actinomycin-D	Inhibits RNA(ribonucleic acid) polymerase activity	Rhabdomyosarcoma & Wilms tumor	Unusual cutaneous toxicity (Kanwar et al., 1995)

## 1.10 Clinically Valid Anticancer Targets and Respective Targeted Drugs

Several targeted drugs were approved by the FDA (food and drug administration) for routine clinical use as first line therapy. Some are described below. Many targeted drugs specifically towards tumor cell are in the pipeline at various stages of preclinical and clinical testing.

### 1.10.1 Bcr-Abl & Imatinib, Dasatinib, Nilotinib

Translocation of a part of the BCR (breakpoint cluster region) gene on Chromosome 22 translocation to ABL (abelson) gene on chromosome 9 results in Philadelphia chromosome. Bcr-Abl is a tyrosine kinase that has constitutive activity in myeloid cells and drives continuous abnormal proliferation (Figure 24). Novartis developed Imatinib, which can selectively bind to Bcr-Abl to inhibit its activity in CML (chronic myelogenous leukemia) cells. Imatinib induced 98% hematological response, 65% cytogenetic response, and complete response in 50% of patients (**Kantarjian et al., 2002**). Imatinib is under the routine use for the first line treatment of CML patients. Imatinib is the first generation drug that gained much attention in the context of targeted therapy.

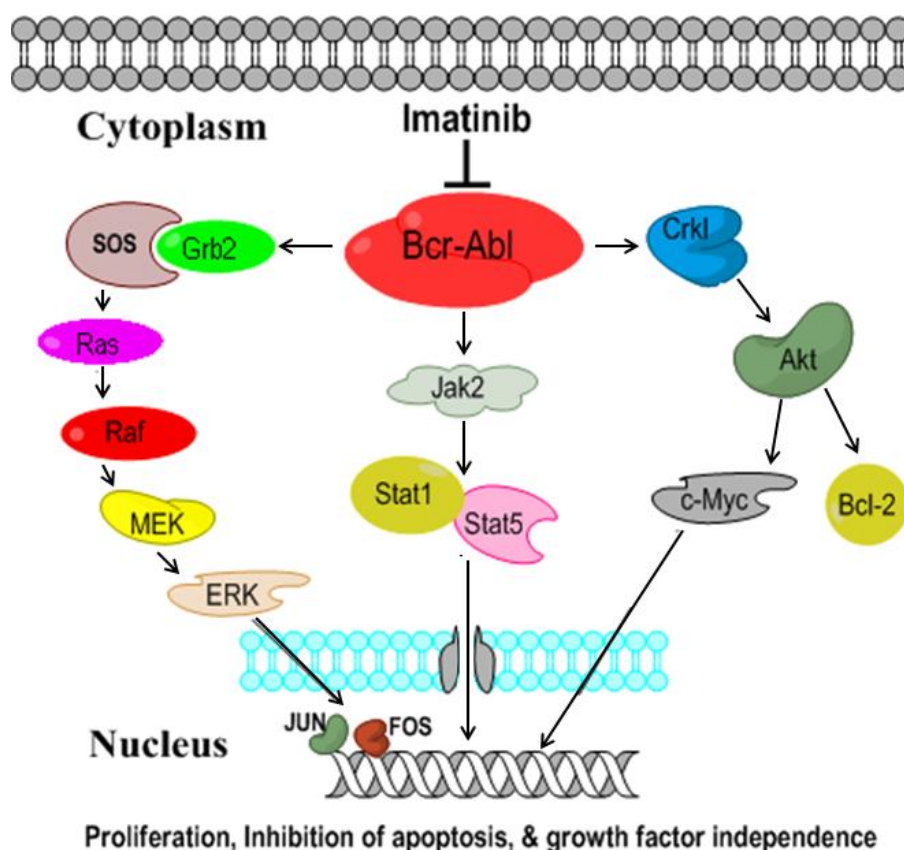


**Figure 24.** Pathways activated by Bcr-Abl fusion protein (All pathways were drawn using ChemDraw software)

Dasatinib and nilotinib are second generation Bcr-Abl inhibitors that are particularly effective in patients resistant to imatinib and in patients who did not tolerate the imatinib. Dasatinib is highly specific and ultra potent (325 times lower IC50 value (inhibitory concentration)) compared to imatinib (**Abbott 2012**). In Phase II study, dasatinib was able to induce complete cytogenetic response in 53% of patients and major molecular response in

47% patients. After 2 years the overall survival rate was 94%. Nilotinib has also been shown to be particularly effective in patients who cannot tolerate or are resistant to imatinib. 55% of patients achieved a confirmed cytogenetic response and 31% displayed complete hematological response (**Ie Coutre et al., 2011**). Overall survival and progression free survival rates were 70% and 33% respectively. Both dasatinib and nilotinib were shown to have favorable safety profiles and can induce long-term survival rates in relapsed CML patients.

### 1.10.2 B-Raf (V600E) & PLX4032

B-Raf kinase (rapidly accelerated fibrosarcoma) is a proto-oncogene and is mainly involved in cell proliferation signaling. 40-60% of melanoma patients harbor V600E B-Raf mutations, which makes B-Raf downstream MAP kinase (mitogen-activated protein) pathway continuously active (Figure 25). Malignant melanoma is very aggressive and significant benefits from conventional drugs were not achieved. PLX4032 is an inhibitor specific to mutated B-Raf, but not to cells containing wild type B-Raf. 81% of patients with B-Raf mutation showed complete or partial tumor regression (**Flaherty et al., 2010**). Toxicities observed were less severe and dose proportional. PLX4032 has been approved by FDA for the treatment of late stage melanoma, and on February 20, 2012 it was approved by the European commission.

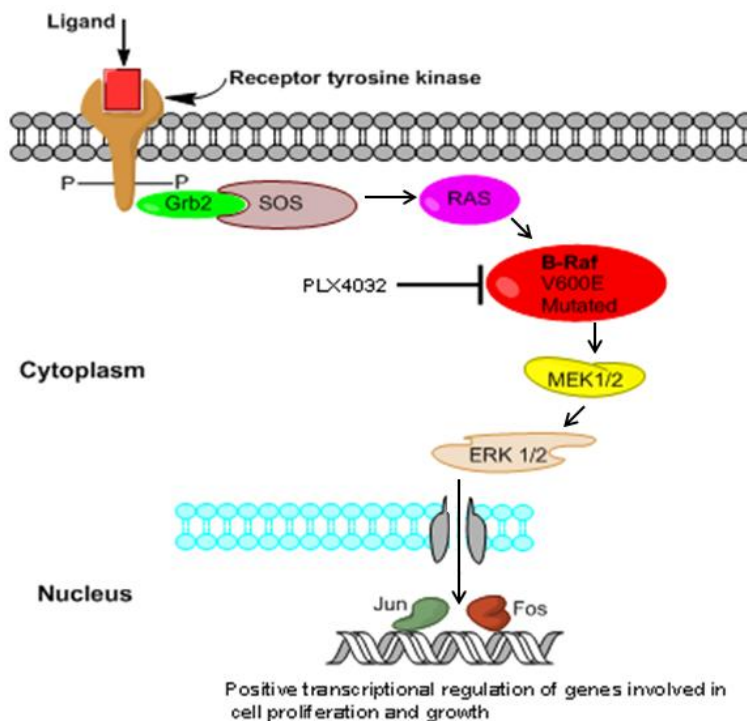


**Figure 25.** Mutated B-Raf constitutively activates MAP kinase pathway

### 1.10.3 EGFR & Gefitinib, Erlotinib

EGFR (epidermal growth factor receptor) overexpression and mutations have been described in many advanced non-small cell lung cancers and breast cancers. These events lead to abnormal activation of Ras signaling cascade, which induces uncontrolled cell proliferation (Figure 26). Hence targeting EGFR in those patients provides significant

therapeutic window and therapeutic index. Gefitinib is an orally available highly specific inhibitor of EGFR. Particularly patients with EGFR mutations were highly sensitive to Gefitinib. Patients showed significant longer progression-free disease (10.4 months) compared to conventional chemotherapy (5.5 months). One year progression-free survival was 42.1% and 3.2% in targeted and conventional chemotherapies respectively (**Maemondo et al., 2010**). Overall objective response rate was significantly higher in Gefitinib group (73.7%) compared to chemotherapy group (30.7%). Gefitinib has become a routine targeted first line therapy for EGFR mutated cancer patients.

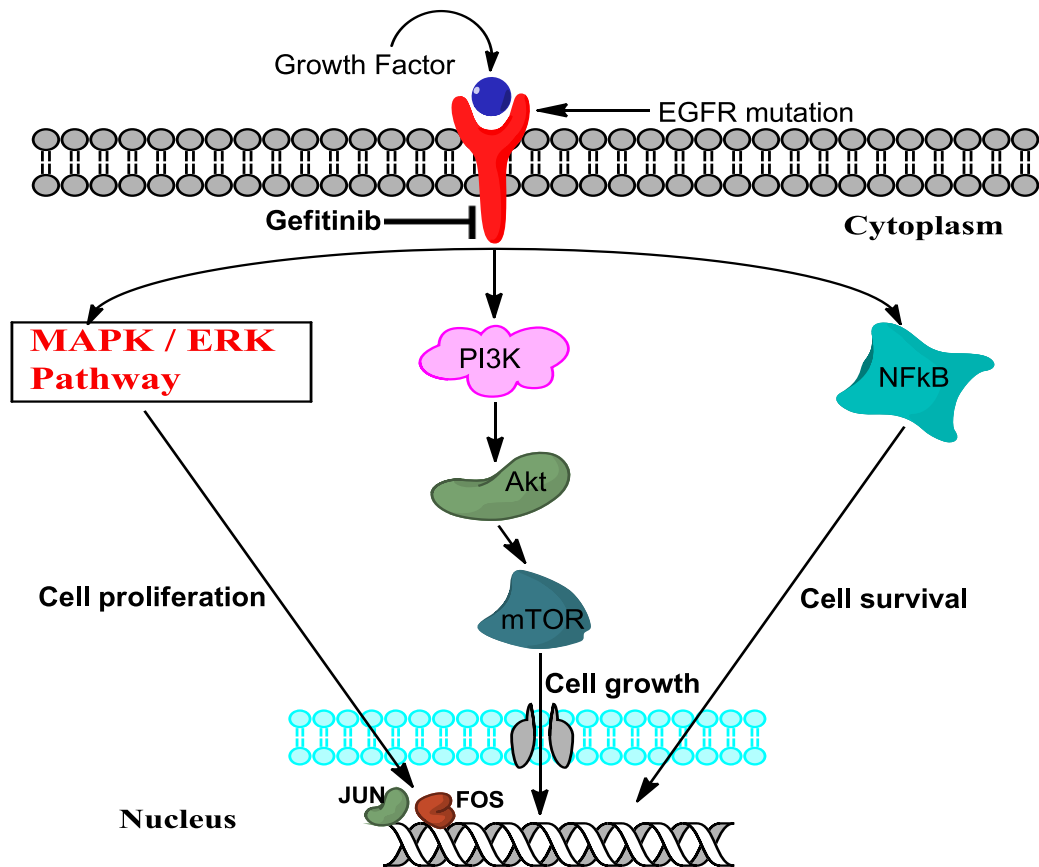


**Figure 26.** Mutated EGFR constitutively activates several oncogenic pathways

Erlotinib is another FDA approved EGFR inhibitor, currently in clinical use for the treatment of non-small cell lung cancer and pancreatic cancer. Erlotinib particularly benefits patients who relapsed to first line platinum based therapy. In one Phase III study 731 patients were randomly assigned either to erlotinib group (488) or placebo group (243) (**Shepherd et al., 2005**). In the erlotinib group complete and partial response rates were 0.7% and 8.2 %, respectively. In placebo group, the rate of partial response was <1%. 45% disease control rate was achieved after erlotinib treatment. In the same the association of EGFR expression (10% of tumor cells) with responsiveness to erlotinib was reported.



#### 1.10.4 EGFR/HER2 & Lapatinib, Herceptin

HER2 (human epidermal growth factor receptor) and EGFR (HER1) are receptor tyrosine kinases, whose overexpression and constitutive activation leads to transformation. EGFR and HER2 oncogenic signaling pathways partly overlap. Many breast cancers are described as HER2 positive and also HER1 to a lesser extent. These are proto-oncogenes primarily involved in cell survival, proliferation and transformation (Figure 27). Inhibition of both kinases would be advantageous; otherwise the EGFR activity may potentially bypass the need for HER2 inhibition to kill the tumor cells. Lapatinib is a dual EGFR and HER2 inhibitor which is very effective in HER2 positive breast cancers. In Phase Ib clinical study, 12 patients overexpressing either EGFR or HER2 achieved stable disease upon Lapatinib administration (**Burris 2004**). Lapatinib was also very effective in trastuzumab refractory breast cancer patients. It was well tolerated at all doses employed in Phase I study. Lapatinib is currently used as front line therapy in Triple positive breast cancers (ER+/EGFR+/HER2+). ER+ is an abbreviated form of estrogen receptor.

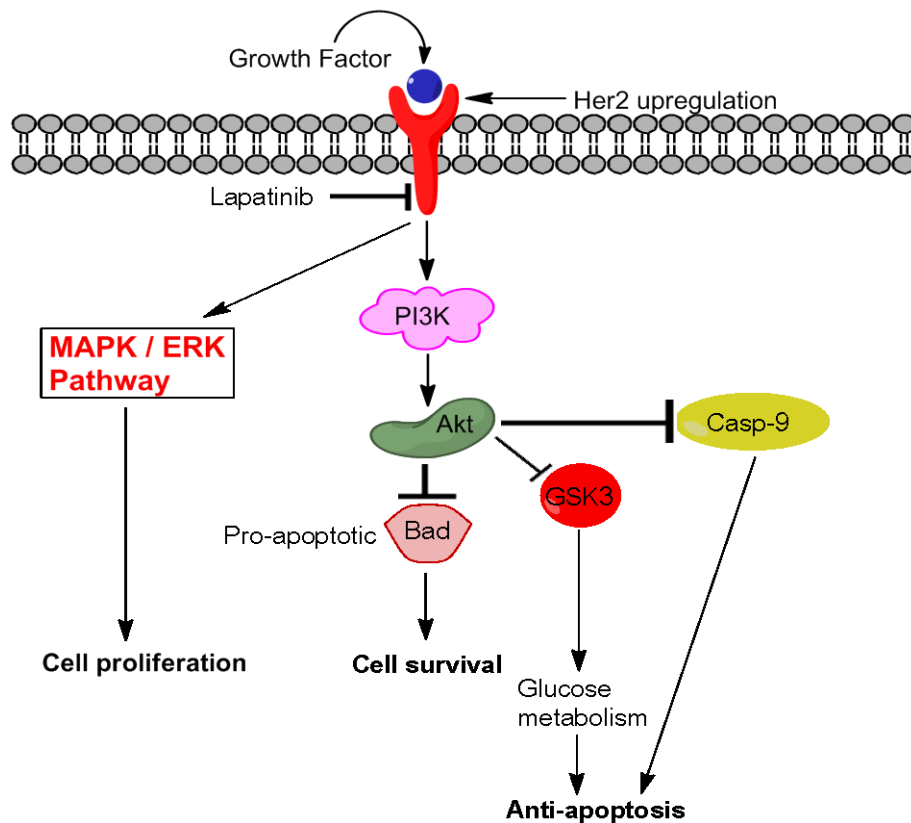


**Figure 27.** Overexpression of HER2 leads to activation of MAP kinase and PI3K pathways

HER2, which is a growth factor receptor, is amplified in approximately 25% to 35% in breast cancers. Overexpression of HER2 activates MAPK, PI3K/Akt (phosphoinositide 3-kinase/ v-akt murine thymoma viral oncogene homolog), and protein kinase C pathways, which promotes cell proliferation and inhibits apoptosis (**Vogel et al., 2002**). HER2 also regulates adhesion, migration, differentiation, and other cellular responses. Hence blocking the activity of HER2 is essential to slow down the progression of cancer and to improve the survival rates. Herceptin (Trastuzumab), which was discovered and developed by Genentech, is under routine clinical use. Herceptin is a monoclonal antibody that interferes with HER2

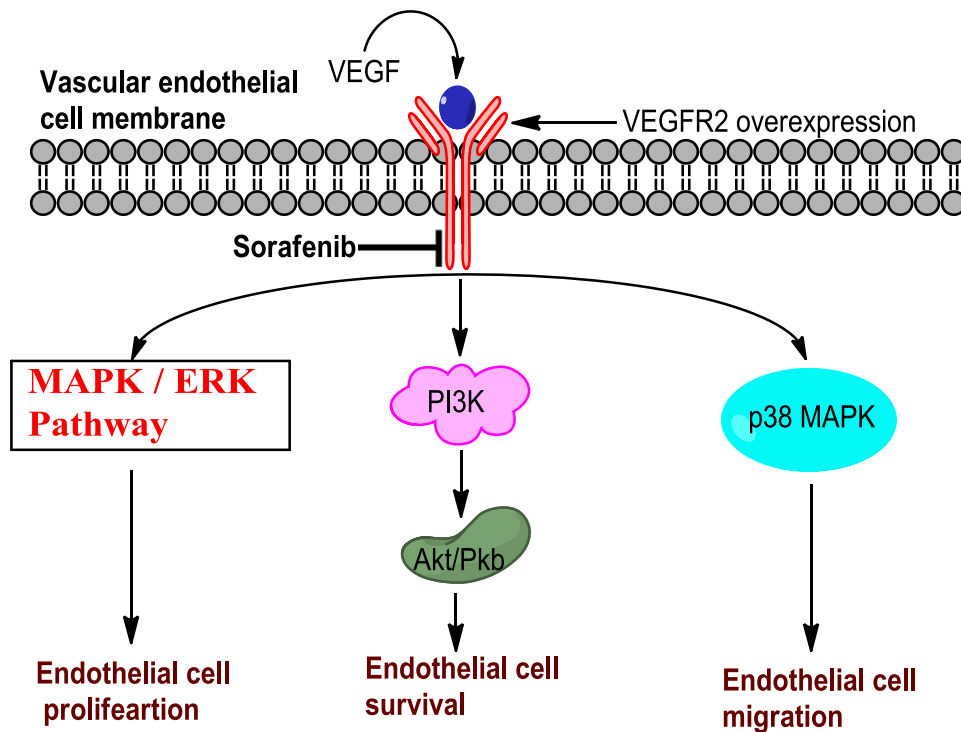
receptor. In Phase I clinical study, investigators enrolled 114 metastatic breast cancer patients with 2+ and 3+ (IHC: Immunohistochemistry) HER2 expression. They reported 7 complete and 23 partial responses, for an objective response rate of 26%. 13 patients displayed minor response or stable disease for longer than 6 months for a clinical benefit rate of 38%. Profound responses were reported in patients overexpressing HER2 at 3+ levels. 57% of patients who responded to herceptin displayed disease free progression for 12 months or more (Vogel et al., 2002).

#### **1.10.5 VEGFR/PDGFR/Raf/c-KIT & Sorafenib, Sunitinib**

Loss of Von-Hippel Lindau gene is the main driving event in clear-cell renal-cell carcinoma. The downstream molecular effects of the loss of this gene include accumulation of VEGF (vascular endothelial growth factor) and PDGF (platelet-derived growth factor), resulting in increased angiogenesis and blood vessel density. Hence targeting selectively VEGFR (vascular endothelial growth factor receptor) and PDGFR (platelet-derived growth factor receptor) provides robust rationale for renal-cell carcinoma (Figure 28). 5.5 months median progression-free survival was achieved in Sorafenib treated group compared to 2.8 months in placebo group (Escudier et al., 2007). Of 335 patients in Sorafenib group 7 patients achieved partial response, 261 patients achieved stable disease, and 29 patients did not respond. In further studies one patient had a complete response and increase number of stable diseases compared to placebo (Escudier et al., 2007).

VEGF and Raf-1 have been implicated in the transformation of hepatocellular carcinoma. As Sorafenib inhibits the activity of Raf-1, its activity was tested in hepatocellular cancers. Patients who have undergone treatment have 3 months survival benefit compared to placebo and this advantage has not reported with conventional chemotherapy (Llovet et al., 2008). Activated c-KIT (proto-oncogene tyrosine-protein kinase KIT) mutations are common in some cancers including GIST (gastrointestinal stromal cancer) and thymic cancers. A 47 year old patient with relapsed thymic cancer (c-KIT exon 11 deletion mutation amplification) benefited significantly from Sorafenib treatment (Disel et al., 2011). After 12 weeks, tumor size reduced to 50% and pleural nodules disappeared. Currently Sorafenib is used as front line therapy in cancer patients with above mentioned molecular defects.

Sunitinib discovered and developed by Pfizer is also a VEGFR2 and PDGFR inhibitor. It also cross-reacts with FLT-3 (fms-related tyrosine kinase) and c-KIT. Sunitinib is under routine clinical use as a first line therapy in patients with renal cell carcinoma and gastrointestinal cancers. In 2009 an expanded-access trial efficacy results from 4564 metastatic renal cell carcinoma patients world-wide were reported. Results were evaluated in 3464 patients (Gore et al., 2009). Objective response rates were achieved in 17% of patients and median progression-free survival was 10.9 months. Overall survival rate was 18.4 months.

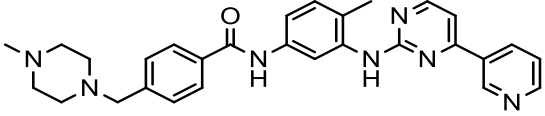
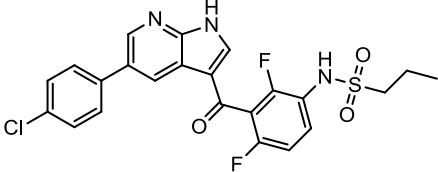
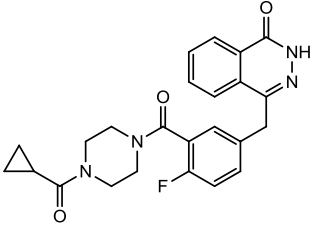
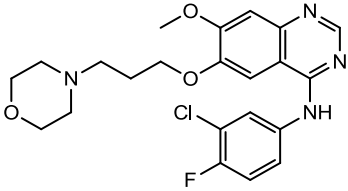
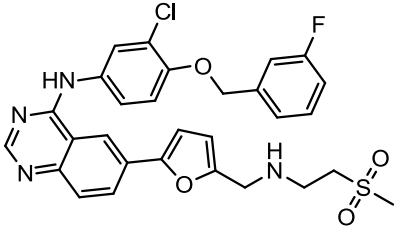
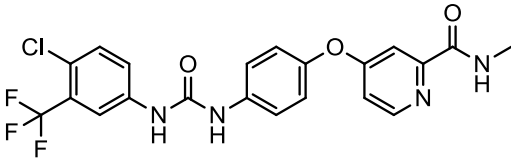


**Figure 28.** Overexpression of VEGFR2 leads to endothelial cell proliferation, survival, and migration, which aids in de-regulated angiogenesis

### 1.10.6 ALK & Crizotinib

Crizotinib discovered and developed by Pfizer has been recently approved by FDA for treatment of NSCLC (non-small cell lung cancer) patients. Crizotinib inhibits both mutated ALK receptor tyrosine kinase (anaplastic lymphoma kinase) and aberrantly activated oncogenic EML4-ALK fusion (echinoderm microtubule-associated protein-like 4) product, which is a consequence of chromosomal rearrangements. Activating mutations or fused product activates signaling pathways involved in proliferation and cell growth. Crizotinib has also been shown to inhibit c-MET (hepatocyte growth factor receptor). Abnormal activation of ALK has also been reported in anaplastic large-cell lymphoma and neuroblastoma. In one Phase I study, crizotinib showed highly significant antitumor activity in ALK positive NSCLC patients. Out of total 119 evaluable patients, objective response rate was 61% and clinical benefit rate was reported as 88%. Preliminary median progression-free survival was reported as 10 months. One patient with ALK rearranged inflammatory myofibroblastic tumor showed substantial response (**Camidge et al., 2011**).

**Table 3: Structures of selected targeted drugs and therapeutic uses**

Company & Structure	Comments
<p><b>Imatinib</b> - Novartis</p> 	<p>Approved for routine clinical use. Front line monotherapy in CML and GIST patients.</p>
<p><b>PLX4032</b> - Plexxikon &amp; Genentech</p> 	<p>Currently undergoing Phase III clinical studies. Its routine clinical use in advanced melanoma patients with V600E B-Raf mutation is anticipated.</p>
<p><b>Olaparib</b> - AstraZeneca</p> 	<p>Currently undergoing Phase II clinical studies. High possibility of its routine use in cancers with BRCA (breast cancer gene) mutations.</p>
<p><b>Gefitinib</b> - AstraZeneca &amp; Teva</p> 	<p>Under regular clinical use. Front line therapy in cancers with EGFR mutations.</p>
<p><b>Lapatinib</b> - GlaxoSmithKline</p> 	<p>Front line therapy in HER2 positive breast cancers.</p>
<p><b>Sorafenib</b> - Bayer</p> 	<p>Front line therapy in advanced renal cell carcinoma and hepatocellular cancers.</p>

## 1.11 Investigational Targeted Drugs

Vigorous research on the identification of targets involved in initiation and progression of cancer led to the marketing of several targeted drugs. In addition to the above, several targeted drugs are in clinical trials and some are still in preclinical studies. Below we describe few drugs, which have potential for FDA approval and routine clinical use.

### 1.11.1 PARP & Olaparib

BRCA1 (breast cancer 1, early onset) and BRCA2 (breast cancer 2, early onset) mutations are the most common causes of ovarian and breast cancers. These genes are mainly involved in double strand DNA break repair mechanisms. In the absence of BRCA1 and BRCA2 functions, PARP1 (poly ADP ribose polymerase) can complement their functions; otherwise PARP mainly participates in single strand DNA repair. Inhibition of PARP with small molecule drugs leads to synthetic lethality (Figure 29). Toxicities are less severe; as normal cells containing wild type BRCA has at least one intact DNA repair pathways. Olaparib, which is a highly specific PARP1 inhibitor, was active only on BRCA mutated tumors. Six patients with BRCA mutation showed 50% reduction of tumor upon Olaparib treatment (Fong et al., 2009). One patient with BRCA1 mutation showed complete regression of peritoneal tumor nodule. Eight patients with advanced ovarian cancer showed partial response. Effect of Olaparib was not noticed in patient with wild type BRCA. Olaparib was shown to be effective in prostate cancers carrying BRCA2 mutations (Fong et al., 2009).

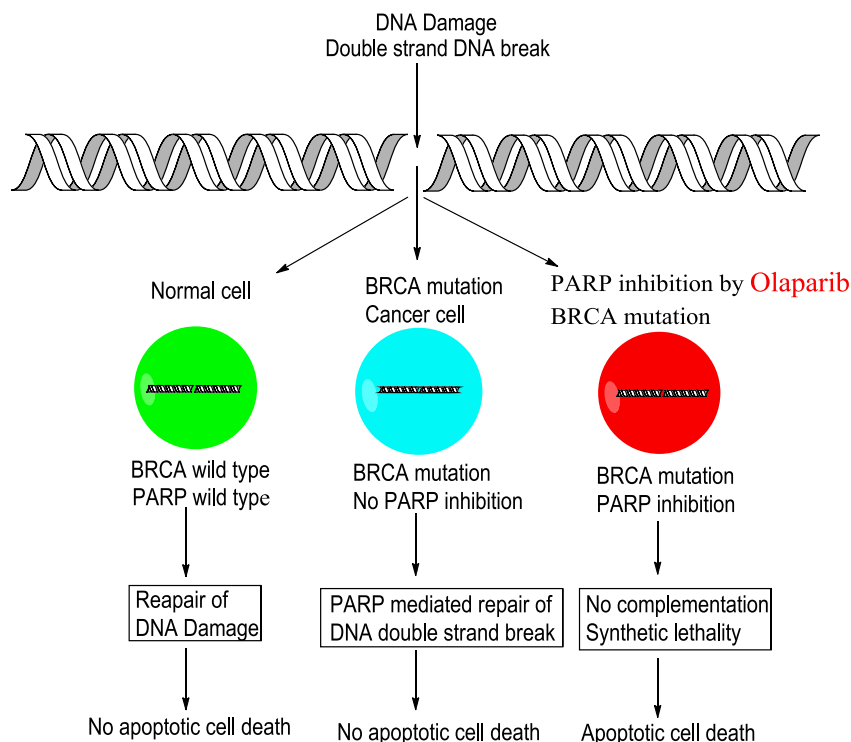


**Figure 29.** Schematic diagram showing synthetic lethality of Olaparib

### 1.11.2 c-Met & Foretinib (GSK1363089, XL880)

Foretinib discovered by Exelixis (being developed by GlaxoSmithKline) is an investigational drug that inhibits c-MET. It has also been shown to inhibit VEGFR2. Currently it is being evaluated in Phase II trials in patients with advanced solid cancers. Overexpression of MET and specific mutations activates tumor growth and angiogenesis and also promotes metastasis. It has also been implicated in several signaling pathways including K-Ras (v-Ki-ras2 Kirsten rat sarcoma viral oncogene homolog), PI3K, STAT (signal transducer and activator of transcription),  $\beta$ -catenin, and NOTCH. Deregulated expression of MET has been reported in several cancers including kidney, thyroid, liver, breast, and stomach. Recently a Phase I efficacy data of foretinib has been reported. 40 patients (8 cohorts) with advanced solid cancers were enrolled for treatment. Out of 40 patients, 3 patients achieved partial response and in these patients the duration of response lasted for 10-12 months. 22 patients displayed stable diseases which lasted for 1-10 months (**Eder et al., 2010**). Some Phase II studies were already completed and few are underway for foretinib

## 2. AIMS OF THE STUDY

To identify and understand potential resistance mechanisms towards Aurora kinase inhibitors, CYC116 and ZM447439, the following objectives were formulated. As mentioned earlier we used two cell line and two Aurora kinase inhibitors to generate and select resistant clones.

The study objectives can be classified into two sections, first section includes characterization studies, and the second includes identification of resistance mechanisms.

### A. Characterization Studies

- To establish drug resistant HCT116 and HCT116 p53-/- clones towards CYC116 and ZM447439
- Confirmation of resistance to selecting agents by cell proliferation assay
- Verification of cross-resistance to other well known Aurora kinases inhibitors
- Verification of multidrug resistance phenotype to approved anticancer agents
- Determination of Aurora kinase inhibition responsive biomarkers

### B. Identification of Resistance Mechanisms

- Analysis of cell cycle to examine the ploidy of cell lines
- Expression of Aurora kinases
- DNA sequencing of Aurora A, B, and C – Detection of drug target mutations
- Global microarray gene expression studies (CYC116-induced resistance signature)
- Validation of candidate genes expression from microarray data using qRT-PCR (quantitative reverse transcriptase-polymerase chain reaction)
- Comparison of CYC116 clones gene expression profiles in CYC116 resistant primary tumors
- Reversal of resistance

Apart from the main experimental part which formed the basis for thesis, we also comprehensively reviewed and published:

- Aurora kinase biology in relation to cancer (**section 3.2**)
- Preclinical and clinical Aurora kinase inhibitors status and their future (**section 3.3**)

### 3. EXPERIMENTAL PART AND SURVEY OF THE RESULTS

#### 3.1 Thesis Background

##### 3.1.1 Resistance mechanisms towards Aurora kinase inhibitors (section 3.4)

CYC116 is a novel pan-Aurora kinase and VEGFR2 inhibitor, which has been discovered and developed by Cyclacel Ltd. In preclinical studies it displayed broad anticancer activity and it has been evaluated in a Phase I clinical study. Emergence of drug resistance towards CYC116 as well as other Aurora kinase inhibitors in the clinic is possible.

Our work was focused on identification and characterization of potential cancer cell resistance mechanisms towards CYC116, alongside with ZM447439, an experimental Aurora kinase inhibitor. We chose HCT116 p53 proficient (p53+/+) and p53 deficient (p53-/-) colorectal cancer isogenic cell line pairs to identify and characterize CYC116 and ZM447439 induced resistance mechanisms. The main reasons to select these isogenic cell pairs include: Firstly, the Aurora kinases were shown to overexpress consistently in colorectal cancers (**Bischoff et al., 1998, Katayama et al., 2009**), Secondly, to delineate CYC116 induced resistance mechanisms in the presence or absence of p53, Thirdly, HCT116 cancer cell line is genetically deficient in recombinational DNA repair, hence they are prone to frequent DNA mutations. These cells lines are good models to identify drug induced Aurora mutations. In these cell lines mutations were expected to be induced rapidly. We also questioned ourselves whether the induced mutations are different based on p53 status. Also to determine expression levels of drug transporters in CYC116 and ZM447439 resistant cells in the presence or absence of p53. Lastly, cancer cells without p53 tend to become chromosomally unstable, hence to determine cell cycle profiles and ploidy status in the presence or absence of p53 in drug resistance cells; we took advantage of these isogenic cell line pairs.

We generated several HCT116 resistant clones on both p53+/+ and -/- backgrounds by exposing cells to cytotoxic concentrations of CYC116 and ZM447439. HCT116:CYC116, HCT116p53-/-:CYC116, HCT116:ZM447439, HCT116p53-/-:ZM447439 clones were 9 to 82 folds, 36 to 64 folds, 18 to >83 folds and 33 to 39 folds more resistant to selecting agents, respectively. Resistant clones also displayed cross-resistance to other clinical Aurora kinase inhibitors and multidrug resistance to some anticancer agents tested. CYC116 clones, but not ZM447439 acquired polyploidy during the selection. Aurora B phosphorylates serine 10 residue of histone H3. Inhibition of Aurora B, suppress histone H3 phosphorylation (ser10). Hence histone H3 phosphorylation is a conventional marker to follow Aurora kinase inhibitors specificity. CYC116 and ZM447439 inhibited histone H3 phosphorylation in parent sensitive cells lines; however phosphorylation was not inhibited in all resistant clones, indicating that Aurora B is catalytically active in the presence of its inhibitors. As expected, all resistance clones did not show up-regulation of common drug transporters including PgP and MRP1. Also we did not observe significant changes in Aurora kinases expression. ZM447439, but not CYC116 induced three novel mutations in Aurora B, namely I216L, L152S, and N76V. Structural modeling studies revealed that L152S may significantly affect the ZM447439 binding. However CYC116 binding was not affected with the L152S Aurora B mutation also with most of the Aurora B mutations reported previously (**Girdler et al., 2008**).



Pangenomic microarray expression studies revealed that 885, 1085, 224, and 212 number of gene sets were differentially expressed (ANOVA  $p < 0.001$ ) in p53<sup>+/+</sup>:CYC116, p53<sup>-/-</sup>:CYC116, p53<sup>+/+</sup>:ZM447439, and p53<sup>-/-</sup>:ZM447439 groups compared to paternal cell lines, respectively. 28 genes were selected from all groups for qRT-PCR validation studies. Nearly 100% match and significant correlation was observed between the gene expression data and qRT-PCR. 23 most relevant genes were selected from all groups for qRT-PCR validation studies on human primary tumors *in vitro* sensitive/resistant to CYC116. Interestingly, majority of cell line findings were confirmed also on primary human cells, suggesting validity of these genes as biomarkers of drug susceptibility or resistance.

An apoptotic gene Bcl-xL (B-cell lymphoma-extra large) was found to be significantly upregulated in CYC116 resistant clones, particularly in p53<sup>+/+</sup> cells. Knock-down of Bcl-xL using RNAi (RNA interference) technology partially reversed the resistance to CYC116. Moreover, Bcl-xL overexpressing p53<sup>+/+</sup> CYC116 clones were highly sensitive to a synthetic Bcl-xL inhibitor, ABT-263, compared to the parent cells.

Our data cumulatively provide a genetic basis of resistance to Aurora kinase inhibitors, which could be used to predict clinical response and also to select patients who might benefit from Aurora kinase inhibition. Moreover, our study suggest a role of Bcl-2 protein family inhibitors for reversal of drug resistance against Aurora kinase inhibitors and their possible significance for therapy of tumors primarily or secondary resistant to these drugs.

### **3.1.2 Proteome analysis of CYC116 and ZM447439 resistant clones (section 3.5)**

This original work was mainly focused on identification and characterization of resistant clones towards Aurora kinase inhibitors. To identify resistance mechanisms we did DNA sequencing of drug targets and global gene expression profiles and validation by qRT-PCR. Based on the gene expression profiles and qRT-PCR studies we selected Bcl-xL overexpression at protein level. Overexpression of Bcl-xL at transcriptional level corresponded to its upregulation at protein level. This is the only minor protein analysis we conducted. To determine most abundant differentially regulated proteins we performed proteomics study in collaboration with Dr. Hana Kovarova, Institute of Animal Physiology and Genetics, AS CR, v.v.i., Laboratory of Biochemistry and Molecular Biology of Germ Cells, Libechov, and Institute of Microbiology, AS CR., v.v.i., Laboratory of Molecular Structure Characterization, Prague.

All protein samples for proteomic study were prepared at the Institute of Molecular and Translational Medicine, Palacky University, Olomouc, under the guidance of Dr. Marian Hajduch. Proteome analysis and identification of differentially regulated proteins were performed at the above mentioned institutes.

The key findings of this proteomics study include:

- Majority of proteins identified as differentially expressed were involved in metabolic processes which may reflect general response of cells to toxicity. Combining clones with the same phenotype has led to the elimination of proteins expressed differently as a result of sporadic response to anti-cancer treatment.

- CYC116 caused a more specific and amplified response in resistant cells. Unlike ZM447439, CYC116 resistant cells expressed 5 proteins differently regardless of p53. Hence, we hypothesize that colon cancer cells resort to different mechanisms in order to resist cell death induced by CYC116 and ZM447439.
- Elongation factor 2 was the only protein regulated specifically in all p53<sup>+/+</sup> cells resistant to both AURK inhibitors. p53 might regulate translation in HCT116 cells and contribute to the development of resistance to Aurora kinase inhibitors by preventing translation of proteins required for apoptosis.
- Resistant cells with loss of p53 were characterized by differential expression of lysozyme C, a protein known to protect cells against oxidative stress. Therefore, such protective mechanism may contribute to resistance to AURK inhibitors in p53 null cells. The second protein specifically regulated in all p53<sup>-/-</sup> resistant cells was 78 kDa glucose-regulated protein which can also prevent cancer cells from oxidative stress. Moreover this protein has also anti-apoptotic effects.
- Serine hydroxymethyltransferase reversibly catalyses the conversion of serine into glycine while hydroxymethyl group is transferred to tetrahydrofolate which is the sole precursor of purine biosynthesis. The verified up-regulation of this enzyme in all clones resistant to CYC116 suggests that despite the treatment, the enzyme is expressed by cancer cells and promote DNA replication, an important step in cell division. We also found extremely high level of serpin B5 in most resistant cells. Instead of promoting proliferation, serpin B5 most likely prevent cancer cells from apoptosis as previously reported in colorectal cancer. With regard to the revealed overexpression of serine hydroxymethyltransferase and serpin B5 in cancer cells of different histogenetic origin resistant to diverse drugs with no apparent impact of p53, we propose these proteins as target molecules that may resolve the problem of drug resistance to cancer therapy.
- Our finding also indicated substantial overexpression of other proteins involved in controlling apoptosis, such as calretinin and voltage-dependent anion-selective channel protein 2. These proteins might promote tumour survival by regulating mitochondrial membrane permeability and by calcium buffering which are critical processes of apoptosis. Hence, we propose these proteins as target molecules for therapy of cancer patients with solid tumours.

Taking into consideration that serpin B5 and calretinin were up-regulated with the highest fold-changes in almost all resistant cells used in this study, they ultimately represent the most promising molecules for cancer therapy monitoring.

## AURORA KINASES: STRUCTURE, FUNCTIONS AND THEIR ASSOCIATION WITH CANCER

Madhu Kollareddy<sup>a</sup>, Petr Dzubak<sup>a</sup>, Daniella Zheleva<sup>b</sup>, Marian Hajduch<sup>a\*</sup>

<sup>a</sup> Laboratory of Experimental Medicine, Department of Pediatrics, Faculty of Medicine, Palacky University, Puskinova 6, 775 20 Olomouc, Czech Republic

<sup>b</sup> Cyclacel Pharmaceuticals, Inc. Dundee Technopole, James Lindsay Place, Dundee, Scotland, UK, DD1 5JJ  
 e-mail: hajduchm@gmail.com

Received: November 30, 2007; Accepted: January 18, 2008

Key words: Aurora kinases/Serine/threonine/Spindle/Centrosomes/Cytoskeleton/Cytokinesis/Oncogenes

**Background:** Aurora kinases are a recently discovered family of kinases (A, B & C) consisting of highly conserved serine/threonine protein kinases found to be involved in multiple mitotic events: regulation of spindle assembly checkpoint pathway, function of centrosomes and cytoskeleton, and cytokinesis. Aberrant expression of Aurora kinases may lead to cancer. For this reason the Aurora kinases are potential targets in the treatment of cancer. In this review we discuss the biology of these kinases: structure, function, regulation and association with cancer.

**Methods and Results:** A literature search.

**Conclusion:** Many of the multiple functions of mitosis are mediated by the Aurora kinases. Their aberrant expression can lead to the deregulation of cell division and cancer. For this reason, the Aurora kinases are currently one of the most interesting targets for cancer therapy. Some Aurora kinase inhibitors in the clinic have proven effectively on a wide range of tumor types. The clinical data are very encouraging and promising for development of novel class of structurally different Aurora kinase inhibitors. Hopefully the Aurora kinases will be potentially useful in drug targeted cancer treatment.

### INTRODUCTION

#### *Aurora Kinases and the Cell Cycle*

The Cell cycle is an ordered set of events, culminating in cell growth and division into two daughter cells. The segregation of genetic material into two exact halves is the hallmark of cell division. The chromosomal DNA is replicated during S phase (DNA synthesis). The G1 phase or first gap phase is the interval between mitosis and DNA replication. The G2 phase or second gap phase is the interval between completion of DNA replication and mitosis. Mitosis is divided into five distinct stages (prophase, prometaphase, metaphase, anaphase and telophase) and the end of mitosis, two daughter cells are formed from one parent cell by cytokinesis. In brief, prophase begins after the transition from G2 to mitosis and chromosome condensation and disassembly of the nuclear envelope are key events. Attachment of chromosome kinetochores to microtubules and the assembly of chromosomes at the center of the cell to form the metaphase plate are the main events in prometaphase and metaphase respectively. Sister chromatids move to opposite pole and the poles move apart during anaphase. During telophase, the chromosomes recondense and the nuclear envelop reforms around genetic material. The most dramatic change in cellular structure at this time is constriction of the cleavage furrow and subsequent cytokinesis (Fig. 1).

These strict molecular events taking place in strict order during the cell cycle is responsible for reliable cell division to produce two daughter cells as precise copies of the parent cell. Biochemical points termed checkpoints,

control transitions in the cell cycle to ensure the fidelity and progression into following stage. Mutations or over expression of the genes involved in these checkpoints can cause cancer. Such genes are called oncogenes. The first checkpoint occurs at the end of G1 phase and before S phase, called G1 checkpoint or restriction checkpoint. The second checkpoint occurring at the end of G2 phase and before mitotic phase is called the G2 checkpoint. Apart from these two checkpoints one more stage called

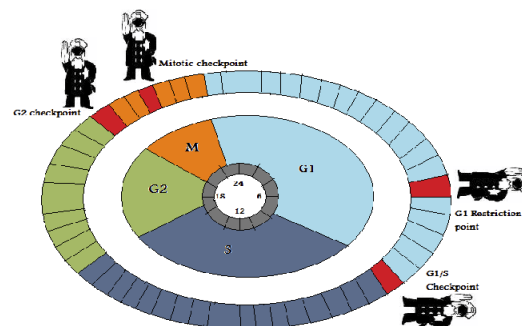


**Fig. 1.** Schematic cell cycle diagram showing phases of cell cycle and checkpoints. G1, S, G2, & M phase are represented by different colors. Red boxes represent the checkpoints at each phase of the cell cycle. At each checkpoint stop signal exist represented by policeman, to prevent uncontrolled cell division.

anaphase checkpoint occur during metaphase and checks for proper alignment of metaphase chromosomes, which should be in a state of bipolar tension. Checkpoints involve orderly synthesis, activation, degradation, phosphorylation and dephosphorylation of different proteins involved in cell cycle (Fig. 1).

The Aurora kinases are importantly involved in cell cycle and they exhibit most of their known functions in mitosis. They are involved in some checkpoint regulation pathways including spindle assembly checkpoint, alignment of metaphase chromosomes and chromosomal bi-orientation. Aberrant expression of Aurora kinases may disturb checkpoint functions particularly in mitosis and this may lead to genetic instability and trigger the development of tumors. Aurora kinases have gained much attention since they were identified as bona fide oncogenes.

### Structure

Aurora kinases, divided into A, B, and C have an amino acid sequence length ranging from 309-403 (ref.<sup>1</sup>). They have N-terminal domain (39-129), a protein kinase domain and C-terminal domain (15-20) (Fig. 2). Aurora A and B share 71% identity in their C-terminal catalytic domain<sup>2</sup>. The high percentage of conservation is very important in relation to the specificity of substrates and inhibitors. The mean proportion of similar amino acids estimated by pair-wise sequence comparisons is significantly higher among different families of Aurora A, B and C in vertebrates ( $0.84 \pm 0.5$ ) than within the same family (Aurora A or B) in vertebrates and invertebrates species ( $0.69 \pm 0.3$  for both). This suggests a recent evolutionary radiation of Aurora families within vertebrates<sup>3</sup>. Structural and motif based comparison suggested an early divergence of Aurora A from Aurora B and Aurora C (ref.<sup>4</sup>). Aurora A, B, & C have been mapped on chromosomes 20q13.2, 17p13.1, and 10q13 respectively<sup>5-7</sup>.

Aurora kinases show little variability in their amino acid sequence and this is very important for interaction with different substrates specific for each Aurora kinase and for their different subcellular localizations<sup>8</sup>. ATP binding active site in all Aurora kinases are lined by 26 residues

and three variants: Leu215, Thr217, R220 are specific to Aurora A. Aurora A, B, and C share identical sequences in their active site<sup>3</sup>.

### Aurora Kinase Geography and Substrates

Aurora kinases are nuclear proteins having different sub cellular locations. Aurora A localizes within the centrosomes from the time of duplication of centrosomes until mitotic exit<sup>2</sup>. Bischoff et al.<sup>5</sup> using indirect immunofluorescence with Aurora A antibodies found the specific localization of Aurora A. Aurora A localizes to centrosomes, spindle poles, spindle from prophase to metaphase but predominantly to the spindle during telophase<sup>5</sup> (Fig. 3). Northern blot analysis has confirmed Aurora A expression in thymus, testis and fetal liver and low expression in bone marrow, lymph node and spleen<sup>5</sup>. Late mitosis or early G1 stage is the degradation point for Aurora A. Aurora B, known as chromosomal passenger protein localizes to kinetochores from prophase to metaphase, in the mid zone during anaphase and eventually to the midbody in cytokinesis<sup>5</sup> (Fig. 3). Northern blot has shown that human Aurora B expression level is high in normal thymus and fetal liver<sup>5</sup>. Aurora C localizes to centrosomes from anaphase to cytokinesis<sup>9</sup>. It is predominantly expressed in testis and isolated from cDNA library<sup>7</sup>.

A number of substrates of Aurora kinases have been reported by several studies. Some substrates activate Aurora kinases, while others are activated by Aurora kinases. The best-known substrate of Aurora A is TPX2. During mitosis Aurora A is activated by autophosphorylation through the interaction with TPX2. Hence TPX2 is considered a substrate and activator of Aurora A (ref.<sup>10</sup>). Other substrates of Aurora A include LIM protein<sup>11</sup>, Eg5 (ref.<sup>12</sup>), CDC25B (ref.<sup>13</sup>), p53 (ref.<sup>14</sup>), and BRCA-1 (ref.<sup>15</sup>). Substrates for Aurora B include histone H3 (Ser10) (ref.<sup>16</sup>), MCAK (ref.<sup>17</sup>), histone H2A (T119) (ref.<sup>18</sup>), Topoisomerase II (ref.<sup>19</sup>), INCENP, survivin<sup>20</sup>, and CENP-A (ref.<sup>21</sup>). The only best-known substrate for Aurora C is INCENP (ref.<sup>22</sup>). Identification of further substrates is important to develop biomarkers for assessing the efficacy of targeted drug cancer treatment.

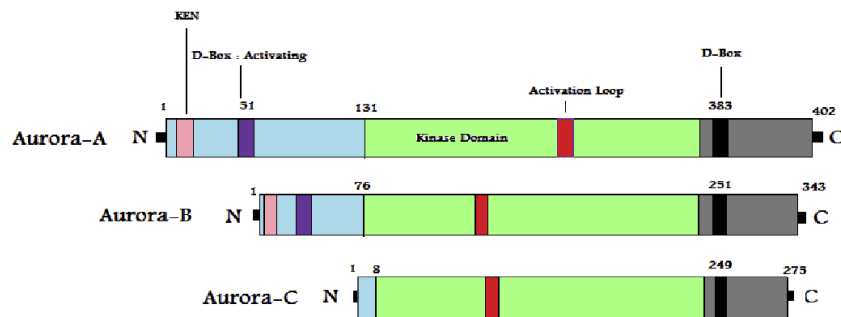


**Fig. 2.** Schematic diagram representing the Aurora A, B, & C kinases domains. N & C terminal domains contain most of the regulatory sequences. The central domain consist of catalytic kinase domain and activation loop. D-Box at the c-terminal domain is the destruction box.

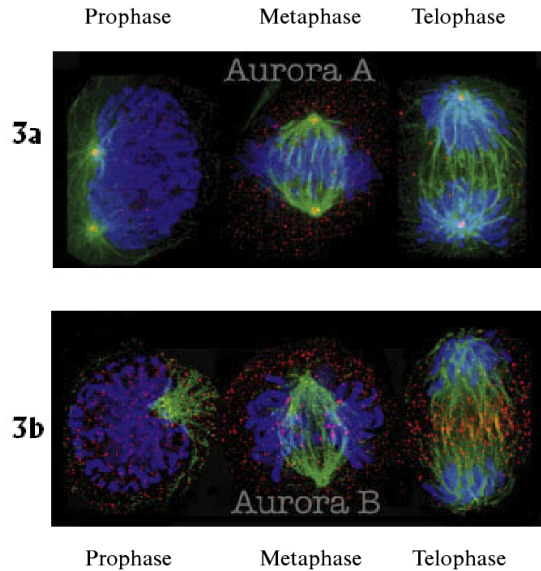


**Fig. 3.** Comparative localization of Aurora A and B. (a) Aurora A in prophase predominantly stained (green) around centrosomes, on the microtubules near spindle poles in metaphase and polar microtubules during anaphase & telophase. (b) Aurora B (red) localized to inner centromere during prophase and metaphase, spindle mid-zone microtubules in anaphase, and subsequently localized to midbody during cytokinesis. (Images taken from the permission of Dr. Andrews, P.D. Home page, University of Dundee)

#### Aurora Kinases Functions

Aurora kinases are involved in multiple functions of mitosis. Aurora A is involved in mitotic entry, separation of centriole pairs, accurate bipolar spindle assembly, and alignment of metaphase chromosomes and completion of cytokinesis<sup>23</sup>. The activity of Aurora A is closely related to centrosomes. It plays a role in bipolar spindle assembly, maturation of duplicated centrosomes by recruiting proteins including D-Tacc<sup>24</sup>,  $\gamma$ -tubulin<sup>25</sup>, SPD-2 (ref.<sup>26</sup>), and centromeric ChToh<sup>27</sup>. Recently role of Aurora A in the promotion of nuclear envelop breakdown has been described<sup>28</sup>. Aurora B is one of the main components of the chromosomal passenger complex, which is a functional mitotic structure. It is involved in chromosomal bi-orientation, regulating kinetochores microtubule association and cytokinesis<sup>29</sup>. Incorrect attachments of sister chromatid kinetochores to microtubules can be resolved by Aurora B<sup>17,30</sup> (Fig. 4). Inhibition of Aurora B by small molecule inhibitor, Hesperadin, significantly increased syntelic attachment, which may lead to genetic instability<sup>30</sup> (Fig. 4). Aurora B is specifically enriched at merotelic attachment sites and is involved in the release of

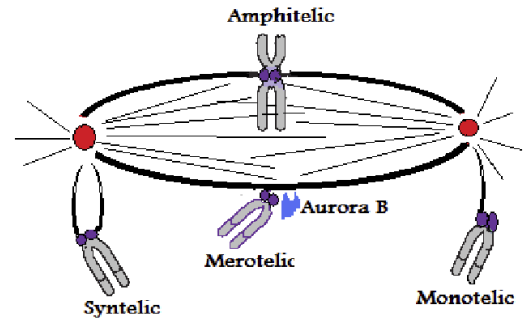


**Fig. 4.** Schematic diagram of centrosomes (red), spindle (microtubule-black lines), various chromosome orientations (gray) or attachments to spindle microtubules, and Aurora B (blue). Amphitelic attachment of sister chromatid kinetochores, where both the kinetochores are attached to opposite poles is the correct attachment (biorientation). Defects in chromosome biorientation leads to monotelic (one kinetochore attached to spindle pole), merotelic (one kinetochore attached to both spindle poles), and Syntelic attachments (both kinetochores attached to same spindle pole). Aurora B is involved in correcting merotelic and syntelic attachments. Aberrant expression of Aurora B compromises chromosomal biorientation (amphitelic) leading to genetic instability (aneuploidy).

improper kinetochore microtubule attachments during chromosomal bi-orientation<sup>17</sup> (Fig. 4). Aurora B phosphorylates histone H3 (Ser 10), which is believed to aid in chromatin condensation and separation<sup>16</sup>. Aurora C exhibits similar functions to those assigned to Aurora B and is required for cytokinesis<sup>22</sup>. Hence Aurora C may be as important a kinase as other kinases in the regulation of various mitotic events.

Recently, the involvement of Aurora B in phosphorylation of centromere-specific histone 2A at T119, which may be crucial for regulation of chromatin structure and function, has been described<sup>18</sup>. Li et al.<sup>22</sup> found that direct association with INCENP activates Aurora C, suggesting the cooperation of Aurora A and B in the regulation of mitotic events. This led to the question, whether Aurora C can fulfill the functions of Aurora B. Indeed, recent publications show that Aurora C can complement the functions of Aurora B. It co-localizes with Aurora B and survivin as a chromosomal passenger protein and is able to rescue polyploidy induced by inactive Aurora B. In summary Aurora C appears to exhibit functions similar to those for Aurora B and is required for cytokinesis<sup>22</sup>.

### Regulation of Aurora Kinases

Phosphorylation, dephosphorylation are the two predominant mechanisms regulating Aurora A activity most of which have been deduced from invertebrates. Generally, phosphorylation of Aurora kinase stimulates kinase activity and three phosphorylation sites in *Xenopus* have been identified by mass spectrometry. Littlepage, L.E. et al. mapped recombinant Aurora A by mass spec sequencing activated by metaphase arrested *Xenopus* eggs extracts<sup>31</sup>. Three phosphorylation sites Ser-53, Thr-295, and Ser-349 were identified. Mutations in Thr-295 and Ser-349 reduced or abolished the activity of Aurora A<sup>31</sup>. Specifically phosphorylation of Thr-295 is required for kinase activation and a protein kinase (PKA) can phosphorylate (Thr-295) and activate the kinase *In vitro*<sup>31</sup>. Mutation in Ser-53 abolished Cdh1 mediated degradation, showing that phosphorylation is involved in the regulation of degradation. PP1 phosphatase negatively regulates Aurora A by dephosphorylating T288 (ref.<sup>32</sup>). In mitosis Aurora A is activated by autophosphorylation through the interaction with TPX2 and could be at least partly due to PP1 antagonism<sup>10</sup>. Kei Honda et al.<sup>33</sup> demonstrated that Aurora A is turned over by APC-ubiquitin-proteasome pathway. Aurora A degradation is mediated by Cdh1 or Fizzy related once the D-box is recognized<sup>34</sup>.

It has also been shown that Chk1 can phosphorylate Aurora B *In vitro*, enhancing the kinase activity to augment spindle checkpoint signalling<sup>35</sup>. To date the best known regulators of Aurora B include Survivin and INCENP. Survivin binds to the catalytic domain of Aurora B and enhances the kinase activity and targeting to its substrates<sup>36</sup>. Lower levels of phosphorylated Histone H3 correlates with the absence of Survivin, confirming that Aurora B activity is enhanced by survivin<sup>36</sup>. Survivin is also involved in the localization of Aurora B to different locations during mitosis. Kie Honda et al. described

activation of Aurora B by C-terminal region of INCENP (ref.<sup>37</sup>). Aurora B is activated upon binding of INCENP resulting in the phosphorylation of the conserved motif of INCENP. These events are critical for full activation of Aurora B/INCENP complex<sup>37</sup>. CENP-A is also involved in the regulation of Aurora B localization to centromeres and spindle midzone<sup>21</sup>. Cdh1 and cdc20 are involved in Aurora B degradation and require intact KEN boxes and A-boxes, which are located within the first 65 amino acids<sup>38</sup>. Levels of Aurora C peak later stages of mitosis after Aurora B. Aurora C is regulated by INCENP like Aurora B, through the C-terminal region. Aurora C may rescue the genetic stability of the cells complementing Aurora B functions in its absence<sup>39</sup>. However regulation of Aurora C is not completely known and further work is needed. Aurora C is predicted to turn over by APC-ubiquitin-proteasome pathway through the recognition of D-box.

### Aurora Kinases and Cancer

Aurora kinases perform important functions during mitosis and hence their aberrant expression can lead to the cell transformations underlying cancer. In many tissues, Aurora kinase over-expression leads to genetic instability (aneuploidy), which may cause cancer. Aneuploidy, a condition where the cells have altered, DNA content may arise from mitotic defects including centrosome duplication, centrosome separation, cytokinesis and chromosomal bi-orientation errors. In all these processes Aurora kinases are involved. Therefore it is tempting to state that the aberrant expression of Aurora kinases may lead to aneuploidy. Hence Aurora genes have been classified as bona fide oncogenes.

Aurora A gene was first named as BTAK (Breast Tumor Activated Kinase), because its mRNA is found to over-expressed in breast tumors and plays a critical role in breast tumor cells transformation<sup>40</sup>. In fact the

**Table 1.** Over-expression or amplification of Aurora kinases in wide variety of tumors types, making them as an attractive targets.

Aurora Kinase	Tumor type	Reference
Aurora A	Breast Cancer	[41]
Aurora A	Human Gliomas	[48]
Aurora A	Ovarian	[41]
Aurora A	Prostrate	[41, 49]
Aurora A	Cervical	[41]
Aurora A	Colon	[41]
Aurora A	Pancreatic	[50]
Aurora A	Lung Cancer	[43]
Aurora B	Colon Cancer	[44]
Aurora B	Thyroid cancer	[45]
Aurora B	Oral	[46]
Aurora B	Non small cell lung carcinoma	[47]
Aurora B	Breast cancer	[42]
Aurora C	Breast cancer	[9]
	Liver cancer	[9]

presence of 20q13 amplicon in breast tumor is a poor prognostic indicator. Two groups independently reported that ectopic over-expression of Aurora A can transform NIHT3 and rat1 cells<sup>5</sup>, which can induce tumors in nude mice. These reports are a break-through and the Aurora kinases came into light attracting more attention than ever before. Zhou et al.<sup>41</sup> performed northern-blot and southern-blot and reported 2.5-8 fold amplification of Aurora A in many cell tumors including breast (BT474, MDA-MB-231), ovarian (2774, SK-OV3), colon (HCT116, HT29, SW480), prostate (DU145, PC3), leukemia (HL60, K562), neural (HTB10) and cervical (SW756). Functional polymorphism due to transitions resulting Phe31Ile has been observed and polymorphism is associated strongly with human colon tumors<sup>42</sup>. Recently similar polymorphisms have been reported in lung cancer predominant in Caucasians<sup>43</sup>. Apart from these tumor types, Aurora A over-expression has been reported in many other tumors (Table 1). Taken together these data, suggest that Aurora A can be characterized as a bona fide oncogene.

Aberrant expression of Aurora B also induces tumor formation and this is not surprising as the kinase is involved in many functions during mitosis. Hence it is logical to classify Aurora B as an oncogene. Katayama et al. performed in situ hybridization, northern and western blot studies from surgically resected colon tumor specimens and reported the over-expression of Aurora B and tumor progression<sup>44</sup>. This significant research stimulated interest in the development of new drugs against Aurora B. Malignant progression of thyroid anaplastic carcinoma cells correlates with the over-expression of Aurora B<sup>45</sup>. Over-expression of Aurora B has also been reported in oral cancer<sup>46</sup> and primary non-small cell lung carcinoma<sup>47</sup>. Aurora B has found to be over-expressed in some other tumor types (Table 1). Aurora C has been found to be over-expressed in some cancer cell lines including HepG2, HUH7, MDA-MB-453 and HeLa. However its correlation with cancer progression is unclear<sup>9</sup>. Hence active research is underway to determine Aurora C as an oncogene.

Based on these reports it is reasonable to classify Aurora kinases as oncogenes. They are not aberrantly expressed in one particular type of tumors only, unlike some other oncogenic kinases. Hence developing potential Aurora kinase inhibitors can target wide range of tumor types. Development of drugs that focus on the Aurora kinases could be promising in the treatment of various cancers. Some Aurora kinases inhibitors have been developed recently and indeed some drugs are in preclinical stage and phase I and phase II clinical trials. Further research on Aurora kinases is required to determine their regulation and their interaction with other partners.

## CONCLUSION

Chromosomal duplication and cell division are very critical, where one copy of each duplicated chromosome segregates to each of two daughter cells. In order to ensure the fidelity of the cell cycle, various proteins

regulate the orderly events at each stage of the cell cycle checkpoints. Mutations or aberrant expression of these proteins involved in the cell cycle regulation may lead to tumorigenesis. The importance of evolutionary conserved Aurora kinases in the regulation of mitotic events came into light recently. They are involved in the regulation of microtubule dynamics, chromosomal segregation, and cytokinesis. These kinases are frequently over-expressed in human tumors resulting in genomic instability. Hence they are clearly implicated in tumorigenesis. Recently Aurora kinases are considered as interesting targets for the development of anticancer drugs. Some Aurora kinases developed recently have proven effective in the clinic on a wide range of tumors. Further understanding the regulation and functions of Aurora kinases deeply, may help to develop potentially useful drugs for targeted cancer treatment.

## ACKNOWLEDGEMENTS

*This work was kindly supported in parts by grants awarded by the Czech Ministry of Education (MSM 6198959216 and LC07017). We are thankful to Dr. Andrews, P.D. University of Dundee for kindly providing Aurora A and Aurora B immunohistochemical images.*

## REFERENCES

1. Bolanos-Garcia M. Aurora Kinases. *Int. J. Biochem. & Cell Biol.* 2004; 37:1572-7.
2. Carmena M, Earnshaw WC. The Cellular Geography of Aurora Kinases. *Nat. Rev. Mol. Cell. Biol.* 2003; 4:842-54.
3. Brown JR, Koretke KK, Birkeland ML, Sanseau P, Patrick DR. Evolutionary relationships of Aurora kinases: Implications for model organism studies and the development of anti-cancer drugs. *BMC Evol. Biol.* 2004; 4:1-10.
4. Cheetam GMT, Knegtel RMA, Coll JT, Renwick SB, Swenson L, Weber P, Lippke, JA, Austen DA. Crystal Structure of Aurora-2, an Oncogenic Serine/Threonine Kinase. *J. Biol. Chem.* 2000; 277:42419-22.
5. Bischoff JR, Anderson L, Zhu Y, Mossie K, Ng L, Souza B, Schryver B, Flanagan P, Clairvoyant F, Ginther C, Chan CS, Novotny M, Slamon DJ, Plowman GD. A Homologue of Drosophila Aurora kinase is Oncogenic and amplified in human colorectal cancers. *EMBO J.* 1998; 17:3052-65.
6. Kimura M, Matsuda Y, Yoshioka T, Sumi N, Okano Y. Identification and characterization of STK12/Aik2: a human gene related to aurora of Drosophila and yeast IPL1. *Cytogenet. Cell Genet.* 1998; 82:147-52.
7. Bernard M, Sanseau P, Henry C, Couturier A, Prigent C. Cloning of STK13, a third human protein kinase related to Drosophila aurora and budding yeast Ipl1 that maps on chromosome 19q13.3-ter. *Genomics* 1998; 53:406-9.
8. Adams RR, Carmena M, Earnshaw WC. Chromosomal passengers and the (aurora) ABCs of mitosis. *Trends Cell Biol.* 2001; 1:49-54.
9. Kimura M, Matsuda Y, Yoshioka T, Okano Y. Cell cycle-dependent expression and centrosome localization of a third human Aurora/Ipl1-related protein kinase, AIK3. *J. Biochem.* 1999; 274:7334-40.
10. Eyers PA, Erikson E, Chen LG, Maller JL. A novel mechanism for activation of the protein kinase Aurora A. *Curr. Biol.* 2003; 13:691-7.

11. Hirota T, Kunitoku N, Sasayama T, Marumoto T, Zhang D, Nitta M, Hatakeyama K, Saya H. Aurora-A and an interacting activator, the LIM protein Ajuba, are required for mitotic commitment in human cells. *Cell* 2003; 114:585-98.
12. Giet R, Uzbekov R, Cubizolles F, Le Guellec K, Prigent C. The *Xenopus laevis* aurora-related protein kinase pEg2 associates with and phosphorylates the kinesin-related protein XIEg5. *J. Biol. Chem.* 1999; 274:15005-13.
13. Dutertre S, Cazales M, Quaranta M, Froment C, Trabut V, Dozier C, Mirey G, Bouché JP, Theis-Febvre N, Schmitt E, Monsarrat B, Prigent C, Ducommun B. Phosphorylation of CDC25B by Aurora-A at the centrosome contributes to the G2-M transition. *J. Cell. Sci.* 2004; 117:2523-31.
14. Liu Q, Kaneko S, Yang L, Feldman RI, Nicosia SV, Chen J, Cheng JQ. Aurora-A Abrogation of p53 DNA binding and transactivation activity by phosphorylation of serine 215. *J. Biol. Chem.* 2004; 279:52175-82.
15. Ouchi M, Fujiuchi N, Sasai K, Katayama H, Minamishima YA, Ongusaha PP, Deng C, Sen S, Lee SW, Ouchi T. BRCA1 phosphorylation by Aurora-A in the regulation of G2 to M transition. *J. Biol. Chem.* 2004; 279:19643-8.
16. Goto H, Yasui Y, Nigg EA, Inagaki M. Aurora B phosphorylates Histone H3 at serine28 with regard to the mitotic chromosome condensation. *Genes Cells* 2002; 7:11-7.
17. Knowlton AL, Lan W, Stukenberg P. Aurora B is enriched at merotelic attachment sites, where it regulated MCAK. *Curr. Biol.* 2006; 16:1705-10.
18. Brittle AL, Nanba Y, Ito T, Ohkura H. Concerted action of Aurora B, Polo and NHK-1 kinases in centromere-specific histone 2A phosphorylation. *Exp. Cell Res.* 2007; 313:2780-5.
19. Morrison C, Henzing AJ, Jensen ON, Osheroff N, Dodson H, Kandels-Lewis SE, Adams RR, Earnshaw WC. Proteomic analysis of human metaphase chromosomes reveals topoisomerase II alpha as an Aurora B substrate. *Nucleic Acids Res.* 2002; 30:5318-27.
20. Spelotes EK, Uren A, Vaux D, Horvitz HR. The survivin-like *C. elegans* BIR-1 protein acts with the Aurora-like kinase AIR-2 to affect chromosomes and the spindle midzone. *Mol. Cell* 2000; 6:211-23.
21. Zeitlin SG, Shelby RD, Sullivan KF. CENP-A is phosphorylated by Aurora B kinase and plays an unexpected role in completion of cytokinesis. *J. Cell Biol.* 2001; 155:1147-57.
22. Li X, Sakashita G, Matsuzaki H, Sugimoto K, Kimura K, Hanaoka F, Taniguchi H, Furukawa K, Urano T. Direct association with inner centromere protein (INCENP) activates the novel chromosomal passenger protein, Aurora-C. *J. Biol. Chem.* 2004; 279:47201-11.
23. Marumoto T, Honda S, Hara T, Nitta M, Hirota T, Kohmura E, Saya H. Aurora-A Kinase Maintains the Fidelity of Early and Late Mitotic events in HeLa Cells. *J. Biol. Chem.* 2003; 278:51786-95.
24. Berdnik D, Knoblich JA. *Drosophila* Aurora-A is required for centrosome maturation and actin-dependent asymmetric protein localization during mitosis. *Curr. Biol.* 2002; 12:640-7.
25. Hannak E, Kirkham M, Hyman AA, Oegema K. Aurora-A kinase is required for centrosome maturation in *Caenorhabditis elegans*. *J. Cell Biol.* 2001; 155:1109-16.
26. Kemp CA, Kopish KR, Zipperlin P, Ahringer J, O'Connell KF. Centrosome maturation and duplication in *C. elegans* require the coiled-coil protein SPD-2. *Dev. Cell* 2004; 6:511-23.
27. Conte N, Delaval B, Ginestier C, Ferrand A, Isnardon D, Larroque C, Prigent C, Séraphin B, Jacquemier J, Birnbaum D. TACC1-chTOG-Aurora A protein complex in breast cancer. *Oncogene* 2003; 22:8102-16.
28. Portier N, Audhya A, Maddox PS, Green RA, Dammermann A, Desai A, Oegema K. A microtubule-independent role for centrosomes and Aurora A in nuclear envelope breakdown. *Dev. Cell* 2007; 12:515-29.
29. Adams RR, Maiato H, Earnshaw WC, Carmena M. Essential Roles of *Drosophila* Inner Centromere Protein (INCENP) and Aurora B in Histone H3 Phosphorylation, Metaphase Chromosome Alignment, Kinetochores Disjunction, and Chromosome Segregation. *J. Biol. Chem.* 2001; 15:865-80.
30. Hauf S, Cole RW, LaTerra S, Zimmer C, Schnapp G, Walter R, Heckel A, van Meel J, Rieder CL, Peters JM. The small molecule Hesperadin reveals a role for Aurora B in correcting kinetochore-microtubule attachment and in maintaining the spindle assembly checkpoint. *J. Biol. Chem.* 2003; 16:281-94.
31. Littlepage LE, Wu H, Andresson T, Deanehan JK, Amundadottir LT, Ruderman JV. Identification of phosphorylated residues that affect the activity of the mitotic kinase Aurora A. *Proc. Natl. Acad. Sci. U.S.A.* 2002; 99:15440-5.
32. Walter AO, Seghezzi W, Korver W, Sheung J, Lees E. The mitotic serine/threonine kinase Aurora 2/AIK is regulated by phosphorylation and degradation. *Oncogene* 2000; 19:4906-16.
33. Honda K, Mihara H, Kato Y, Yamaguchi A, Tanaka H, Yasuda H, Furukawa K, Urano T. Degradation of human Aurora2 protein kinase by the anaphase-promoting complex-ubiquitin-proteasome pathway. *Oncogene* 2000; 19:2812-9.
34. Castro A, Arlot-Bonnemains Y, Vigneron S, Jean-Claude L, Prigent C, Lorca T. APC/Fizzy-Related targets Aurora-A kinase for proteolysis. *EMBO Rep.* 2002; 3:457-62.
35. Zachos G, Black E, Walker M, Scott M, Vagnarelli P, Earnshaw W. Chk1 is required for spindle checkpoint function. *Dev. Cell* 2007; 12:247-60.
36. Chen J, Jin S, Tahir SK, Zhang H, Liu X, Sarthy AV, McGonigal TP, Liu Z, Rosenberg SH, Ng SC. Survivin enhances Aurora-B kinase activity and localizes Aurora B in human cells. *J. Biochem.* 2003; 278:486-90.
37. Honda R, Korner R, Nigg EA. Exploring the functional interactions between Aurora B, INCENP, and survivin in mitosis. *Mol. Biol. Cell* 2003; 14:3325-41.
38. Nguyen HG, Chinnappan D, Urano T, Ravid K. Mechanism of Aurora-B Degradation and Its Dependency on Intact KEN and A-Boxes: Identification of an Aneuploidy-promoting Property. *Mol. Cell. Biol.* 2005; 25:4977-92.
39. Sasai K, Katayama H, Stenoien DL, Fujii S, Honda R, Kimura M, Okano Y, Tatsuka M, Suzuki F, Nigg EA, Earnshaw WC, Brinkley WR, Sen S. Aurora-C is a novel chromosomal passenger protein that can complement Aurora-B kinase function in mitotic cells. *Cell Motil. Cytoskeleton* 2004; 59:249-63.
40. Sen S, Zhou H, White RA. A putative serine/threonine kinase encoding gene BTAK on chromosome 20q13 is amplified and overexpressed in human breast cancer cell lines. *Oncogene* 1997; 14:2195-200.
41. Zhou H, Kuang J, Zhong L, Kuo WL, Gray JW, Sahin A, Brinkley BR, Sen S. Tumour amplified kinase STK15/BTAK induces centrosome amplification, aneuploidy and transformation. *Nat. Genet.* 1998; 20:189-93.
42. Tchatchou S, Wirtenberger M, Hemminki K, Sutter C, Meindl A, Wappenschmidt B, Kiechle M, Bugert P, Schmutzler RK, Bartram CR, Burwinkel B. Aurora kinases A and B and familial breast cancer risk. *Cancer Lett.* 2007; 247:266-72.
43. Gu J, Gong Y, Huang M, Lu C, Spitz MR, Wu X. Polymorphisms of STK15 (Aurora-A) gene and lung cancer risk in Caucasians. *Carcinogenesis* 2007; 28:350-5.
44. Katayama H, Ota T, Jisaki F, Ueda Y, Tanaka T, Odashima S, Suzuki F, Terada Y, Tatsuka M. Mitotic kinase expression and colorectal cancer progression. *J. Natl. Cancer Inst.* 1999; 91:1160-2.
45. Sorrentino R, Libertini S, Pallante PL, Troncone G, Palombini L, Bavetsias V, Spalletti-cernia D, Laccetti P, Linardopoulos S, Chieffi P, Fusco A, Portell G. Aurora B overexpression associates with the thyroid carcinoma undifferentiated phenotype and is required for thyroid carcinoma cell proliferation. *J. Clin. Endocrinol. Metab.* 2004; 90:928-35.
46. Guangying Q, Ikuko O, Yasusei K, Mutsumi M, Siriwardena B, Fumio S, Masaaki M, Takashi A. Aurora-B overexpression and its correlation with cell proliferation and metastasis in oral cancer. *Springer* 2007; 450:297-302.
47. Smith SL, Bowers NL, Betticher DC, Gautschi O, Ratschiller D, Hoban PR, Booton R, Santibáñez-Koref MF, Heighway J. Overexpression of aurora B kinase (AURKB) in primary non-small



- cell lung carcinoma is frequent, generally driven from one allele, and correlates with the level of genetic instability. *Br. J. of cancer* 2005; 93:719-29.
48. Reichardt W, Jung V, Brunner C, Klein A, Wemmert S, Romeike BFM, Zang KD, Urbschat S. The putative serine/threonine kinase gene STK15 on chromosome 20q13.2 is amplified in human gliomas. *Oncol. Rep.* 2003; 10:1275-9.
49. Buschhorn HM, Klein RR, Chambers SM, Hardy MC, Green S, Bearss D, Nagle RB. Aurora-A over-expression in high-grade PIN lesions and prostate cancer. *The Prostate* 2005; 64:341-6.
50. Li D, Zhu J, Firozi PF, Abbruzzese JL, Evans DB, Cleary K, Friess H, Sen S. Overexpression of oncogenic STK15/BTAK/Aurora A kinase in human pancreatic cancer. *Clin. Cancer Res.* 2003; 9:991-7.

## Aurora kinase inhibitors: Progress towards the clinic

Madhu Kollareddy · Daniella Zheleva · Petr Dzubak ·  
Pathik Subhashchandra Brahmshatriya ·  
Martin Lepsik · Marian Hajduch

Received: 13 December 2011 / Accepted: 29 January 2012  
© The Author(s) 2012. This article is published with open access at Springerlink.com

**Summary** The Aurora kinases (serine/threonine kinases) were discovered in 1995 during studies of mutant alleles associated with abnormal spindle pole formation in *Drosophila melanogaster*. They soon became the focus of much attention because of their importance in human biology and association with cancer. Aurora kinases are essential for cell division and are primarily active during mitosis. Following their identification as potential targets for cancer chemotherapy, many Aurora kinase inhibitors have been discovered, and are currently under development. The binding modes of Aurora kinase inhibitors to Aurora kinases share specific hydrogen bonds between the inhibitor core and the back bone of the kinase hinge region, while others parts of the molecules may point to different parts of the active site via noncovalent interactions. Currently there are about 30 Aurora kinase inhibitors in different stages of pre-clinical and clinical development. This review summarizes the characteristics and status of Aurora kinase inhibitors in pre-clinical, Phase I, and Phase II clinical studies, with particular emphasis on the mechanisms of action and resistance to these

promising anticancer agents. We also discuss the validity of Aurora kinases as oncology targets, on/off-target toxicities, and other important aspects of overall clinical performance and future of Aurora kinase inhibitors.

**Keywords** Aurora kinases · Aurora kinase inhibitors · Cell division · Resistance · Mitosis · Serine/threonine kinases · Spindle pole

### Introduction

In 1995, David Glover discovered a new family of mitotic kinases while studying mutant alleles associated with defective spindle pole organization in *Drosophila melanogaster*. This family of kinases, which has been highly conserved during evolution, became known as the Aurora kinases (AKs) [1]. Humans have three homologous AKs, designated A, B and C. AKs are nuclear proteins, but they each have different sub-cellular locations. Aurora A is localized at the centrosome from the time of centrosome duplication through to mitotic exit [2, 3]. Aurora B, which is also known as the chromosomal passenger protein, is localized to the centromeres from the prophase to the metaphase-anaphase transition. Thereafter, it is localized to midzone spindle microtubules during telophase and subsequently to midbody during cytokinesis [2, 3]. Aurora C is also a chromosomal passenger protein considered to have a similar sub-cellular location to Aurora B. Aurora C is localized to centromeres during the prophase to metaphase and is redistributed to midzone microtubules during anaphase [4].

AKs are known to play multiple roles in mitosis, and their distribution correlates strongly with their functions. Aurora A is involved in mitotic entry, separation of centriole pairs, accurate bipolar spindle assembly, alignment of metaphase

M. Kollareddy · P. Dzubak · M. Hajduch (✉)  
Laboratory of Experimental Medicine,  
Institute of Molecular and Translational Medicine,  
Palacky University,  
Puskinova 6,  
Olomouc 77520, Czech Republic  
e-mail: marian.hajduch@upol.cz

D. Zheleva  
Cyclacel Ltd,  
1 James Lindsay place,  
Dundee DD1 5JJ, UK

P. S. Brahmshatriya · M. Lepsik  
Institute of Organic Chemistry and Biochemistry, v.v.i. and Gilead  
Sciences and IOCB Research Center,  
Academy of Sciences of the Czech Republic,  
166 10 Prague, Czech Republic

Published online: 18 February 2012

 Springer

chromosomes, and completion of cytokinesis [5]. Recently, the role of Aurora A in the promotion of nuclear envelope breakdown has been described [6]. Aurora B is involved in chromosomal bi-orientation, regulating the association between kinetochores and microtubules, and cytokinesis [7]. Aurora B is also involved in the release of abnormal kinetochore microtubule attachments during chromosomal bi-orientation [8]. Aurora B is known to phosphorylate Histone H3 (Ser10), which then aids in chromatin condensation and separation [9]. It has been shown that Aurora C exhibits similar functions to those assigned to Aurora B and share the same substrates [10, 11].

Direct association with inner centromere protein (INCENP) activates Aurora C *in vivo*, which results in further complexation with Aurora B, suggesting the cooperation of Aurora B and C in the regulation of mitosis [10]. Like Aurora B, Aurora C associates with survivin and may be essential for cytokinesis. Wild-type Aurora C has also been reported to rescue multinucleation induced by enzymatically inactive Aurora B, indicating that Aurora C may complement the functions of Aurora B [11]. In summary, AKs play prominent roles in maintaining the genetic stability of cells. Aberrant expression of AKs leads to genomic instability or aneuploidy, hallmark of cancer cells [12].

#### Aurora kinases as targets for cancer therapy

The Aurora A gene was originally named BTAK (breast tumor activated kinase) because its mRNA is overexpressed in breast tumors and it plays a critical role in the transformation of breast tumor cells [13]. Similarly, the Aurora A gene has been found to be amplified in human gliomas [14]. Using Northern and Southern blotting, Zhou et al. observed 2.5 to 8-fold amplification of Aurora A in many tumor cell lines [15]. Furthermore, Aurora A has been characterized as a potential low-penetrance tumor susceptibility gene, since the Phe31Ile functional polymorphism is strongly associated with familial breast cancer [16]. Similarly, Katayama et al. reported a correlation between overexpression of Aurora B and tumor progression in surgically resected colon tumor specimens [17]. The malignant progression of thyroid anaplastic carcinoma has also been shown to correlate with the overexpression of Aurora B [18]. The silent functional polymorphism, Ser295Ser (885 A > G) in the C-terminal end of Aurora B has been associated with an elevated risk of familial breast cancer [16], and overexpression of Aurora B has been correlated with decreased survival in glioblastoma patients [19].

In addition, aberrant expression of AKs has been shown to impair the functions of tumor suppressor genes, thereby generating aggressive tumors. Liu et al. reported that when overexpressed, Aurora A specifically phosphorylates p53 at

Ser215 and inhibits its DNA binding and transcriptional activities [20]. Thus, inhibition of Aurora A may rescue the function of tumor suppressor genes.

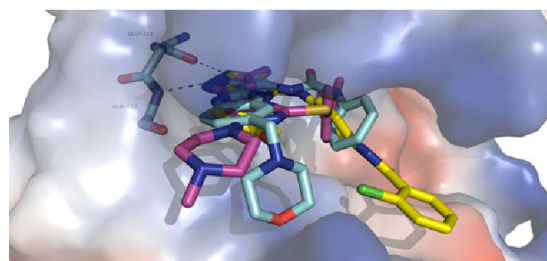
Since AKs are aberrantly expressed in many cancer tissue types, and thereby generate aggressive tumors, they are regarded as important new-generation targets for cancer therapy.

#### Small molecule Aurora kinase inhibitors (AKIs)

The discoveries of small molecule AKIs have been fuelled by the use of a variety of experimental and theoretical approaches. Examples include also structure-based drug design, especially in a fragment-based setup [21–24], structure-based virtual screening [25], FRET-based biochemical cell proliferation assay [26], and rational design followed by combinatorial expansion [27, 28].

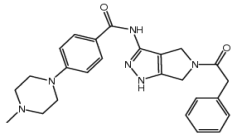
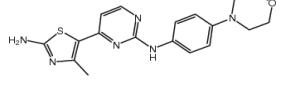
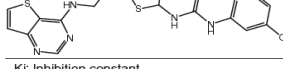
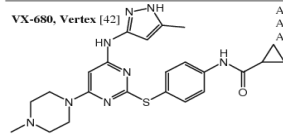
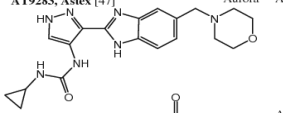
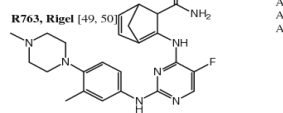
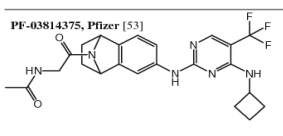
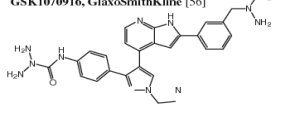
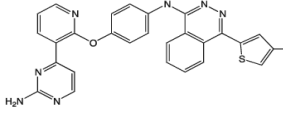
Currently, more than 30 AKIs are in various stages of preclinical and clinical studies. Their core binds via specific hydrogen bonds to the hinge region of Aurora A [21, 29, 30]. The other parts of AKIs may span different regions of the active site and interact via various types of noncovalent interactions or stick to the solvent (Fig. 1). The interaction modes of two clinical compounds (AT-9283 and VX-680) and one bisanilinopyrimidine based preclinical AKI (Genentech, Aurora A: 3 nM IC<sub>50</sub>) have determined using PyMol, ver. 0.99 (Fig. 1).

In the following sections we discuss pan-Aurora kinase inhibitors (Table 1), the characteristics of specific inhibitors of Aurora A and Aurora B which are in clinical studies (Table 2), AKIs in advanced preclinical studies (Table 3), and finally AKIs in early preclinical studies and first generation AKIs (Table 4).

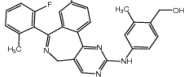
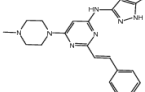
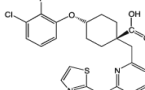
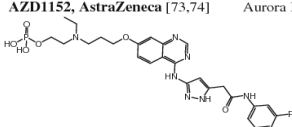


**Fig. 1** The crystallographic binding modes of three AKIs (in sticks, cyan—AT-9283, PDB (protein data bank) code 2W1E; yellow—bisanilinopyrimidine-based AKI, PDB code 3H0Y; violet—VX-680, PDB code 3E5A in the Aurora kinase A binding cleft (shown as surface). Specific hydrogen bonds to the backbone of residues Glu-211 and Ala-213 in the hinge region are shown by dotted lines. Color coding: oxygen—red, nitrogen—blue, chlorine—green, carbon—different colors. The figure was prepared using PyMol, ver. 0.99 [31]

**Table 1** Pan-Aurora kinase inhibitors in clinical trials

Compound, company, & code	<i>In vitro</i> potency	<i>In vitro</i> cellular potency (IC <sub>50</sub> )	Preclinical activity	Clinical development
<b>PHA-739358, Nerviano</b> [33, 34] 	Aurora A <sub>(IC50)</sub> - 13 nM Aurora B <sub>(IC50)</sub> - 79 nM Aurora C <sub>(IC50)</sub> - 61 nM	28 - 300 nM	Solid tumors & CML	Phase II Advanced solid and blood cancers. Partial response in one patient. 28 patients displayed stable disease. One CML patient showed complete hematological response
<b>CYC116, Cyclacel</b> [36] 	Aurora A <sub>(IC50)</sub> - 44 nM Aurora B <sub>(IC50)</sub> - 19 nM Aurora C <sub>(IC50)</sub> - 65 nM	34 - 1370 nM	Solid tumors. Reduced tumor weights in various solid tumors & leukemia xenografts	Phase I Advanced solid tumors
<b>SNS-314, Sunesis</b> [40] 	Aurora A <sub>(IC50)</sub> - 9 nM Aurora B <sub>(IC50)</sub> - 31 nM Aurora C <sub>(IC50)</sub> - 3 nM	1.8 - 24.4 nM	Solid tumors & leukemias	Phase I Advanced solid tumors. 6 patients displayed stable disease
<b>Ki: Inhibition constant</b>				
Compound, Company, & Code	<i>In vitro</i> potency	<i>In vitro</i> cellular potency (IC <sub>50</sub> )	Preclinical activity	Clinical Development
<b>VX-680, Vertex</b> [42] 	Aurora A <sub>(Ki)</sub> - 0.7 nM Aurora B <sub>(Ki)</sub> - 18 nM Aurora C <sub>(Ki)</sub> - 4.6 nM	15 - 113 nM	Solid tumors	Terminated due to severe toxicities
<b>AT9283, Astex</b> [47] 	Aurora A & B <sub>(IC50)</sub> - 3 nM	-	Solid tumors, CML & AML (acute myeloid leukemia)	Phase II Refractory solid and blood cancers. 4 patients with NSCLC and colorectal carcinoma showed stable disease
<b>R763, Rigel</b> [49, 50] 	Aurora A <sub>(IC50)</sub> - 4.0 nM Aurora B <sub>(IC50)</sub> - 4.8 nM Aurora C <sub>(IC50)</sub> - 6.8 nM	2-19 nM	Solid tumors	Phase I Advanced solid tumors. Good tolerability and efficacy reported in patients. Hematological malignancies-on going
Compound, company, & code	<i>In vitro</i> potency	<i>In vitro</i> cellular potency (IC <sub>50</sub> )	Preclinical activity	Clinical development
<b>PF-03814375, Pfizer</b> [53] 	Aurora A <sub>(IC50)</sub> - 5.0 nM Aurora B <sub>(IC50)</sub> - 0.8 nM	42-150 nM	Solid tumors	Phase I Advanced solid tumors. 19 patients achieved stable disease
<b>GSK1070916, GlaxoSmithKline</b> [56] 	Aurora B <sub>(IC50)</sub> - 3.5 nM Aurora C <sub>(IC50)</sub> - 6.5 nM	Median IC <sub>50</sub> is 8 nM	Solid tumors and blood cancer xenografts. Stable disease in several solid cancer xenograft models	Phase I Advanced solid tumors & leukemias
<b>AMG-900, Amgen</b> [57] 	Aurora A <sub>(IC50)</sub> - 5 nM Aurora B <sub>(IC50)</sub> - 4 nM Aurora C <sub>(IC50)</sub> - 1 nM	0.7-5.3 nM	Solid tumors. Active in multidrug resistant xenograft models	Phase I Advanced solid tumors and acute leukemias

**Table 2** Aurora A or Aurora B inhibitors in the clinical trials

Compound, company, & code	<i>In vitro</i> potency	<i>In vitro</i> cellular potency (IC50)	Preclinical activity	Clinical development
<b>MLN8237, Millennium</b> [62] 	Aurora A <sub>(IC50)</sub> - 1 nM	Pediatric cancer cell lines: Median IC50 is 61 nM	Solid tumors and leukemias	Phase II Advanced solid and blood cancers. Good pharmacokinetic profile
<b>ENMD-2076, Entremed</b> [66] 	Aurora A <sub>(IC50)</sub> - 14 nM	25 - 700 nM	Solid tumors & multiple myeloma. Induced 51% TGI & 70% tumor regression in MDA-MB-231 xenograft	Phase II Partial response in two platinum refractory ovarian cancer patients
<b>MK-5108, Vertex</b> [68] 	Aurora A <sub>(IC50)</sub> - 0.064 nM	0.16-6.4 μM	Solid tumors. 58% TGI was achieved at 45 mg/kg in SW48 xenograft model	Phase I Advanced and refractory solid tumors
<b>AZD1152, AstraZeneca</b> [73,74] 	Aurora B <sub>(IC50)</sub> - 0.37 nM	3 - 40 nM (leukemia cell lines)	Solid tumors & AML	Phase II Advanced solid and blood cancers. Overall 25% response rate. Stable disease in some patients

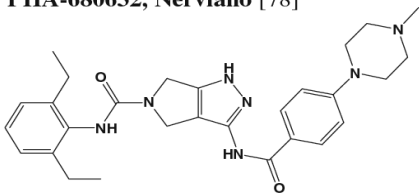
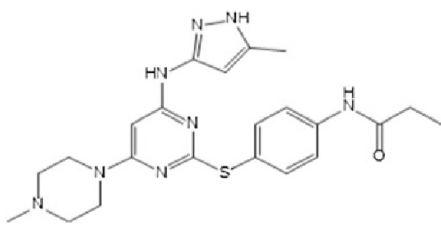
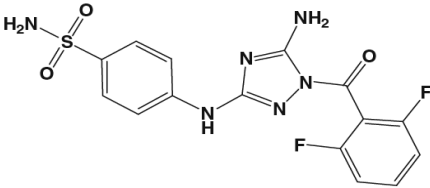
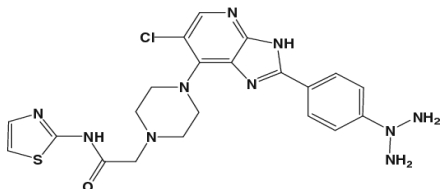
### Pan-Aurora kinase inhibitors in clinical trials

#### PHA-739358

PHA-739358 (Danusertib), which was discovered and developed by Nerviano Medical Sciences, is currently in Phase II clinical studies. This inhibitor features a pyrrolopyrazole scaffold which had previously been identified as an ATP-mimetic pharmacophore suited for kinase binding [27]. The SAR (structure activity relationship) analysis of several pyrrolopyrazole subclasses resulted in the synthesis of PHA-680632 which showed high anti-cancer activity *in vitro* and *in vivo* and have thus become a preclinical candidate [27]. The X-ray crystallographic structure of PHA-680632 in complex with Aurora A guided further design. Through combinatorial expansion of a related 1,4,5,6-tetrahydropyrrolo[3,4-*c*]pyrazole core and SAR refinements of the 5-amido-pyrrolopyrazole series a potent Aurora kinase inhibitor PHA-739358 was identified [28]. It has been shown to inhibit Aurora A, B, and C in biochemical competitive assays with IC50 values of 13, 79, and 61 nM, respectively [28]. However, this study also demonstrated that PHA-739358 predominantly has an Aurora B inhibition phenotype in cell cultures. At high concentrations, it has been reported to cross-react with Abl (Abelson), Ret (rearranged during transfection), Trk-A, and FGFR1 (fibroblast growth factor receptor 1) kinases [32]. In this latter study, cell lines exposed to PHA-739358 were found to be sensitive to concentrations in the range 28 to 300 nM and the mode of action of PHA-739358 corresponded to Aurora B

inhibition as assessed by phospho-histone H3(Ser10) inhibition. In addition, cells with tetraploid (4n) and polyploid (>4n) DNA content were observed to accumulate upon treatment with PHA-739358 [32]. Preclinical efficacy and toxicity studies were also performed in nude mice transplanted with several human xenografts, employing maximum tolerated doses (MTD) of 60 mg/kg/day for 5 days, 30 mg/kg/day for 10 days, or 45 mg/kg/day for 10 days. Tumor growth inhibition (TGI) was observed to be 66% to 98%; the compound was fairly well tolerated with only mild weight loss and myelosuppression. PHA-739358 has also been tested in a rat model having DMBA (9,10-Dimethylbenz-A-Anthracene) induced mammary carcinomas. At 25 mg/kg, TGI was measured as 75% and a complete cure was achieved in one rat [32]. Recently a Phase I study results were reported. Pharmacokinetic profiles were linear, and dose and time dependent. Of 80 patients assessed, stable disease was observed in 28, and in seven cases, this lasted for six months [33]. In another Phase I study, 56 patients divided into two parts (part 1 has 40 patients and part 2 has 16 patients) received escalating doses (45, 90, 180, 360, 500, 580, 650 mg/m<sup>2</sup>: 24 h infusion every 14 days) of PHA-739358 [34]. In part 1, patients received escalating doses of PHA-739358 without the co-administration of G-CSF (granulocyte stimulating factor). Doses were further escalated in part 2 in the presence of G-CSF. The MTD established in part 1 was 500 mg/m<sup>2</sup>. DLTs (dose limiting toxicity) were reported in 6 patients, which include neutropenia, grade 4 mucositis, and neutropenic infection. In part 2, 16 patients received the escalating doses of 500, 750, and 1000 mg/m<sup>2</sup>

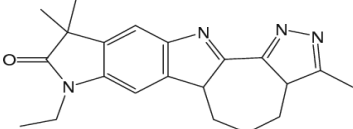
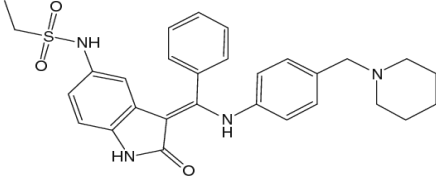
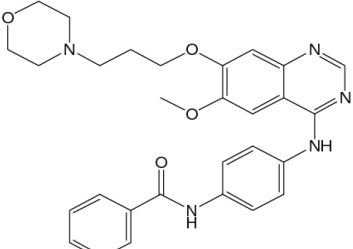
**Table 3** AKIs in advanced preclinical development

Compound, company & code	<i>In vitro</i> potency	<i>In vitro</i> cellular potency (IC <sub>50</sub> )	Preclinical activity
<b>PHA-680632, Nerviano [78]</b> 	Aurora A <sub>(IC<sub>50</sub>)</sub> - 27 nM Aurora B <sub>(IC<sub>50</sub>)</sub> - 135 nM Aurora C <sub>(IC<sub>50</sub>)</sub> - 120 nM	0.06 - 7.15 μM	Solid tumors and leukemia. 85% TGI resulted in HL60 human xenograft model. Similar results in A2780 and HCT116 xenograft models
<b>VE-465, Merck [80]</b> 	Aurora A <sub>(K<sub>i</sub>)</sub> - 1 nM Aurora B <sub>(K<sub>i</sub>)</sub> - 26 nM Aurora C <sub>(K<sub>i</sub>)</sub> - 8.7 nM	-	Up to 77% of mean tumor volume reduction achieved in Huh-7 xenograft model
<b>JNJ-7706621, Johnson [84]</b> 	Aurora A <sub>(IC<sub>50</sub>)</sub> - 11 nM Aurora B <sub>(IC<sub>50</sub>)</sub> - 15 nM	112 - 514 μM	Solid tumors. 93% TGI achieved in A375 human melanoma xenograft model
<b>CCT129202, Chroma [85]</b> 	Aurora A <sub>(IC<sub>50</sub>)</sub> - 42 nM Aurora B <sub>(IC<sub>50</sub>)</sub> - 198 nM	GI50 0.08 - 1.7 μM	Solid tumors. Induced TGI in HCT116 human xenograft model

along with G-CSF. No severe DLTs in the presence of G-CSF were reported even at maximum dose administered (1000 mg/m<sup>2</sup>). The dose 1000 mg/m<sup>2</sup> of PHA-739358 along with G-CSF induced objective response in one refractory

small cell lung cancer patient. This is the first time that the partial responses have been reported for an AKI with minimum toxicities. Several prolonged disease stabilizations were also reported in part 1 schedule. Phase II and Phase

**Table 4** AKIs in early preclinical development and first generation AKIs

Compound, company & code	<i>In vitro</i> potency	<i>In vitro</i> cellular potency (IC <sub>50</sub> )	Preclinical activity & comments
<b>Telik's dual Aurora A &amp; B inhibitor</b> Structure not available [86]	Inhibits Aurora A & B in 1-10 nM IC <sub>50</sub> range	15 - 500 nM	Solid tumors and hematological cancers. 72% TGI was achieved in HL60 xenograft
<b>AKI-001, Roche [87]</b> 	Inhibits Aurora A & B at nanomolar concentrations	>100 nM	Solid tumors. 92% TGI achieved in HCT116 xenograft
<b>Hesperadin, Boehringer Ingelheim [89]</b> 	Inhibits Aurora B at nanomolar range concentration	-	Many mitotic functions of Aurora B were discovered using Hesperadin, including its role in chromosomes attachment to mitotic spindle, conversion of monotelic to syntelic forms, and recruitment of BubR1 and Bub1
<b>ZM447439, AstraZeneca [90]</b> 	Aurora A <sub>(IC<sub>50</sub>)</sub> - 1 μM Aurora B <sub>(IC<sub>50</sub>)</sub> - 0.05 μM	-	Using ZM447439, Aurora B roles in recruitment of Cenp-E and BubR1 towards kinetochore, chromosome alignment and spindle check point regulations were discovered

BubR1: Budding uninhibited by benzimidazoles 1 homolog beta

Bub1: Budding uninhibited by benzimidazoles 1

Cenp-E: Centromere protein E

III single agent studies without G-CSF are underway in 7 types of solid tumors [34]. However, G-CSF is also being considered in further clinical studies. In addition to AKs, PHA-739358 has been also shown to inhibit BCR-ABL kinase (breakpoint cluster region-abelson) [35]. Many chronic myeloid leukemia (CML) patients acquire resistance to the BCR-ABL inhibitor imatinib by specific BCR-ABL mutations, particularly the T315I gate-keeper mutation.

Interestingly, PHA-739358 inhibited both wild type BCR-ABL (25 nM) and T315I mutated protein in kinase assays. Moreover, PHA-739358 reportedly has a higher affinity for the T315I form (5 nM) than the Abl wild type (21 nM) [35], which may prove advantageous for clinical treatment. This compound is currently in Phase II studies, being investigated in imatinib-resistant CML patients [33]. Twelve CML patients were enrolled and received doses from 250 to 400 mg/m<sup>2</sup>/day

(3 consecutive weeks every 4 weeks). Two patients with T315I BCR-ABL achieved complete hematological response. One patient displayed complete cytogenetic and molecular response after 3 months. PHA-739358 was well tolerated and only grade 3/4 neutropenia has been reported. As part of the pharmacodynamic study, CRKL phosphorylation was decreased in majority of treated patients. Additional studies in CML resistant patients are underway [33].

#### CYC116

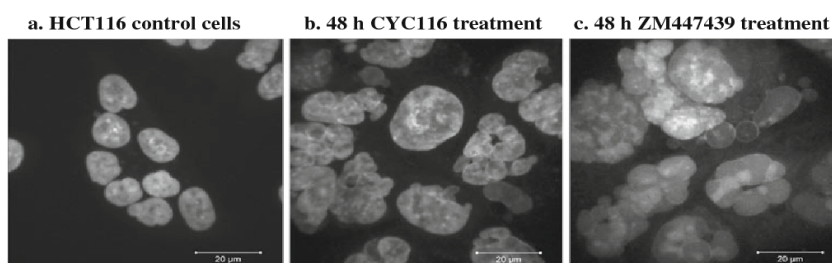
CYC116, discovered by Cyclacel Ltd., is an orally available AKI that has been tested in a Phase I trial. CYC116 was designed from the subset of lead N-phenyl-4-(thiazol-5-yl) pyrimidin-2-amines through cell-based screening of kinase-directed compound library [36]. The potency and specificity of CYC116 to Aurora kinases A and B was rationalized using X-ray crystal structure of the CDK2/CYC116 complex and docking to Aurora A structural model; indeed, specific residues responsible for the (differential) activity were identified [36]. It has been found to inhibit Aurora A, B, and C with IC50 values of 44, 19, and 65 nM, respectively, and also VEGFR2 (vascular endothelial growth factor receptor 2) with an IC50 of 69 nM [37]. In this study, the proliferations of various cancer cell lines with different genetic backgrounds were inhibited with IC50 values of 34 to 1370 nM. CYC116 is a targeted drug that has antimetabolic and anti-angiogenesis properties [36]. It was shown to inhibit autophosphorylation of Aurora A and B in A549 lung cancer cell lines, demonstrating its specificity against AKs, and it also induced failed mitosis, resulting in polyploidy (Fig. 2), which eventually killed the cells by apoptosis [36]. Further, CYC116 exhibited antitumor activity in various leukemia, solid tumor xenograft and leukemic syngenic models [36]. In mice with P388/D1 leukemia, it suppressed angiogenesis, decreased phosphorylation of histone H3, and induced accumulation of 4n and >4n DNA in cells [37]. It was reported to significantly reduce tumor neovascularization in a dose-dependent manner, possibly due to inhibition of VEGFR2 [38]. In P388D1 mouse leukemia model, at 45 and 67 mg/kg twice daily, the drug

increased the life span of 172% and 183%, respectively. Oral administration of CYC116 in NCI-H460 xenograft, at 75 and 100 mg/kg for 5 days caused significant tumor growth delays. Adverse side effects have not been reported. A Phase I trial in advanced solid tumors has been conducted to determine its MTD and evaluate its pharmacokinetic properties [36].

#### SNS-314

SNS-314 is a pan-Aurora kinase inhibitor discovered and developed by Sunesis pharmaceuticals which has been tested in a Phase I clinical trial. It was designed from the lead molecule, 2-aminoethyl phenyl benzamide through structure-activity optimizations. It has been reported to inhibit Aurora A, B, and C with IC50s of 9, 31, and 3 nM, respectively [39]. Additionally, it was shown to inhibit 24 other kinases with higher IC50 values. It inhibited cell proliferation in different human cell lines with IC50 values of 1.8 to 24.4 nM, and induced polyploidy. Histone H3 phosphorylation was significantly inhibited in all 6 cell lines tested with IC50 values 9–60 nM. The anti-tumor activity of SNS-314 was tested in several solid tumor xenograft models [39]. Preliminary in vivo study to determine dosing and schedules was performed in HCT116 xenograft. This study involved administration on a biweekly schedule for three weeks and reported 54–91% TGI at 170 mg/kg in breast, prostate, lung, ovarian, and melanoma xenografts. Single dose of SNS-314, 50 or 100 mg/kg, led to the complete inhibition of histone H3 phosphorylation as early as 3 h after administration in HCT116 xenograft model. This corresponded to the appearance of polyploid cells and caspase-3 activation [39]. The drug has been subjected to a Phase I clinical trial involving 32 advanced solid tumor patients, divided into 8 cohorts with doses ranging from 30 to 1800 mg/m<sup>2</sup> [40]. Only Grade 1 and 2 toxicities were observed, suggesting it was well tolerated. A dose limiting toxicity, namely neutropenia (Grade 3), was observed at a dose of 1440 mg/m<sup>2</sup>. Plasma levels of SNS-314 were dose-proportional and no drug accumulation was reported. Stable disease has been reported in 6 patients with advanced solid tumors [40].

**Fig. 2** Confocal microscopic images of HCT116 colorectal cancer cells treated with CYC116 and ZM447439. a) DAPI (4',6-diamidino-2-phenylindole) staining of diploid HCT116 parent cell line. b) & c) CYC116 and ZM447439 treatments resulted in the formation of polyploid cells





## VX-680

VX-680 was discovered by Vertex Pharmaceuticals, Oxford, UK. It was designed during the SAR exploitation of a lead molecule amino pyrazole linked to 2-substituted quinazoline [41]. It has been shown to inhibit Aurora A, B, and C with  $K_i$  values of 0.7, 18, and 4.6 nM, respectively [42]. In cytotoxicity assays with several tumor cell lines, VX-680 was reported to inhibit proliferation with  $IC_{50}$  values ranging from 15 to 130 nM. It was also observed to disrupt mitosis in a wide variety of tumor cell lines by affecting chromosome segregation and cytokinesis, eventually inducing the accumulation of cells with 4n DNA content, activating checkpoints, and subsequently inducing apoptosis [42]. Despite promising results, clinical trials involving this compound were suspended due to its toxicity profile (one case of heart failure). However, the compound has been tested in patients with advanced CML, acute lymphoblastic leukemia (ALL), and myelodysplastic syndromes because it has been found to successfully inhibit the T315I mutated form of BCR-ABL, which is resistant to imatinib. This surprising result prompted a re-examination of other clinical compounds against drug-resistant kinases. VX-680 has been observed to bind to wild type BCR-ABL with a dissociation constant  $K_d$  of ~20 nM and to T315I (as well as other Abl mutants) with a  $K_d$  of 5 nM. In vitro assays have shown that VX-680 inhibits the activity of wild type BCR-ABL and BCR-ABL (T315I) with  $IC_{50}$  values of 10 and 30 nM, respectively [43].

## AT9283

AT9283 developed by Astex Therapeutics is the first AKI discovered through the company's proprietary fragment-based screening approach. The pyrazole-benzimidazole hit compound was improved by SAR to a lead. The lead optimization was guided by X-ray crystallography and finally resulted in AT9283 as a clinical candidate [21]. It is currently in several Phase II studies under the Cancer Research UK. It has been shown to be an inhibitor of several kinases, including Aurora A (3 nM), Aurora B (3 nM), JAK2 (janus kinase) (1.2 nM), JAK3 (1.1 nM), and Abl (4.0 nM, T315I) [21]. HCT116 cells exposed to AT9283 exhibited polyploid phenotypes, which are typically associated with predominant Aurora B inhibition [21]. Like PH3-739358, AT9283 was found to inhibit wild-type BCR-ABL and T315I BCR-ABL ( $IC_{50}$  values of 110 and 4 nM, respectively) [44]. AT9283 has also been observed to inhibit proliferation of BaF3 cells with both wild type BCR-ABL and T315I BCR-ABL ( $IC_{50}$  values of 13 and 11 nM, respectively). In cellular assays, it inhibited the proliferation of BCR-ABL driven chronic myelogenous leukemia (BaF3) cells as judged by the inhibition of CRKL (v-crck sarcoma virus CT10 oncogene homolog (avian)-like) phosphorylation. In vivo efficacy of AT9283 was tested in

BaF3 xenograft with either BCR-ABL wild type or T315I mutation. At 12.5 mg/kg for 5 days, followed by 2-day drug holiday AT9283 significantly inhibited tumor growth without severe toxicities. It has also been found to induce significant reductions of tumor volume in K562 (CML, BCR-ABL positive) xenograft mouse model at 12.5 mg/kg [44].

In one trial, skin punch biopsies were taken for subsequent immunohistochemical studies from patients treated with AT9283, as well as serum samples collected at regular intervals. Inhibition of histone H3 phosphorylation, p53 stabilization, reduction of PCNA and Ki67 were detected. Analysis of the serum samples indicated elevation of M30 and M65 apoptotic markers and caspase activation [45]. The safety, tolerability, and preliminary efficacy of this compound are currently being evaluated in Phase I/II clinical studies. In one study, 30 patients with different refractory leukemias were enrolled for part of a Phase I trial. Patients were treated with escalating doses of AT9283, rising from 3 to 162 mg/m<sup>2</sup>/day [46]. No DLT was observed at doses below 72 mg/m<sup>2</sup>/day, except in one patient who developed tumor lysis syndrome at 12 mg/m<sup>2</sup>/day. At the maximum administered dosage, two DLTs and three deaths were reported, so further attention was focused on sub-maximum doses. Commonly observed DLTs included septicemia, pneumonia, and mucositis [46]. In a second study, 40 patients (five cohorts) with refractory solid tumors were enrolled as part of a second Phase I clinical study. Patients were treated with escalating doses, rising from 1.5 to 12 mg/m<sup>2</sup>/day. No DLTs were observed at doses below 6 mg/m<sup>2</sup>/day. At 12 mg/m<sup>2</sup>/day, two patients developed febrile neutropenia; 9 mg/m<sup>2</sup>/day was identified as the MTD. At this dosage, 3% of patients showed a partial response and 30% displayed stable disease [47].

## R763

R763 (AS703569), which was discovered and developed by Rigel, is an orally available Aurora inhibitor, currently in Phase I study. It was designed and developed based on a image-based phenotypic screen. It has been reported to inhibit Aurora A, B, and C with  $IC_{50}$  values of 4, 4.8, and 6.8 nM, respectively and to inhibit Abl, FLT1 (fms-related tyrosine kinase), and FLT3 oncogenic kinases [48]. In this study, Colo205, MiaPaCa-2, HeLa, and MV4-11 cells were observed to be most sensitive to R763 ( $IC_{50}$ =2 to 8 nM), but primary proliferating cells were also sensitive despite having higher  $IC_{50}$  values ( $IC_{50}$ =31 to 160 nM). This could be due to slower cell proliferation and intact cell cycle checkpoints. No effect was observed on non-dividing cells at the highest concentration tested. R763 appeared to induce endoreduplication within 48 h as evidenced by the accumulation of 4n and 8n cells. Colo205, HeLa, and MiaPaCa-2 underwent apoptosis after 48 h. In a preclinical phase, the in vivo efficacy of R763 was tested in MiaPaCa-2, adriamycin-resistant tumor,

MOLT-4, and MV4-11 xenograft models. Significant reduction in tumor volumes did not occur in the MiaPaCa-2 xenograft model, but histological regression and reduction in histone H3 phosphorylation (Ser10) was observed. In contrast, tumor volumes were significantly reduced in adriamycin-resistant tumors. Treatment of the MOLT-4 xenograft model resulted in a 5–10% reduction in the total number of bone marrow cells. The percentages of leukemia cells were significantly reduced, whereas control groups were not affected. In the MV4-11 xenograft, R763 induced pronounced anticancer activity in a dose-dependent manner. For a dose of 20 mg/kg/day, undetectable levels of tumors were seen in 17% of animals. Increased life span was observed in all treated groups, whereas all control mice died early [48].

Two Phase I studies were completed and one study is underway. Data from two studies were reported at international meetings. Initial clinical studies have been performed with two different dosing regimens to determine the compound's MTD, toxicity, and pharmacodynamic profile [49]. Cohorts of three patients were assigned to one of the two regimens. The starting dose was 6 mg/m<sup>2</sup> *p.o.* (Per Os) per 21-day cycle divided into two or three doses. Regimen 1 involved dosing on days 1 and 8, while regimen 2 involved dosing on days 1, 2, and 3. 15 patients were enrolled, including three with uterine, three with cervical, and two with breast cancer. Initially, two cohorts of three patients were treated at dose level 1, and no significant toxicity or adverse side effects were observed. Two patients did not receive effective treatment and one patient withdrew consent. During this study, two patients received 4+ dosing cycles and one received 3+. Overall, both dose levels (6 and 12 mg/mg<sup>2</sup>) were well tolerated [49]. Further dose escalations were carried out in patients with hematological malignancies in a second Phase I study [50]. Two dosing regimens were tested: days 1–3 and 8–10 of a 21-day cycle (regimen 1) and days 1–6 of a 21-day cycle (regimen 2). In regimen 1, 24 patients were treated up to dose levels of 47 mg/m<sup>2</sup>. At the maximum dose of 47 mg/m<sup>2</sup>, two grade 3 diarrheas have been reported. In regimen 2, 21 patients were also treated up to dose levels of 47 mg/m<sup>2</sup>. At this dose two DLTs namely, one neutropenic infection and two grade 4 mucositis have been reported. In this Phase I study, the established MTD was 37 mg/m<sup>2</sup>. Other reported toxicities include neutropenia, anemia, thrombocytopenia, and gastrointestinal disorders. One patient with CML (T315I) displayed hematological and cytogenetic response, one CML patient had a partial response, three AML patients achieved reduction in peripheral blasts, and several disease stabilizations were also reported [50]. Further enrollment of patients was ongoing at the time of report. Another Phase I study of R763 in combination with gemcitabine in advanced malignancies was recently completed.

#### PF-03814735

Pfizer's PF-03814735 is another orally available dual Aurora-A and Aurora-B inhibitor, which is currently in a Phase I study. It was discovered by SAR exploitation of lead pyrimidine scaffold. PF-03814735 was eventually designed by SAR optimizations at C2 and C4 positions of pyrimidine scaffold [51]. It has been found to inhibit recombinant Aurora A and Aurora B with IC<sub>50</sub> values of 5 and 0.8 nM, respectively, as well as FLT1, FAK (focal adhesion kinase), TrkA, MET, and FGFR1 kinases at higher IC<sub>50</sub> values [52]. It has also been shown to inhibit the proliferation of various human tumor cell lines (IC<sub>50</sub>=42 to 150 nM). In this study, phosphorylation of Aurora B (Thr232) was reduced significantly in MDA-MB-231, using a concentration of PF-03814735 close to the IC<sub>50</sub> (about 20 nM). It was also found to inhibit phosphorylation of histone H3 (Ser10) with an IC<sub>50</sub> value of ~50 nM. Aurora A autophosphorylation (Thr288) was also inhibited at an IC<sub>50</sub> value of ~150 nM, which is 3-folds higher than histone H3 (Ser10) phosphorylation inhibitor. PF-03814735 was shown to inhibit Aurora A and Aurora B rapidly and reversibly in cell cultures. When HCT116 cells were treated with PF-03814735, initially 4n DNA content cells accumulated followed by ≥8n DNA content, consistent with failed mitosis. At similar concentrations, inhibition of phospho-histone H3 was observed in athymic mice bearing HCT116 xenograft. Mice bearing HCT116 tumors were treated once daily with 10, 20, or 30 mg/kg for 10 days. Significant tumor growth inhibition (≥50%) occurred at ≥20 mg/kg. Moreover, significant antitumor efficacy was observed when PF-03814735 was tested in A2780, MDA-MB-231, Colo-205, and HL-60 xenograft models. Mice xenograft models tolerated various dosing schedules with very few toxic effects [52]. In Phase I initial clinical study, 57 patients with solid tumors were treated [53]. In schedule A, 32 patients received 5–100 mg/day for 5 days; or in schedule B patients (25) received 40–60 mg/day for 10 days of 21-day cycles. The MTD for schedule A was 80 mg/day. One patient in schedule A experienced grade 3 proctalga and two patients experienced grade 3 and grade 4 febrile neutropenia. The MTD for schedule B is 50 mg, where two patients experienced grade 3 increase of aspartate aminotransferase and grade 2 ventricular dysfunction. PF-03814735 was rapidly absorbed, appeared in circulation within 6 h of dosing, and it exhibited favorable linear pharmacokinetics. Pharmacodynamics of PH-03814735 was evaluated using phospho-histone H3 (Ser10) staining of mitotic cells as a surrogate biomarker. In comparison to the baseline, phospho-histone H3 levels decreased in 10 patients and paradoxically increased in two treated patients. In terms of efficacy, 19 patients achieved stable disease. Moreover in schedule A, five patients with stable disease displayed low tumor shrinkage [53].

## GSK1070916

GlaxoSmithKline's GSK1070916 is a reversible Aurora B and C inhibitor that is currently studied by Cancer Research UK in a Phase I clinical study. It was designed from the various SAR refinements of a lead 7-azaindole series [54]. It has been shown to inhibit Aurora B-INCENP and Aurora C-INCENP with IC<sub>50</sub> values of 3.5 and 6.5 nM, respectively, and to cross-react with FLT1, TIE2 (tyrosine kinase with immunoglobulin-like and EGF-like domains 1), SIK (salt inducible kinase), FLT4, and FGFR1 at higher concentrations [55]. The *in vitro* activity of GSK1070916 has been tested on 161 tumor cell lines and found to inhibit the proliferation of cancer cell lines with a median IC<sub>50</sub> of 8 nM [56]. It did not show any potent anticancer effects on non-proliferating HUVEC cells (IC<sub>50</sub>=3900 nM). In A549 cell line, it induced polyploidy and apoptosis in a dose dependent manner, which is consistent with Aurora B inhibition. Apoptotic cell death was evidenced by induction of caspase-3 and PARP cleavage in Colo205 cells. *In vivo* efficacy was tested in several xenograft models at 25, 50, or 100 mg/kg once daily for five consecutive days, followed by two days off, for two or three cycles. Complete or partial regressions were achieved in A549, HCT116, HL60, and K562 xenograft models and stable disease was observed in Colo205, H460, and MCF-7 xenografts. Adverse toxicities were not reported for this compound. Its efficacy was also tested in two human leukemia models: MV-4-11 and HL60. Significant dose-dependent increase in median survival times were reported [56]. GSK1070916 Phase I clinical study is currently recruiting patients with advanced solid tumors.

## AMG-900

Amgens's AMG-900 is an orally available pan-Aurora kinase inhibitor that is currently in Phase I clinical studies. It has been shown to inhibit Aurora A, B, and C with IC<sub>50</sub> values of 5, 4, and 1 nM, respectively [57]. It has also been shown to cross-react with other kinases including p38 $\alpha$ , TYK2 (tyrosine kinase 2), JNK2, MET, and TIE2 with IC<sub>50</sub> values in the range of 53–650 nM. It has been found to inhibit the proliferation of 26 diverse cancer cell lines with IC<sub>50</sub> values between 0.7–5.3 nM. Interestingly it was able to overcome the resistance in PgP (P-glycoprotein) expressing multidrug resistant cancer cell lines, as it inhibited colony formation of resistant and parent cell lines uniformly. Strikingly other AKIs (AZD1152, VX-680, PHA-739358) were less potent than AMG-900, when tested on these multidrug resistant cell lines. Moreover, the compound was also shown to inhibit AZD1152 resistant HCT116 cell line harboring Aurora B mutation (W221L). AMG-900 inhibited both parent and AZD1152

HCT116 resistant cell lines with equal potencies in colony formation assay [57], while human foreskin fibroblasts were relatively insensitive to the drug. However, it induced cell death in proliferating human bone marrow mononuclear cells at nanomolar concentrations, suggesting its high activity in cycling cells. AMG-900 inhibited autophosphorylation of Aurora A (Thr288) and histone H3 phosphorylation (Ser10) in a dose-dependent manner, with IC<sub>50</sub> values of 6.5 and 8.2 nM, respectively. AMG-900 predominantly showed Aurora B inhibition phenotype, as evidenced by the appearance of polyploid HeLa cells due to failed cytokinesis. Appearance of polyploid cells corresponded to the induction of p53 and p21 levels, which are widely accepted biomarkers related to Aurora inhibition. The compound induced time-dependent induction of apoptosis, as evidenced by the increase in the caspase-7 levels over the period of time. In HCT116 xenograft model it inhibited histone H3 phosphorylation in a dose-dependent manner. As expected it also suppressed histone H3 phosphorylation in mouse bone marrow cells. Treatment of mice with AMG-900 at 3.75, 7.5, and 15 mg/kg/twice daily for 2 consecutive days/week/3 weeks resulted in dose-dependent TGI's in the range 40 to 75%. Toxicities reported include moderate weight loss and myelosuppression. Dose-dependent TGI's were also reported in an alternate daily dosing schedule. It has also been tested in other xenograft models and 3 multidrug resistant (MDR) xenograft models. Two schedules were employed for this study. The xenografts were treated at 15 mg/kg b.i.d/2 consecutive days/week or 3 mg/kg b.i.d/day. AMG-900 exhibited significant antitumor activity (50–97% TGI) in all the xenograft models including MDR xenografts. It was able to overcome the drug resistance of MDR xenografts, otherwise insensitive to docetaxel or paclitaxel at their respective MTDs. Importantly, inhibition of histone H3 phosphorylation correlated with plasma drug concentrations [57]. Overall AMG-900 displayed favorable pharmacokinetic and pharmacodynamic profiles with anticipated minimum toxicities. Importantly, AMG-900 has great potential to overcome both the tumor multidrug resistance and to show activity in cancers resistant to other AKI due to mutation of the Aurora kinase B binding site. Currently two Phase I studies are underway in patients with advanced solid tumors and acute leukemias.

## Aurora A inhibitors in clinical trials

## MLN8237

MLN8237 (Alisertib) discovered by Millennium pharmaceuticals has been reported to be a highly specific and potent inhibitor of Aurora A (IC<sub>50</sub>=1 nM) [58].

This is a second generation Aurora A inhibitor from this company, as the predecessor to MLN8054. MLN8054 was terminated in Phase I studies due to off-target toxicities observed. This led to the development of new Aurora A specific inhibitor by the company, with a code name, MLN8237. MLN8237 was designed through SAR optimization of lead 5-H-pyrimido[5,4-d][2]benzazepine. It is currently in numerous Phase II clinical studies. It does not appear to have any significant off-target effects towards other kinases included in the panel, but it has been shown to inhibit wild-type BCR-ABL and T3151 BCR-ABL effectively in both kinase assays and in vitro cell cultures [59]. It has also been found to inhibit growth in HCT116, PC3, SK-OV-3, and LY-3 cancer cell lines in cell proliferation assays, with GI50 values between 16 and 469 nM [58]. The specificity of MLN8237 has been tested in multiple myeloma (MM) cell lines [60]. In this study, autophosphorylation of Aurora A (Thr 288) was markedly inhibited at 0.5  $\mu\text{M}$  in MM cell lines. MLN8247 induced 2 to 6-fold accumulation of G2/M followed by apoptosis, as evidenced by cleavage of PARP, caspase-9, and caspase-3. In addition, cell death by senescence was predominant after long exposure of MM cell lines. The efficacy of MLN8237 was tested in vivo in a MM xenograft model implanted in SCID (severe combined immune deficiency) mice. Tumor volumes were found to be significantly reduced at 30 mg/kg, and TGI was determined to be 42% and 80% at 15 and 30 mg/kg, respectively. Further, the overall survival rates of animals were significantly prolonged [60]. MLN8237 has also been tested on many pediatric cancer cell lines including rhabdomyosarcoma, Ewing sarcoma, glioblastoma, neuroblastoma, ALL, and AML [61]. In this study, the median IC50 was reported as 61 nM, ALL cell lines displaying the highest sensitivity and rhabdomyosarcoma cell lines were the least sensitive. Disease-free survival was improved in 80% of solid tumor models and 100% in ALL models, even more promising, a sustained complete response was achieved in 3 of 7 neuroblastoma models and the activity was much higher than standard anti-cancer agents [61]. Phase I dose escalation and dose-limiting toxicity studies involving cohorts of three patients with advanced solid tumors have been completed [62]. Each patient was given an oral dose once per day for seven days in a 21-day cycles, with the dosage increasing from 5 to 150 mg/day until DLTs were observed in more than two patients. DLTs were not reported for doses of 5–80 mg/day. However, in some patients mixed DLTs were reported at 150 mg/day, including G3 and 4 neutropenia, G3 somnolence, G3 mucositis or oral candidiasis, confusion, agitation, and alopecia. Aurora A kinase inhibition was inferred from the accumulation of mitotic cells in skin and tumor biopsies [62]. Plasma levels of MLN8237 were found to

be dose-proportional, suggesting MLN8237 has a good pharmacokinetic profile. Currently multiple Phase II MLN8237 studies are recruiting patients with a wide range of solid cancers and blood cancers for optimal dosing regimen, efficacy, and MTD determination.

#### ENMD-2076

EntreMed's ENMD-2076, currently in Phase II clinical trials, has been shown to selectively inhibit Aurora A with an IC50 of 14 nM measured in biochemical assays [63]. The molecule was designed by SAR optimization of a lead imidazole-vinyl-pyrimidine scaffold. It was also found to inhibit multiple oncogenic kinases, namely FLT3 (3 nM), Src (sarcoma) (20 nM), VEGFR2 (36 nM), and FGFR1 (93 nM), as well as the growth of various cancer cell lines (IC50=25 to 700 nM) [63]. It was observed that 5  $\mu\text{M}$  ENMD-2076 induced G2/M arrest in HCT116 cells consistent with Aurora A inhibition, rapidly inducing apoptosis. Recently, ENMD-2076 has also been shown to be highly effective against MM cell lines and primary MM cells derived from patients [64]. In this study, ENMD-2076 was found to cause 50% cell death in MM cell lines at a concentration of 3  $\mu\text{M}$  for 72 h of exposure. It also induced apoptotic cell death after only 6 h of exposure as evidenced by annexin-V staining, PARP cleavage, and activation of caspase-9, 8, and 3. In MM cells it significantly reduced autophosphorylation of Aurora A (Thr288) after 24 h of exposure. However, it also inhibited Aurora B at concentrations that resulted in cell death, as shown by down-regulation of histone H3 phosphorylation (Ser10). The in vivo efficacy was tested in a H929 human plasmocytoma xenograft model at doses of 50, 100, and 200 mg/kg. A dose-dependent efficacy was observed in all animals and maximum effect was achieved at 200 mg/kg with good tolerability. Immunohistochemistry on sacrificed animals revealed reduced Ki67 levels, increased caspase-3 levels, and decreased phospho-histone levels in treated animals compared to an untreated control [64]. When a HT-29 xenograft model was dosed at 100 or 200 mg/kg once per day, the tumor volumes remained static until around 17 days, and moderate regression was subsequently observed for 200 mg/kg. Immunohistochemistry revealed there was a corresponding reduction in Ki67 levels. ENMD-2076 has also been tested in a patient-derived colorectal cancer (CRC) xenograft where it was found to induce TGI in all cases (K-ras mutant) [65]. In the MDA-MB-231 mouse xenograft model, ENMD-2076 has been observed to reduce tumor growth by 51% at a dose of 50 mg/kg per day and to cause tumors to regress by 70% at a dose of 200 mg/kg [63]. Recently, Phase I study results were reported including pharmacokinetic, pharmacodynamic, and antitumor activity profiles. Patients with refractory advanced solid tumors were treated with continuous

oral daily dosing. Doses in the range 60 to 200 mg/m<sup>2</sup> were tested in a standard 3+3 design. Totally 67 patients were enrolled for this study [66]. At 200 mg/m<sup>2</sup>, two patients displayed grade 3 hypertension and 160 mg was reported as MTD. ENMD-2076 has linear pharmacokinetic profile and displayed significant antitumor activity including decreased VEGFR2 levels in plasma. The highest activity was reported in ovarian cancers, where two patients with platinum refractory disease showed partial responses [66]. Three Phase I studies are currently underway being tested in advanced solid tumors and multiple myeloma.

#### MK-5108

MK-5108 (VX689), discovered and developed by Vertex Pharmaceuticals, has been studied in a Phase I clinical trial in patients with advanced solid tumors. It has been shown to inhibit Aurora A with an IC<sub>50</sub> value of 0.064 nM [67]. It also inhibited Aurora B and Aurora C at higher IC<sub>50</sub> values (220 and 190 folds higher than Aurora A). It has been shown to inhibit the proliferation of 17 diverse cancer cell lines with IC<sub>50</sub> values ranging from 0.16 to 6.4 μM. MK-5108 significantly enhanced the efficacy of docetaxel in HeLa-S3 and ES-2 cell lines. MK-5108 and docetaxel combination also showed similar efficacy in HeLa-luc and ES-2 xenograft models. In cell lines it predominantly showed Aurora A inhibition phenotype (G2/M arrest), as histone H3 phosphorylation was not inhibited, which is a marker for Aurora B inhibition. MK-5108 inhibited Aurora A, as also evidenced by the inhibition of Aurora A autophosphorylation (Thr288). MK-5108 induced greater accumulation of phospho-histone H3 at much lower concentrations compared to MLN8054, a well known Aurora A specific inhibitor [67]. In vivo efficacy of MK-5108 was tested in HCT116 and SW48 xenograft models. Doses of 15 and 30 mg/kg were administered twice daily for 12 days. MK-5108 treatment resulted in TGI's of 10% and 17% at doses 15 mg/kg and 30 mg/kg, respectively in HCT116 xenograft model. In SW48 xenograft model, intermittent doses (twice daily/2 days/week/3 weeks) of 15 mg/kg and 45 mg/kg resulted in 35% and 58% TGI's, respectively. MK-5108 was well tolerated and adverse toxicities were not reported.

MK-5108 was tested in patients with advanced solid tumors either as a single agent or in combination with docetaxel. Febrile neutropenia and myelotoxicity were reported as DLTs in the combination treatment regimen. However, no significant toxicities were reported in the monotherapy arm. Disease stabilization was reported in 32% patients from both arms and partial responses were reported in 12% of patients only from the combination arm [68].

#### Aurora B inhibitors in clinical trials

##### AZD1152

AZD1152 (Barasertib) is an AstraZeneca compound which has been shown to be a highly specific inhibitor of Aurora B (0.37 nM) [69], and is currently in Phase II clinical studies. It was designed and developed from the lead pyrazole-acetanilide-substituted quinazoline by SAR exploitation [70]. It has been found to exhibit varying potency across different types of leukemia cells (ALL, PALL-2, MOLM13, MV4-11) inhibiting their proliferation with IC<sub>50</sub>s ranging from 3 to 40 nM, and also inhibits the proliferation of freshly isolated patient leukemia cells (IC<sub>50</sub>=3 nM). In this work, exposure of MOLM13 and PALL-2 to AZD1152 resulted in accumulation of 4n/8n DNA cells, which subsequently underwent apoptotic cell death as demonstrated by annexin-V staining [69]. In SW620 colon cancer cells, it has been observed to inhibit the phosphorylation of histone H3 in a dose-dependent manner, which is indicative of Aurora B inhibition [71]. Furthermore, it caused potent dose-dependent growth inhibition of human xenograft models in nude mice, including SW620, HCT116, Colo205, A549, Calu-6, and HL-60. In these experiments, the extent of growth inhibition ranged from 55 to 100%; the HL-60 model was the most responsive (complete regression was observed). Elevated caspase-3 levels were observed in all tumors isolated for histological assessment. The mechanism of AZD1152 action was found to be similar in both in vitro and in vivo conditions. AZD1152 was well-tolerated at doses required for efficacy; myelosuppression is the primary problem associated with high doses [71]. Treatment of the human MOLM13 xenograft immunodeficient murine model with AZD1152 at a dose of 25 mg/kg per day caused significant reductions in tumor weight and growth [69]. However, none of the mice showed any signs of side effects, which suggest that it was well tolerated.

Initial clinical study was conducted on 13 patients having colon cancer, melanoma or some other solid tumors. The compound was administered via intravenous (i.v.) infusion (2 hrs per week) in a dose-escalating manner (100–450 mg) on days 1, 8 and 15 of a 28-day cycle. Doses up to 300 mg were well tolerated, but neutropenia was observed in three patients at 450 mg. Significant disease stabilization was observed in progressive cancers [72]. AZD1152 recently entered Phase I/II clinical trials focusing on its safety, tolerability, pharmacokinetics, and efficacy profiles in AML patients [73]. Treatment of AML patients was performed in two parts; in part A, 32 individuals were treated (continuous 7-day infusion every 21 days) at doses ranging from 50 to 1600 mg. Grade 3/4 stomatitis or mucosal inflammation were reported as DLTs at doses ranging from 800 to 1600 mg. Most of the toxicities resolved following dose

delay and no treatment related deaths have been reported. This part of the study established MTD as 1200 mg. Consequently, another 32 patients received 1200 mg in part B of the study. For combined part A and part B, the overall response rate was 25% in both newly diagnosed and relapsed AML patients. The pharmacokinetic profiles were favorable as assessed by the AZD1152 blood levels and distribution to tissues [73]. Recently, barasertib has been tested in patients with advanced solid malignancies using escalating doses from 100 mg to 650 mg per day [74]. In schedule A, 2 h i.v. infusion was given for every 7 days across four escalating doses (100, 200, 300, and 450 mg). In schedule B, the drug was administered every 14 days across five escalating doses (200, 300, 450, 550, and 650 mg). Schedule A included 19 patients and schedule B included 40 patients. Doses 250 mg and 400 mg per day were the MTDs in schedules A and B, respectively. Neutropenia and leukopenia were the most common side effects. Objective antitumor effects were not observed, however, stable disease achieved in 15 patients overall. In this study, the linear pharmacokinetics has also been reported, as the systemic exposure to AZD1152-HPQA (active drug) was observed by 1 h into the infusion [74]. Currently AZD1152 is being tested in a Phase II trial in large B-cell lymphoma patients.

#### BI 811283

Boehringer-Ingelheim's BI 811283 is a Aurora B inhibitor that is currently in a Phase II clinical study. It has been shown to inhibit Aurora B with IC<sub>50</sub> value of 9 nM and also inhibited the proliferation of 24 diverse cancer cell lines with an IC<sub>50</sub> value <14 nM [75]. Chemical structure of BI 811283 is not disclosed by the company. Treatment of cancer cell lines with BI 811283 resulted in polyploidy within 48 h due to failed mitosis. It dominantly induced senescence (based on SA-beta-GAL staining) within 96 h and only 7% cells showed apoptotic phenotype (PARP cleavage and nuclear fragmentation) after 96 h. In vivo efficacy of BI 811283 was tested in NSCLC and colorectal cancer cell line xenograft models. The compound was administered once weekly by 24 h s.c. infusion. It inhibited tumor growth of xenografts in dose-dependent manner and at the MTD (20 mg/kg), tumor regression was reported in some animals. Accumulation of larger and multinucleate cells were reported, which is consistent with the Aurora B inhibition phenotype [75].

In Phase I dose escalation study, BI 811283 has been tested in advanced and metastatic solid tumors [76]. Patients were randomized into two schedule treatment groups, q2w and q3w in a bicentric Phase I dose escalation. In 3-week treatment schedule, patients were treated with BI 811283 as 24 h i.v. infusion on day 1 of each 21-day treatment cycle. The MTD was reported to be 230 mg/kg. The main side

effects include reversible hematotoxicity, neutropenia, and febrile neutropenia. However, accumulated toxicity was not reported in two patients that are treated for >16 courses. As part of the efficacy, stable disease was reported in 33.3% of patients [76]. In another 4-week treatment schedule, patients received BI 811283 (5–140 mg/kg) as 24 h i.v. infusion on days 1 and 15 of each treatment cycle [77]. The MTD was reported to be 140 mg/kg. The dose limiting toxicities were almost identical to previous schedule. Stable disease was reported in 29% of patients. Pharmacokinetic profiles were near-linear and the half-life was 11.9 to 26 h. Additional dosing schedules in expanded patient cohorts were also completed. However, the results are not yet published. A Phase II clinical study in combination with cytarabine is currently underway.

#### AKIs in advanced preclinical studies

##### PHA-680632

PHA-680632 is another pan-Aurora kinase inhibitor from Nerviano. It emerged from SAR modifications of several pyrrolopyrazole core sub-classes of ATP-mimetic pharmacophores [27]. It has been reported to inhibit Aurora A, B, and C with IC<sub>50</sub> values of 27, 135, and 120 nM, respectively, and to cross-react with FGFR1 (IC<sub>50</sub>=390 nM) [78]. It has also been shown to inhibit proliferation of various cancer cell lines with different genetic backgrounds (IC<sub>50</sub>=0.06 to 7.15 μM). Further, this study found that PHA-680632 selectively generated polyploidy in a cancer cell line—HCT116, but not in a normal cell line. Treatment of cells with anti-Aurora A siRNA, but not anti-Aurora B siRNA induced accumulation of active caspase 9 and 3. Similarly PHA-680632 induced accumulation of active caspase 9 and 3, which is an indicative of predominant Aurora A inhibition related apoptosis. Treatment of HeLa cells with 2 μM PHA-680632 for 24 h resulted in dramatic down-regulation of phospho histone H3 (Ser10). Its efficacy and toxicity were tested in human tumor xenograft models, and in mouse and rat syngenic models. These tests involved administration of PHA-680632 at a dose of 45 mg/kg for five consecutive days to mice bearing the HL60 tumor and resulted in a TGI of 85% compared to tumor growth in control animals treated only with the vehicle. Similar effects were observed in A2780 and HCT116 models. In A2780 mouse xenograft model, inhibition of histone H3 phosphorylation was observed within 8 h of dosing at 60 mg/kg. No toxicities were reported at any of the doses employed [78]. Treatment of HCT116p53<sup>-/-</sup> cells with PHA-680632 after ionising radiation exposure (IR) has been shown to result in enhanced cell killing (with additive effect) as determined by annexin-V staining, micronuclei and BRCA-1 foci

formation. Correspondingly, combined treatment of IR and PHA-680632 in HCT116p53<sup>-/-</sup> mice xenograft model showed enhanced tumor growth delay [79].

#### VE-465

VE-465 is another pan-Aurora kinase inhibitor discovered by Vertex pharmaceuticals. The chemical structure is similar to that of VX-680. VE-465 was designed by SAR optimization of the lead amino pyrazole. Using ATP (adenosine triphosphate) competitive binding assays it has been shown to inhibit Aurora A, B, and C with  $K_i$  values of 1, 26, and 8.7 nM, respectively [80]. In preclinical studies it exhibited anticancer effects on two hepatocellular carcinomas, Huh-7 and HepG2. It also suppressed Aurora B activity in a dose-dependent manner within 1 h treatment of both cell lines. Immunocytochemistry studies in Huh-7 and HepG2 using anti  $\alpha$ -tubulin and DAPI indicated that VE-465 causes the formation of abnormal prometaphase cells, affecting centrosome maturation and spindle bipolarity. These effects are entirely consistent with inhibition of Aurora A in the treated cells. VE-465 also induced mitotic abnormalities associated with Aurora B inhibition, namely dispersal of the chromosomes. It induced endoreduplication and cell cycle arrest as early as 24 h. At slightly higher concentrations, VE-465 induced apoptotic cell death in both Huh-7 and HepG2, as measured by annexin-V staining [80]. It has also been shown to have significant activity against paclitaxel-resistant ovarian carcinoma at higher doses, causing an 8-fold increase in apoptotic cell death at 100 nM [81]. Recently it was demonstrated to have significant activity against a panel of resistant and non-resistant multiple myeloma cell lines [82]. In this study, VE-465 inhibited proliferation of MM cells at concentrations of 400 nM or less. G2/M, 8n, and sub G1 populations were observed to accumulate with increasing exposure time, and correspondingly apoptotic markers appeared, including cleavage of PARP, caspase-3, 8, and 9. However, primary MM cells from patients are relatively insensitive to VE-465. Further it was shown that the effects of VE-465 were additive alongside with anti-MM agents [82]. In vivo efficacy was tested in Huh-7 xenograft model at 15, 25, and 35 mg/kg doses, administered twice daily for 14 days. These treatments caused reductions in the mean tumor volume of 59%, 59%, and 77% respectively [80]. In this study, VE-465 was also observed to inhibit histone H3 phosphorylation and to induce apoptosis in the tumors in a dose-dependent manner.

#### JNJ-7706621

Johnson & Johnson's JNJ-7706621 is an Aurora A and B kinase inhibitor. It was designed by the refinement of a series of acyl-substituted 1,2,4-triazole-3,5-diamine analogues [83].

The molecule has been reported to inhibit Aurora A and B with  $IC_{50}$  values of 0.011 and 0.015  $\mu$ M, respectively [84]. However, in this study, it was also shown to inhibit CDK1 (cyclin dependent kinases), CDK2, CDK3, CDK4, and CDK6 ( $IC_{50}$ =0.009 to 0.175  $\mu$ M). Further, it inhibited proliferation of various cancer cell lines ( $IC_{50}$ =0.112 to 0.514  $\mu$ M), but showed less potency against normal cell lines, which were several-fold less sensitive. Moreover, it inhibited cell proliferation of both drug-sensitive and drug-resistant MES-SA cell lines at almost identical  $IC_{50}$  values, suggesting that PgP expression has no effect on JNJ-7706621 activity. Long-term effects of this compound on cell proliferation were determined by colony formation assay. HeLa cells were treated with either 1  $\mu$ M or 3  $\mu$ M concentrations for 48 h, followed by removal of the compound, and cells were then monitored for 7 days. Colony formation inhibition of 55% (1  $\mu$ M) and 95.5% (3  $\mu$ M) compared to control cells was reported. JNJ-7706621 induced apoptosis in the U937 histiocytic lymphoma cell line in a dose- and time-dependent manner, as evaluated by annexin-V staining. It also induced G2/M cell cycle arrest and polyploidy, which is one of the major phenotypic responses associated with Aurora kinase inhibition. The compound inhibited histone H3 phosphorylation at concentrations of 1 to 4  $\mu$ M, which is again consistent with activity against Aurora B. The compound has been subjected to preclinical in vivo testing using the A375 human melanoma xenograft model, at doses of 100 and 125 mg/kg. Although daily dosing was the most efficient, five out of six test animals died after 22 days of treatment. However, an alternative '7 days on, 7 days off' dosing schedule resulted in 93% TGI with no treatment-related deaths [84].

#### CCT129202

Chroma's CCT129202 has been shown to have high activity against Aurora A and Aurora B. It was developed through SAR optimization of an imidazopyridine scaffold. The compound has been reported to inhibit Aurora A, B, and C with  $IC_{50}$  values of 0.042, 0.198, and 0.027 nM, respectively [85]. It was also shown to cross-react with FGFR3, PDGFR $\beta$  (platelet-derived growth factor receptor), and GSK3 $\beta$  (glycogen synthase kinase 3 beta) at high concentrations. The effect of this compound on cancer cell line proliferation was tested on Colo205, SW620, HCT116, HT29, KW12, HeLa, A2780, OVCAR8, MDA-MB-157, and MV4-11 cells, and was found to have a half-maximal growth inhibition concentration ( $GI_{50}$ ) in the range 0.08 to 1.7  $\mu$ M. In preclinical studies, it induced the accumulation of HCT116 cells with  $\geq 4$  N DNA content, accompanied by the appearance of subG1 apoptotic cells and accumulation of PARP cleavage. In HCT116 colon carcinoma cells, CCT129202 inhibited histone H3

phosphorylation after 15 min of treatment. The same effect was observed in the HCT116 xenograft model, i.e., inhibition of histone H3 phosphorylation after 15 minutes at a dose of 100 mg/kg. Furthermore, it induced stabilization of p53 (consistent with Aurora A inhibition). CCT129202 was administered at a dose of 100 mg/kg once a day for 9 days to HCT116 colon tumor xenografts in athymic mice to test its effects on TGI. The compound was well tolerated and induced significant TGI. Studies in mice also indicated that the compound has a favorable pharmacokinetic profile [85].

### AKIs in early preclinical studies

#### Telik's dual AKIs

Telik's Aurora A and B inhibitors are at early preclinical stage. Telik's Aurora inhibitors were designed by using proprietary drug discovery technology called TRAP (Target-Related Affinity Profiling). They have been reported to inhibit Aurora A, B, and VEGFR2 with IC50s of 1–10 nM [86]. Telik's compounds have also been shown to inhibit proliferation of various colon, leukemia, lung, pancreatic, ovarian, and prostate cancer cell lines, with IC50s in the range 15 to 500 nM. Mechanistic actions consistent with Aurora inhibition were observed, including inhibition of histone H3 phosphorylation and polyploidy. The *in vivo* activity of TLK60404, one of Telik's specific AKI was tested in human HCT116 and HL-60 mouse xenograft models. No toxicity or drug-related weight loss was observed. In addition, tumor growth was inhibited by 72% in HL-60 human xenograft model [86].

#### AKI-001

Roche's AKI-001 is an inhibitor of Aurora A and Aurora B that is in initial preclinical studies. AKI-001's core, the pyridinyl pyrimidine amide scaffold, was discovered by high-throughput screening against Aurora-A kinase [87]. Further optimization and inclusion of lactam ring and hydrocarbon constraint to pentacyclic scaffold led to the discovery of the highly potent AKI-001 which is orally bioavailable phthalazine derivative with improved enzyme and cellular activity and a high level of kinase selectivity. AKI-001 has been shown to inhibit recombinant Aurora A and Aurora B at low nanomolar concentrations in ATP-competition assays. The compound also inhibited the proliferation of various cancer cell lines with IC50 values below 100 nM. In cellular assays, both Aurora A and Aurora B inhibition phenotypes were reported. AKI-001 had good oral bioavailability and was well tolerated at 5 mg/kg daily in the HCT116 xenograft

model. At this dose AKI-001 induced 92% inhibition of tumor growth [87].

#### CHR-3520

After screening many small molecule inhibitors, Chroma Therapeutics selected CHR-3520 for entry into preclinical studies. Initial studies have indicated that CHR-3520 is an inhibitor of AKs and other kinases related to cancer. Details of the specificity and cellular potency of CHR-3520 in relation to the AKs have not yet been disclosed [88].

#### Other AKIs

In addition to these compounds, many biotechnology and pharmaceutical companies are developing novel AKIs. Cetek selected CTK110, an AKI with promising *in vitro* and *in vivo* anticancer activity, from a series of potential compounds. Ambit Biosciences have used their KinomeScan technology to select a lead AKI. KinomeScan is a novel and highly promising chemogenomics-based technique that is able to screen and characterize whole libraries of compounds across 400 kinases.

### First generation AKIs

#### Hesperadin

Hesperadin is the first generation AKI discovered by Boehringer Ingelheim. Treatment of cancer cell lines with hesperadin resulted in Aurora B inhibition phenotype. The specificity of hesperadin towards Aurora A and C is unknown. Most of the basic functions of Aurora B in mitosis and its role in cancer cell proliferation were discovered by inhibiting it with Hesperadin [89].

#### ZM447439

ZM447439, discovered by AstraZeneca, was the first AKI to be thoroughly characterized [90]. ZM447439 has been used extensively to study the biology of AKs and in their validation as targets for anti-cancer drug development.

### Natural AKI

#### Jadomycin-B

Discovery of Jadomycin B (an Aurora B inhibitor) is attributed to structure-based virtual screening. Virtual screening against Aurora B (PDB code 2BFY) resulted in 22 compounds amongst a database of nearly 15,000 microbial natural



products among which Jadomycin showed dose-dependent inhibition of Aurora B and several human cancer cell lines [25].

### Drug resistance to AKIs

Over the last 15 years, cancer chemotherapy has been greatly improved by the discovery of targeted drugs. In particular, some targeted drugs have achieved complete cures in some patients. However, the primary drug resistance or its development after few courses of chemotherapy is a major obstacle in the clinic. Many drug discovery companies are now focusing on drug resistance after realizing its importance in clinical trials and the clinic. Studies of drug-induced resistance in cell line models in parallel with preclinical development can be expected to yield significant information, and the findings of such studies can be used to circumvent drug resistance in clinical studies by designing combinations of anticancer agents.

Until recently, very little was known about drug-induced resistance mechanisms towards AKIs. One study found that SW620 (colon carcinoma) and MiaPaca (pancreatic carcinoma) cell lines became resistant to 1  $\mu$ M AZD1152 over the course of three months exposure [91]. The resistant cells were maintained for further three months in the presence or absence of AZD1152. Genome-wide screening studies revealed that the expression of the ABCB1 (ATP-binding cassette, subfamily B, member 1/Multidrug resistance protein 1) gene was 70-fold higher in the SW620 AZD1152-resistant clones than in the SW620 cell line. At the same time, LC-MS (Liquid chromatography-mass spectrometry) analysis showed decreased drug accumulation in cytoplasm of resistant cells. When drug resistant SW620 cell line was treated with either 50 or 100 mg/kg of AZD1152, no decrease in tumor size was observed. By contrast, the MiaPaca pancreatic carcinoma cell line became resistant to AZD1152 following overexpression of the ABCG2 (ATP-binding cassette, subfamily G, member 2/Breast cancer resistance protein) drug transporter. Microarray analysis revealed that the expression of this gene was increased 98-fold relative to controls. [91].

Seamon et al. obtained JNJ-7706621 resistant HeLa cell line by exposing the cells to increasing concentrations over a 12 month period [92]. A LC-MS study on these resistant lines showed a highly significant reduction of intracellular drug accumulation. Quantitative RT-PCR (Real time polymerase chain reaction) studies revealed a 163-fold increase in ABCG2 (BCRP/Breast cancer resistance protein) transporter gene expression, a 37-fold increase in ABCC2 (ATP-binding cassette, subfamily C, member 2), and a 3-fold increase in ABCB1. Treatment of the resistant HeLa cell line with the ABCG2 inhibitor fumitremorgin C restored the sensitivity to JNJ-7706621 and mitoxantrone [92].

Unlike previous studies, in which resistant cell cultures were developed by prolonged exposure to slowly-increasing levels of AKIs, Girdler et al. [93] treated the HCT116 cell line with a supra-lethal dose of ZM447439 (1  $\mu$ M) for four weeks. While most of the cells died, 20 drug resistant colonies were appeared and among them seven clones were selected for further characterization. Colony formation and cell proliferation assays demonstrated that the clones R1 and R2 were highly resistant to ZM447439 compared to controls. cDNA sequencing of Aurora B from these resistant clones (designated R1-R7), revealed five point mutations. R3, R4, and R6 harbored two point mutations. H250Y was common to all three of these clones, whereas G160V was specific to R3 and R4, while G160E was specific to R6. The R1, R2, R5, and R7 clones contained the G160E, Y156H and L308P, H250Y, and Y156H mutations, respectively. Ectopic expression of the Y156H, G160V, and H250Y mutants in DLD-1 cells revealed that they retained catalytic activity. The Y156H genotype along with G160V and G160E showed strong cross-resistance to VX-680 and hesperadin, but not H250Y. Advanced crystallographic studies revealed that these Aurora B mutations increase the steric hindrance in the active site of Aurora B, inhibiting the binding of ZM447439, but not that of ATP [93].

### Validity of Aurora kinases as oncology targets

Although AKs are widely considered as oncogenes, many questions were raised regarding their role in cancer initiation. Despite their overexpression in many tumors, no clear role for the AKs in tumorigenesis has been established. Probably the overexpression of AKs may not be the main cause of cancer initiation in primary tumors, rather it could be a late event. Bischoff et al. showed that overexpression of wild type Aurora A is sufficient to transform rat1 and NIH3T3 fibroblasts. Authors also speculated that additional oncogenic events may be required for transformation [94]. However, another similar study performed by Tatsuka et al., did not observe transforming potential of Aurora A alone in BALB/c 3T3A31-1 cells. Interestingly in co-transfection study, Aurora A forced expression potentiated G12V H-Ras induced transformation [95]. Ota et al. reported that overexpression of Aurora B induced histone H3 phosphorylation (Ser10) and mitotic phenotype in Chinese hamster embryo cells [96]. Further, when these cells were xenografted into mice, they were able to form aggressive and invasive tumors compared to control cells that express low Aurora B. Nonetheless, another similar study performed by Kanda et al. did not observed transforming potential of Aurora B alone in BALB/c 3T3 A31-1-1 cells. Here also forced expression of Aurora B augmented the frequency of G12V H-Ras induced transformation [97]. Role of Aurora C in transformation has not been yet established. All these studies

clearly suggest that AKs may not be directly involved in cancer initiation, but rather cooperate with or complement other oncogenes. Overexpression of AKs and their association with poor prognosis were reported consistently in many cancers, indicating that AKs are required for tumor maintenance, progression, and survival. These important functions of AKs are sufficient to consider them as viable targets in cancer disease, even though their clinical validation is still awaited.

Among the AKs, which Aurora kinase is the best target for effective cancer treatment has become an interesting topic of debate. Some reports suggest Aurora A inhibition has more cytotoxic than cytostatic effects [98], while others suggest targeting Aurora B is more effective [99]. MLN8237 is a highly specific and potent Aurora A inhibitor, which has been shown to induce apoptosis rapidly compared to other AKIs. It has also been shown to have anticancer activity on a wide range of cancer cell lines, such as MM cell lines. In clinical studies, it produced few side effects and had good pharmacokinetics and efficacy. Interestingly, MLN8237 has also displayed higher anticancer activity than standard agents in childhood cancer cell lines and their xenograft models. However, its efficacy under the pediatric clinical setting needs further studies. AZD1152 is a specific and potent Aurora B inhibitor, which is currently at the forefront of clinical studies compared to other Aurora inhibitors. It has been found to induce anticancer activity in both leukemias and solid tumors. It also induces rapid apoptosis in many cancer cell lines, suggesting it has cytotoxic activity. After AZD1152 administration, 15 patients with progressive cancer showed stable disease.

#### Dose limiting target toxicities of AKIs

Under in vitro conditions AKIs displayed broad anticancer activity in rapidly proliferating cancer cells, but not in resting cells. Hence it is likely that chemotherapy with AKIs may be toxic to rapidly dividing hematological cells. As anticipated, the most common on-target toxicity reported for many AKIs is grade 3/4 neutropenia. The other on-target toxicities reported include wide range of hematological toxicities including leukopenia and myelosuppression. Few cases of septicemia and pneumonia were also reported and they may be the consequences of neutropenia. On the other hand off-target toxicities were also reported for AKIs, which includes hypertension, somnolence, mucositis, stomatitis, proctalgia, grade 3 increase in aspartate aminotransferase, and grade 2 ventricular dysfunction. Importantly most of the side effects were reversible upon drug withdrawal. VX-680 caused cardio-toxicity and was associated with death of one patient, which prompted to suspend the compound from clinical trials recently. Probably the off-target toxicities of AKIs could be due to their cross-reaction with other kinases, since their spectrum varies from among individual AKIs.

AKIs described in this review displayed much high potency in hematological cancers both under in vitro and in vivo conditions compared to solid tumors. This clearly suggests that AKIs are highly active in rapidly cycling cells. This point corresponds to the dose limiting toxicity including bone marrow suppression and associated neutropenia in normal hematological cells. Drug related toxicities of AKIs on hematological cells and associated bone marrow toxicity was reported exceptionally well by Wilkinson et al. [71]. Bone marrow tissue from the AZD1152 treated rats were used to study the effect on rapidly dividing cells. Staining of the tissue revealed signs of atrophy associated with decrease in the total cellular content. However, myelosuppression was reversed within a week of AZD1152 withdrawal. Clinicians should consider intermittent dosings at appropriate intervals or metronomic therapy in order to better target tumor cells and allowing bone marrow cells to recover.

Administration of hematopoietic growth factors in conjunction with anticancer drugs may also help to reduce the severity of bone marrow toxicities. Many clinical studies were performed using growth factors in conjunction with anticancer agents and were successful to limit the bone marrow related toxicities [100]. In the context of AKIs, Cohen et al. used G-CSF in conjunction with PHA-739358 [34]. In this study they were able to escalate the PHA-739358 dose until 1000 mg/m<sup>2</sup> and did not reported any bone marrow related toxicities, particularly neutropenia. This was the first time they were able to achieve objective responses in patients with advanced solid tumors. On the other hand, grade 3/4 neutropenia and neutropenic infection were reported in the absence of G-CSF at around 500 mg/m<sup>2</sup> dose. Conjunctive use of growth factors would be beneficial in significantly reducing drug associated toxicities and also to enhance the efficacy of drugs by dose intensification.

#### Additional features of AKIs

From our review, one can appreciate many important aspects of AKIs. Firstly, almost all the AKIs cross-reacts with many structurally related oncogenic kinases including VEGFR2, FLT3, Bcr-Abl, JAK, and FGFR1. It has been consistently reported that these kinases are involved in the initiation and its progression of cancer. The main advantage of targeting multiple kinases other than AKs is that majority of cancers have abnormalities at multiple targets, thereby increasing the probability of effective treatment. Targeting multiple kinases may also prevent the emergence of resistance during AKI therapy, because resistance towards AKIs in the clinic is highly probable. To support this, recently Girdler et al. reported emergence of resistance in HCT116 cell line due to Aurora B mutations [93].

Secondly, we noticed that some pan-AKIs are significantly effective in drug resistant cancer lines. They were able to inhibit the cell proliferation equally or more efficiently compared to non-resistant parent cell lines. The authors of these studies were also able to successfully validate the AKIs ability to overcome the (multidrug) resistance in xenograft models at least with few AKIs. Hence AKIs may have a huge potential to overcome the resistance in patients with refractory cancers and some clinical studies are underway. Imatinib targeted towards Bcr-Abl has been highly successful in treating CML patients with Bcr-Abl translocation. In some patients complete hematological and cytological responses were achieved. However, during the course of imatinib chemotherapy, many patients acquired Abl kinase domain mutations resulting in imatinib resistance. Among multiple mutations, the gate keeper mutation, namely T315I is very aggressive, which renders complete resistance to imatinib and related compounds. Many AKIs were able to inhibit T315I Bcr-Abl mutations with high specificity than wild type Bcr-Abl. AKIs have also been proved to be efficient in reversal of resistance in T315I Bcr-Abl CML cell lines both *in vitro* and *in vivo*. This sparked the interest of testing the AKIs in refractory CML patients with T315I mutations and many clinical studies are underway. Discovery of AKIs efficiency in inhibiting T315I Bcr-Abl formed a strong rationale in testing the existing second generation kinase inhibitors on drug resistant mutants.

Thirdly, AKIs have a great potential to enhance the efficacy of other anticancer drug and radiation therapies, which can be exemplified by some reports. MK-5108 significantly enhanced the efficacy of docetaxel in HeLa-S3 and ES-2 cell lines both *in vitro* and *in vivo* [67]. Low concentrations of VE-465 alone synergized with paclitaxel and induced 4.5 fold greater apoptosis in 1A9 ovarian cancer cell line [81]. On the other hand AZD1152 [101] and PHA-680632 [79] greatly enhanced the effect of radiation treatment. These findings have potential interest for further clinical development. AKIs have broad anticancer activity in most of the cancer cell lines tested. The above described characteristics of AKIs make them very attractive candidates for targeted therapy.

#### Potential approvable AKIs for routine clinical use

In preliminary clinical studies, AKIs have consistently displayed cytostatic effects, tumor response or stable disease, particularly in solid tumors. However, because of the plethora of synthetic AKIs with diverse chemical structures, target and off-target activities, toxicological profiles, and efficacy, it is difficult to predict which compound(s) will enter clinical use. Certainly, one of the most interesting and advanced inhibitors is PHA-739358. This compound not only inhibits AKs, but it also has an off-target effect on Abl, Ret, and FGFR-1 oncogenic

kinases, which are implicated in many types of malignancies. Moreover, it has been shown to have good pharmacokinetic properties combined with high anticancer activity; 28/80 patients with solid tumors showed stable disease, which lasted for 6 months in six patients. As a result of these attributes PHA-739358 is regarded as a highly promising clinical candidate. Metastasis of a malignant tumor is one of the hallmarks of cancer and its progression. Hence, inhibition of metastasis by suppressing angiogenesis is a novel approach for cancer treatment. Interestingly, CYC116 and ENMD-2076 inhibits VEGFR-2, which directly promotes angiogenesis. These drugs have also exhibited significant anticancer effects on a broad range of cancer cell lines. These properties strongly encourage their further clinical development, which could improve overall survival of patients. AT9283 is a promising multikinase inhibitor with activity against, e.g., AKs, JAK2, JAK3, and Abl. In one clinical trial, 30% of patients showed stable disease, and the compound was well tolerated. One of the common mechanism of cancer cell drug resistance is the overexpression of Pgp, which actively effluxes the anticancer agent before reaching the target. Overexpression of Pgp and associated multidrug resistance was reported in cancer patients that are resistant to many anticancer agents. AMG-900 was able to overcome the resistance particularly in Pgp upregulated multidrug resistant cancer cell lines. AMG-900 may have great potential in both enhancing the therapeutic potential of anticancer agents and also in combating drug specific resistance.

#### Clinical efficacy of Aurora kinase inhibitors

Though AKIs have showed broad range anticancer activity in cell lines and xenograft models, they did not lived up to the expectations in the clinic. Here we speculate some of the reasons; firstly the rationale for targeting AKs is not validated. The main reason for targeting AKs is based on the fact that they are upregulated in many cancer types. It could be possible that tumors cells may not be addicted to AKs for their proliferation and survival as much as to Bcr-Abl, K-ras, or B-Raf oncogenes. Recently many questions were raised regarding the validity of AKs as oncogenes. Probably the role of AKs in inducing malignant phenotype is transient. This is probably one of the reasons that AKIs were not specifically efficient in any cancer type, compared to other routinely used anticancer agents in the clinic. For example platinum drugs are well known agents to treat ovarian and breast cancers, paclitaxel for ovarian and breast cancers, gemcitabine for pancreatic and lung cancers, and bortezomib and thalidomide for multiple myeloma. Secondly, polo-like kinases (PLK) share similar functions that are assigned to AKs [101]. This is strongly supported by the fact that cellular phenotypes overlap with the inhibition of PLKs and AKs. Thus it is likely that PLKs may complement the functions of AKs and may compromise

the AKIs induced effects. Hence outcome of combined inhibition of AKs and PLKs might be desirable compared to single target inhibition. Thirdly, mitotic inhibitors are well validated to treat cancer cells in vitro and in xenograft models, where tumors doubling times are relatively short. However, in real life situation human tumor cells have very long doubling times that may range from months to years. AKIs execute their mode of actions only when the cells are actively proliferating, as AKs are predominantly expressed in mitotic phase. In clinical trials, AKIs mostly induced only stable diseases (only in few patients), but rarely the partial or complete responses and this could be due to high doubling time of tumors cells. Most of the AKIs doses employed in the Phase I studies are relatively low, ranging from 3 to 200 mg/kg, due to DLTs, mainly neutropenia. These doses are well below the therapeutic window for activity. Thus further dose enhancements in Phase II studies in conjunction with growth factors would be beneficial. Cohen et al. successfully escalated the doses upto 1000 mg/m<sup>2</sup> in the presence of G-CSF and reported objective responses with reduced toxicities [34]. One of the solutions could be intermittent dosings at appropriate intervals or metronomic therapy to recover bone marrow cells should be considered.

## Conclusions

The AKs have been the focus of considerable attention since their discovery in *Drosophila* mutants, and many independent studies have contributed to our understanding of their biology. AKs have multiple important functions in mitosis, and their overexpression in some cancers prompted the discovery and development of novel AKIs as therapeutic drugs using a variety of experimental and computational techniques. Less than ten years after AKs were discovered in humans, more than ten Aurora inhibitors had entered clinical trial, and the number of new AKIs entering preclinical development or clinical trials is continuing to increase. No general mechanisms of tumor cell resistance to AKIs have yet been identified, although some preliminary studies suggest that mutations of the targeted Aurora kinase and overexpression of drug-resistance genes may be involved.

Further in-depth clinical studies are now required to evaluate the effectiveness of AKIs. Hence, it is too early to draw any conclusions regarding which compounds are likely to enter the market for routine use. Furthermore, identification of biomarkers based on gene expression studies, that are predictive of anticancer activity for a specific drug in individual patients is important. Some AKIs have been shown to be very effective in single agent or combination studies in some patients. Widely accepted functional pharmacological/surrogate biomarkers are available for both Aurora A and B inhibition, which makes them attractive targets. In the absence of tumor associated

biomarkers, neutropenia per se is a biomarker of Aurora kinase inhibition in the bone marrow cells. Thus, biomarkers that allow the efficacy of given AKI to be assessed offer the promise of individualized therapy, which academic clinicians are keen to pursue. Since AKIs are emerging as targeted cancer therapeutics with interesting off-target effects, one might reasonably hope that they could also be used to tackle the problem of resistance, and thus enhance the treatment of cancer.

**Acknowledgements** This study was supported by grants awarded by the Grant Agency of the Czech Republic (301/08/1649 and 303/09/H048), Internal Grant Agency of Palacky University (IGA UP LF 2011 018) and by a grant from Iceland, Liechtenstein and Norway through the EEA Financial Mechanism (CZ0099). The infrastructural part of this project (Institute of Molecular and Translational Medicine) was supported by the Operational Programme Research and Development for Innovations (project CZ.1.05/2.1.00/01.0030). We are thankful to Martin Mistrik, Ph.D. for confocal microscopy.

**Conflict of interest** The authors declare no conflict of interest.

**Open Access** This article is distributed under the terms of the Creative Commons Attribution License which permits any use, distribution, and reproduction in any medium, provided the original author(s) and the source are credited.

## References

- Glover DM, Leibowitz MH, McLean DA, Parry H (1995) Mutations in Aurora prevent centrosome separation leading to the formation of monopolar spindles. *Cell* 81:95–105
- Andrews PD (2005) Aurora kinases: shining lights on the therapeutic horizon? *Oncogene* 24:5005–5015
- Carmena M, Earnshaw WC (2003) The cellular geography of aurora kinases. *Nat Rev Mol Cell Biol* 4:842–854
- Chen HL, Tang CJ, Chen CY, Tang TK (2005) Overexpression of an Aurora-C kinase-deficient mutant disrupts the Aurora-B/INCENP complex and induces polyploidy. *J Biomed Sci* 12:297–310
- Marumoto T, Honda S, Hara T et al (2004) Aurora-A kinase maintains the fidelity of late and early mitotic events in HeLa cells. *J Bio Chem* 278:51786–1795
- Portier N, Audhya A, Maddox PS, Green RA, Dammermann A, Desai A, Oegema A (2007) A microtubule-independent role for centrosomes and Aurora A in nuclear envelope breakdown. *Dev Cell* 12:515–529
- Adams RR, Maiato H, Earnshaw WC, Carmena M (2001) Essential roles of *Drosophila* inner centromere protein (INCENP) and Aurora B in histone H3 phosphorylation, metaphase chromosome alignment, kinetochore disjunction, and chromosome segregation. *J Biol Chem* 15:865–880
- Knowlton AL, Lan W, Stukenberg P (2006) Aurora B is enriched at merotelic attachment sites, where it regulates MCAK. *Curr Biol* 16:1705–1710
- Goto H, Yasui Y, Nigg EA, Inagaki M (2002) Aurora B phosphorylates histone H3 at serine 28 with regard to the mitotic chromosome condensation. *Genes Cells* 7:11–17
- Li X, Sakashita G, Matsuzaki H, Sugimoto K, Kimura K, Hanaoka F, Taniguchi H et al (2004) Direct association with

- inner centromere protein (INCENP) activates the novel chromosomal protein, Aurora-C. *J Biol Chem* 279:47201–47211
11. Yan X, Cao L, Li Q, Wu Y, Zhang H, Saiyin H, Liu X et al (2005) Aurora C is directly associated with survivin and is required for cytokinesis. *Genes Cells* 10:617–626
  12. Marumoto T, Zhang D, Saya H (2005) Aurora-A—a guardian of poles. *Nat Rev Cancer* 5:42–50
  13. Sen S, Zhou H, White RA (1997) A putative serine/threonine kinase encoding gene BTAK on chromosome 20q13.2 is amplified and overexpressed in human breast cancer cell lines. *Oncogene* 14:2195–2200
  14. Reichardt W, Jung V, Brunner C, Klien A, Wemmer S, Romeike BF, Zang KD, Urbschat S (2003) The putative serine/threonine kinase gene STK15 on chromosome 20q13.2 is amplified in human gliomas. *Oncol Rep* 10:1275–1279
  15. Zhou H, Kuang J, Zhong L, Kuo WL, Gray JW, Sahin A, Brinkley BR, Sen S (1998) Tumour amplified kinase STK15/BTAK induces centrosome amplification, aneuploidy and transformation. *Nat Genet* 20:189–193
  16. Tchatchou S, Wirtzenberger M, Hemminki K, Sutter C, Meindl A, Wappenschmidt B, Kiechle M, Bugert P, Schmutzler RK, Bartram CR, Burwinkel B (2007) Aurora kinases A and B and familial breast cancer risk. *Cancer Lett* 247:66–72
  17. Katayama H, Ota T, Jisaki F, Ueda Y, Tanaka T, Odashima S, Suzuki F, Terada Y, Tatsuka M (1999) Mitotic kinase expression and colorectal cancer progression. *J Natl Cancer Inst* 91:1160–1162
  18. Sorrentino R, Libertini S, Pallante PL, Troncone G, Palombini L, Bavetsias V, Spalletti-Cernia D et al (2004) Aurora B overexpression associates with the thyroid carcinoma undifferentiated phenotype and is required for thyroid carcinoma cell proliferation. *J Clin Endocrinol Metab* 90:928–935
  19. Zeng WF, Navaratne K, Prayson RA, Weil RJ (2007) Aurora B expression correlates with aggressive behaviour in glioblastoma multiforme. *J Clin Pathol* 60:218–221
  20. Liu Q, Kaneko S, Yang L, Feldman RI, Nicosia SV, Chen J, Cheng JQ (2004) Aurora-A abrogation of p53 DNA binding and transactivation activity by serine 215. *J Biol Chem* 279:52175–52182
  21. Howard S, Berdini V, Boulstridge JA, Carr MG, Cross DM, Curry J, Devine LA et al (2009) Fragment based discovery of the pyra-4-yl-urea (AT9283), a multitargeted kinase inhibitor with potent aurora kinase activity. *J Med Chem* 52:379–388
  22. Mortlock AA, Keen NJ, Jung FH, Heron NM, Foote KM, Wilkinson RW, Green S (2005) Progress in the development of selective inhibitors of aurora kinases. *Curr Top Med Chem* 5:199–213
  23. Warner SL, Bashyam S, Vankayalapati H, Bearss DJ, Han H, Mahadevan D, Von Hoff DD, Hurley LH (2006) Identification of a lead small-molecule inhibitor of the Aurora kinases using a structure assisted, fragment-based approach. *Mol Cancer Ther* 5:1764–1773
  24. Cancilla MT, He MM, Viswanathan N, Simmons RL, Taylor M, Fung AD, Cao K, Erlanson DA (2008) Discovery of an Aurora kinase inhibitor through site-specific dynamic combinatorial chemistry. *Bioorg Med Chem Lett* 18:3978–3981
  25. Fu DH, Jiang W, Zheng JT, Zhao GY, Li Y, Yi H, Li ZR et al (2008) Jadomycin B, an Aurora-B kinase inhibitor discovered through virtual screening. *Mol Cancer Ther* 7:2386–2393
  26. Oslob JD, Romanowski MJ, Allen DA, Baskaran S, Bui M, Elling RA, Flanagan WM et al (2008) Discovery of potent and selective aurora kinase inhibitor. *Bioorg Med Chem Lett* 18:4880–4884
  27. Fancelli D, Berta D, Bindi S, Cameron A, Cappella P, Carpinelli P, Catana C et al (2005) Potent and selective Aurora inhibitors identified by a novel scaffold for protein kinase inhibition. *J Med Chem* 48:3080–3084
  28. Fancelli D, Moll J, Varasi M, Bravo R, Artico R, Berta D, Bindi S et al (2006) 1, 4, 5, 6-tetrahydropyrrolo [3, 4-c] pyrazoles: identification of a potent Aurora kinase inhibitor with a favorable antitumor kinase inhibition profile. *J Med Chem* 49:7247–7251
  29. Aliagas-Martin H, Burdick D, Corson L, Dotson J, Drummond J, Fields C, Huang OW et al (2009) A class of 2,4-bisaminopyrimidine Aurora A inhibitor with unusually high selectivity against Aurora B. *J Med Chem* 52:3300–3307
  30. Zhao B, Smallwood A, Yang J, Koretke K, Nurse K, Calamari A, Kirkpatrick RB, Lai Z (2008) Modulation of kinase-inhibitor interactions by auxiliary protein binding: crystallography studies on Aurora A interactions with VX-680 and with TPX2. *Protein Sci* 17:1791–1797
  31. De Lano WL (2002) The PyMOL molecular graphic system. De Lano Scientific LLC, San Carlos
  32. Carpinelli P, Ceruti R, Giorgini ML, Cappella P, Gianellini L, Croci V, Degrassi A et al (2007) PHA-739358, a potent inhibitor of Aurora kinases with a selective target inhibition profile relevant to cancer. *Mol Cancer Ther* 6:3158–3168
  33. Paquette R, Shah N, Sawyers C, Martinelli G, Nicoll J, Chalukya M, Locatelli G, Capolongo L, Moll J, Comis S, Laffranchi B (2008) PHA-739358: a pan-Aurora kinase inhibitor. *Haematol Meet Rep* 2:92–93
  34. Cohen RB, Jones SF, Aggarwal C, von Mehren M, Cheng J, Spigel DR, Greco FA et al (2009) A phase I dose-escalation study of danusertib (PHA-739358) administered as a 24-hour infusion with and without granulocyte colony-stimulating factor in a 14-day cycle in patients with advanced solid tumors. *Clin Cancer Res* 15:6694–6701
  35. Modugno M, Casale E, Soncini C, Rosettani P, Colombo R, Lupi R, Rusconi L et al (2007) Crystal structure of the T3151 Abl mutant in complex with the aurora kinases inhibitor PHA-739358. *Cancer Res* 67:7987–7990
  36. Wang S, Midgley CA, Scaerou F, Grabarek JB, Griffiths G, Jackson W, Kontopidis G et al (2010) Discovery of N-Phenyl-4-(thiazol-5-yl)pyrimidin-2-amine Aurora kinase inhibitors. *J Med Chem* 53:4367–4378
  37. Griffiths G, Scaerou F, Sorrell D, Duckmanton A, Tosh C, Lewis S, Midgley C et al (2008) Anti-tumor activity of CYC116, a novel small molecule inhibitor of aurora kinases and VEGFR2. *AAO Annual Meeting*; 12–16 April 2008, San Diego, CA, USA, Abstract 651
  38. Hajdudich M, Vydra D, Dzubak P, Stuart I, Zheleva D (2008) *In vivo* mode of action of CYC116, a novel small molecule inhibitor of Aurora kinases and VEGFR2. *AAO Annual Meeting*; 12–16 April 2008, San Diego, CA, USA, Abstract 5645
  39. Arbitrario JP, Belmont BJ, Evanchik MJ, Flanagan WM, Fucini RV, Hansen SK, Harris SO et al (2010) SNS-314, a pan-Aurora kinase inhibitor, shows potent anti-tumor activity and dose flexibility *in vivo*. *Cancer Chemother Pharmacol* 65:707–717
  40. Robert F, Hurwitz H, Verschraegen CF, Verschraegen R, Advani R, Berman C, Taverna P, Evanchik M (2009) Phase 1 trial of SNS-314, a novel selective inhibitor of aurora kinases A, B, and C, in advanced solid tumor patients. *ASCO Annual Meeting*; 29 May–2 June 2009, Orlando, FL, USA, Abstract 14642
  41. Bebbington D, Binch H, Charreir JD, Everitt S, Fraysee D, Golec J, Kay D et al (2009) The discovery of potent aurora inhibitor MK-0457 (VX-680). *Bioorg Med Chem Lett* 19:3586–3592
  42. Harrington EA, Bebbington D, Moore J, Rasmussen RK, Ajose-Adeogun AO, Nakayama T, Graham JA et al (2004) VX-680, a potent and selective small-molecule inhibitor of the Aurora kinases, suppresses tumor growth *in vivo*. *Nat Med* 10:262–267
  43. Cheetam GM, Charlton PA, Golec JM, Pollard JR (2007) Structural basis for potent inhibition of the Aurora Kinases and a T135I multi-drug resistant form of Abl kinase by VX-680. *Cancer Lett* 251:323–329
  44. Tanaka R, Squires MS, Kimura S, Yokota A, Nagao R, Yamauchi T, Takeuchi M et al (2010) Activity of multitargeted kinase

- inhibitor, AT9283, in imatinib-resistant BCR-ABL-positive leukemia cells. *Blood* 116:2089–2095
45. Lyons J, Curry J, Reule M et al (2008) Biomarker identification of AT9283: a multitargeted kinase inhibitor with Aurora A and Aurora B activities from pre-clinical models to clinical trials. AACR centennial conference; 20–23 July 2008, California, USA
  46. Foran JM, Ravandi F, O'Brien SM, Borthakur G, Rios M, Boone J, Worrell K et al (2008) A phase I and pharmacodynamic trial of AT9283, an aurora kinase inhibitor in patients with refractory leukemia. ASCO Annual Meeting; 30 May–3 June 2008, Chicago, IL, USA, Abstract 2518
  47. Kristeleit R, Calvert H, Arkenau H, Olmos D, Adam J, Plummer ER, Lock V et al (2009) A phase I study of AT9283, an aurora kinase inhibitor in patients with refractory solid tumours, ASCO Annual Meeting; 29 May–2 June 2009, Orlando, FL, USA, Abstract 2566
  48. McLaughlin J, Markovtsov V, Li H, Wong S, Gelman M, Zhu Y, Franci C et al (2010) Preclinical characterization of Aurora kinase inhibitor R763/AS703569 identified through an image-based phenotypic screen. *J Cancer Res Clin Oncol* 136:99–113
  49. Renshaw JS, Patnaik A, Gordon M, Beerman M, Fischer D, Gianella-Borradori A, Lin C, Mendelson D (2007) A phase I two arm trial of AS703569 (R763), an orally available aurora kinase inhibitor, in subjects with solid tumors: preliminary results. ASCO Annual Meeting; 30 May–3 June 2007, Chicago, IL, USA, Abstract 14130
  50. Sonet A, Graux C, Maertens J et al (2008) Phase I, dose-escalation study of 2 dosing regimens of AS703569, an inhibitor of aurora and other kinases, administered orally in patients with advanced hematological malignancies. *Blood (ASH Annual Meeting)* 2008:112
  51. Bhattacharya S, Wishka D, Luzzio M, Arcari J, Bernardo V, Briere D, Boyden T et al (2008) SAR and chemistry of Aurora kinase inhibitors: discovery of PF-3814735, an oral clinical candidate. AACR Annual Meeting; 12–16 April 2008, San Diego, CA, USA
  52. Jani JP, Arcari J, Bernardo V (2010) PF-03814735, an orally bioavailable small molecule Aurora kinase inhibitor for cancer therapy. *Mol Cancer Ther* 9:883–894
  53. Schoffski P, Jone SF, Dumez H, Infante JR, Van Mieghem E, Fowst C, Gerletti P et al (2011) Phase I, open-label, multicentre, dose-escalation, pharmacokinetic and pharmacodynamic trial of the oral aurora kinase inhibitor PF-03814735 in advanced solid tumours. *Eur J Cancer* 47:2256–2264
  54. Adams ND, Adams JL, Burgess JL, Chaudhari AM, Copeland RA, Donatelli CA, Drewry DH et al (2010) Discovery of GSK1070916, a potent and selective inhibitor of Aurora B/C kinase. *J Med Chem* 53:3973–4001
  55. Anderson K, Lai Z, McDonald OB, Stuart JD, Nartey EN, Hardwicke MA, Newlander K et al (2009) Biochemical characterization of GSK1070916, a potent and selective inhibitor of aurora B and aurora C kinases with an extremely long residence time. *Biochem J* 13:259–265
  56. Hardwicke MA, Oleykowski CA, Plant R, Wang J, Liao Q, Moss K, Newlander K et al (2009) GSK1070916, a potent Aurora B/C kinase inhibitor with broad antitumor in tissue culture cells and human tumor xenografts models. *Mol Cancer Ther* 8:1808–1817
  57. Payton M, Bush TL, Chung G, Ziegler B, Eden P, McElroy P, Ross S et al (2010) Preclinical evaluation of AMG 900, a novel potent and highly selective pan-aurora kinase inhibitor with activity in taxane-resistant tumor cell lines. *Cancer Res* 70:9846–9854
  58. Sells T, Ecsedy J, Stroud S et al (2008) MLN8237: an orally active small molecule inhibitor of Aurora A kinase in phase I clinical trials. AACR Annual Meeting; 12–16 April 2008, San Francisco, CA, USA, Abstract 237
  59. Kelly KR, Ecsedy J, Medina E, Mahalingam D, Padmanabhan S, Nawrocki ST, Giles FJ, Carew JS (2011) The novel Aurora A kinase inhibitor MLN8237 is active in resistant chronic myeloid leukemia and significantly increases the efficacy of nilotinib. *J Cell Mol Med* 15:2057–2070
  60. Gorgun G, Calabrese E, Hideshima E, Ecsedy J, Perrone G, Mani M, Ikeda H et al (2010) A novel Aurora-A kinase inhibitor MLN8237 induces cytotoxicity and cell-cycle arrest in multiple myeloma. *Blood* 115:5202–5213
  61. Maris JM, Morton CL, Gorlick R, Kolb EA, Lock R, Carol H, Keir ST et al (2010) Initial testing of Aurora A inhibitor MLN8237 by the pediatric preclinical testing program. *Pediatr Blood Cancer* 55:26–34
  62. Infante J, Dees EC, Cohen RB (2008) Phase I study of the safety, pharmacokinetics (PK), and pharmacodynamics (PD) of MLN8237, a selective Aurora A kinase inhibitor, in the United States. *Eur J Cancer Suppl* 6:90–91, Abstract 280
  63. Fletcher GC, Brokx RD, Denny TA, Hembrough TA, Plum SM, Fogler WE, Sidor CF, Bray MR (2010) ENMD-2076 is an orally-active kinase inhibitor with antiangiogenic and antiproliferative mechanisms of action. *Mol Cancer Ther* 10:126–137
  64. Wang X, Sinn AL, Pollok A, Sandusky G, Zhang S, Chen L, Liang J et al (2010) Preclinical activity of a novel multiple tyrosine kinase and aurora kinase inhibitor, ENMD-2076, against multiple myeloma. *Br J Haematol* 150:313–325
  65. Tentler JJ, Bradshaw-Pierce EL, Serkova NJ, Hassebrook KM, Pitts TM, Diamond JR, Fletcher GC, Bray MR, Eckhardt SG (2010) Assessment of the *in vivo* antitumor effects of ENMD-2076, a novel multitargeted kinase inhibitor, against primary and cell line-derived human colorectal cancer xenograft models. *Clin Cancer Res* 16:2989–2998
  66. Diamond JR, Bastos BR, Hansen RJ, Gustafson DL, Eckhardt SG, Kwak EL, Pandya AA et al (2011) Phase I safety, pharmacokinetic, and pharmacodynamic study of ENMD-2076, a novel angiogenic and Aurora kinase inhibitor, in patients with advanced solid tumors. *Clin Cancer Res* 17:849–860
  67. Shimomura T, Hasako S, Nakatsuru Y, Mita T, Ichikawa K, Kodera T, Sakai T et al (2010) MK-5108, a highly selective Aurora-A kinase inhibitor, shows antitumor activity alone and in combination with docetaxel. *Mol Cancer Ther* 9:157–166
  68. Minton SE, LoRusso P, Lockhart AC et al (2010) A phase I study of MK-5108, an oral aurora A kinase inhibitor, in both monotherapy and in combination with docetaxel in patients with advanced solid tumors. *J Clin Oncol* 28;15s suppl:abstr e13026
  69. Yang J, Ikezoe T, Nishioka C, Tasaka T, Taniguchi A, Kuwayama Y, Komatsu N et al (2007) AZD1152, a novel and selective aurora B kinase inhibitor, induces growth arrest, apoptosis and sensitization for tubulin depolymerizing agent or topoisomerase II inhibitor in human acute leukemia cells *in vitro* and *in vivo*. *Neoplasia* 110:2034–2040
  70. Mortlock AA, Foote KM, Heron NM, Jung FH, Pasquet G, Lohmann JJ, Warin N et al (2007) Discovery, synthesis, and *in vivo* activity of a new class of pyrazoloquinazolines as selective inhibitors of aurora B kinase. *J Med Chem* 50:2213–2224
  71. Wilkinson RW, Odedra R, Heaton SP, Wedge SR, Keen NJ, Crafter C, Foster JR et al (2007) AZD1152, a selective inhibitor of aurora B kinase, inhibits human tumor xenograft growth by inducing apoptosis. *Clin Cancer Res* 13:3682–3688
  72. Schellens JH, Boss D, Witteveen PO, Zandvliet A, Beijnen JH, Voogel-Fuchs M, Morris C, Wilson D, Voest EE (2006) Phase I and pharmacological study of the novel Aurora kinase inhibitor AZD1152. *J Clin Oncol* 24:3008 (suppl)
  73. Lowenberg B, Muus P, Ossenkoppele G, Rousselot P, Cahn JY, Ifrah N, Martinelli G et al (2011) Phase I/II study to assess safety, efficacy, and pharmacokinetics of barasertib (AZD1152) in patients with advanced acute myeloid leukemia. *Blood* 118:6030–6036

74. Boss DS, Witteveen PO, Van der sar J, Lolkema MP, Voest EE, Stockman PK, Ataman O, Wilson D, Das S, Schellens JH (2010) Clinical evaluation of AZD1152, an i.v. inhibitor of Aurora B kinase, in patients with solid malignant tumors. *Ann Oncol* 22:431–437
75. Gurtler U, Tontsch-Grunt U, Jarvis M, Zahn SK, Boehmelt G, Quant J, Adolf GR et al (2010) Effect of BI 811283, a novel inhibitor of Aurora B kinase, on tumor senescence and apoptosis. *J Clin Oncol* 28;suppl:abstr e13632
76. Mross KB, Scheulen ME, Frost A, Scharf D, Richly H, Nokay B, Lee K et al (2010) A phase I dose-escalation study of BI 811283, an Aurora B inhibitor, administered every three weeks in patients with advanced solid tumors. *J Clin Oncol* 28; 15s suppl:abstr 3011
77. Scheulen ME, Mross KB, Richly H, Nokay B, Frost A, Lee K, Saunders O et al (2010) A phase I dose-escalation study of BI 811283, an Aurora B inhibitor, administered day 1 and 15, every four weeks in patients with advanced solid tumors. *J Clin Oncol* 28; 15s suppl:abstr e13065
78. Soncini C, Carpinelli P, Gianellini L, Fancelli D, Vianello P, Rusconi L, Storicci P et al (2006) PHA-680632, a novel aurora kinase inhibitor with potent antitumoral activity. *Clin Cancer Res* 12:4080–4089
79. Tao Y, Zhang P, Frascogna V, Lecluse Y, Auperin A, Bourhis J, Deutsch E (2007) Enhancement of radiation response by inhibition of Aurora-A kinase using siRNA or a selective Aurora kinase inhibitor PHA680632 in p53-deficient cancer cells. *Br J Cancer* 97:1664–1672
80. Lin ZZ, Hsu HC, Hsu CH, Yen PY, Huang CY, Huang YF, Chen TJ et al (2009) The Aurora kinase inhibitor VE-465 has anticancer effects in pre-clinical studies of human hepatocellular carcinoma. *J Hepatol* 50:518–527
81. Scharer CD, Laycock N, Osunkoya AO, Logani S, McDonald JF, Benigno BB, Moreno CS (2008) Aurora kinase inhibitors synergize with paclitaxel to induce apoptosis in ovarian cancer cells. *J Transl Med* 6:1–13
82. Negri JM, McMillin DW, Delmore J, Mitsiades N, Hayden P, Klippel S, Hideshima T et al (2009) *In vitro* anti-myeloma activity of the Aurora kinase inhibitor VE-465. *Br J Hematol* 147:672–676
83. Lin R, Connolly PJ, Huang S, Wetter SK, Lu Y, Murray MV, Emanuel SL et al (2005) 1-Acyl-1H-[1,2,4]triazole-3,5-diamine analogues as novel and potent anticancer cyclin-dependent kinase inhibitors: synthesis and evaluation of biological activities. *J Med Chem* 48:4208–4211
84. Emanuel S, Rugg CA, Gruninger RH, Lin R, Fuentes-Pesquera A, Connolly PJ, Wetter SK et al (2005) The *In vitro* and *In vivo* effects of JNJ-7706621: A dual inhibitor of cyclin-dependent kinases and aurora kinases. *Cancer Res* 65:9038–9046
85. Chan F, Sun C, Perumal M, Nguyen QD, Bavetsias V, McDonald E, Martins V et al (2007) Mechanism of action of the aurora kinase inhibitor CCT129202 and *in vivo* quantification of biological activity. *Mol Cancer Ther* 6:3147–3157
86. Aurora kinase/VEGFR2 inhibitors (2010). <http://www.telik.com/pdf/targets/Aurora.pdf>. Accessed 6 May 2010
87. Rawson TE, Ruth M, Blackwood E, Burdick D, Corson L, Dotson J, Drummond J et al (2008) A pentacyclic aurora kinase inhibitor (AKI-001) with high *in vivo* potency and oral bioavailability. *J Med Chem* 51:4465–4475
88. CHR-3520: Potent Aurora/multi-kinase inhibitor (2010). [http://www.chromatherapeutics.com/Aurora-Kinase\\_backup.html](http://www.chromatherapeutics.com/Aurora-Kinase_backup.html). Accessed 26 April 2010
89. Hauf S, Cole RW, LaTerra S, Zimmer C, Schnapp G, Walter R, Heckel A, van Meel J, Rieder CL, Peters JM (2003) The small molecule Hesperadin reveals a role for Aurora B in correcting kinetochore-microtubule attachment and in maintaining the spindle assembly checkpoint. *J Cell Biol* 161:281–294
90. Ditchfield C, Johnson VL, Tighe A, Ellston R, Haworth C, Johnson T, Mortlock A, Keen N, Taylor SS (2003) Aurora B couples chromosome alignment with anaphase by targeting BubR1, Mad2, and Cenp-E to kinetochores. *J Cell Biol* 161:267–280
91. Guo J, Anderson MG, Tapang P, Palma JP, Rodriguez LE, Niquette A, Li J et al (2009) Identification of genes that confer tumor cell resistance to the Aurora B kinase inhibitor AZD1152. *Pharmacogenomics J* 9:90–102
92. Seamon JA, Rugg CA, Emanuel S, Calcagno AM, Ambudkar SV, Middleton SA, Butler J, Borowski V, Greenberger LM (2006) Role of the ABCG2 drug transporter in the resistance and oral bioavailability of a potent cyclin-dependent kinase/Aurora kinase inhibitor. *Mol Cancer Ther* 5:2459–2467
93. Girdler F, Sessa F, Patercoli S, Villa F, Musacchio A, Taylor S (2008) Molecular basis of drug of resistance in Aurora kinases. *Chem Biol* 15:552–562
94. Bischoff JR, Anderson L, Zhu Y, Mossie K, Ng L, Souza B, Schryver B et al (1998) A homologue of drosophila Aurora kinase is oncogenic and amplified in human colorectal cancers. *EMBO J* 17:3052–3065
95. Tatsuka M, Sato S, Kitajima S, Suto S, Kawai H, Miyachi M, Ogawa I et al (2005) Overexpression of Aurora-A potentiates H-RAS-mediated oncogenic transformation and is implicated in oral carcinogenesis. *Oncogene* 24:1122–1127
96. Ota Y, Suto S, Katayama H, Han ZB, Suzuki F, Maeda M, Tanino M et al (2002) Increased mitotic phosphorylation of mitotic histone H3 attributable to AIM-1/Aurora B overexpression contributes to chromosome number instability. *Cancer Res* 62:5168–5177
97. Kanda A, Kawai H, Suto S, Kitajima S, Sato S, Takata T, Tatsuka M (2005) Aurora-B/AIM-1 kinase activity is involved in Ras-mediated cell transformation. *Oncogene* 24:7266–7272
98. Warner SL, Munoz RM, Stafford P, Koller E, Hurley LH, Von Hoff DD, Han H (2006) Comparing aurora A and aurora B as molecular targets for growth inhibition of pancreatic cancer cells. *Mol Cancer Ther* 5:2450–2458
99. Girdler F, Gascoigne KE, Evers PA, Hartmuth S, Crafter C, Foote KM, Keen NJ, Taylor SS (2006) Validating aurora B as an anti-cancer drug target. *J Cell Sci* 119:3664–3675
100. Crawford J, Ozer H, Stoller R, Johnson D, Lyman G, Tabbara I, Kris M et al (1991) Reduction by granulocyte colony-stimulating factor of fever and neutropenia induced by chemotherapy in patients with small-cell lung cancer. *N Engl J Med* 325:164–170
101. Tao Y, Zhang P, Girdler F, Frascogna V, Castedo M, Bourhis J, Kroemer G, Deutsch E (2008) Enhancement of radiation response in p53-deficient cancer cells by Aurora-B kinase inhibitor AZD1152. *Oncogene* 22:3244–3255
102. Len SM, Voest EE, Medema RH (2010) Shared and separate functions of polo-like kinases and aurora kinases in cancer. *Nat Rev Cancer* 10:825–841

### 3.4

#### **Identification and characterization of drug resistance mechanisms in cancer cells against Aurora kinase inhibitors CYC116 and ZM447439**

Madhu Kollareddy<sup>1</sup>, Daniella Zheleva<sup>2</sup>, Petr Džubák<sup>1</sup>, Josef Srovnal<sup>1</sup>, Lenka Radová<sup>1</sup>, Dalibor Doležal<sup>1</sup>, Vladimíra Koudeláková<sup>1</sup>, Pathik Subhashchandra Brahmshatriya<sup>3</sup>, Martin Lepšík<sup>3</sup>, Pavel Hobza<sup>3</sup>, and Marián Hajdúch<sup>1</sup>

**Authors Affiliations:** <sup>1</sup>Institute of Molecular and Translational Medicine, Faculty of Medicine, Palacky University, Olomouc, Czech Republic; <sup>2</sup>Cyclacel Ltd, Dundee, United Kingdom, <sup>3</sup>Institute of Organic Chemistry and Biochemistry, v.v.i. and Gilead Sciences and IOCB Research Center, Academy of Sciences of the Czech Republic, 166 10 Prague, Czech Republic

**Running title:** Resistance mechanisms against Aurora kinase inhibitors

**Key words:** CYC116, resistance, polyploidy, Bcl-xL, ABT-263

**Grant Support:** This study was supported by the Grant Agency of the Czech Republic (301/08/1649 and GAČR 303/09/H048) and Internal Grant Agency of the Palacky University (IGA UP LF 2011 018). Infrastructural part of this project (Institute of Molecular and Translational Medicine) was supported by the Operational Programme Research and Development for Innovations (project CZ.1.05/2.1.00/01.0030).

The modeling part of the work was supported by a part of research project no. RVO: 61388963 of the IOCB, Academy of Sciences of the Czech Republic and was supported by Czech Science Foundation [P208/12/G016]. This work was also supported by the Operational Program Research and Development for Innovations - European Science Fund (CZ.1.05/2.1.00/03.0058). The support of Praemium Academiae of the Academy of Sciences of the Czech Republic awarded to P.H. in 2007 is also acknowledged. The financial support from the Gilead Sciences and IOCB Research Center, Prague, is also acknowledged.

**Corresponding Author:** Marian Hajduch, Institute of Molecular and Translational Medicine, Faculty of Medicine, Palacky University, Hnevotinska, Olomouc 775 15. Czech Republic, Phone: 00420-58-563-2082; Fax: 00420-58-585-2527; E-mail: marian.hajduch@upol.cz

**Disclosure of Potential Conflicts of Interest:** Daniella Zheleva is an employee of Cyclacel Ltd. No potential conflicts of interests were disclosed



## Abstract

CYC116 is a selective Aurora kinase inhibitor that has been tested in a Phase I study in patients with advanced solid tumors. Although CYC116 has shown desirable preclinical efficacy, the potential for emergence of resistance has not been explored. We established several CYC116 resistant clones from isogenic HCT116 and HCT116 p53<sup>-/-</sup> cell line pairs. We also generated resistant clones towards ZM447439 (quinazoline derivative), a model Aurora inhibitor. The selected clones were 10-80 fold resistant to CYC116 and cross-resistant to other synthetic Aurora inhibitors including AZD1152, VX-680, and MLN8054. Resistant clones displayed multidrug resistant phenotypes, tested by using 13 major cytostatics. All clones were highly resistant to etoposide followed by other drugs. Interestingly, all CYC116 clones but not ZM447439 became polyploid. ZM447439, but not CYC116 induced three novel mutations in Aurora B. Leu152Ser significantly affected ZM447439 binding, but not CYC116. Gene expression studies revealed differential expression of more than 200 genes. Some of these genes expression profiles were also observed in CYC116 resistant primary tumors. Bcl-xL (BCL2L1) was found to be overexpressed in CYC116 clones and its knockdown resensitized the p53<sup>+/+</sup> resistant clones to CYC116. Finally Bcl-xL overexpressing p53<sup>+/+</sup> CYC116 clones were highly sensitive to navitoclax (ABT-263) compared to parent cells. The data shed light on the genetic basis for resistance to Aurora kinase inhibitors which could be used to predict and monitor clinical response, to select patients who might benefit from therapy and to suggest suitable drug combinations for a particular patient population.

## Introduction

A major approach for effective cancer treatment in recent years is the development of targeted therapy. Focused research on biochemical pathways, involved in cancer genesis and progression, and evaluating differences between normal and transformed cells, allowed identifying new cancer targets. Few important examples of targets which are particularly involved in the transformation of a cell are cyclin dependent kinases (1), protein kinase B (Akt) (2), Bcl-2 (3), VEGFR-2 (4), B-RAF (5), BCR-ABL (6), and polo like kinases (7). Aurora kinases (AKs) (serine/threonine) have recently emerged as interesting drug targets. They are involved in the regulation of the cell cycle and have multiple functions in mitosis. AKs A, B, and C are highly conserved and each has distinct and overlapping functions and sub-cellular locations. One of the hall marks of cancer cell is genomic instability. Since AKs regulate genomic stability, it is not surprising that their aberrant expression leads to cancer. Several reports have been published that many cancers overexpress AKs, which leads to enhanced proliferation and genomic instability. AKs are widely considered as oncogenes (8).

Several Aurora kinase inhibitors (AKIs) are in various phases of anticancer clinical trials and some are in preclinical development (9). CYC116 ([4-(2-amino-4-methyl-thiazol-5-yl)pyrimidin-2-yl]-(4-morpholin-4-ylphenyl)-amine) is a novel pan-Aurora kinase (Aurora A: 44 nM, B: 16 nM, & C: 95 nM IC50s) and VEGFR2 (IC50: 69 nM) inhibitor, which has been tested in a Phase I study. It showed significant antiproliferative activity on various cancer cell lines and solid xenograft models (10). Its suppressed angiogenesis, inhibited histone H3 phosphorylation (pH3ser10), and induced accumulation of 4n and >4n DNA in mice with P388D1 leukemia (Hajduch M et al., AACR 2008, Abstract 5645). Also tumor neovascularization was reduced significantly, possibly due to the VEGFR2 inhibition. CYC116 is a promising anticancer compound with significant specificity and potency, which could benefit patients with various cancers. As with most of the targeted drugs, primary or acquired resistance to CYC116 is expected to occur in the clinic.

Our study was focused on identification of potential cancer cell resistance mechanisms towards CYC116 alongside the first tool AKI, ZM447439 (11). Two isogenic colon cancer cell lines; HCT116 p53+/+ and HCT116 p53-/- were used as models in order to investigate role of the p53 gene. Here, we report the identification and characterization of potential tumor cell resistance mechanisms towards CYC116 and ZM447439. All selected clones were highly resistant and also cross-resistant to other AKIs and to some approved cancer drugs. We found overexpression of antiapoptotic Bcl-xL (BCL2L1) in CYC116 resistant clones, particularly the one with p53. Knockdown of Bcl-xL significantly restored the sensitivity to CYC116. Further, navitoclax (ABT-263), a small molecule Bcl-2 inhibitor (12) showed high activity selectively on Bcl-xL overexpressing resistant clones. These data suggest that the upregulation of Bcl-xL could limit the clinical response to CYC116. Additionally, ZM447439 resistant clones acquired Aurora B mutations, which significantly affected drug binding and anti-proliferative activity.

## **Materials and Methods**

### **Cell lines & Proliferation assay**

HCT116 p53<sup>+/+</sup> and HCT116 p53<sup>-/-</sup> cell lines were purchased from Horizon discovery. All cell lines were cultured in Dulbecco's modified eagles media (DMEM) (Sigma-Aldrich) supplemented with 10% FBS, 100 µg/mL streptomycin, and 100 U/mL MTT (3-(4,5-Dimethylthiazol-2-yl)-2,5-diphenyltetrazolium bromide) based proliferation assay was performed as described previously (13).

### **AKIs and anticancer drugs**

CYC116 was provided by Cyclacel Ltd. ZM447439 was purchased from Tocris. AZD1152, VX680, and MLN8054 were purchased from Selleckchem. Anticancer drugs were purchased from Bristol-Myers Squibb (paclitaxel), Ebewe (doxorubicin, 5-fluorouracil, etoposide), Sigma (daunorubicin), Lachema (cisplatin, carboplatin, oxaloplatin), Lilly (gemcitabine), Unipharma (cladribine), Ovation (actinomycin-D), Glaxo (topotecan), Janssen-Cilag (bortezomib), and signalling inhibitors (ABT-263).

### **Cell cycle analysis and pH3 (ser10) staining**

The cell cycle analysis was carried out in three replicates as described previously (14). For phospho-histone H3 (ser10) staining, cells were harvested and fixed following the cell cycle method. The cells were washed in PBS (phosphate saline buffer) containing 1% fetal bovine serum (FBS) solution. The pellet was suspended in PBS, 0.25% Triton X-100 (Sigma) and incubated on ice for 15 min. The pellet was washed with PBS, 1% FBS solution and stained with 100 µl of phospho-histoneH3 antibody (Upstate 1:500) for 1 h. The unbound antibody was washed out and suspended in 100 µl of secondary Alexa flour 488 goat anti-rabbit IgG (Invitrogen, 1:500) and incubated for 30 min. After washing, the pellet was suspended in DNA staining/RNase solution (50 µg/ml propidium iodide, 0.5 mg/ml RNase in PBS, 1%FBS) and incubated in dark at 37°C for 30 min and finally analyzed by flowcytometry (FACSCalibur, Becton Dickinson).

### **Computational modeling**

Interactions of ZM447439 and CYC116 with the wild-type and several mutants of Aurora B kinase were studied using SQM/MM-based PM6-D3H4X method. Details of the computational methodologies are described in supplementary information.

### **Western blotting**

Western blotting was performed as described previously (15). The membranes were probed with pH3ser10 (06-570, Millipore), anti-Aurora A (N-20, Santa Cruz), anti-Aurora B (E-15, Santa Cruz), anti-p53 (BP53-12, Sigma), anti-Bcl-xL (clone 4A9, Origene), and β-tubulin (clone TU-06, Exbio) or β-actin (clone AC-74, Sigma) antibodies.

### **DNA sequencing**

Genomic DNA and RNA were isolated and cDNA (complimentary DNA) was prepared as described previously (16). 25-50 ng of cDNA or gDNA (genomic DNA) was amplified by PCR using Phusion® Hot Start High-Fidelity DNA Polymerase (Finnzymes) and specific primers. Approximately 50 ng of amplified cDNA (Aurora A, B, C) and gDNA (Aurora B,

C) were used in each sequencing reaction. Sequencing was performed on ABI Prism® 3100-Avant Genetic Analyzer using Applied Biosystems chemistry. RidomTraceEdit (Ridom GmbH) and VectorNTI/ContigExpress (Invitrogen) softwares were used to align sequenograms and to check mutations. The primers used for sequencing can be found in supplemental Table S1.

### **Gene expression and copy number studies and analysis**

100 ng of RNA were used for preparation of biotinylated sense-strand DNA targets according to Affymetrix protocol. The fragmented and labeled sample was hybridized to Affymetrix Human Gene 1.0 ST Array. Expression profiles were examined from three independent biological replicates. All statistical analyses of expression arrays were carried out using either an assortment of R system software (<http://www.R-project.org>, version 2.11.0) packages including those of Bioconductor (version 2.7) by Gentleman et al. (17) or original R code. We used the affyQCReport Bioconductor R package to generate a quality control report for all chips. Chips that did not pass this filter were not included. Raw feature data from the expression chips were normalized in batch using robust multi-array average (RMA) method by Irizarry et al. (18), implemented in R package affy. Based on the RMA  $\log_2$  single-intensity expression data, we used Limma moderate T-tests (Bioconductor package limma (19) to identify differentially expressed genes. The p.adjust function from stats R package was used to estimate the false discovery rate using the Benjamini-Hochberg (BH) method (20). Expression data have been deposited in Array Express under accession number E-MEXP-3526. Parallel gene copy number analysis was evaluated in parent and resistant cells as described in supplementary information.

### **Validation of differently expressed genes using qRT-PCR**

The RNA was extracted using Trizol reagent (Ambion) followed by cDNA synthesis (Promega and Fermentas kits) and SYBR Green (Invitrogen) based qRT-PCR (Thermoscientific kit) (Rotor gene 6000 cycler). All gene primers were purchased from Genie Biotech. Thermal profiles were: 96° C for 15 m denaturation, then 95° C for 15 s amplification, and 66 or 64 or 62° C for 15 sec extension steps for 50 cycles. The specificity of gene primers and melting temperatures were optimized and the products were examined using Agilent DNA chips and analyzed using Agilent bioanalyser 2100. Target gene expression was normalized against to GAPDH (glyceraldehyde-3-phosphate dehydrogenase) housekeeping gene and  $2^{-\Delta\Delta Ct}$  method was used to calculate the relative gene expression. Gene primers and thermal profiles are listed in supplemental Table S2.

### **Validation of candidate genes using CYC116 *in vitro* sensitive and resistant primary human tumors**

59 primary human tumor samples were used for analysis of *in vitro* response to CYC116 as described previously (21). and parallel tumor sample was snap frozen and stored at -80°C in tumor bank. Then, 13 the most sensitive and 14 the most resistant tumors were selected for further validation study. RNA isolation, cDNA synthesis and qRT-PCR analysis was carried out for selected genes as mentioned above for the cell line experiments. The gene expression profiles were compared between CYC116 *in vitro* sensitive and resistant tumors. The Ct values were normalized against GAPDH. To calculate relative gene expression of resistant

samples the following statistical method was applied: The mean was calculated (value A) from the normalized Ct values of a gene from all sensitive and resistant samples. Then normalized Ct value of each gene from each sample was subtracted from value A. The obtained value is designated as value B. Finally the mean values were calculated and compared for sensitive sample and resistant sample groups. These values were plotted in a chart to show relative gene expression differences between the sensitive and resistant samples.

#### **siRNA mediated Bcl-xL knockdown**

$1.5 \times 10^5$  cells were seeded in 6-well plates and incubated for 24 hours. Anti-Bcl-xL siRNAs (Origene) was diluted in jetPRIME (Polyplus transfection, France) buffer and transfection reagent, subsequently added to cells at a final concentration of 10 nM. After 24 hours of transfection, fresh media were replaced. Cellular lysates were prepared after 96 hours to follow the knockdown by western blotting. Control (buffer) and negative control siRNA were also included during the optimization. Negative siRNA control was a scrambled RNA duplex and has no homology to any human gene, useful to validate the anti-Bcl-xL siRNAs specificity. Among the three unique 27mer siRNA duplexes (named as A, B, and C) B and C types of siRNAs were very effective in the Bcl-xL depletion. Combinations of B and C siRNAs at 5 nM each were therefore used for transfection followed by cell proliferation assay.

## **Results**

### **Generation and selection of resistant clones**

HCT116 p53<sup>+/+</sup> and HCT116 p53<sup>-/-</sup> were exposed to cytotoxic concentrations (1  $\mu$ M: above IC<sub>50</sub>) of CYC116 and ZM447439 in Petri dishes, which resulted in four groups of drug treated cell cultures: [1] p53<sup>+/+</sup>:CYC116, [2] p53<sup>-/-</sup>:CYC116, [3] p53<sup>+/+</sup>:ZM447439, and [4] p53<sup>-/-</sup>:ZM447439. During the course of selection, cells became polyploid, which is in agreement with Aurora B inhibition phenotype. Most of the cells died due to drug-induced effects. However, a small sub-population survived and formed colonies after 5 weeks. At least 10 colonies were isolated from each group and 3 clones were selected for further studies. Clones from each group were designated as: Group 1. [R1.1, R1.2, R1.3: CYC116 p53<sup>+/+</sup>], Group 2. [R2.1, R2.2, R2.3: CYC116 p53<sup>-/-</sup>], Group 3. [R3.1, R3.2, R3.3: ZM447439 p53<sup>+/+</sup>], and Group 4. [R4.1, R4.2, R4.3: ZM447439 p53<sup>-/-</sup>]. All clones were maintained continuously in 1  $\mu$ M CYC116 or ZM447439 respectively.

### **Clones displayed high resistance and cross-resistance to AKIs**

p53<sup>+/+</sup>:CYC116 clones (R1.1, R1.2, R1.3) were 9, 82, and 62 folds less sensitive to CYC116 than the parent cells (Table 1). The differences in resistant factor values might be due to genetic heterogeneity within the clones in the course of selection process. Similarly p53<sup>-/-</sup>:CYC116 clones (R2.1, R2.2, R2.3) displayed high resistance to CYC116. Two clones from p53<sup>+/+</sup>:ZM447439 group exhibited very high resistance, >83 fold increase in IC<sub>50</sub> values (R3.1, R3.2), where as the other clone (R3.3) is only 18 fold resistant. Degree of resistance was similar in p53<sup>-/-</sup>:ZM447439 group clones, - 33, 38, and 39 folds respectively.

Overall, p53+/+ background displayed higher resistance to both AKIs. This preliminary study confirmed the resistance of clones to selecting agents.

Cross-resistance profiles were tested using AKIs that have been tested in clinical trials. p53+/+:CYC116 clones were highly cross-resistant to AZD1152 (1100-1800 fold) followed by MLN8054 (79-163 fold), and VX-680 (33-67 fold) (Table 1). Interestingly, they were more resistant to AZD1152 and MLN8054 than CYC116. Two clones (R2.1, R2.3) from p53-/-:CYC116 group were highly resistant to MLN8054 (176 & 106 fold) (Table 1). They were 20-24 fold more resistant to VX-680. AZD1152 was unable to reach the IC50 in p53-/- HCT116 cells - both parent and resistant clones even at the highest concentration tested (50  $\mu$ M). p53+/+:ZM447439 clones presented variable resistance towards AZ1152 – from low to extremely high (7-3600 fold). They also displayed resistance to VX680 and MLN8054. p53-/-:ZM447439 clones were highly resistant to MLN8054 followed by VX680.

Interestingly, the p53-/-:ZM447439 cells were more resistant to MLN8054 than to the selecting agent. Overall, our data confirm wide cross-resistance among individual AKIs and suggest for shared mechanisms of drug resistance. All CYC116 and ZM447439 clones also acquired multidrug resistance phenotype as tested by using 13 approved anticancer drugs. Particularly all clones were highly resistant to etoposide. (supplemental Table S3). However, resistant clones were also more sensitive to several anticancer drugs compared to parent cell lines, particularly antimetabolites (5-fluorouracil and gemcitabine), DNA intercalators (daunorubicin and doxorubicin) and proteasome inhibitor bortezomib. Combination of these agents may have potential to prevent and/or overcome drug-induced resistance in concomitant or sequential administration.

**Table 1.** Resistance and cross-resistance profiles of parental versus CYC116 or ZM447439 resistant cells against various synthetic AKIs

Clone	CYC116	ZM447439	AZD1152	VX-680	MLN8054
<b>HCT116 p53+/+</b>	0.5	0.6	0.01	0.03	0.19
<b>CYC116(p53+/+)</b>					
R1.1	<b>4.4 (9)</b>	7 (12)	17 (1700)	1.9 (63)	31 (163)
R1.2	<b>41 (82)</b>	12 (20)	18 (1800)	2.0 (67)	15 (79)
R1.3	<b>31 (62)</b>	5 (8)	11 (1100)	1.0 (33)	16 (84)
<b>HCT116 p53-/-</b>	0.66	1	>50	0.1	0.17
<b>CYC116(p53-/-)</b>					
R2.1	<b>42 (64)</b>	12 (12)	>50	4.0 (40)	30 (176)
R2.2	<b>27 (41)</b>	7 (7)	>50	2.0 (20)	3 (18)
R2.3	<b>24 (36)</b>	8.8 (8.8)	>50	2.4 (24)	18 (106)
<b>ZM447439(p53+/+)</b>					
R3.1	7 (14)	<b>&gt;50 (&gt;83)</b>	36 (3600)	2.6 (87)	2.0 (10)
R3.2	1 (2)	<b>&gt;50 (&gt;83)</b>	8 (800)	0.7 (23)	2.0 (10)
R3.3	1 (2)	<b>11 (18)</b>	0.07 (7)	0.09 (3)	0.4 (2)
<b>ZM447439(p53-/-)</b>					
R4.1	4.5 (7)	<b>33 (33)</b>	>50	0.8 (8)	22 (129)
R4.2	3.0 (5)	<b>38 (38)</b>	>50	1.5 (15)	18.6 (109)
R4.3	3.0 (5)	<b>39 (39)</b>	>50	3.0 (30)	39 (229)

All values in the above table represent average IC50s in  $\mu\text{M}$  calculated from three independent experiments, each done in two technical replicates. The SD values for the above data were typically within 10-15% of the mean values. The values in parentheses are fold increase calculated by dividing average IC50 value of respective clones by the IC50 values of parent p53+/+ or p53-/- cells respectively.

### **CYC116 clones, but not ZM447439 became polyploid irrespective of p53 status**

Treatment of parent cells with either CYC116 or ZM447439 at a concentration of 1  $\mu\text{M}$  for 48 h induced the mitotic failure and accumulation of G2/M and >G2/M cells in both p53+/+ and p53-/- cell lines (Fig. 1) and eventually apoptosis. Interestingly, all p53+/+:CYC116 clones have 4n (tetraploid) DNA content and p53-/-:CYC116 clones have slightly less than 4n DNA content (>3n-<4n) (Fig. 1C & 1D). On contrary to this, all ZM447439 clones were diploid (Fig. 1E & 1F). p53 levels in p53+/+ clones were equal or slightly up-regulated compared to controls (Fig. 1K).

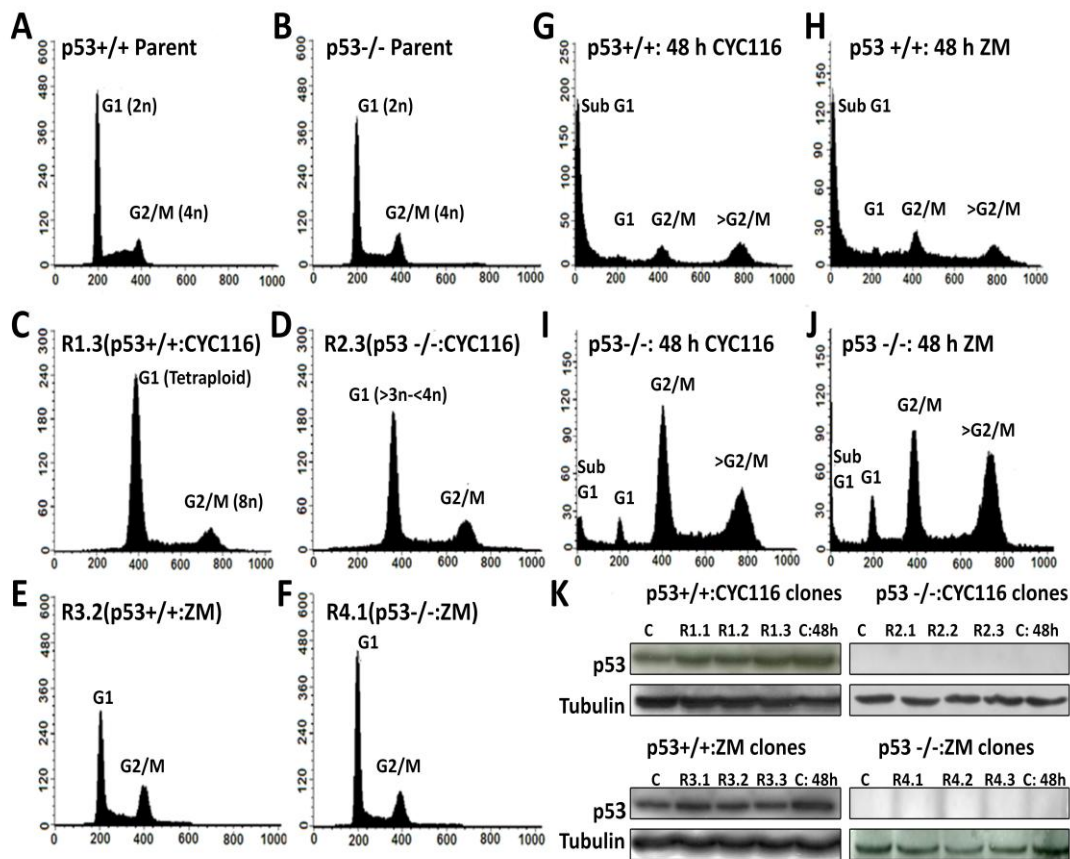


**Figure 1.** Cell cycle profiles of parent cell lines and resistant clones. A & B, Diploid parent HCT116 and HCT116 p53<sup>-/-</sup>. Cell cycle profiles for a representative clone from each group are shown. G, H, I, J, Cell cycle effects of CYC116 or ZM447439 on parent cell lines. C & D, Cell cycle profiles of CYC116 resistant clones. E & F, cell cycle profiles of ZM447439 clones. K, p53 induction levels in parent (C=DMSO: 48 h), resistant, and parent cell lines treated for 48 hours (C: 48 h).

### ZM447439, but not CYC116 induced mutations in Aurora B kinase and modeling of their impact on drug binding

DNA sequencing of AKs (A, B and C) revealed only three novel Aurora B mutations in ZM447439 clones (sequenograms in supplementary Fig. S1). One common mutation was detected in all p53<sup>+/+</sup>:ZM447439 clones i.e. I216L (mutant-1). Similarly one common mutation was detected in all p53<sup>-/-</sup>:ZM447439 clones, which is L152S (mutant-3). However R4.1 clone harbored L152S and one additional mutation, N76V (mutant-2). We carried out modeling of all three induced mutant proteins (mutant-1: I216L; mutant-2: N76V, L152S; mutant-3: L152S) to describe in structural and energy terms their effects on the interaction with ZM447439 and CYC116. Judging from the crystal structure of ZM447439 in complex with the wild-type Aurora B kinase (PDB (protein data bank) code 2VRX) (22), the binding seems to be chiefly governed by dispersion (L83, L138, E125, L152, L154) with only one classical H-bond (hydrogen bond) interaction (with A157) and one weaker C-H...O interaction with E155. The I216L mutation is far from the inhibitor (>7Å) and thus it does not directly influence the binding of the inhibitor (Supplemental Table S4). Further, it was seen that the side chain of I216 is buried in a pocket made up of I137, A187, L188, L184,



L201, and L214. Our modeling study showed that I216L might lose some interactions (L184 & L214), which may clarify the resistance towards ZM447439. On the other hand, the terminal C $\delta$ 1 of L152 residue has three direct CH... $\pi$  interactions with the inhibitor (23) (Fig. 2A). Thus its change to a smaller serine residue in both mutant-2 and mutant-3 is assumed to perturb these interactions. N76V is quite far from the binding site and hence it is beyond the scope of our study. However, it should be noted that this mutation disrupts the strong electrostatic interactions of Aspartate with T73, which might be one of the reasons for resistance.

For CYC116, we performed docking to Aurora B kinase structure (PDB code 2VRX) and rescored the best docked pose. Interestingly, our docking results could identify identical interactions to those reported in previous studies which used a different docking program (10). CYC116 interacted differently with Aurora B kinase as compared to ZM447439 (Figure 2B). A prominent novel interaction was H-bond formed between the amino moiety of CYC116 and the side chain of E161. Similar to ZM447439, mutant-1 had a minor effect on the interactions as it is far ( $>7\text{\AA}$ ) from the active site. In contrast to ZM447439, L152 did not show any interactions with CYC116 as it was quite far from CYC116 (Figure 2B). Hence, we assume that CYC116 will not lose interactions against mutant-2 and mutant-3 proteins. The calculated binding energies between CYC116 and ZM447439 Aurora B mutants can be found in the supplemental Table S4.

Girdler et al. reported seven sets of Aurora B mutations induced by ZM447439 (22). Particularly G160E, Y156H, and G160V significantly affected ZM447439 binding. We performed modeling studies on these mutants using the CYC116 docked pose. We predict replacement of Gly with charged Glu might lead to some unknown quantum chemical phenomenon within the protein (e.g. electrostatic repulsion). This mutation also seemed to render cross-resistance to CYC116 significantly. For Y156H, in wild type (Y156), the phenyl ring of tyrosine showed  $\pi$ - $\pi$  stacking interactions with pyrimidine ring of CYC116. Similarly, imidazole ring of histidine also interacted by stacking interactions and hence we assume that this mutation may not affect CYC116 binding. Like wild type G160, the mutant G160E conserved the CH... $\pi$  stacking interactions with the aromatic ring of CYC116. Hence we believe that this mutation would not affect CYC116 binding. The binding energies can be found in the supplemental Table S4.

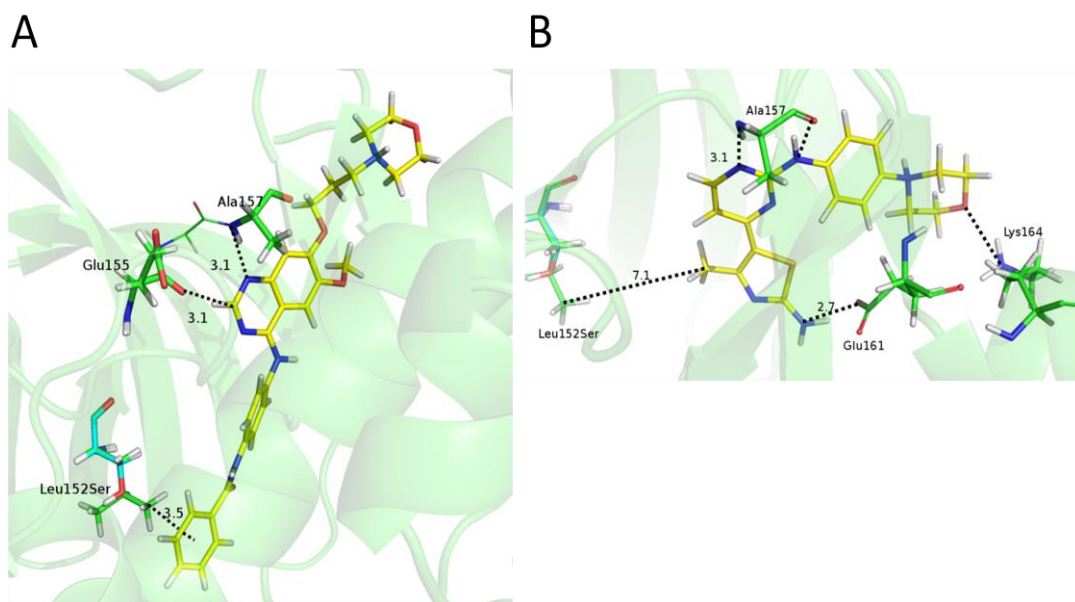


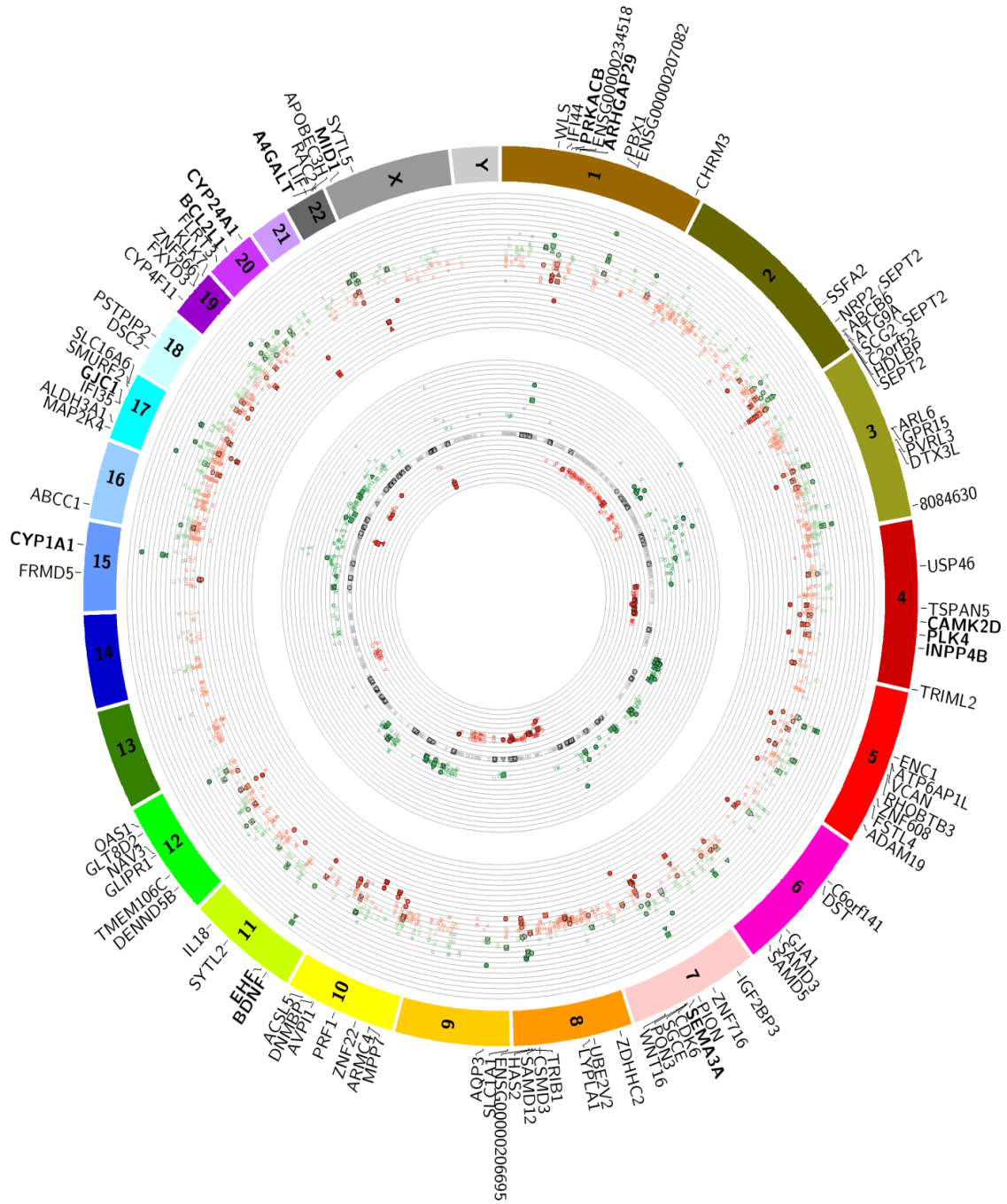
**Figure 2.** A close-up view of the binding interactions of ZM447439 and CYC116 in wild-type and in mutant-2 and 3 Aurora B kinases. A, The C-H... $\pi$  interactions between L152 of Aurora B kinase and the terminal phenyl group ZM447439 are lost upon L152S mutation, which is not seen with CYC116. B, Specific hydrogen bond to the backbone of A157 and C-H...O H-bond to the backbone of E155 are shown along with two additional H-bond interactions (E161 and K164) in CYC116. Color coding: Ligand carbon in yellow, amino acids carbon in green, Ser152 carbon in cyan, nitrogen in blue, oxygen in red, hydrogen in white.

### Microarray based gene expression analysis

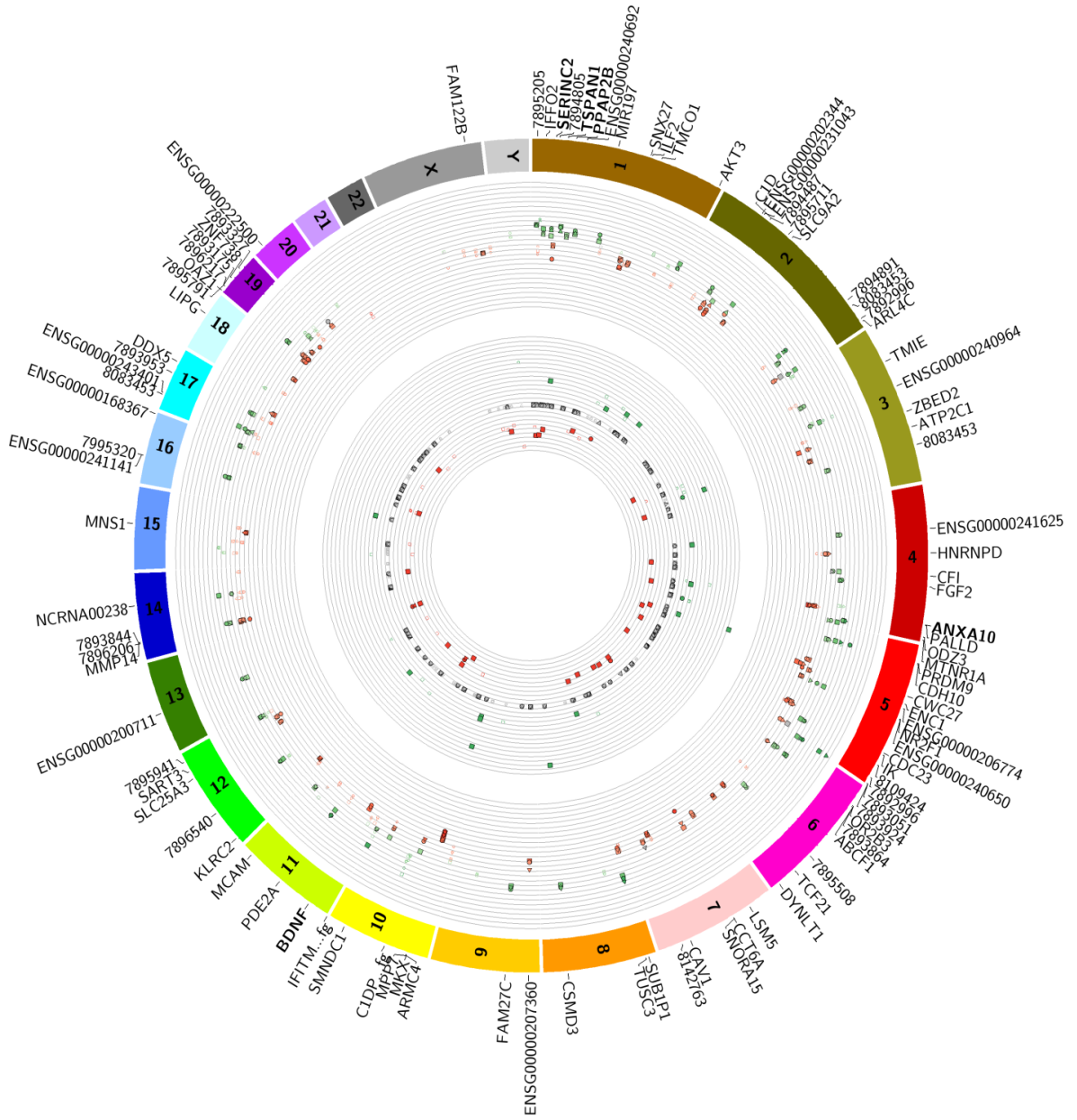
Whole human genome transcript array analysis was carried out to identify significant gene expression changes. The unsupervised clustering pattern suggest that majority of the gene expressions are common between the clones of each group. The clones were clustered (unsupervised clustering) with respect to p53 background and AKI used for selection of resistant clones (supplemental Fig. S2A). 50 genes were identified which mostly affect each of the first, second, and third component in PCA (principle component analysis) from all clones to generate the heat map (supplemental Fig. S2B). 885, 1085, 224, and 212 number of gene sets were differentially expressed (ANOVA  $p < 0.001$ ) in p53+/+:CYC116, p53-/:CYC116, p53+/+:ZM447439, and p53-/:ZM447439 groups, respectively. The fold changes of all gene sets of each group and corresponding copy number changes were presented in the form of circular plots (Fig. 3). The top 100 genes from all four groups were listed (supplemental Tables S5A, S5B, S5C, S5D). Highly differentially expressed genes, common genes between the groups, and some based on biological relevance were further validated by qRT-PCR. Altogether 28 genes were selected from all groups (supplemental Table S6). Nearly 100% match and significant correlation was noticed between microarray data and qRT-PCR validation, although the fold changes varied between the assay formats (supplemental Fig. S3).



B



C



D

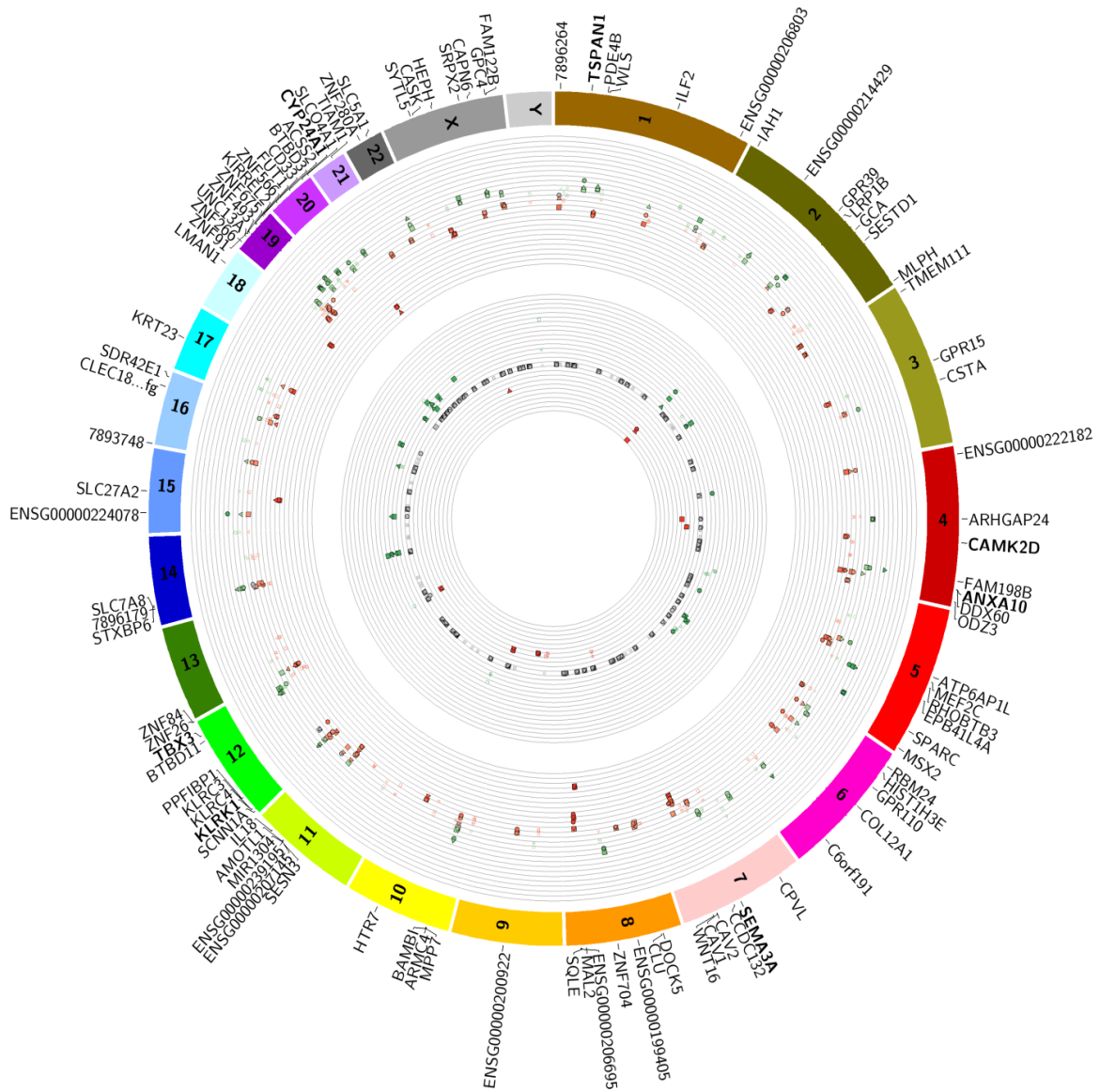


**Figure 3.** Circos visualization plots. The outer circular panel represents gene expression fold changes (logFC: fold change) of three clones from one group. Overexpression is color coded in green, whereas down-regulation in red. Grey color indicates no change in expression (-0.15 to 0.15). Inner circle represents corresponding gene copy number changes. Amplifications are color coded in green (>2 copies) and deletions in red (0-2). Grey color indicates no change in gene copy number. Each part of the circle coded in different colors represents chromosome number. Top 100 genes were highlighted in each group. The genes validated by qRT-PCR were marked as bold. Each clone was marked with a different symbol. A, HCT116: CYC116 (R1.1-□, R1.2-○, R1.3-△) B, HCT116 p53<sup>-/-</sup>:CYC116 (R2.1-□, R2.2-○, R2.3-△) C, HCT116:ZM447439 (R3.1-□, R3.2-○, R3.3-△) D, HCT116 p53<sup>-/-</sup>:ZM447439 (R4.1-□, R4.2-○, R4.3-△).

Since the number of differentially expressed genes is high, it is difficult to predict the affected pathways that influence AKIs induced resistance. We used GeneGo-system biology software to identify and prioritize most relevant pathways affected in resistant clones (Table 2). For HCT116 p53<sup>+/+</sup>:CYC116 clones the top scored common pathway map is apoptosis

and survival-BAD phosphorylation (supplemental Fig. S4A). In HCT116 p53<sup>-/-</sup>:CYC116 clones the most relevant commonly affected pathway is retinol metabolism, where CYP1A1, CYP1B1, and CYP4F11 showed altered expression (supplemental Fig. S4B). The top common pathway that is affected in HCT116 p53<sup>-/-</sup>:ZM447439 clones is immune response-human NKG2D signaling (supplemental Fig. S4C). Finally the most relevant pathway affected in HCT116 p53<sup>-/-</sup>:ZM447439 is cell cycle regulation of mitosis (supplemental Fig. S4D). Some gene expressions which are altered in the above mentioned pathways were successfully validated by qRT-PCR (**Bcl-xL**, CYP1A1, PRKACB, KLRK1, and Cyclin H). Common or differentially affected pathways based on p53 background for CYC116 or ZM447439 resistant clones are shown in supplemental Table S7.

**Table 2.** List of commonly affected pathways in each group of resistant clones

Group	Commonly affected pathways and genes involved
HCT116 p53 <sup>+/+</sup> CYC116 clones	Apoptosis and survival-BAD phosphorylation ( <b>Bcl-xL</b> ↑, <b>PKA-cat</b> ( <b>PRKACB</b> ) ↓, AKT3↑, GNG5 (G-protein beta/gamma) ↓, PP2C (PDP1) ↓ (supplemental Fig. S4A), Development-PIP3 signaling (GNG5↓, AKT3↑, <b>Bcl-xL</b> ↑, Cyclin D1↑), Development-A3 receptor signaling (GNG5↓, AKT3↑, <b>PKA-cat</b> ↓, Cyclin D1↑), Development-IGF-1 receptor signaling (IBP (IGFBP3 & IGFBP6)↑, <b>Bcl-xL</b> ↑, AKT3↑, Cyclin D1↑), PGE2 pathways in cancer (GNG5 ↓, GNAI1 (G-protein alpha-1) ↓, AKT3↑, Axin2↑, <b>PKA-cat</b> ↓, Cyclin D1↑)
HCT116 p53 <sup>-/-</sup> CYC116 clones	Retinol metabolism ( <b>CYP1A1</b> ↑, CYP1B1↑, DHA6↑) (supplemental Fig. S4B), Cell-adhesion-Alpha-4 integrins in cell migration and adhesion ( FN1 (Fibronectin)↑, ITGB7↑, alpha-4/beta-7 integrin↑, <b>PKA-cat</b> ↓), Immune response-Antigen presentation by MHC class II (MHC class II↑, HLADRA↑)
HCT116 p53 <sup>+/+</sup> ZM447439 clones	Immune response-NK2D signaling ( <b>KLRK1</b> ↓, AKT↑, AP-1↓, c-Jun/c-Fos↓) (supplemental Fig.S4C), Development ligand-dependent activation of ESR/AP1 pathway (RIP140↓, c-Jun/c-Fos↓), Muscle contraction regulation of eNOS activity in endothelial cells (CAV1↓, AKT↑, c-Jun↓, ETV4 (PEA3)↑)) Reproduction-GnRH signaling ( <b>PKA-cat</b> ↓, AP-1↓, c-Jun/c-Fos↓, AP-1↓)
HCT116 p53 <sup>-/-</sup> ZM447439 clones	Cell cycle-Initiation of mitosis ( <b>Cyclin H</b> ↓, APC↓, CAK complex↓, CDC25C↓, Weel↓) (supplemental Fig. S4D), Cell cycle-Regulation of G1/S transition (Cak complex ↓, Cyclin A↓), Cholestrol and sphingolipids transport (CAV1↓, CAV2↓, ARH↑), Histamine metabolism (ALDH2↑, MAOB↑, MAOA↑)

↓-down-regulation, ↑-up-regulation. Genes marked in bold were validated by qRT-PCR

## Comparison of drug resistant gene expression signatures in primary tumor biopsies sensitive/resistant to CYC116

Previously, several primary tumor samples (various solid and hematological cancers) were tested for sensitivity towards CYC116 under *in vitro* condition. 13 sensitive (average IC50: 4.42  $\mu$ M) and 14 resistant samples (average IC50: 95  $\mu$ M) were selected to validate gene expression signatures associated with response to AKIs. 23 most relevant genes were selected for qRT-PCR validation studies on human primary tumors *in vitro* sensitive/resistant to CYC116. Interestingly, majority of the cell line findings were also confirmed on primary human cells, suggesting validity of these genes as biomarkers of drug susceptibility or resistance (Fig. 4). Moreover, 5 genes expression were statistically significant in this limited sample set.

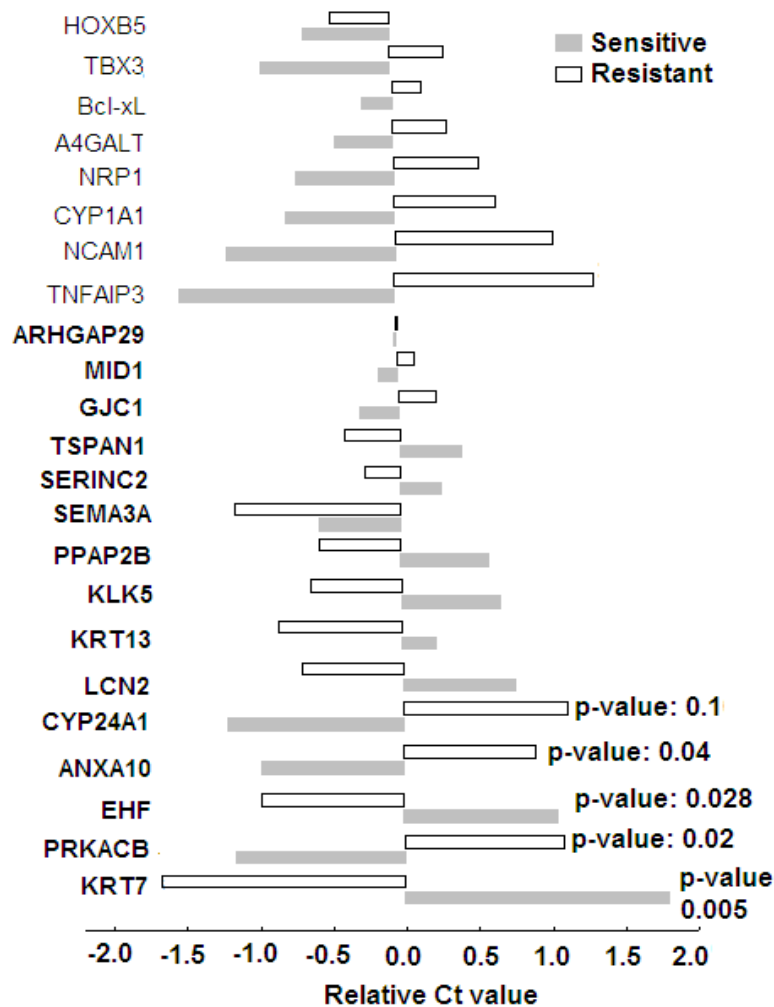


**Figure 4.** Validation of drug resistant gene expression signatures from cell lines in primary tumor biopsies sensitive/resistant to CYC116. The Ct value is reciprocal to the expression level. Gene expression trends that match to CYC116 resistant clones are marked in bold. Five genes expression trends shown from the bottom of the chart were statistically significant: KRT7, PRKACB, EHF, ANXA10, and CYP24A1.



## Bcl-xL is overexpressed and its inhibition re-sensitized resistant clones towards CYC116

All CYC116 clones, but not ZM447439 showed upregulation of Bcl-xL at RNA and protein level. Expression of Bcl-xL in p53<sup>+/+</sup> CYC116 resistant clones was much higher than p53<sup>-/-</sup> clones (Fig. 5A). We selected one resistant clone for optimization of Bcl-xL knockdown. Both B and C types of siRNAs (see Materials and Methods) were effective in depletion of Bcl-xL (Fig. 5B). Cell proliferation/cytotoxicity assay was performed following Bcl-xL knock down on two selected CYC116 resistant clones. Anti-Bcl-xL siRNA did not sensitize parent cells towards CYC116. Strikingly, depletion of Bcl-xL particularly in p53<sup>+/+</sup> resistant clone significantly reversed the resistance. (Fig. 5C). We were able to reach the IC<sub>50</sub> value at a level close to the sensitive parent cell line. Sensitization effect was much higher in p53<sup>+/+</sup> than p53<sup>-/-</sup> background.

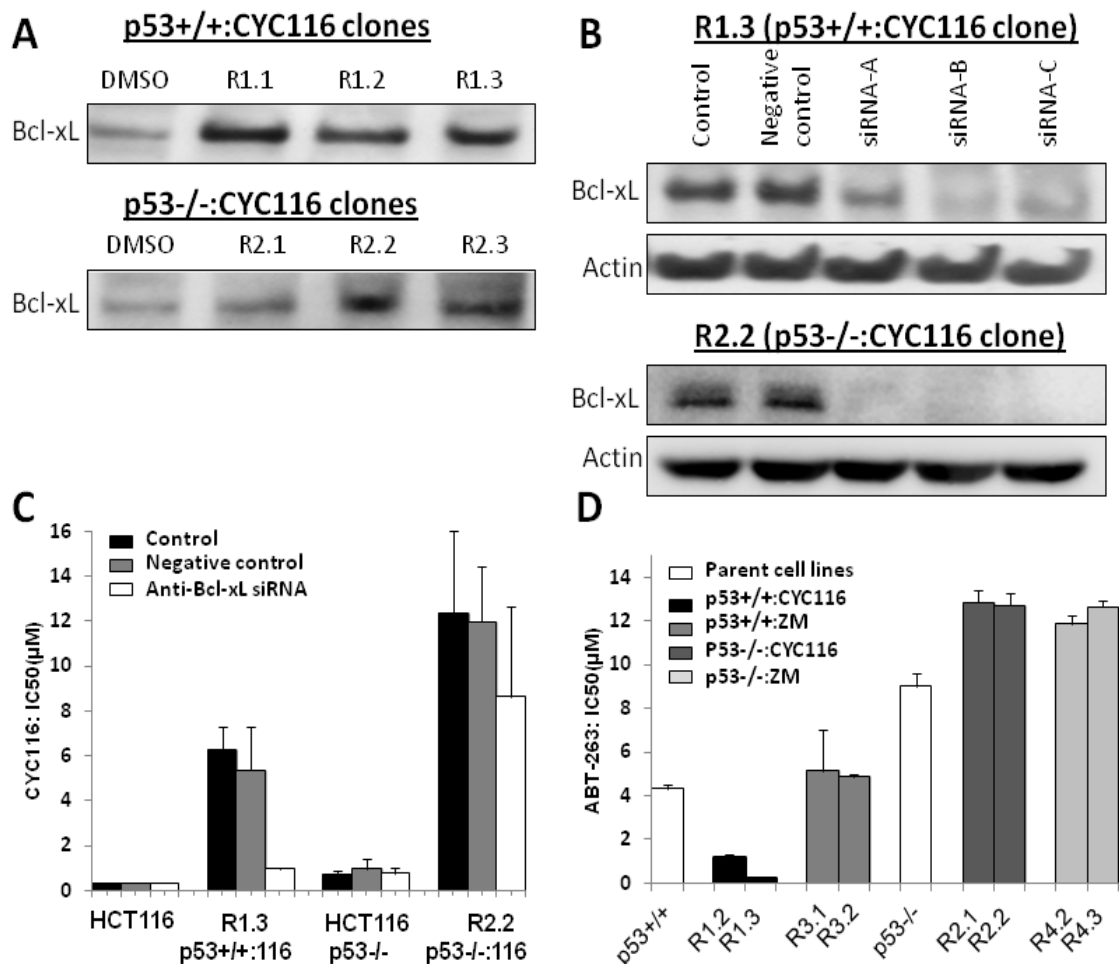


**Figure 5.** Inhibition of Bcl-xL expression restores response of CYC116 resistant cells to Aurora kinase inhibition. A, Bcl-xL expression in CYC116 resistant clones. Tubulin was used as a loading control as shown in Fig. 1 (same lysates were used for Bcl-xL expression also). B, Knockdown of Bcl-xL significantly by B and C types of anti-Bcl-xL siRNAs in R1.3 (p53<sup>+/+</sup>:CYC116) and R2.2 (p53<sup>-/-</sup>:CYC116) clones. C, IC<sub>50</sub> values (n=3) of CYC116 after Bcl-xL knockdown in one p53<sup>+/+</sup> & one p53<sup>-/-</sup> selected CYC116 resistant clones. D, IC<sub>50</sub> values of ABT-263 on two selected resistant clones from each group (n=3).

## **Bcl-xL expression correlates to the sensitivity of its pharmacological inhibition**

Navitoclax (ABT-263) is a potent inhibitor of Bcl-2, Bcl-xL, and Bcl-w, which is currently in Phase II clinical studies in refractory cancers. Bcl-xL overexpressing CYC116 clones with p53 background were more sensitive (R1.2: 4 fold, R1.3: 17 fold) to ABT-263 than HCT116 parent cells (Fig. 5D). However, p53<sup>-/-</sup> CYC116 clones were resistant, suggesting a p53-dependent mode of action. All ZM447439 clones with no change in Bcl-xL expression were equally sensitive or slightly resistant to navitoclax. Cellular Bcl-xL levels significantly influenced the response to ABT-263 in p53<sup>+/+</sup> CYC116 clones. In contrary, Bcl-xL expression in p53<sup>-/-</sup> cells (slightly up-regulated) did not modulate the response to ABT-263. This result was very much in line with siRNA mediated Bcl-xL knockdown, where Bcl-xL depletion sensitized p53<sup>+/+</sup> CYC116 clone to a greater extent compared to p53<sup>-/-</sup> clone.

## **Discussion**

Understanding of genetic anomalies paved the way in identification of several targets and biomarkers specific to a cancer cell. This laid the rationale for so-called ‘personalized’ medicine and several targeted agents evolved and proved to be successful. Drug-induced resistance to these targeted agents is likely and has been evident in the clinic. Hence it is crucial to understand the genetic basis of resistance, which provides additional filter to stratify, select, and treat patients that would benefit from therapy.

Abnormal cell proliferation is one of the main hall marks of a cancer cell, which mainly depends on uninterrupted cell cycle progression. Several drugs were targeted to various essential nodes in the cell cycle machinery. AKs are one such entity, which are essential for cell cycle progression through mitosis. Aberrant expressions of AKs have been reported in several cancers (24-29), which formed the rationale for targeted therapy. CYC116 is a novel AKI with broad anticancer activity. We selected HCT116 to study CYC116-induced resistance, as they express little or no multidrug transporters (30), thereby reducing the chance of resistance due to drug pumps. Supporting this, flow cytometry based analysis of PgP and MRP1 expression revealed no induction in resistant clones (data not shown). Histone H3 is a direct downstream substrate of Aurora B, and inhibition of its ser10 phosphorylation is a hallmark of Aurora B kinase inhibition (31). pH3ser10 was not inhibited in resistant clones in the presence of AKIs as determined by flowcytometry and western blotting (supplemental Fig. S5). Western blotting revealed no significant changes in the expression levels of Aurora A and B in all resistant clones (supplemental Fig. S6). The CYC116 resistant and polyploid cell lines displayed altered cell cycle kinetics as evidenced by increase in doubling time to 1.2-2 folds. However all clones were actively cycling as evidenced by BrdU (bromodeoxyuridine-DNA synthesis) and BrU (bromouridine-RNA synthesis) staining (data not shown). Further, the CYC116 resistant clones were highly proliferative, when xenografted into mice, suggesting that they did not lose tumorigenicity during the selection process (supplemental Fig. S7). Aneuploidy, frequently associated with chromosomal instability, has been consistently reported to associate with MDR (multidrug resistance) both in cell lines and patients. Castedo et al. established tetraploid HCT116 clones by treatment with other mitotic agents cytochalasin-D or nocodazole. They also selected tetraploid clones from diploid RKO (rectal carcinoma) cell lines by limiting dilutions (32). These clones were particularly resistant to DNA damaging agents including cisplatin, oxaloplatin, camptothecin, and etoposide. However, inhibition or knockdown of p53 partially

restored the cisplatin sensitivity. Our polyploid HCT116:CYC116 clones were also cross-resistant to some DNA damaging agents (supplemental Table 3), which is in line with their results. On the other hand, p53<sup>-/-</sup> CYC116 clones were either less resistant or sensitive to DNA damaging agents than p53<sup>+/+</sup>, which is again in agreement with their findings. Yuan et al. reported tetraploid clones in lenalidomide and bortezomib resistant multiple myeloma patient (33). Although this patient responded well initially, evolution of tetraploidy made resistant to lenalidomide and bortezomib with worsened prognosis. Lee et al. also reported worse prognosis in colorectal cancer patients with CIN<sup>+</sup> (chromosomal instability) following 5-FU adjuvant therapy compared to CIN<sup>-</sup> tumors (34). Polyploidy per se provides survival advantage, because alterations in gene dosage can affect the target and drug stoichiometric ratios. In our CYC116 clones, AKs were most probably amplified as a consequence of polyploidy, which could manifest drug resistance by target amplification indirectly. Based on the CYC116 mode of action i.e. induction of mitotic failure, the polyploid clones evolved were likely due to failed cytokinesis.

Our study also indicated that the CYC116 may be relatively ineffective in tumors that overexpress antiapoptotic Bcl-xL protein. The tumors which overexpress Bcl-xL may be also potentially insensitive to AZD1152, VX680, and MLN8054, as CYC116 clones are highly cross-resistant to these AKIs. Bcl-xL mediated drug resistance and relatively worse prognosis was reported consistently in the clinic (35). Here we report a novel resistance mechanism in the context of Aurora inhibition. Guo et al. found that SW620 and MiaPaca (pancreatic cancer cell line) cell lines became resistant to AZD1152 (Aurora B inhibitor) by upregulation of PgP and BCRP, respectively (36). Seamon et al. showed upregulation of BCRP in JNJ-7706621 (Aurora A and B inhibitor) resistant HeLa cell line (37). Girdler et al. found several Aurora B mutations in ZM447439 (Aurora B specific) resistant HCT116 cell line, including H250Y, G160V, G160E, Y156H, and L308P (22).

Inhibition of Bcl-xL partially restored the sensitivity of resistant clones to CYC116; suggesting involvement of additional mechanisms. Indeed our geneGO analysis showed few relevant pathways affected in resistant clones including anti-apoptotic survival and drug metabolism pathways. The pathway analysis predicted the regulation of Bcl-xL by AKT via BAD phosphorylation in HCT116 p53<sup>+/+</sup>: CYC116 clones. AKT phosphorylates BAD and inhibits its association with Bcl-xL, there by inhibiting apoptosis. In CYC116 clones both AKT and Bcl-xL are overexpressed. Previously it was shown that CYC116 induced some CYP1A in human hepatocytes (10). Pathway analysis showed interaction of up-regulated CYP1A1 (cytochrome P450, family 1, member A1) with retinoic acid derivatives. These interactions indicate the possibility of CYC116 as a substrate for CYP1A and related genes. Moreover some pathways relevant to Aurora kinase inhibition were also affected including cell cycle regulation of G1/S transition, initiation of mitosis, spindle assembly and chromosome separation, and DNA damage. Role of other observed affected pathways in the context of CYC116 and ZM447439-induced drug resistance are not clear. Taken together, the results suggest that tumor resistance towards CYC116 and ZM447439 is not mediated by one gene or one pathway, rather it is multifactorial. The drug resistance gene expression signatures specific to CYC116, could be used in the clinic to predict therapeutic response. As the mode of action of CYC116 and ZM447439 (almost identical to AZD1152) are similar to other AKIs, and CYC116 and ZM447439 resistant clones were cross-resistant to AZD1152,

VX680, and MLN8054, the genetic fingerprint we have identified may be useful to predict the response to AKIs in general. Interestingly, CYC116 did not induce AK mutations as a mechanism of induced resistance, which could be advantageous in the clinic to design combinations to overcome relatively less aggressive resistant mechanisms. Moreover, our modeling studies showed that CYC116 can potentially inhibit the Aurora kinase with ZM447439-induced mutations that are likely to occur in the clinic. This is further supported by the fact that the cell lines harboring these mutations are significantly less cross-resistant to CYC116 (Table 1).

In conclusion, we have i) described mechanisms underlying resistance to novel AKI CYC116 in comparison to model compound ZM447439 and other clinically relevant AKIs; ii) identified and validated gene signatures associated with response to AKIs potentially usable for patient stratification; iii) showed that CYC116 is fully or partially active in mutant forms of Aurora B kinase associated with resistance against quinazoline class of AKIs; iv) and showed that resistance phenotype can be reversed, at least partially, using genetic or pharmacological inhibition of Bcl-xL protein. Thus, the CYC116 in combination with Bcl-xL inhibitors might be potentially useful to overcome or even prevent the emergence of resistance against AKIs, and the Bcl-xL inhibitors might be highly active in tumors resistant or refractory to synthetic AKIs.

### **Acknowledgements**

We are thankful to Cancer Research Foundation in Olomouc for fellowship awarded to Madhu Kollareddy.

### **References**

1. An HX, Beckmann MV, Reifemberger G, Bender HG, Niederacher D. Gene amplification and overexpression of CDK4 in sporadic breast carcinomas is associated with high tumor cell proliferation. *Am J Pathol* 1999;154:113-18.
2. Roy HK, Olusola BF, Clemens DL, Karolski WJ, Ratashak A, Lynch HT, et al. AKT proto-oncogene overexpression is an early event during sporadic colon carcinogenesis. *Carcinogenesis* 2002;23:201-05.
3. Coustan-Smith E, Kitanaka A, Pui CH, McNinch L, Evans WE, Raimondi SC, et al. Clinical relevance of BCL-2 overexpression in childhood acute lymphoblastic leukemia. *Blood* 1996;87:1140-46.
4. Joensuu H, Puputti M, Sihto H, Tynninen O, Nupponen NN. Amplification of genes encoding KIT, PDGFR $\alpha$  and VEGFR2 receptor tyrosine kinases is frequent in glioblastoma multiforme. *J Pathol* 2005;207:224-31.
5. Karasarides M, Chiloeches A, Hayward R, Niculescu-Duvaz D, Scanlon I, Friedlos F, et al. B-RAF is a therapeutic target in melanoma. *Oncogene* 2004;23:6292-98.
6. John M, Goldman DM, Melo JV. Targeting the BCR-ABL tyrosine kinase in chronic myeloid leukemia. *N Engl J Med* 2001;344:1084-86.
7. Jang YJ, Kim YS, Kim WH. Oncogenic effect of Polo-like kinase 1 expression in human gastric carcinomas. *Int J Oncol* 2006;29:589-94.
8. Kollareddy M, Dzubak P, Zheleva D, Hajdуч M. Aurora kinases: structure, functions, and their association with cancer. *Biomed Pap* 2008;152:27-33.

9. Kollareddy M, Zheleva D, Brahmshatriya PS, Dzubak P, Hajduch M. Aurora kinase inhibitors: progress towards the clinic. *Invest New Drugs* 2012; 30:2411-2432.
10. Wang S, Midgley CA, Scaërou F, Grabarek, JB, Griffiths G, Jackson W, et al. Discovery of N-phenyl-4-(thiazol-5-yl)pyrimidin-2-amine aurora kinase inhibitors. *J Med Chem* 2010;53:4367-78.
11. Ditchfield C, Johnson VL, Tighe A, Ellston R, Haworth C, Johnson T, et al. Aurora B couples chromosome alignment with anaphase by targeting BubR1, Mad2, and Cenp-E to kinetochores. *J Cell Biol* 2003;161:267-80.
12. Tse C, Shoemaker AR, Adickes J, Anderson MG, Chen J, Jin S, et al. ABT-263: a potent and orally bioavailable Bcl-2 family inhibitor. *Cancer Res* 2008;68:3421-28.
13. Dzubak P, Hajduch M, Gazak R, Svobodova A, Psotova J, Walterova D, et al. New derivatives of silybin and 2,3-dehydrosilybin and their cytotoxic and P-glycoprotein modulatory activity. *Bioorg Med Chem* 2006;14:3793-810.
14. Brulikova L, Dzubak P, Hajduch M, Lachnitova L, Kollareddy M, Kolar M, et al. Synthesis of 5-[alkoxy-(4-nitro-phenyl)-methyl]-uridines and study of their cytotoxic activity. *Eur J Med Chem* 2010;45:3588-94.
15. Paprskarova, Krystof V, Jorda R, Dzubak P, Hajduch M, Wesierska-Gadek J, Strnad M. Functional p53 in cells contribute to the anticancer effect of the cyclin-dependent kinase inhibitor roscovitine. *J Cell Biochem* 2009;107:428-37.
16. Radilova H, Libra A, Holasova S, Safarova M, Viskova A, Kunc F, Buncek M. COX-1 is coupled with mPGES-1 and ABCC4 in human cervix cancer cells. *Mol Cell Biochem* 2009;330:131-40.
17. Gentleman RC, Carey VJ, Bates DM, Bolstad B, Dettling M, Dudoit S, et al. Bioconductor: open software development for computational biology and bioinformatics. *Genome Biol* 2004;5:R80.
18. Irizarry RA, Hobbs B, Collin F, Beazer-Barclay YD, Antonellis KJ, Scherf U, et al. Exploration, normalization, and summaries of high density oligonucleotide array probe level data. *Biostatistics* 2003;4:249-64.
19. Smyth GK (2005). Limma: linear models for microarray data. In: 'Bioinformatics and Computational Biology Solutions using R and Bioconductor'. R. Gentleman, V. Carey, S. Dudoit, R. Irizarry, W. Huber (eds), Springer, New York, pages 397-420.
20. Benjamini Y, Hochberg Y. Controlling the false discovery rate: a practical and powerful approach to multiple testing. *J Roy Statist Soc Ser* 1995;57:289-300.
21. Hajduch M, Mihal V, Minarik J, Faber E, Safarova M, Weigl E, Antalek P. Decreased in vitro chemosensitivity of tumor cells in patients suffering from malignant diseases with poor prognosis. *Cytotechnology* 1996;19:243-45.
22. Girdler F, Sessa F, Patercoli S, Villa F, Musacchio A, Taylor S. Molecular basis of drug resistance in aurora kinases. *Chem Biol* 2008;15:552-62.
23. Tsuzukis S, Fuji A. Nature and physical origin of CH/pi interaction: significant difference from conventional hydrogen bonds. *Phys Chem Chem Phys* 2008;10:2584-94.
24. Bischoff JR, Anderson L, Zhu Y, Mossie K, Ng L, Souza B, Schryyer B, Flanagan P, Clairvoyant F, Ginther C, Chan CS, Novotny M, Slamon DJ, Plowman GD. A homologue of *Drosophila* aurora kinase is oncogenic and amplified in colorectal cancers. *EMBO J* 1998;17:3052-65.

25. Katayama H, Ota T, Jisaki F, Ueda Y, Tanaka T, Odashima S, Suzuki F, Terada Y, Tatsuka M. Mitotic kinase expression and colorectal cancer progression. *J Natl Cancer Inst* 1999;91:1160-62.
26. Sen S, Zhou H, White RA. A putative serine/threonine kinase encoding gene BTAK on chromosome 20q13 is amplified and overexpressed in human breast cancer cell lines. *Oncogene* 1997;14:2195-200.
27. Zhou H, Kuang J, Zhong L, Kuo WL, Gray JW, Sahin A, Brinkely BR, Sen S. Tumour amplified kinase STK15/BTAK induces centrosome amplification, aneuploidy and transformation. *Nat Genet* 1998;20:189-93.
28. Sorrentino R, Libertini S, Pallante PL, Troncone G, Palombini L, Bavetsias V, Spalletti-Cernia D, et al. Aurora B overexpression associates with the thyroid carcinoma undifferentiated phenotype and is required for thyroid carcinoma cell proliferation. *J Clin Endocrinol Metab* 2004;90:928-35.
29. Zeng WF, Navaratne K, Prayson RA, Weil RJ. Aurora B expression correlates with aggressive behaviour in glioblastoma multiforme. *J Clin Pathol* 2007;60:218-21.
30. Teraishi F, Wu S, Zhang L, Guo W, Davis JJ, Dong F, Fang B. Identification of a novel synthetic thiazolidin compound capable of inducing c-Jun NH2-terminal kinase-dependent apoptosis in human colon cancer cells. *Cancer Res* 2005;65:6380-87.
31. Adams RR, Maiato H, Earnshaw WC, Carmena M. Essential roles of *Drosophila* inner centromere protein (INCENP) and Aurora B in histone H3 phosphorylation metaphase chromosome alignment, kinetochore disjunction, and chromosome segregation. *J Cell Biol* 2001;153:865-79.
32. Castedo M, Coquelle A, Vivet S, Vitae I, Kauffmann A, Dessen P, Pequignot MO, et al. Apoptosis regulation in tetraploid cancer cells. *EMBO J* 2006;25:2584-95
33. Yuan J, Shah R, Kulharya A, Ustun C. Near-tetraploidy clone can evolve from a hyperdiploidy clone and cause resistance to lenalidomide and bortezomib in a multiple myeloma patient. *Leuk Res* 2010;34:954-57.
34. Lee AJ, Endesfelder D, Rowan AJ, Walther A, Birbak NJ, et al. Chromosomal instability confers intrinsic multidrug resistance. *Cancer Res* 2011;71:1858-70.
35. Williams J, Lucas PC, Griffith KA, Choi M, Fogoros S, Hu YY, Liu JR. Expression of Bcl-xL in ovarian carcinoma is associated with chemoresistance and recurrent disease. *Gynecol Oncol* 2005;96:287-95.
36. Guo J, Anderson MG, Tapang P, Palm JP, Rodriguez LE, Niguette A, et al. Identification of genes that confer tumor cell resistance to the Aurora B kinase inhibitor AZD1152. *Pharmacogenomics J* 2009;9:90-102.
37. Seamon JA, Rugg CA, Emanuel S, Calcagno AM, Ambudkar SV, Middleton SA, et al. Role of the ABCG2 drug transporter in the resistance and oral bioavailability of a potent cyclin-dependent kinase/Aurora kinase inhibitor. *Mol Cancer Ther* 2006;5:2459-67.

## Supplemental materials and methods

### Computational modeling

#### ZM447439 in complex with Aurora B kinase

The X-ray crystal structure of Aurora B kinase in complex with ZM447439 was taken from the PDB database (code 2VRX) (1). The complex was prepared in the following way: hydrogens were added to the protein using the Reduce (2) and LEaP programs (3) and to the ligands using Chimera, ver. 1.5.3 (4). The parameters for the protein were acquired from the ff03 force field (5) and for the ligands from the gaff force field (6). Charges for the ligands were calculated using the RESP procedure (7) at the HF/6-31G\* level. The complex was relaxed in several steps. First, the hydrogens were optimized using AMBER program (3) for 2000 steps followed by a short high-temperature molecular dynamics (1 ps, starting from 1700 K, cooled down to 10 K).

Based on this structure, three different mutant proteins (mutant-1: I216L; mutant-2: N76V, L152S; mutant-3: L152S) were built automatically using the LEaP (3) program and adjusted manually by use of Pymol (8). Subsequently, the modeled residues were relaxed using AMBER minimization for 5000 steps, followed by 1 ps molecular dynamics (with three independent calculations starting at 300, 600 or 1200 K; and cooled down to 10 K). However, all molecular dynamics run resulted into almost identical geometries and hence only one of them was used for the optimization. The relaxed mutant proteins were further treated as the wild-type protein.

The protein-inhibitor interaction energies were calculated using our SQM/MM procedure (semiempirical quantum chemistry linked to molecular mechanics) for optimization and scoring (9,10). The SQM part comprised the ligand and the amino acids of the protein extending to 6 Å from the ligand. The rest of the protein was calculated using MM (AMBER) and kept frozen. The surrounding was modeled using the generalized Born (GB) solvation model mimicking the solvent (11). All complexes were optimized in a SQM/MM setup using our in-house program linking the SQM program (MOPAC2009) and the MM program (AMBER) (3). The SQM part was treated by the newly parametrized PM6-D3H4X method (12) which was shown to reproduce experimental binding constants closely (10). The MOZYME approximation was used to speed up the calculations. The SQM/MM optimizations were performed in several rounds until the energy and gradient convergence criteria ( $\Delta E = 0.005$  kcal/mol, maximum gradient of 1 kcal/mol/Å, root-mean-square of the gradient of 0.5 kcal/mol/Å) were met. The SQM/MM optimized structures were subsequently scored using our recently developed scoring methods (9).

#### Docking of CYC116 in Aurora B kinase using Glide and SQM/MM rescoring

Aurora B kinase complex (code 2VRX) was subjected to preparation steps using the Protein Preparation Wizard in Maestro (13): waters were removed, bond orders were assigned and hydrogens were added. Next, the orientation of amide (Asn and Gln), hydroxyl (Ser, Thr, and Tyr), and thiol groups (Cys) and the protonation and tautomeric state of His residues were optimized using the exhaustive sampling option. For generation of receptor grids, a grid box of  $20 \times 20 \times 20$  Å<sup>3</sup> with a default inner box ( $10 \times 10 \times 10$  Å<sup>3</sup>) was centered on the corresponding ligand. Default parameters were used, and no constraints were

included. Docking calculations were performed using Glide Extra Precision (XP) (14) algorithm along with postdocking minimization introduced as default in the Glide 5.5 for XP docking as postprocessing. In the protocol, Glide was set to write out the 5 best poses per ligand. The best pose was reoptimized and rescored using our SQM/MM-based (PM6-D3H4X) scoring function in the manner analogous to that in case of ZM447439.

### **Cytogenetic arrays**

DNA was extracted from one million cells using DNeasy blood and tissue kit (QIAGEN). Extracted genomic DNA was processed exactly according to manufacturer's protocol (Affymetrix, Santa Clara, CA). 100 ng of DNA was amplified by whole genome amplification. After product purification with magnetic beads, DNA was quantified, fragmented, labeled, and hybridized to Cytogenetics Whole-Genome 2.7M array. Arrays were washed, stained and scanned. We used software Partek Genomics Suite to analyze CGH arrays. Corresponding copy number changes for differentially expressed genes ( $p < 0.001$ ) were shown in the circos plots and also in the supplementary tables S5, S6, S7, and S8.



## Supplemental Figures

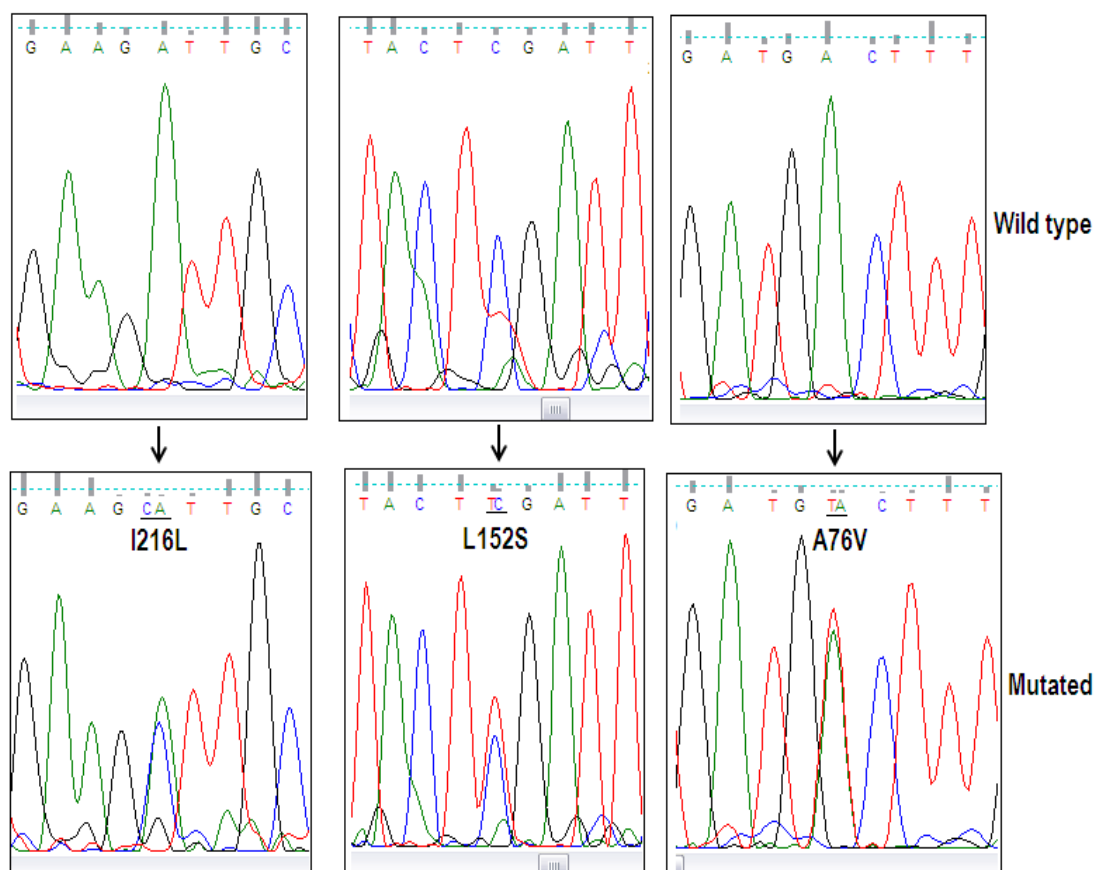


**Figure S1.** Sequenograms of wild-type and mutated Aurora B. Aurora B sequencing revealed three novel point mutations in ZM447439 resistant clones. cDNA sequences of Aurora B in parent cell lines (upper panel) vs. ZM447439 resistant clones at specific mutation site is presented in the sequenograms.

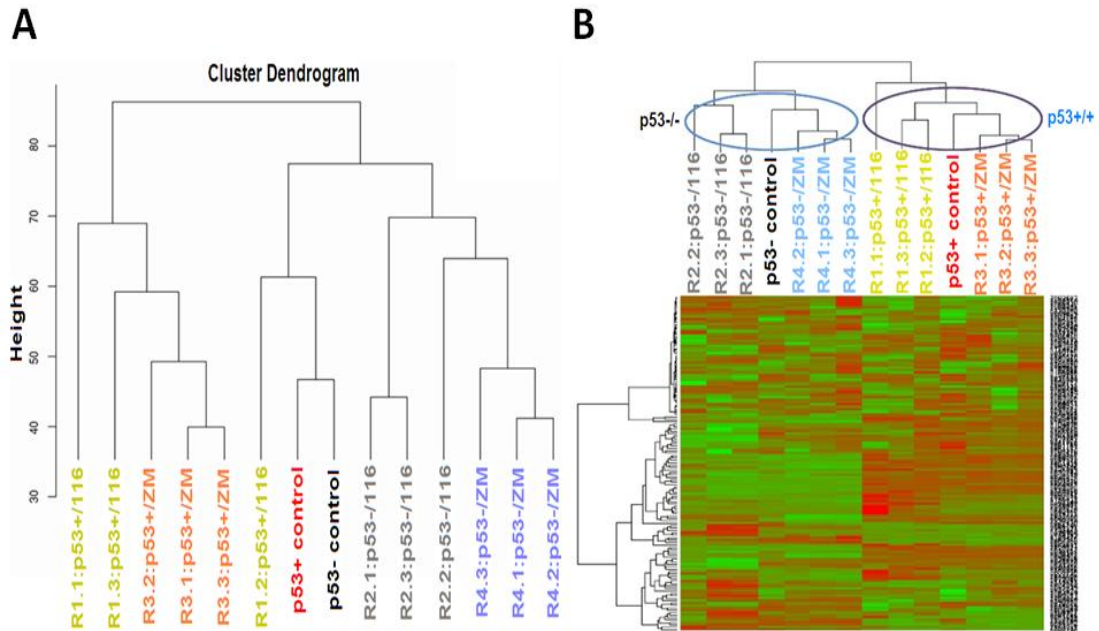


**Figure S2.** Unsupervised clustering of resistant clones and parent cell lines based on global gene expression patterns and heatmap created based on 50 genes, which mostly affect each of the first, second, and third component in PCA (total 138 genes, 12 genes overlap between the components of PCA). A, Dendrogram was created based on the global gene expression of all three clones (average of expression from three replicates) from all groups. Clones were clustered (unsupervised clustering) with respect to p53 background and compound used to generate resistant clones. This indicates that majority of the genes expression trends were common between the clones. B, 50 genes were selected, which mostly affect the first, second, and the third component (totally 138 genes, 12 genes overlap between the three components) in PCA, to create the heatmap. Here also the clones were clustered with respect to p53 background and compound used to generate resistant clones.

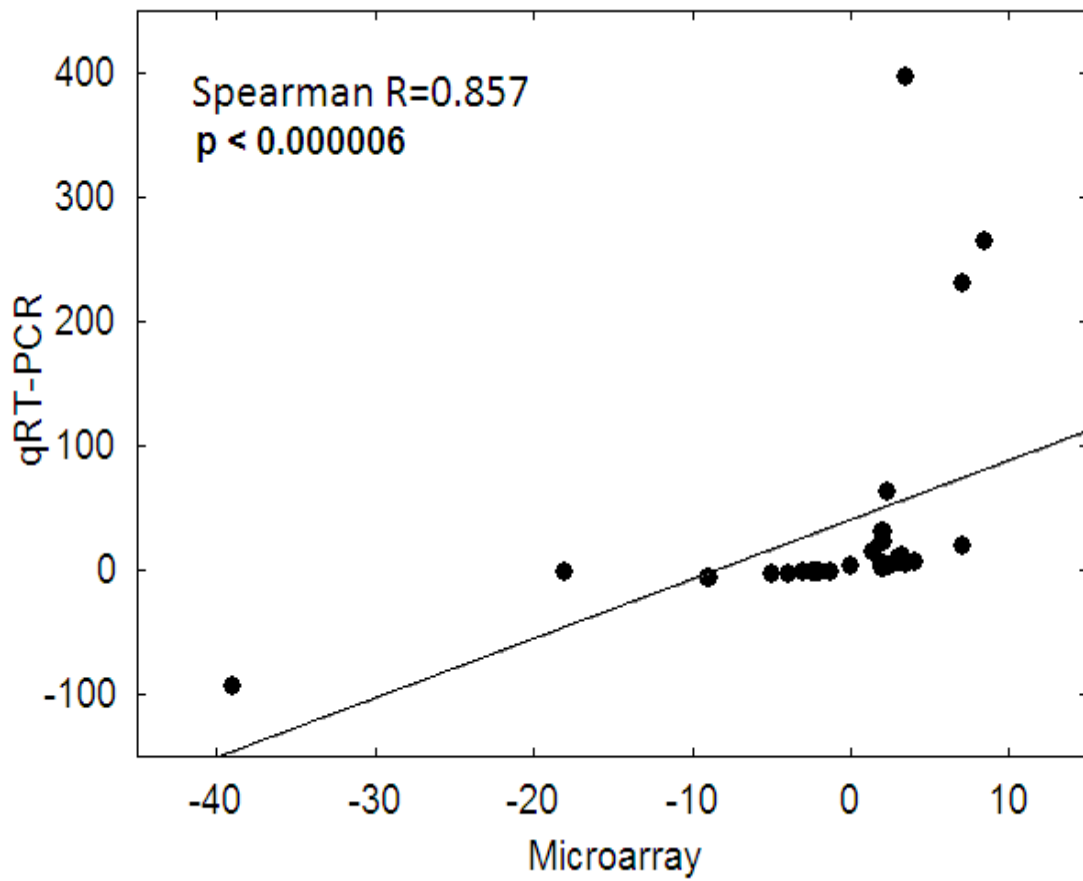
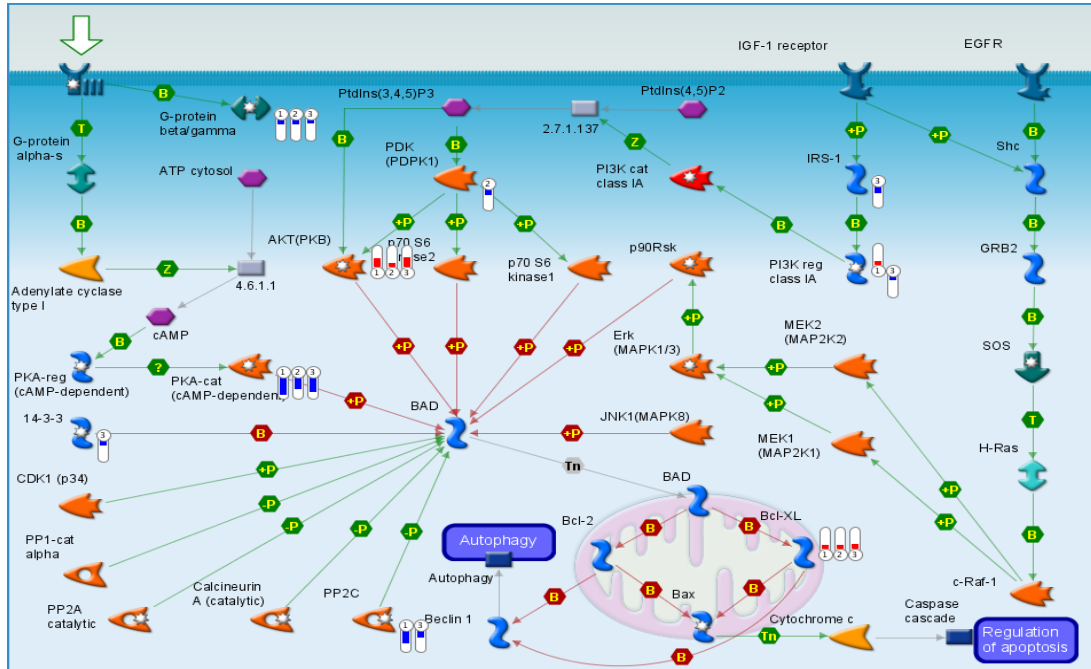
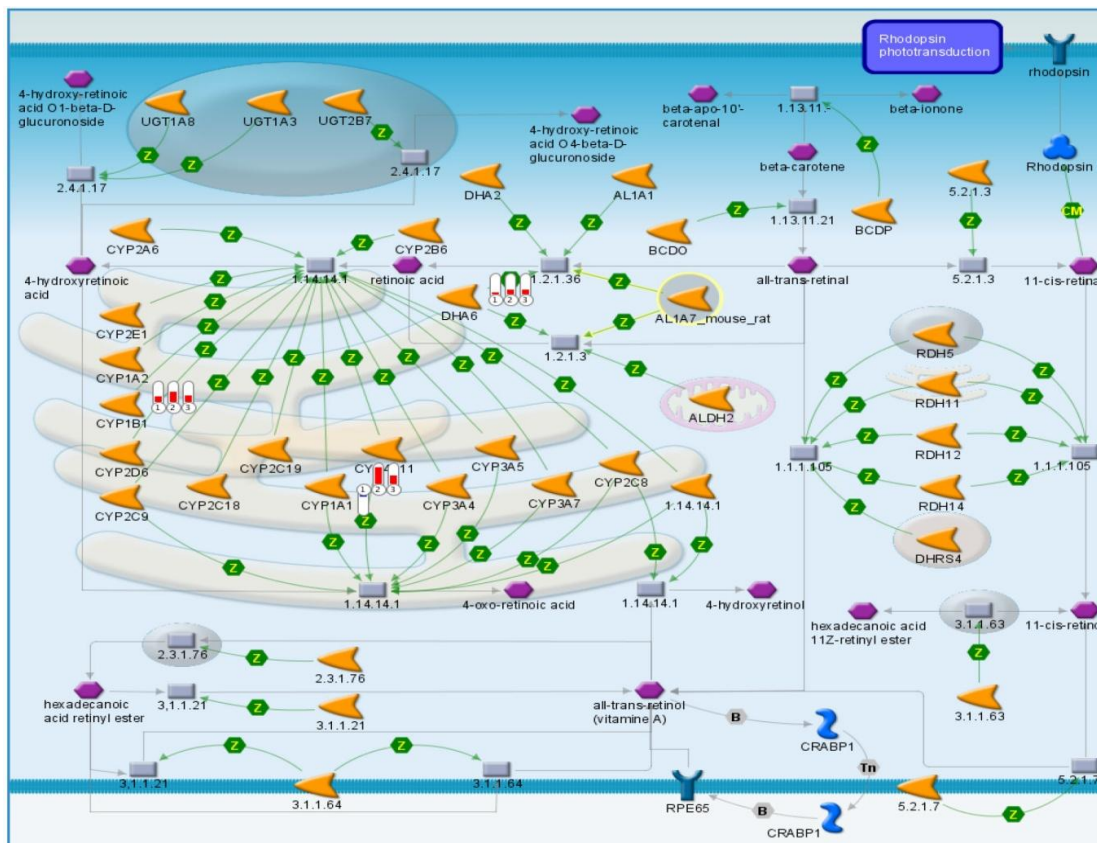


**Figure S3.** Correlation plot of 28 selected genes showing similar gene expression patterns between the microarray analysis and qRT-PCR analysis. Significant correlation ( $R=0.857$ ,  $p<0.000006$ ) was achieved between the assay formats

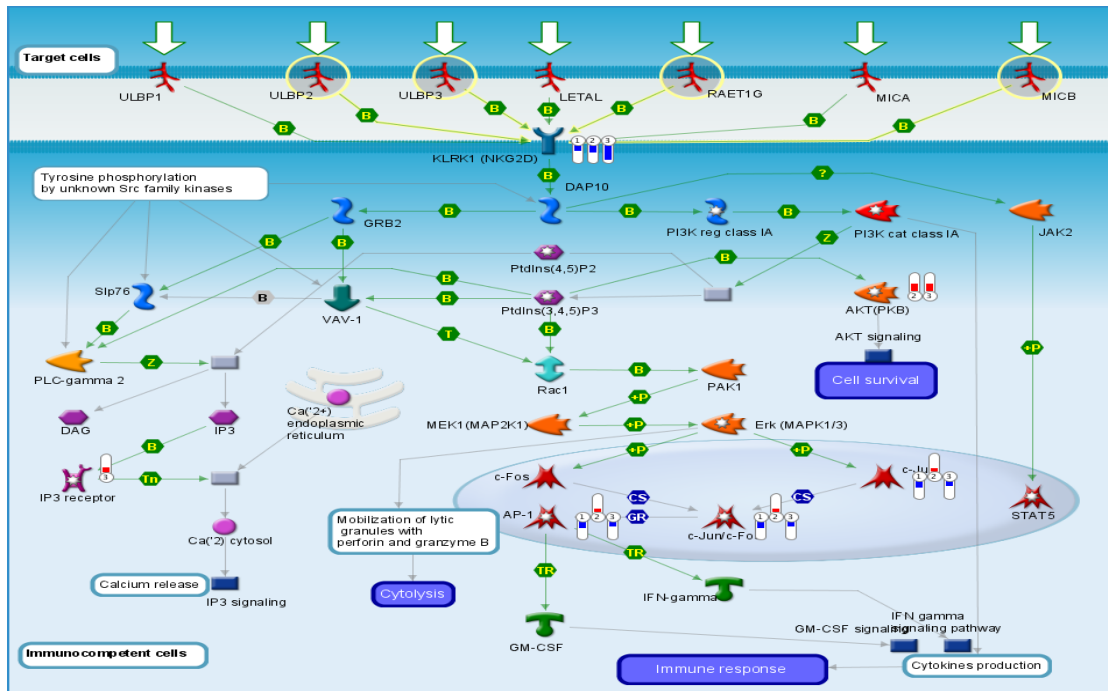
A



B



C



D

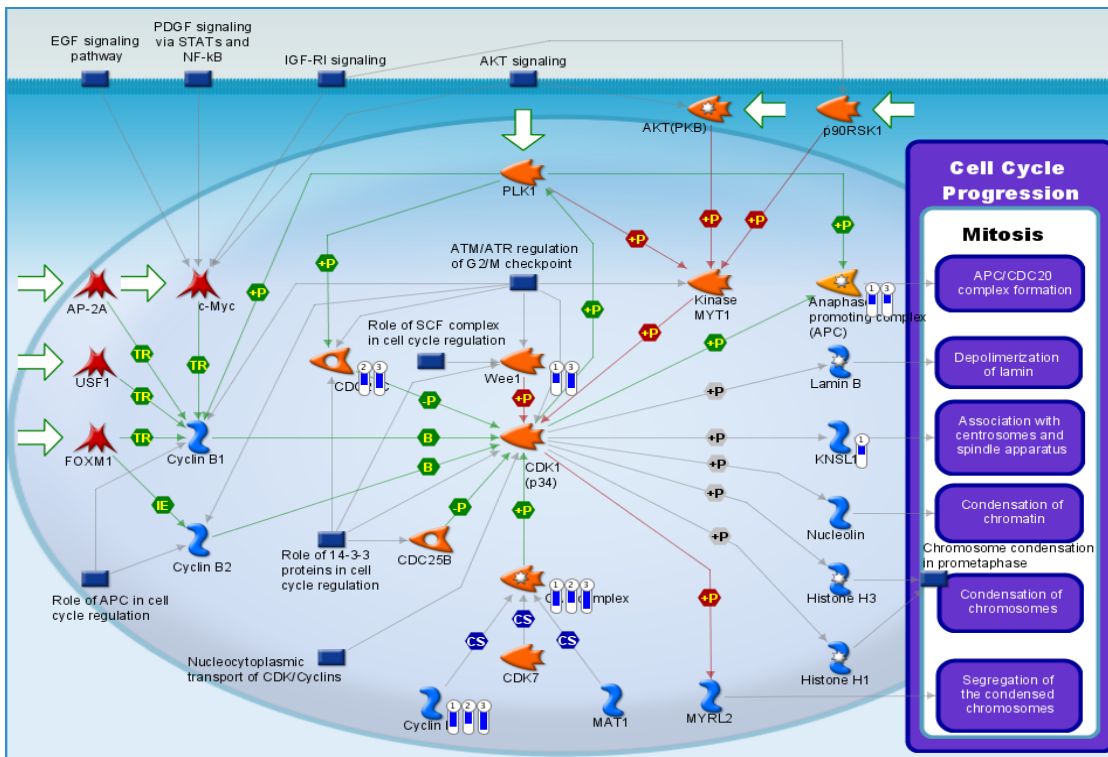


**Figure S4.** GeneGo pathway analysis of top commonly affected pathway in each group of resistant clones. Top common pathway for each group of resistant clones is shown. A, Apoptosis and survival BAD phosphorylation pathway in HCT116 p53<sup>+/+</sup>:CYC116 clones. B, Retinol metabolism pathway in HCT116 p63<sup>-/-</sup>:CYC116 clones. C, Immune-response-NK2D signaling in HCT116 p53<sup>+/+</sup>:ZM447439 clones. D, Cell cycle regulation of mitosis in HCT116 p53<sup>-/-</sup>:ZM447439 clones.

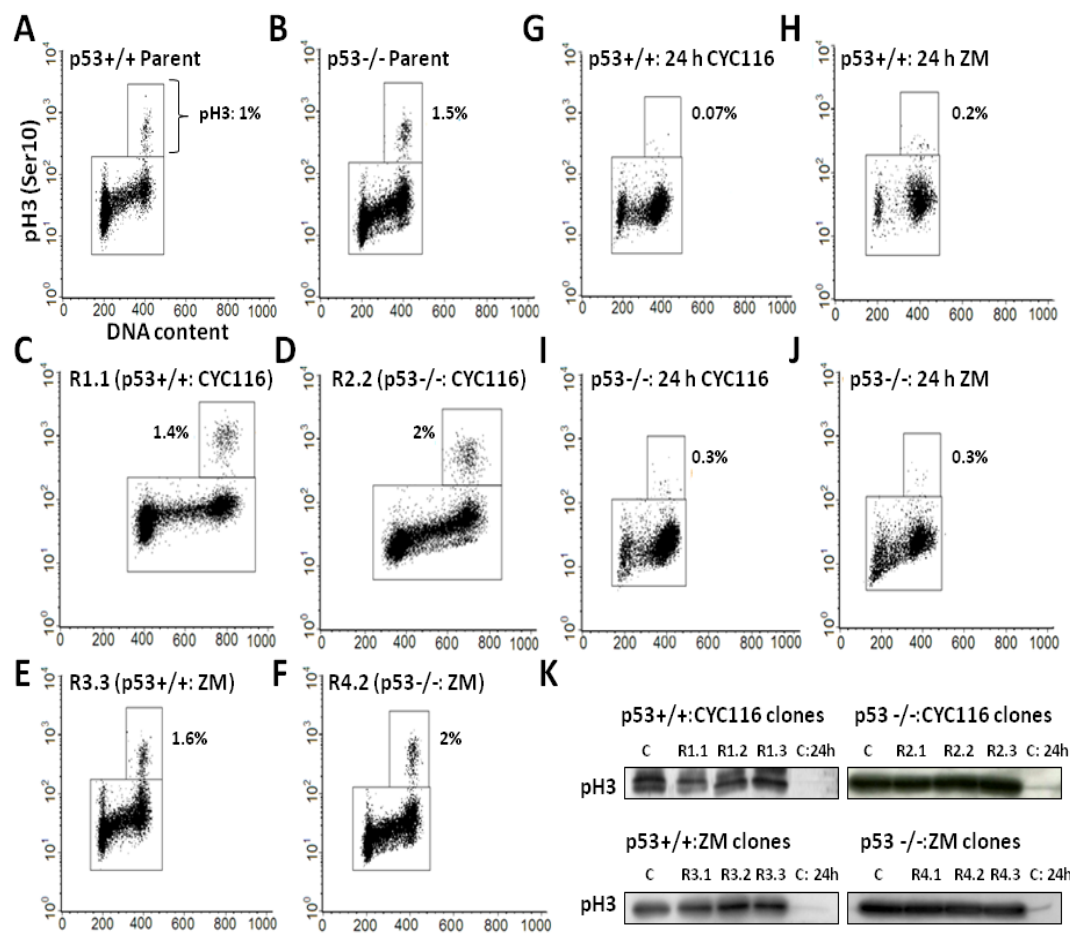


**Figure S5.** Biomarker modulations in resistant clones in comparison to parent cell lines. A & B are the dot plots of parent DMSO controls. No inhibition of phospho-histone H3 can be seen. Here also from each group one resistant clone is shown. C, D, E, F, represents pH3 levels in resistant clones. G, H, I, J are parent controls treated with either CYC116 or ZM447439 for 24 h. Flow cytometry based assay for each sample was done in 3 biological replicates. K: The same profile can be noticed from western blotting (C=DMSO, C: 24 h = parent cell line treated with either CYC116 or ZM447439 for 24 h). Tubulin was used as loading control as shown in Fig. 1 (same lysates were used to determine phospho histone H3 (ser10) levels also).

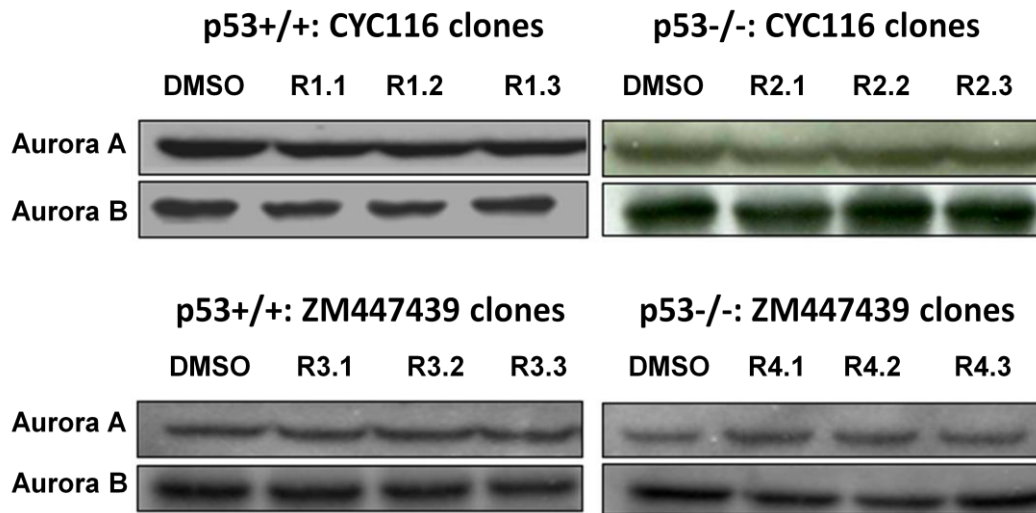


**Figure S6.** Western blot showing protein expression levels of Aurora A and B in all CYC116 and ZM447439 resistant clones in comparison to DMSO controls. Tubulin was used as loading control as shown in Fig. 1 (same lysates were used for Aurora A and B expression studies also)

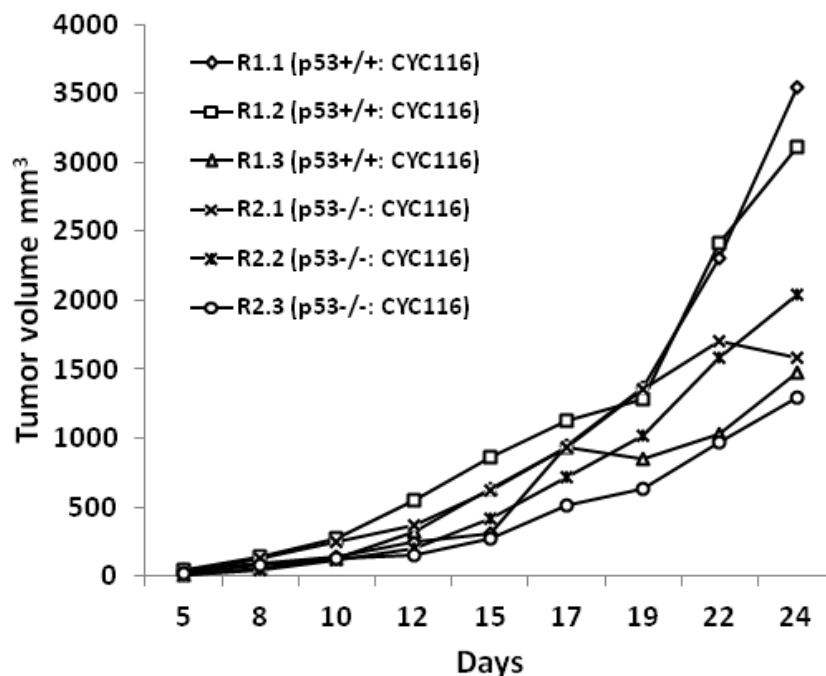


**Figure S7.** Tumorigenicity of CYC116 resistant clones. All CYC116 resistant clones were subcutaneously xenografted on both right and left side flanks of SCID (severe combined immunodeficiency) mice. On each side  $5-10 \times 10^6$  cells were injected. The tumor volumes were measured from all three replicates. As shown in the graph, the tumor volumes of the xenograft increased significantly in a time dependent manner, indicating the proliferative and tumorigenic potential of the CYC116 resistant clones.

**Supplemental Table S1.** Primers used for DNA sequencing of Aurora kinases

<b>Aurora Kinase</b>	<b>Reverse</b>	<b>Forward</b>
Aurora A (cDNA <sup>a</sup> )	(1) TCAGGATTATTTTCAGGTGCCG (3) AGAGAGTGGTCCTCCTGG	(2) TCCTTCAAATTCTTCCCAGCG (3) TGGCAAGAGAAAAGCAAAGCAAG (4) TGCCCTGTCTTACTGTCATTCTG (5) GCAAACACATACCAAGAGACC
Aurora B (cDNA)	(1) GTAGAGACGCAGGATGTTGG	(2) TTGATGACTTTGAGATTGGGCG (3) GGAGGAAGACAATGTGTGGC
Aurora B (gDNA <sup>b</sup> ) Exon2		(1) TAGATCAGAGGGTCCGTTGG
Aurora C (gDNA) Exons 1-4	(1) AAAGAAGAGCGTTGGGGAGG (2) CGGAGGGAAAGTCAGGGATG (4) TTCTCAGAAGGCAATGCGGA	(3) GAACTACTGATAGGGCTGGG
Aurora C (cDNA) Exons 5-7	(1) GACAAATGAGGTGGCAGAGC	(2) AGCGAGAAATTAGATGAACAGCG

<sup>a</sup>cDNA, <sup>b</sup>gDNA, Primer sequences used for Aurora A, B, and C kinases sequencing



**Supplemental Table S2.** Primers and thermal profiles used for qRT-PCR

<b>Gene Symbol</b>	<b>Forward primer</b>	<b>Reverse primer</b>	<b>Thermal profiles</b>
CYP24A1	CTGGGATCCAAGGCATTCTA	ATGGTGCTGACACAGGTGAA	62° C/15 s
BCL2L1	CTGGCTCCCATGACCATACT	GCTGAGGCCATAAACAGCTC	62° C/15 s
GJC1	ATGGTGTTACAGGCCTTTGC	GAGTCTCGAATGGTCCCAA	62° C/15 s
NCAM1	TGAGTGGAGAGCAGTTGGTG	TTGGCATCATAACCACTTGG	62° C/15 s
KLK5	CTCGTGTCTGGGGAGATTA	TGAACTTGCAGAGGTTTCGTG	62° C/15 s
KRT7	GATGCTGCCTACATGAGCAA	TGAGGGTCCTGAGGAAGTTG	62° C/15 s
LCN2	CAAGGAGCTGACTTCGGAAC	GACAGGGGAAGACGATGTGGT	64° C/15 s
TNFAIP3	ATGCACCGATACACACTGGA	GGATGATCTCCCGAAACTGA	62° C/15 s
KRT13	CGAGAGCCTGAATGAAGAGC	CGACCACCTGGTTGCTAAAT	62° C/15 s
PPAP2B	AAATGACGCTGTGCTCTGTG	ACCGCGACTTCTTCAGGTAA	62° C/15 s
TBX3	GGGACATCGAACCTCAAAGA	CCATGCTCCTCTTTGCTCTC	62° C/15 s
SERINC2	CGTGTGGGTGAAGATCTGTG	CAGGGTCCACAGGTAGAGGA	66° C/15 s
HOXB5	AGGGCCCAAAGCTTGTAAT	GCATCCACTCGCTCACTACA	62° C/15 s
ANXA10	GTCCTATGGGAAGCCTGTCA	GCTCTTGTTCACAGGATCA	60° C/15 s
CYP1A1	GACAGATCCCATCTGCCCTA	CGAAGGAAGAGTGTGCGAAG	62° C/15 s
PRKACB	GAGACCGTCCTTGTGAAGC	ACGGGATGATGGCAATAAAG	60° C/15 s
A4GALT	GACCACTACAACGGCTGGAT	CGGATGGAACACCACTTCTT	62° C/15 s
ARHGAP29	CATGGCAGCTGAATCTTTGA	AGCCAGATGACAGGAGCCTA	62° C/15 s
NRP1	CAAGGCGAAGTCTTTTGAGG	TCTCGGGTAGATCCTGATG	64° C/15 s
KLRK1	GCCACAGCAGAGAGACACAG	CCCATTAAAAGTGGCAGCAT	62° C/15 s
MID1	ACCCAACATCAAGCAGAACC	GGCCTTGACCATGAAGATGT	64° C/15 s
EHF	AGGTGATGCATCCTCCTCAC	AATGTTACCTCCCTTGACG	62° C/15 s
SEMA3A	TGCCAAGGCTGAAATTATCC	GCCAAGCCATTGAAAGTGAT	62° C/15 s
PLK4	TCCTTTTCCATTTGCAGACC	GCAGATTCCCAAACCACTGT	64° C/15 s
INPP4B	GTGCTCCTTCAGGAACCTGC	AGTGCTTGGCTGAAGACGAT	64° C/15 s
CAMK2D	CAGTACATGGATGGCAGTGG	TGCCACACACGAGTCTCTTC	62° C/15 s
BDNF	CAAGGGGACCCATAGGAAAT	GAGCAAGGCACCTTCAAGTC	62° C/15 s
TSPAN1	CCTTTCTGCTCCAGACTTGG	AAGTCAGGCATCGCCTAAAA	62° C/15 s
GAPDH	GAAGATGGTGATGGGATTTT	GAAGGTGAAGGTCTGGAGT	60° C/30 s

Primer sequences and thermal profiles used for qRT-PCR based microarray validations.

**Supplemental Table S3. Multidrug resistance and sensitivity profiles of resistant clones**

Drug	HCT116 p53+/+	R1.2:116 (p53 WT)	R1.3:116 (p53WT)	Drug	HCT116 p53-/-	R2.1:116 (p53 null)	R2.2:116 (p53 null)
Etoposide	1.3	45 (34)	71 (53)	Etoposide	1.84	14 (8)	8.5 (5)
Gemcitabine	0.08	2.3 (29)	0.3 (4)	Act-D	0.0015	0.004 (3)	0.005 (3)
Daunorubicin	0.03	0.33 (11)	0.4 (16)	Carboplatin	9.9	27 (3)	26.3 (3)
Act-D	0.0006	0.0027 (5)	0.003 (6)	Paclitaxel	0.004	0.008 (2)	0.008 (2)
Topotecan	0.01	0.045 (4.5)	0.17 (17)	Cladribine	7.6	16.5 (2)	8 (1)
Bortezomib	0.03	0.12 (4)	0.3 (10)	Cisplatin	2.1	3.35 (1.6)	4.3 (2)
Paclitaxel	0.0015	0.0055 (4)	0.007 (5)	Topotecan	0.155	0.21 (1.4)	0.115 (0.7)
Cisplatin	0.9	3.3 (4)	2.37 (3)	5-Flurouracil	1.2	1.5 (1.3)	1 (0.8)
Carboplatin	7	22 (3)	12 (2)	Oxaloplatin	3.3	2.05 (0.6)	2.46 (0.7)
Oxaloplatin	0.9	2.8 (3)	1.2 (1)	Gemcitabine	1.1	0.64 (0.6)	0.63 (0.6)
Doxorubicin	0.1	0.17 (1.7)	0.2 (2)	Doxorubicin	0.6	0.2 (0.3)	0.32 (0.5)
Cladribine	3.7	4.7 (1)	4 (1)	Daunorubicin	0.7	0.225(0.3)	0.3 (0.4)
5-Flurouracil	0.9	0.78 (0.8)	1 (1)	Bortezomib	0.28	0.04 (0.1)	0.047 (0.2)

	R3.1:ZM (p53 WT)	R3.2:ZM (p53WT)	R4.2:ZM (p53 null)	R4.3:ZM (p53 null)
Etoposide	40 (30)	1.72 (1.3)	39 (21)	37 (20)
Daunorubicin	0.25 (10)	0.05 (2)	Topotecan	0.4 (2.6)
Topotecan	0.04 (4)	0.016 (2)	5-Flurouracil	2 (1.6)
Carboplatin	25 (3.6)	14 (2)	Cladribine	16.5 (2)
Taxol	0.005 (3)	0.001 (6)	Oxaloplatin	5.9 (2)
Cisplatin	2.4 (3)	2.42 (3)	Bortezomib	0.5 (2)
Oxaloplatin	2.9 (3)	1 (1)	Paclitaxel	0.006 (1.5)
Act-D	0.002 (3)	0.0009 (2)	Act-D	0.002 (1.3)
Doxorubicin	0.19 (2)	0.0355(0.4)	Carboplatin	12 (1.2)
Cladribine	6.3 (2)	2.3 (0.6)	Cisplatin	2.27 (1)
5-Flurouracil	1.4 (1.5)	0.46 (0.5)	Gemcitabine	0.35 (0.3)
Gemcitabine	0.06 (0.8)	0.026 (0.3)	Doxorubicin	0.1 (0.15)
Bortezomib	0.006 (0.2)	0.03 (1)	Daunorubicin	0.1 (0.14)

**MDR and sensitivity profiles of CYC116 and ZM447439 resistant clones.** All IC50 values in the above table are in micrograms (except bortezomib:  $\mu\text{M}$ ), calculated from 3 independent replicates, each two technical replicates. The SD values for the above data are in the range  $\pm 0.000007$  -  $\pm 4$ . IC50 values were also shown for p53+/+ and p53-/- parent cell lines. From each group two clones were selected to verify multidrug resistant phenomenon using 13 approved anticancer agents.

**Supplemental Table S4.** Binding free energies  $\Delta G_{\text{int}}^{\text{w}}$  (kcal/mol) of ZM447439 and CYC116 with the wild type and mutated Aurora B proteins.

<b>Protein</b>	<b><math>\Delta G_{\text{int}}^{\text{w}}</math> (kcal/mol)</b>	
	<b>ZM447439</b>	<b>CYC116</b>
Wild type Aurora B	-79.9	-68.5
I216L	-80.3	-67.5
L152S N76V	-76.4	-66.0
L152S	-77.9	-66.0
G160E	-	-60.19
G160V	-	-71.4
Y156H	-	-69.8

**Supplemental Table S5.** Top 100 common differentially expressed genes (Cumulative p-value <0.001) and corresponding copy number changes in HCT116:CYC116 group. <sup>a</sup>Chr. - Chromosome, <sup>b</sup>logFC – Fold change, <sup>c</sup>Amp. – Amplification, <sup>d</sup>Del. – Deletion, <sup>e</sup>Nd - No description. For some genes, identity number is presented more than once as respective Affymetrix probe binds to one more than one location of the genome having same recognition sequence. The same Gene IDs represented more than once, have unique ENSEMBL IDs.

Gene ID	Gene Symbol	Chr. <sup>a</sup>	R1.1 logFC <sup>b</sup>	R1.2 logFC	R1.3 logFC	logFC Mean	R1.1 Copy No.	R1.2 Copy No.	R1.3 Copy No.
8067140	CYP24A1	20	-6.68	-3	-6.17	-4.99			
8047738	NRP2	2	4.04	0.82	0.89	1.435			
8065569	BCL2L1	20	0.80	0.71	0.91	2.000	Amp. <sup>c</sup>	Amp.	
8047763	Nd <sup>e</sup>	2	4.03	0.45	1.25	1.309			
7964927	TSPAN8	12	4.64	4.48	0.96	2.711			
7944931	SLC37A2	11	3.79	1.09	0.66	1.396	Amp.	Amp.	
8016094	GJC1	17	-3.63	-0.44	-1.8	-1.42			
8152617	HAS2	8	-0.42	4.5	1.68	1.476			
7961891	BHLHE41	12	2.71	-0.01	0.06	0.096			Amp.
7963614	ITGB7	12	3.93	1.06	1.4	1.802			
8101828	TSPAN5	4	-4.39	-0.78	-1	-1.51			
8150529	DKK4	8	-0.05	-0.07	3.56	0.233			
8070574	TFF2	21	2.02	-0.25	0.14	0.411		Amp.	Amp.
7935553	LOXL4	10	3.21	0.04	0.77	0.447			
7943892	NCAM1	11	2.87	-0.1	2.94	0.944	Amp.	Amp.	
8038670	KLK5	19	4.23	0.37	1.17	1.227		Amp.	
7955613	KRT7	12	3.71	-0.22	1.29	1.018			
8158167	LCN2	9	5.3	1.71	2.22	2.723		Amp.	
8122265	TNFAIP3	6	2.36	0.65	3.11	1.686			
8015323	KRT13	17	5.5	0.72	1.37	1.755		Amp.	
8020740	DSG4	18	2.69	0.23	-0.15	0.455			
8123936	NEDD9	6	2.47	0.03	0.27	0.262			Del. <sup>d</sup>
8173261	ZC4H2	X	0.3	-0.05	-1.82	-0.29			
8152606	SNTB1	8	0.12	3.06	1.84	0.872			
8016994	RNF43	17	-2.98	0.58	0.09	-0.54			
8168749	SRPX2	X	2.71	0.28	0.78	0.84			
8112615	ENC1	5	-2.39	-1.49	-2.01	-1.93			
7916493	PPAP2B	1	1.57	0.03	1.53	0.433			
8081548	PVRL3	3	-3.43	0.18	-1.01	-0.85			
8090180	MUC13	3	1.12	3.14	0.16	0.818		Amp.	
8135763	WNT16	7	-2.96	0.23	-1.1	-0.91	Amp.	Amp.	
8138566	IGF2BP3	7	-3.22	0.26	0.31	-0.64	Amp.	Amp.	
8068633	B3GALT5	21	2.21	-0.16	0.27	0.454			Amp.
8140955	CDK6	7	-0.99	0.64	1.49	0.98	Amp.		
8176174	MPP1	X	-1.87	-0.06	0.06	-0.19			
8026468	CYP4F12	19	2.49	0.62	0.85	1.095			
8174598	IL13RA2	X	3.4	0.58	0.35	0.881			
8129677	SGK1	6	2.27	1.61	1.44	1.739			
8120043	RUNX2	6	2.58	2.09	0.96	1.733			
8038725	KLK10	19	3.93	0.78	1.73	1.746		Amp.	
8096116	AGPAT9	4	2.68	1.14	-0.58	1.211			
8148548	PSCA	8	2.34	-0.04	0.47	0.339		Amp.	
8161964	FRMD3	9	3.14	0.39	0.32	0.734			
7970954	DCLK1	13	-0.44	2.21	3.21	1.463			Del.
7966690	TBX3	12	2.29	1.39	1.58	1.714			Amp.
7899615	SERINC2	1	2.44	2.13	2.37	2.312		Amp.	

8049349	UGT1A	2	1.28	-0.11	0.17	0.288			
8106986	RHOBTB3	5	-1.64	0.15	-3	-0.91			
8027748	FXYD3	19	3.4	1.02	1.88	1.868			
7973433	DHRS2	14	0.45	0.87	2.2	0.95	Del.	Del.	
8101675	ABCG2	4	2.87	1.01	0.27	0.922			
8151730	CALB1	8	3.44	0.8	1.74	1.683			
7927215	ALOX5	10	2.78	0.73	1.59	1.479			
8045889	TANC1	2	1.68	0.3	0.33	0.552			
7925531	AKT3	1	1.98	0.91	2.19	1.578		Amp.	
8098441	ODZ3	4	1.57	0.28	1.61	0.896			Del.
8044574	IL1RN	2	1.81	0.1	0.24	0.354		Del.	
8038683	KLK6	19	3.25	0.93	0.87	1.381		Amp.	
7922773	NCF2	1	1.59	0.09	0.65	0.454			
8068100	NCRNA00189	21	0.11	0.29	1.35	0.347			Amp.
8037205	CEACAM1	19	3.05	0.75	1.64	1.556		Amp.	
7918657	PTPN22	1	3.67	1.53	0.72	1.591			
8098263	PALLD	4	-1.96	-1.72	-2.27	-1.97			Del.
8053417	CAPG	2	1.43	-0.7	-0.23	0.616		Amp.	
8016457	HOXB5	17	1.49	1.97	2.44	1.927			
8067055	ATP9A	20	1.07	0.04	-0.64	0.301			
7902104	PDE4B	1	-2.32	-0.11	-2.07	-0.8			
8077899	PPARG	3	2.26	0.56	0.56	0.89			
8015016	TNS4	17	0.52	0.83	1.68	0.895			
7915472	SLC2A1	1	-1.73	0.8	1.04	1.13			
8095728	EREG	4	-1.52	0.1	-3.87	-0.83			
7923958	C1orf116	1	2.01	0.54	0.82	0.96			
7955694	IGFBP6	12	2.27	1.12	1.5	1.56			
8112803	LHFPL2	5	1.39	0.1	-0.15	0.273			
8033780	ZNF426	19	-1.11	1.12	-0.92	-1.04			
8016463	HOXB6	17	1.53	2.06	2.45	1.979			
7940643	ASRGL1	11	-1.35	0.56	0.01	-0.2		Amp.	
7961182	KLRC2	12	-3.17	-0.99	-1.91	-1.82			Amp.
8038695	KLK7	19	2.78	0.72	0.82	1.178		Amp.	
7950534	WNT11	11	2.45	0.77	0.45	0.951	Amp.	Amp.	
7986214	SLCO3A1	15	2.27	0.53	1.26	1.148			
8098246	ANXA10	4	-0.19	-1.75	-1.4	-0.77			
7990391	CYP1A1	15	2.51	1.14	0.91	1.374			
7946781	PLEKHA7	11	1.68	0.52	0.43	0.722	Amp.	Amp.	
8070411	C21orf88	21	1.43	-0.21	0.11	0.32			Amp.
7920128	S100A11	1	1.24	0.69	1.6	1.108		Amp.	
7902594	PRKACB	1	-3.7	-2.59	-3.14	-3.11			
7957023	LYZ	12	3.63	0.7	1.24	1.466			
8150509	PLAT	8	1.92	-0.61	0.77	0.968			
					-7.87E-				
7920285	S100A2	1	1.43	-0.12	0.05	0.024			Amp.
7976425	OTUB2	14	1.56	0.69	0.81	0.957	Del.		
8122146	Nd	6	-2.21	0.89	0.2	-0.74			
8042993	CTNNA2	2	1.1	-0.03	0.33	0.227			
8076497	A4GALT	22	1.39	1	2.15	1.439		Amp.	
8073068	APOBEC3C	22	1.82	1.35	1.77	1.633		Amp.	
7917850	ARHGAP29	1	-4.1	-1.54	-1.73	-2.22			
7938035	TRIM22	11	1.04	1.76	0.49	0.964	Amp.		
7932985	NRP1	10	2.95	-0.18	0.18	0.458			
7961151	KLRK1	12	-4.33	-0.91	-2.15	-2.04			Amp.
7963333	KRT80	12	1.51	-0.15	-0.03	0.199			

**Supplemental Table S6.** Top 100 common differentially expressed genes (Cumulative p-value <0.001) and corresponding copy number changes in HCT116 p53<sup>-/-</sup>:CYC116 group.

Gene ID	Gene symbol	Chr.	R2.1 logFC	R2.2 logFC	R2.3 logFC	logFC Mean	R2.1 Copy No.	R2.2 Copy No.	R2.3 Copy No.
8135763	WNT16	7	-0.6	-3.9	-0.38	-0.95			
7906954	PBX1	1	1.38	4.11	1.36	1.98			
8140955	CDK6	7	-2.05	1.29	-1.69	-1.65		Amp.	
8171297	MID1	X	-3.99	-4	-4.66	-4.19	Del.	Del.	Del.
7939314	EHF	11	5.37	1.13	4.74	3.07			
8013384	ALDH3A1	17	0.5	3.72	0.24	0.76			Del.
8046726	SSFA2	2	-0.47	-2.1	-0.51	-0.8	Del.		Del.
8152376	CSMD3	8	-0.3	1.67	-0.12	0.39		Del.	
8067140	CYP24A1	20	-5.54	-3.7	-5.79	-4.92			
8140468	PION	7	4.09	-0.2	3.51	1.44			
7895417	SEPT2	2	-1.83	-0.1	-2.04	-0.6			
8106727	ATP6AP1L	5	2.49	-0.2	2.26	1.01	Amp.	Amp.	Amp.
7951686	IL18	11	0.6	-1.7	0.58	-0.84	Amp.	Amp.	Amp.
8148309	Nd	8	-1.39	-1.7	-1.18	-1.42		Del.	
8140668	SEMA3A	7	0.48	-2.5	0.56	-0.87			
8081548	PVRL3	3	-0.51	-2.4	-0.6	-0.9		Amp.	
7950810	SYTL2	11	1.44	-1.6	1.2	1.42	Amp.	Amp.	Amp.
7910915	CHRM3	1	-0.19	2.02	0.13	0.37		Del.	
8038695	KLK7	19	1.48	0.1	1.61	0.61			
7917850	ARHGAP29	1	-1.95	-3.9	-1.25	-2.11			
8113761	ZNF608	5	-1	-1.7	-0.98	-1.19	Amp.	Amp.	Amp.
8076497	A4GALT	22	0.89	1.68	1.1	1.18			
8122634	SAMD5	6	2	-0.3	1.6	1			
7957298	NAV3	12	-0.04	-2	0.11	-0.21			
8073096	APOBEC3H	22	1.71	0.86	1.84	1.39			
8114119	FSTL4	5	1.54	1.3	1.58	1.47	Amp.		Amp.
7958884	OAS1	12	0.3	2.31	0.37	0.64			
8121749	GJA1	6	0.25	-0	1.86	0.28	Amp.	Amp.	Amp.
8065569	BCL2L1	20	0.53	0.86	0.41	1.5			
7965941	GLT8D2	12	0.94	-0.8	0.88	0.86			
8141066	PON3	7	-2.23	-2.2	-1.95	-2.11			
7906969	Nd	1	0.05	1.85	0.13	0.23			
8023043	PSTPIP2	18	-0.01	-1.3	-0.24	-0.15	Amp.	Del.	
8097356	PLK4	4	-1.31	-0.8	-1.42	-1.16	Del.	Del.	Del.
7962151	DENND5B	12	0.96	1.65	0.86	1.11			
7932744	ARMC4	10	-0.38	-1.9	-0.33	-0.62			
7934161	PRF1	10	-2.9	-2.2	-2.8	-2.63	Amp.	Amp.	Amp.
8127234	DST	6	-1.27	-2.2	-1.36	-1.57	Amp.	Amp.	Amp.
8084630	Nd	3	1.37	2.24	1.15	1.52		Amp.	
8084630	Nd	3	1.37	2.24	1.15	1.52		Amp.	
8084630	Nd	3	1.37	2.24	1.15	1.52		Amp.	
8007446	IFI35	17	-0.46	2.23	-0.45	0.77			
8115490	ADAM19	5	0.68	-2	0.4	-0.81			
8082075	DTX3L	3	-0.45	1.39	-0.12	0.42		Amp.	
8075310	LIF	22	1.3	-0.2	1.35	0.66			
8102950	INPP4B	4	-0.68	-2.7	-1.01	-1.23	Del.	Del.	Del.
8027748	FXVD3	19	0.74	2.71	0.76	1.15			
8065071	FLRT3	20	0.34	1.64	0.21	0.49			
8101828	TSPAN5	4	-1.08	-2.8	-1.11	-1.49	Del.	Del.	Del.
8166747	SYTL5	X	0.85	-2.4	0.9	-1.22			

7990391	CYP1A1	15	2.56	4.74	2.21	2.99			Amp.
8152506	SAMD12	8	1.51	1.81	1.63	1.64		Del.	Del.
7927202	ZNF22	10	-2.48	-2	-2.29	-2.23	Amp.	Amp.	Amp.
7902594	PRKACB	1	-1.56	-2	-1.35	-1.62	Amp.	Amp.	Amp.
8036318	ZNF566	19	-0.68	1.35	-0.8	-0.9		Del.	
7935521	AVPI1	10	1.08	1.17	1.19	1.15	Amp.	Amp.	Amp.
8022711	DSC2	18	-0.02	-1.5	-0.34	-0.22	Amp.	Del.	Amp.
7932765	MPP7	10	-0.12	-1.4	-0.17	-0.3		Del.	Del.
7957260	GLIPR1	12	-0.81	-2.7	-0.48	-1.01			
7916862	WLS	1	1.12	-0.6	1.21	0.93			
8102415	CAMK2D	4	-0.66	-1.7	-0.77	-0.95	Del.	Del.	Del.
8150830	LYPLA1	8	-1.23	-1.1	-1.07	-1.12	Del.	Del.	Del.
8154135	SLC1A1	9	1.03	-1.8	0.97	1.21	Amp.	Del.	
8148304	TRIB1	8	0.03	-0.9	0.23	-0.18		Del.	
8106743	VCAN	5	1.05	-2.6	1.14	-1.47	Amp.	Amp.	Amp.
8005029	MAP2K4	17	-1.2	-0.6	-1.38	-1.01	Del.		Del.
8138566	IGF2BP3	7	-2.63	-0.3	-1.63	-1.05		Amp.	
8059716	C2orf52	2	1.18	0.75	1.54	1.11	Amp.	Amp.	Amp.
8106986	RHOBTB3	5	-0.41	-2	-0.54	-0.76	Amp.	Amp.	Amp.
8016094	GJC1	17	-2.55	-1.9	-2.36	-2.24	Amp.	Amp.	
8133018	ZNF716	7	0.05	2.51	0.53	0.39	Amp.	Amp.	Amp.
8144758	ZDHHC2	8	0.41	-0.8	0.45	0.53	Del.	Del.	Del.
8129482	SAMD3	6	-0.07	-1.2	-0.1	-0.2	Amp.		
7917528	Nd	1	-0.34	0.6	-0.68	-0.52			
8100328	USP46	4	-0.84	0.11	-0.85	-0.43	Del.	Amp.	Del.
8047738	NRP2	2	-0.01	1.1	0.34	0.17		Amp.	
7947230	BDNF	11	-0.29	-2.2	-0.35	-0.6			
8081214	GPR15	3	1.42	-1.3	1.03	1.23		Amp.	
8104107	TRIML2	4	-1.78	-2	-1.6	-1.78			
7892605	SEPT2	2	-1.5	0.12	-1.33	-0.62			
8120176	C6orf141	6	0.27	-1.2	0.64	-0.59	Amp.	Amp.	Amp.
7930498	ACSL5	10	-1.7	-2	-1.18	-1.59			
8060225	HDLBP	2	-0.91	-0.1	-1.07	-0.38		Amp.	Amp.
8152617	HAS2	8	2.11	0.03	2.25	0.53		Del.	Del.
7935660	DNMBP	10	-0.34	-1.7	-0.44	-0.64	Amp.		
8075910	RAC2	22	-0.01	-1.2	-0.06	-0.08			
8059345	SCG2	2	-1.05	0.23	-1.16	-0.65		Amp.	
8081158	ARL6	3	-0.24	0.98	-0.09	0.27		Amp.	
8035095	CYP4F11	19	-1.87	-0.7	-2.06	-1.36			Amp.
8160670	AQP3	9	0.41	2.75	0.25	0.65			
8141035	SGCE	7	-1.18	0.39	-0.64	-0.67			
8059111	ABCB6	2	-0.21	0.74	-0.34	0.37		Amp.	Amp.
8059111	ATG9A	2	-0.21	0.74	-0.34	0.37		Amp.	Amp.
7988260	FRMD5	15	-1.5	-1.7	-1.38	-1.52	Amp.		Amp.
7896498	SEPT2	2	-0.81	-0	-1.07	-0.33			
8017651	SMURF2	17	-1.08	-1	-1.14	-1.06	Amp.		
8146379	UBE2V2	8	-0.81	-0.5	-0.92	-0.71	Del.	Del.	Del.
7993478	ABCC1	16	-0.2	1.12	-0.17	0.33		Amp.	
8017843	SLC16A6	17	2.4	-0.6	2.61	1.6			
8112615	ENC1	5	0.09	-1.5	0.39	-0.38	Amp.	Amp.	Amp.

**Supplemental Table S7.** Top 100 common differentially expressed genes (Cumulative p-value <0.001) and corresponding copy number changes in HCT116:ZM447439 group. <sup>a</sup>fg: family gene

Gene ID	Gene symbol	Chr.	R3.1 logFC	R3.2 logFC	R3.3 logFC	logFC Mean	R3.1 Copy No.	R3.2 Copy No.	R3.3 Copy No.
8098441	ODZ3	4	1.949	1.872	2.185	1.998	Del.		
7932744	ARMC4	10	-2.59	-2.67	-2.52	-2.59	Amp.		
8144726	TUSC3	8	1.872	2.211	2.602	2.209	Amp.		
8098263	PALLD	4	-2.18	-2	-1.99	-2.05	Amp.		
7989146	MNS1	15	-1.61	-1.56	-1.35	-1.5			
7894805	Nd	1	-0.43	-1.91	-0.55	-0.77			
8021169	LIPG	18	-1.03	-1	-1.22	-1.08			
8059854	ARL4C	2	1.866	0.953	1.152	1.27			
7893924	Nd	5	4.604	6.218	5.593	5.43			
7895294	ILF2	1	-1.37	-1.33	-0.49	-0.96			
8122176	TCF21	6	-1.22	-0.97	-1.06	-1.08			
7932765	MPP7	10	-2.08	-2.28	-2.2	-2.18	Amp.		
7895205	Nd	1	1.628	1.559	1.57	1.586			
7894487	Nd	2	-1.06	-1.46	-0.28	-0.75			
7893953	Nd	17	0.941	1.278	1.175	1.122			
7975154	NCRNA00238	14	1.573	0.154	0.215	0.373	Del.		
7896206	Nd	14	-0.39	-1.42	-0.71	-0.73			
7932733	MKX	10	-1.76	-1.68	-1.75	-1.73	Amp.		
8152376	CSMD3	8	1.521	1.813	1.934	1.747	Amp.		
8112615	ENC1	5	-1.86	-1.39	-0.99	-1.37	Amp.		
8102328	CFI	4	0.822	0.178	0.071	0.218	Del.		
8088952	Nd	3	1.552	0.431	0.654	0.759			
7893175	Nd	19	1.829	1.995	1.755	1.857			
8089467	ZBED2	3	-1.75	-0.71	-0.47	-0.83	Amp.	Amp.	
8013519	Nd	17	1.872	1.107	0.327	0.878			
8013519	Nd	5	1.872	1.107	0.327	0.878			
8003230	Nd	16	0.991	0.934	1.073	0.998	Del.		
7899615	SERINC2	1	0.523	1.289	1.146	0.917	Del.		
7937335	IFITM...fg <sup>a</sup>	11	2.179	0.229	0.228	0.484	Del.		
7937335	IFITM1	11	2.179	0.229	0.228	0.484	Del.		
7937335	IFITM2	11	2.179	0.229	0.228	0.484	Del.		
7934731	C1DP...fg	10	0.217	-0.9	-1.12	-0.6			
7934731	C1DP2	10	0.217	-0.9	-1.12	-0.6			
7934731	C1DP3	10	0.217	-0.9	-1.12	-0.6			
7934731	C1DP1	10	0.217	-0.9	-1.12	-0.6			
7934731	C1DP4	10	0.217	-0.9	-1.12	-0.6			
7934731	C1D	2	0.217	-0.9	-1.12	-0.6			
7903717	MIR197	1	0.687	1.372	1.049	0.996			
7952205	MCAM	11	0.958	0.824	0.882	0.886	Del.		
7894185	OAZ1	19	-0.71	-1.08	-0.69	-0.81			
8142763	Nd	7	-0.73	-0.58	0.019	-0.2	Del.		
7947230	BDNF	11	-1.14	-1.57	-1.3	-1.32	Del.	Del.	Del.
8135594	CAV1	7	-1.17	-1.22	-1.38	-1.26			
7902265	Nd	1	0.946	1.285	1.087	1.098			
7901175	TSPAN1	1	1.563	1.468	1.121	1.37	Del.		
7916493	PPAP2B	1	0.755	0.616	0.514	0.621	Amp.		
7894891	Nd	2	1.25	2.188	1.987	1.758			
7893711	ABCF1	6	1.828	1.907	1.65	1.792			
7995320	Nd	16	1.188	1.597	1.266	1.339	Amp.		
7995320	Nd	16	1.188	1.597	1.266	1.339	Amp.		
7995320	Nd	16	1.188	1.597	1.266	1.339	Amp.		
7995320	Nd	16	1.188	1.597	1.266	1.339	Amp.		
7895508	Nd	6	0.357	0.815	0.685	0.584			



8155497	FAM27C	9	1.575	1.948	1.795	1.766	Amp.		
7921987	TMCO1	1	-0.6	-0.88	-0.61	-0.69	Del.		
8083453	Nd	17	0.612	0.832	0.776	0.734			
8083453	Nd	17	0.612	0.832	0.776	0.734			
8083453	Nd	17	0.612	0.832	0.776	0.734			
8083453	Nd	17	0.612	0.832	0.776	0.734			
8083453	.nd	2	0.612	0.832	0.776	0.734			
8083453	Nd	2	0.612	0.832	0.776	0.734			
8083453	Nd	2	0.612	0.832	0.776	0.734			
8083453	Nd	2	0.612	0.832	0.776	0.734			
8083453	Nd	3	0.612	0.832	0.776	0.734			
8083453	Nd	3	0.612	0.832	0.776	0.734			
8083453	Nd	3	0.612	0.832	0.776	0.734			
8111255	CDH10	5	0.53	0.763	0.896	0.713		Amp.	
7896217	Nd	19	-0.35	-1.17	-0.48	-0.58			
8132962	CCT6A	7	-0.04	-2.01	-0.52	-0.35	Del.		
8132962	SNORA15	7	-0.04	-2.01	-0.52	-0.35	Del.		
7893844	Nd	14	0.813	1.207	0.819	0.93			
8044080	SLC9A2	2	-0.85	-0.7	-0.73	-0.76	Amp.		
8130499	DYNLT1	6	-0.83	-1.05	-1.02	-0.96	Del.	Del.	
8065082	Nd	20	-0.54	0.106	-0.26	-0.25			
8106923	NR2F1	5	-0.87	-0.73	-0.89	-0.83	Del.		
8097256	FGF2	4	0.977	1.204	1.078	1.083			
8144667	SUB1P1	8	-0.68	-1.04	-0.79	-0.83	Del.		
8082607	ATP2C1	3	-0.86	-0.97	-0.85	-0.89	Del.		
7895711	Nd	2	1.345	-0.05	0.307	0.282			
7912994	IFFO2	1	1.219	0.709	0.66	0.829	Del.		
7925531	AKT3	1	1.595	1.035	1.077	1.212	Amp.	Del.	
7893864	Nd	6	0.227	-0.68	-0.55	-0.44			
7971669	Nd	13	0.7	1.23	0.983	0.946	Del.	Del.	Del.
7895521	HNRNPD	4	-0.61	-0.74	-0.29	-0.51			
7896540	Nd	12	1.524	1.961	1.978	1.808			
8079426	TMIE	3	0.318	0.756	0.443	0.474	Del.		
7895791	Nd	19	-0.69	-1.01	-0.15	-0.47			
7896112	Nd	2	-0.55	-1.16	-0.31	-0.58			
7896112	IK	5	-0.55	-1.16	-0.31	-0.58			
7892996	Nd	2	0.13	-0.82	-0.44	-0.36			
7892996	Nd	5	0.13	-0.82	-0.44	-0.36			
8114396	CDC23	5	-0.69	-1.1	-0.67	-0.8	Del.		
8100376	Nd	4	0.755	0.991	0.717	0.813	Amp.		
7893051	Nd	5	1.731	2.423	2.256	2.115			
8109424	Nd	5	1.109	1.602	1.549	1.402			
8105612	CWC27	5	-0.66	-0.92	-0.73	-0.76	Amp.		
7905444	SNX27	1	-0.49	-0.68	-0.52	-0.56			
8052370	Nd	2	0.843	1.339	0.915	1.011	Amp.		
8098246	ANXA10	4	-1.49	-1.67	-1.5	-1.55	Amp.		
7895085	SMNDC1	10	0.287	-0.72	-0.84	-0.56			

**Supplemental Table S8.** Top 100 common differentially expressed genes (Cumulative p-value <0.001) and corresponding copy number changes in HCT116 p53<sup>-/-</sup>:ZM447439 group.

Gene ID	Gen symbol	Chr.	R4.1 logFC	R4.2 logFC	R4.3 logFC	logFC Mean	R4.1 Copy No.	R4.2 Copy No.	R4.3 Copy No.
8148040	MAL2	8	-5.55	-5.56	-5.68	-5.6			
8067140	CYP24A1	20	-5.5	-5.61	-6.22	-5.77			
8148280	SQLE	8	-2.41	-2.77	-2.47	-2.55			
8030804	CD33	19	1.24	1.81	1.768	1.586	Amp.		Amp.
7983650	SLC27A2	15	-3.43	-3.35	-2.95	-3.24			
7960143	ZNF84	12	0.19	-1.85	-0.5	-0.56			
8113512	EPB41L4A	5	2.47	2.06	2.797	2.421		Amp.	
8055496	LRP1B	2	2.02	0.89	2.048	1.544	Amp.	Amp.	Amp.
8135763	WNT16	7	-0.33	-1.45	-1.41	-0.88			
8129476	C6orf191	6	0.67	0.83	2.264	1.076			
8098246	ANXA10	4	-1.82	-1.3	-1.2	-1.42			
7916862	WLS	1	0.91	0.94	1.253	1.025			
8135587	CAV2	7	-1.53	-1.2	-1.53	-1.41			
8172158	CASK	X	-2.04	-2.02	-1.96	-2.01			Del.
8023561	LMAN1	18	-3.1	-3.36	-3.05	-3.17		Amp.	Amp.
7901175	TSPAN1	1	0.72	1.65	0.988	1.054			
8036318	ZNF566	19	1.19	-0.44	1.368	0.893			
7961166	KLRC4	12	0.38	-0.72	1.128	0.677			
8115327	SPARC	5	2.8	2.76	2.87	2.809			
8148309	ND	8	-1.33	-2	-1.34	-1.53			
8103415	FAM198B	4	0.96	1.29	2.959	1.544			
8028058	KIRREL2	19	1.54	1.43	1.52	1.494			
8135594	CAV1	7	-2.22	-1.89	-2.22	-2.1			
8151496	ZNF704	8	1.4	1.03	1.118	1.174			
8102415	CAMK2D	4	-1.59	-1.38	-1.54	-1.5	Del.		
8038192	FUT1	19	0.58	1.2	0.358	0.629			
8166747	SYTL5	X	-1.53	-1.63	-2.13	-1.74			
8106986	RHOBTB3	5	-0.86	-1.59	-0.8	-1.03			
7977933	SLC7A8	14	1.27	1.11	1.885	1.385	Amp.		Amp.
7902104	PDE4B	1	-1.56	-1.81	-1.36	-1.57			
8003060	SDR42E1	16	-1.4	-1.46	-1.2	-1.35			
7954559	PPFIBP1	12	0.14	-1.05	0.143	-0.28			
8138805	CPVL	7	1.11	0.64	0.932	0.872			
8180200	ZNF493	19	-0.77	-0.72	-1.11	-0.85			
7934970	HTR7	10	-1.28	-1.21	-1.59	-1.35			
7932744	ARMC4	10	0.23	-0.9	0.348	-0.42			
8072587	SLC5A1	22	0.34	0.75	1.506	0.73			
8096160	ARHGAP24	4	1.26	1.28	1.282	1.276	Del.		
7982066	Nd	15	-0.12	2.09	0.734	0.568	Amp.		Amp.
7982066	SNORD115-24	15	-0.12	2.09	0.734	0.568	Amp.		Amp.
7982066	SNORD115-30	15	-0.12	2.09	0.734	0.568	Amp.		Amp.
7982066	SNORD115-42	15	-0.12	2.09	0.734	0.568	Amp.		Amp.
7978376	STXBP6	14	-0.66	0.06	-0.88	-0.33	Amp.	Amp.	Amp.
8127563	COL12A1	6	-0.83	-1.61	-1.24	-1.18		Amp.	
8035847	ZNF675	19	-0.62	-1.4	-0.5	-0.76	Amp.		Amp.
8069880	TIAM1	21	-0.88	-0.8	-1.03	-0.9			
8126820	GPR110	6	-0.4	-1.56	0.481	-0.67			
8040163	IAH1	2	-0.86	-0.89	-0.99	-0.91			
8099393	Nd	4	-1.23	-0.22	-0.75	-0.58		Amp.	
7926875	BAMBI	10	0.42	1.32	1.625	0.964			
8081214	GPR15	3	-1.24	-1.54	-1.3	-1.36			
8167973	HEPH	X	1.31	0.76	0.814	0.933			
8110084	MSX2	5	-1.49	-1.35	-1.44	-1.43			
8174527	CAPN6	X	0.96	0.68	1.222	0.929			

7943263	AMOTL1	11	0.29	-0.79	-0.05	-0.23			
8149927	CLU	8	-0.43	-0.66	-0.73	-0.59			
8085263	TMEM111	3	-1.23	-1.27	-1.3	-1.26			
7960134	ZNF26	12	-1.58	-1.82	-1.32	-1.56			
8175217	GPC4	X	-0.5	0.77	0.551	0.595			
7951077	SESN3	11	-1.87	-1.9	-1.31	-1.67			
8117045	RBM24	6	0.32	-1.09	-0.22	-0.43	Amp.		Amp.
8053325	Nd	2	0.34	0.99	1.27	0.754			
7961175	KLRC3	12	-0.09	-0.79	0.38	-0.3			
8168749	SRPX2	X	-0.93	-0.89	-1.23	-1			
7932765	MPP7	10	0.07	-1.14	-0.2	-0.26	Del.	Del.	Del.
8060988	BTBD3	20	1.37	1.16	1.154	1.222			
8049487	MLPH	2	-1.17	-1.22	-1.38	-1.25	Amp.	Amp.	Amp.
8035842	ZNF91	19	-0.41	-1.51	-1.06	-0.87			Amp.
8033754	ZNF266	19	-1.4	-1.19	-1.22	-1.27			
8062041	ACSS2	20	0.52	1.22	0.291	0.568			
7997010	CLEC18...fg	16	-0.95	0.29	-1.55	-0.75			Amp.
7997010	CLEC18A	16	-0.95	0.29	-1.55	-0.75			Amp.
7997010	CLEC18C	16	-0.95	0.29	-1.55	-0.75			Amp.
8015133	KRT23	17	-2.08	-1.84	-0.81	-1.46	Amp.		Amp.
8074853	ZNF280A	22	-0.78	-0.65	-0.77	-0.73			
7958352	BTBD11	12	1.19	1.37	1.502	1.349			
7951686	IL18	11	-0.85	0.11	-0.08	-0.19			
8175269	FAM122B	X	-0.7	-0.6	-0.55	-0.61			
8045336	GPR39	2	0.29	1.34	-0.07	0.301	Del.	Del.	Del.
7960529	SCNN1A	12	-0.98	-0.23	-1.11	-0.63			
7896179	Nd	14	-0.16	-1.04	0.045	-0.2			
8161737	Nd	9	-0.74	-1.09	-0.64	-0.8	Del.	Del.	Del.
8117415	HIST1H3E	6	0.65	0.56	0.808	0.665	Amp.		Amp.
8145365	DOCK5	8	-0.89	-0.46	-0.73	-0.67			
8063923	SLCO4A1	20	1.07	1.14	0.805	0.995	Amp.		
7961151	KLRK1	12	0.42	-0.32	1.368	0.567			
7893748	Nd	16	-0.42	0	0.633	0.096			
8150862	Nd	8	-0.78	-0.85	-0.86	-0.83			
7951036	SNORD5	11	-0.86	-1.07	-0.83	-0.91			
7951036	SNORA18	11	-0.86	-1.07	-0.83	-0.91			
7951036	MIR1304	11	-0.86	-1.07	-0.83	-0.91			
8082058	CSTA	3	-0.01	1.55	-0.06	0.083			
7966690	TBX3	12	1.25	0.36	1.135	0.802	Del.	Del.	Del.
7894895	ILF2	1	-1.42	-0.49	0.484	-0.7			
8035318	UNC13A	19	0.46	0.83	0.616	0.618	Amp.		Amp.
8134219	CCDC132	7	-0.83	-0.76	-0.5	-0.68			
8106727	ATP6AP1L	5	0	1.25	0.322	0.12			
8140668	SEMA3A	7	0.83	0.53	1.002	0.762			
8103563	DDX60	4	-0.58	-0.34	0.693	-0.52			
8098441	ODZ3	4	-0.86	-0.9	-0.73	-0.82			

**Supplemental Table S9.** Totally 28 genes from microarray data ( $p < 0.001$ ) were validated by qRT-PCR. Nearly 100% correspondence in expression patterns can be noticed. Positive value indicate up-regulation and negative values represent down-regulation. Values from microarray data are represented as fold changes in comparison to control. <sup>a</sup>NC=No change in expression.

Gene	p53+/+:CYC116 clones		p53-/-:CYC116 clones		p53+/+: ZM447439 clones		p53-/-: ZM447439 clones	
	Micro array	qRT-PCR	Micro array	qRT-PCR	Micro array	qRT-PCR	Micro array	qRT-PCR
CYP24A1	-32	-33	-30	-50	NC <sup>a</sup>	NC	-55	-200
Bcl-xL	2	2	1.5	2	NC	NC	NC	NC
GJC1	-3	-3.5	-5	-5	NC	NC	NC	NC
NCAM1	2	22	NC	NC	NC	NC	NC	NC
KLK5	2.34	62	NC	NC	NC	NC	NC	NC
KRT7	2	30	NC	NC	NC	NC	NC	NC
LCN2	7	229	NC	NC	NC	NC	NC	NC
TNFAIP3	3.22	11	NC	NC	NC	NC	NC	NC
KRT13	3.4	396	NC	NC	NC	NC	NC	NC
PPAP2B	1.4	7	NC	NC	2	2.3	NC	NC
TBX3	3.3	11	NC	NC	NC	NC	2	7.4
SERINC2	5	7.4	NC	NC	2	2.1	NC	NC
HOXB5	4	5.4	NC	NC	NC	NC	NC	NC
ANXA10	-2	-2	NC	NC	-3	-6	-3	-1.3
CYP1A1	3	9	8	28	NC	NC	NC	NC
PRKACB	-9	-6	-3	-3	NC	NC	NC	NC
A4GALT	3	6.3	2.3	6.2	NC	NC	NC	NC
ARHGAP29	-5	-5	-4.3	-2.3	NC	NC	NC	NC
NRP1	1.4	14	NC	NC	NC	NC	NC	NC
KLRK1	-4	-3	NC	NC	NC	NC	1.5	1.3
MID1	NC	NC	-18	-3	NC	NC	NC	NC
EHF	NC	NC	8.4	264	NC	NC	NC	NC
SEMA3A	NC	NC	<b>-2</b>	<b>3</b>	NC	NC	2	3
PLK4	NC	NC	-2.2	-1.1	NC	NC	NC	NC
INPP4B	NC	NC	-2.4	-1.2	NC	NC	NC	NC
CAMK2D	NC	NC	-2	-1.4	NC	NC	-3	-3.2
BDNF	NC	NC	-1.5	-1.4	-2.5	-4.5	NC	NC
TSPAN1	NC	NC	NC	NC	2.6	2	2.1	4

**Supplemental Table S10A. Common pathways affected in each group of resistant clones**

<b>Group</b>	<b>Common pathways affected</b>
HCT116 p53+/+ CYC116	Development-IGF-1 receptor signaling, PGE2 pathways in cancer, development-A3 receptor signaling, and development-PIP3 signaling in cardiac myocytes.
HCT116 p53-/- CYC116	Cell adhesion-alpha-4 integrins in cell migration and adhesion, translation-(L)-selenoaminoacids incorporation in proteins during translation, immune response-antigen presentation by MHC class II, and CFTR translational fidelity (class I mutations).
HCT116 p53+/+ ZM447439	Development-Ligand-dependent activation of the ESR1/AP-1 pathway, muscle contraction-regulation of eNOS activity in endothelial cells, and reproduction-GnRH signaling.
HCT116 p53-/- ZM447439	Cholesterol and Sphingolipids transport / Influx to the early endosome in lung and transcription-Ligand-Dependent transcription of retinoid-target genes.

**Supplemental Table S10B. Common and differential affected pathways based on p53 background of CYC116 or ZM447439 resistant clones**

<b>Group</b>	<b>Common pathways</b>	<b>Differential pathways</b>
p53+/+ and p53-/- CYC116 resistant clones	Cell adhesion-alpha-4 integrins in cell migration and adhesion, signal transduction-Erk Interactions, signal transduction-cAMP signaling, transport-ACM3 in salivary glands, and regulation of lipid metabolism-regulation of lipid metabolism by niacin and Isoprenaline.	DNA damage-mismatch repair, cell cycle-Spindle assembly and chromosome separation, and cell cycle-role of APC in cell cycle regulation.
p53+/+ and p53-/- ZM447439 resistant clones	Delta508-CFTR traffic/ER-to-golgi, normal wtCFTR traffic/ER-to-golgi, neurophysiological process-NMDA-dependent postsynaptic long-term potentiation in CA1 hippocampal neurons, neurophysiological process-dopamine D2 receptor transactivation of PDGFR in CNS, and cholesterol and sphingolipids transport/Influx to the early endosome in lung.	Immune response-classical complement pathway, immune response-human NKG2D signaling,

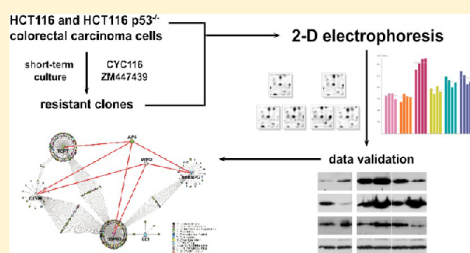
## Supplemental references

1. Girdler F, Sessa F, Patercoli S, Villa F, Musacchio A, Taylor S. Molecular basis of drug resistance in aurora kinases. *Chem Biol* 2008;15:552-62.
2. Word J M, Lovell S C, Richardson J S, Richardson DC. Asparagine and glutamine: using hydrogen atom contacts in the choice of side-chain amide orientation. *J Mol Biol* 1999; 285:1735-1747.
3. Case DA, Darden TA, Cheatham III TE, Simmerling CL, Wang J, Duke RE, et al. AMBER 11, University of California, San Francisco, 2010.
4. Pettersen EF, Goddard TD, Huang CC, Couch GS, Greenblatt DM, Meng EC, Ferrin TE. UCSF—Chimera a visualization system for exploratory research and analysis. *J Comput Chem* 2004;25:1605-1612.
5. Duan Y, Wu C, Chowdhury S, Lee MC, Xiong GM, Zhang W, et al. A point-charge force field for molecular mechanics simulations of proteins based on condensed-phase quantum mechanical calculations. *J Comput Chem* 2003; 24:1999-2012.
6. Wang JM, Wolf RM, Caldwell JW, Kollman PA, Case DA. Development and testing of a general amber force field. *J Comput Chem* 2004; 25:1157-1174.
7. Bayly CI, Cieplak P, Cornell WD, Kollman PA. A well-behaved electrostatic potential based method using charge restraints for determining atom-centered charges: The RESP model. *J Phys Chem* 1993;97:10269-10280.
8. De Lano WL. The PyMOL Molecular Graphics System, DeLano Scientific LLC, San Carlos, CA, 2002
9. Fanfrlík J, Bronowska AK, Řezáč J, Přenosil O, Konvalinka J, Hobza P. A reliable docking/scoring scheme based on the semiempirical quantum mechanical PM6-DH2 method accurately covering dispersion and H-bonding: HIV-1 protease with 22 ligands. *J Phys Chem B* 2010;114:12666-78
10. Dobeš P, Fanfrlík J, Řezáč J, Otyepka M, Hobza P. Transferable scoring function based on semiempirical quantum mechanical PM6-DH2 method: CDK2 with 15 structurally diverse inhibitors. *J Comput Aided Mol Des* 2011; 25:223-35
11. Tsui V, Case DA. Theory and applications of the generalized Born solvation model in macromolecular simulations. *Biopolymers* 2001;56:275-291.
12. Řezáč J, Hobza P. Advanced corrections of hydrogen bonding and dispersion for semiempirical quantum mechanical methods. *J Chem Theory Comput* 2012;8:141-51.
13. Maestro, version 8.5; Schrodinger, LLC: New York, NY 2008.
14. Friesner RA, Murphy RB, Repasky MP, Frye LL, Greenwood JR, Halgren TA, et al. Extra precise glide: docking and scoring incorporating a model of hydrophobic enclosure for protein-ligand complexes. *J Med Chem* 2006; 49:6177–619.

**Cancer Cell Resistance to Aurora Kinase Inhibitors: Identification of Novel Targets for Cancer Therapy**Rita Hrabakova,<sup>†</sup> Madhu Kollareddy,<sup>‡</sup> Jirina Tyleckova,<sup>†</sup> Petr Halada,<sup>§</sup> Marian Hajduch,<sup>‡</sup> Suresh Jivan Gadher,<sup>||</sup> and Hana Kovarova<sup>\*,†</sup><sup>†</sup>Institute of Animal Physiology and Genetics, AS CR, v.v.i., Laboratory of Biochemistry and Molecular Biology of Germ Cells, Rumburska 89, 277 21 Libečov, Czech Republic<sup>‡</sup>Institute of Molecular and Translational Medicine, Laboratory of Experimental Medicine, Palacky University and University Hospital in Olomouc, Faculty of Medicine and Dentistry, Hnevotinska 5, 775 15 Olomouc, Czech Republic<sup>§</sup>Institute of Microbiology, AS CR, v.v.i., Laboratory of Molecular Structure Characterisation, Videnska 1083, 142 20 Prague, Czech Republic<sup>||</sup>Life Technologies, Frederick, Maryland 21704, United States**S** Supporting Information

**ABSTRACT:** Drug resistance is the major obstacle to successful cancer therapy. Our study focuses on resistance to Aurora kinase inhibitors tested as anti-cancer drugs in clinical trials. We have used 2D electrophoresis in the pH ranges of 4–7 and 6–11 followed by protein identification using MALDI-TOF/TOF to compare the protein composition of HCT116 colon cancer cells either sensitive to CYC116 and ZM447439 inhibitors or resistant toward these drugs. The analysis also included p53<sup>+/+</sup> and p53<sup>-/-</sup> phenotypes of HCT116 cells. Our findings demonstrate that platelet-activating factor acetylhydrolase and GTP-binding nuclear protein Ran contribute to the development of resistance to ZM447439 only where resistance is related to p53. On the other hand, serine hydroxymethyltransferase was found to promote the tumor growth in cells resistant to CYC116 without the influence of p53. Computer modeling of interaction networks highlighted a direct link of the p53-independent mechanism of resistance to CYC116 with autophagy. Importantly, serine hydroxymethyltransferase, serpin B5 and calretinin represent the target proteins that may help overcome resistance in combination therapies. In addition, serpin B5 and calretinin appear to be candidate biomarkers that may be accessible in patients for monitoring of cancer therapy with ease.

**KEYWORDS:** Aurora kinase inhibitors, resistance, p53, apoptosis, autophagy, platelet-activating factor acetylhydrolase, Ran, serine hydroxymethyltransferase, serpin B5, calretinin

**■ INTRODUCTION**

Despite significant progress in the development of anti-cancer drugs, there is still a need for novel therapeutic strategies that would overcome development of drug resistance and improve the outcome of cancer patient therapy. Extensive efforts have been made to develop the therapy directed toward specific genetic alterations present predominantly or exclusively in tumors but not in normal cells. Aurora kinases (AURKs), which are comprised of three family members, Aurora-A, Aurora-B, and Aurora-C, are essential regulators of mitotic events including G2/M transition, spindle organization, chromosome segregation, and cytokinesis. Because AURKs are frequently overexpressed in human cancers, they have emerged as attractive therapeutic targets.<sup>1</sup> Accordingly, inhibitors of AURKs with potent anti-proliferative and anti-apoptotic effects have evolved, too.<sup>2</sup>

In the present study, we have taken into account an experimental and well characterized AURK inhibitor

ZM447439, 4-(4-(N-benzoylamino)anilino)-6-methoxy-7-(3-(1-morpholino)propoxy)quinazoline, which has been found to inhibit AURK-A and AURK-B,<sup>3</sup> and a novel AURK inhibitor CYC116, ([4-(2-amino-4-methyl-thiazol-5-yl)pyrimidin-2-yl]-(4-morpholin-4-ylphenyl)-amine), which inhibits not only AURK-A, AURK-B and AURK-C, but also angiogenesis promoter VEGFR2 (vascular endothelial growth factor receptor 2).<sup>2,4</sup>

A major obstacle to successful cancer therapy is the presence of dormant and/or drug resistant cells, which may later evoke disease relapse. In response to anti-cancer treatment, changes in different cellular processes are triggered as tumors struggle to survive where mechanisms of extreme importance including pharmacological, physiological, and altered survival pathway parameters come into play. For instance, the overexpression of

**Received:** August 30, 2012

drug transport pumps can lead to the increased drug efflux, which usually manifests as multi-drug resistance.<sup>5</sup> Additionally, activated DNA repair and impaired apoptosis have been implicated in the development of drug resistance.<sup>6,7</sup> Cancer stem cell phenomenon and epigenetic regulation that simultaneously influence expression of multiple genes might also contribute to the acquisition of drug resistance.<sup>8,9</sup> Nevertheless, molecular mechanisms of drug resistance have not yet been fully elucidated in spite of numerous studies carried out to date.

Previous studies have described mutations in p53 tumor suppressor gene in over 50% of human malignancies including colorectal cancer.<sup>10</sup> Some forms and/or combinations of p53 mutants may also enhance resistance of tumor cells to anti-cancer drugs.<sup>11</sup> In response to genotoxic stress and hypoxia, p53 transcriptionally activates upstream genes important for cell cycle arrest, DNA repair, or apoptosis<sup>12</sup> and can also induce apoptosis by non-transcriptional inhibition of bcl-2 and bcl-xl proteins at the mitochondrial membrane level.<sup>13</sup> Additionally, there is an important interaction between p53 and AURK, and deregulation of functional balance might trigger chromosome instability and carcinogenesis.<sup>14</sup>

Interaction of p53 with AURK-A suppresses its oncogenic activity.<sup>15</sup> On the other hand, AURK-A phosphorylates p53, resulting in p53 protein turnover and its transcriptional activity.<sup>16</sup> It has been shown that pharmacological inhibition of AURK-A provides a growth advantage to cells that have suffered from p53 loss or alternatively may lead to complete loss of wild-type p53 activity.<sup>14</sup> It remains obscure how p53 affects the development of resistance to AURK inhibitors in cancer cells.

Currently, proteomic approaches represent promising tools in our understanding of the molecular mechanisms of various diseases and for a quest for disease biomarkers as well as specific targets for novel drugs. We have used 2D electrophoresis in pH ranges of 4–7 and 6–11 to compare sensitive and resistant HCT116 human colon cancer cells with p53<sup>+/+</sup> (wild-type) and p53<sup>-/-</sup> phenotypes. Using MALDI-TOF/TOF, we have identified proteins that may contribute to the acquisition of resistance toward CYC116 and ZM447439 AURK inhibitors. Such protein alterations have also been examined in CCRF-CEM human T-lymphoblastic leukemia cells carrying p53 mutations<sup>17</sup> and A549 human lung adenocarcinoma cells with p53 wild-type phenotype<sup>18</sup> resistant to diverse anti-cancer drugs. On the basis of our findings, we propose novel targets for drugs, which may prevent or overcome the drug resistance and highlight candidate markers that could be used to monitor anti-cancer therapy in patients.

## ■ EXPERIMENTAL SECTION

### Chemicals

Unless otherwise stated, all chemicals were obtained from Sigma-Aldrich (St. Louis, MO).

### Cell Culture and Sample Preparation

HCT116 p53<sup>+/+</sup> (wild-type) and HCT116 p53<sup>-/-</sup> cell lines derived from a human colon carcinoma were purchased from Horizon Discovery Ltd. (Cambridge, United Kingdom) and cultured in DMEM supplemented with 10% FCS (PAN-Biotech GmbH, Aidenbach, Germany), penicillin (Biotika, Prague, Czech Republic), and streptomycin at 37 °C and 5% CO<sub>2</sub>. Cells resistant to AURK inhibitors were derived by short-term exposure of parental sensitive cells directly to 1 μM (cytotoxic dose above IC<sub>50</sub> for both inhibitors) CYC116 (Cyclacel Ltd., Dundee Technopole, Dundee, Scotland, United Kingdom) or

ZM447439 (AstraZeneca Pharmaceuticals Ltd., London, United Kingdom). After 5 weeks, several colonies were isolated, and a MTT-based proliferation assay was performed as described previously<sup>19</sup> to confirm resistance to AURK inhibitors. The resistance was evaluated as a fold increase calculated by dividing mean IC<sub>50</sub> values of respective resistant clones and parental p53<sup>+/+</sup> and p53<sup>-/-</sup> sensitive cells.

In the present study, two clones resistant to CYC116 with wild-type p53<sup>+/+</sup> alleles (R1.2 and R1.3), two clones resistant to CYC116 with mutated p53<sup>-/-</sup> alleles (R2.1 and R2.2), two clones resistant to ZM447439 with wild-type p53<sup>+/+</sup> alleles (R3.1 and R3.2), and two clones resistant to ZM447439 with mutated p53<sup>-/-</sup> alleles (R4.2 and R4.3) were analyzed. Clones exhibited high resistance with a fold increase of IC<sub>50</sub> as follows: 82 and 63 for R1.2 and R1.3, 64 and 41 for R2.1 and R2.2, 83 for both R3.1 and R3.2, and 38 and 39 for R4.2 and R4.3, respectively. All clones were maintained at 1 μM concentration of AURK inhibitors.

The CCRF-CEM (human T-lymphoblastic leukemia cells) and A549 (human lung adenocarcinoma) cell lines were obtained from American Tissue Culture Collection (ATCC, Manassas, VA). The CCRF-CEM and A549 cells were cultured at 37 °C and 5% CO<sub>2</sub> in RPMI 1640 and DMEM, respectively, with 5 g/L glucose, 2 mM glutamine, 10% FCS (PAN-Biotech GmbH), penicillin (Biotika), and streptomycin. The CCRF-CEM cells resistant to daunorubicin, vincristine, or cytarabine as well as A549 cells resistant to vincristine or paclitaxel were established as described previously<sup>20</sup> and grown in the media mentioned above.

Cells were grown to 80% confluency in Petri dish, rinsed with cold PBS, and solubilized in 500 μL of extraction buffer consisting of 7 M urea, 2 M thiourea, 3% w/v CHAPS (Carl Roth GmbH, Karlsruhe, Germany), 2% v/v Nonidet 40, 5 mM TCEP, protease inhibitor cocktail (complete Mini, Roche, Mannheim, Germany), and phosphatase inhibitor cocktail (PhosSTOP, Roche, Mannheim, Germany). Cell lysates were left for 30 min at room temperature to optimize protein extraction and centrifuged at 20000g at 4 °C for 1 h, and the clarified protein extracts were kept at -80 °C until used. The protein concentration of each sample was estimated using the Pierce 660 nm protein assay kit (Thermo Scientific, Rockford, IL) according to the manufacturer's protocol.

### 2-DE and Evaluation of Protein Spot Differences

2-DE was carried out using Protean IEF Cell (Bio-Rad, Hercules, CA) for the first dimension and Protean II xi Cell (Bio-Rad) for the second dimension. Polyacrylamide gel strips with an IPG of 4–7 and 6–11 (180 mm × 3 mm × 0.5 mm, GE Healthcare, Uppsala, Sweden) were loaded with 100 and 70 μg of proteins, respectively. For the pH range 4–7, protein extracts were diluted to 130 μL with extraction buffer and dissolved in 230 μL of rehydration buffer: 7 M urea, 2 M thiourea, 4% CHAPS, 200 mM DeStreak reagent (GE Healthcare, Uppsala, Sweden), 2% IPG buffer pH 4–7 (GE Healthcare), protease inhibitor cocktail, phosphatase inhibitor cocktail, and a trace of bromophenol blue. Proteins were loaded into IPG strips using overnight in gel rehydration at 50 V, and IEF was performed at the following voltages: 200 V for 10 h, 600 V for 30 min, 1000 V for 30 min, and 5000 V for the time period necessary to reach 50000 Vh in total. After IEF separation, IPG strips were equilibrated in 50 mM Tris-HCl, pH 6.8 (Carl Roth GmbH), 6 M urea, 30% glycerol (Penta, Prague, Czech Republic), 4% SDS, and 100 mM DeStreak reagent for 25 min.



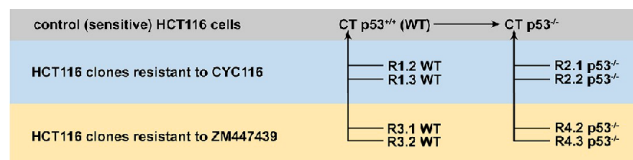


**Figure 1.** Clones resistant to CYC116 or ZM447439 AURK inhibitors analyzed using 2-DE. Wild-type (WT) p53<sup>+/+</sup> resistant cells were compared to sensitive HCT116 p53<sup>+/+</sup> cells, and resistant cells carrying p53<sup>-/-</sup> alleles were compared to sensitive HCT116 p53<sup>-/-</sup> cells.

For the pH range 6–11, IPG strips were passively rehydrated overnight without sample in 340  $\mu$ L of rehydration buffer with 0.5% IPG buffer, pH 6–11 (GE Healthcare), and 30 mM DTT instead of DeStreak reducing agent. Protein extracts were diluted to 150  $\mu$ L with extraction buffer supplemented by 65 mM DTT and 0.5% IPG buffer, pH 6–11. After 15 min, free thiol groups were alkylated by 30 mM iodoacetamide, a trace of bromophenol blue was added, and cup-loading was applied. IEF was performed at the following voltages: 150 V for 12 h, 1000 V for 1 h, 8000 V for 3 h, and 8000 V for the time period necessary to reach 20000 Vh in total. After IEF separation, IPG strips were equilibrated for 20 min as described above but with 8% SDS and without reducing agent (DeStreak).

For preparative gels, IPG strips were loaded with 500 and 130  $\mu$ g of total protein for pH 4–7 and pH 6–11, respectively. Prior to the second dimension, the focused proteins were reduced (1% DTT) and alkylated (4% iodoacetamide) in two 15 min steps via equilibration.

The equilibrated proteins were transferred from the IPG strips onto a 10% SDS-PAGE gels (180 mm  $\times$  180 mm  $\times$  1 mm). SDS-PAGE was carried out at a constant current of 40 mA per gel until the bromophenol blue line reached the bottom of the gel. Analytical gels were stained with SYPRO Ruby protein gel stain (Bio-Rad) and digitized at 500 DPI resolution using a Phoros FX scanner (Bio-Rad). Protein spots on preparative gels were visualized by reverse staining using a zinc salt.<sup>21</sup>

For further evaluation, 2-DE gel images were subjected to REDFIN Solo analysis (<http://www.ludesi.com/>, Ludesi, Malmo, Sweden).<sup>22</sup> All resistant clones were compared in pairs with relevant (sensitive) control either HCT116 p53<sup>+/+</sup> (wild-type) or HCT116 p53<sup>-/-</sup> cell line (Figure 1), and differential expression of proteins was determined by applying the criteria of significance with  $p < 0.05$  and fold-change values  $> \pm 1.20$ . The calculations (Student's  $t$  test) were performed by REDFIN software from the mean normalized volumes of four biological replicates, which were grown and processed independently.

#### Enzymatic In-Gel Digestion

Spots showing a significant expression change ( $p < 0.05$ ) were excised from zinc-stained preparative gels and cut into small pieces. To complex zinc ions, gel pieces were incubated for 5 min in 50 mM Tris-HCl pH 8.3 (Carl Roth GmbH), 200 mM glycine, and 30% acetonitrile (Merck Millipore, Bilerica, MA). The gel pieces became transparent, and after complete destaining, the chelating solution was removed, and gels were rinsed twice with 50 mM Tris-HCl, pH 8.3 (Carl Roth GmbH). Then, gels were washed with water, shrunk by dehydration in acetonitrile, and reswollen in water. The washing step was repeated three times, and gels were partly dried in a SpeedVac concentrator. Gels were rehydrated in a cleavage buffer containing 25 mM 4-ethylmorpholine, 5% acetonitrile, and trypsin (3.3 ng/ $\mu$ L; Promega, Madison, WI) and incubated overnight at 37  $^{\circ}$ C. The digestion

was stopped by the addition of 5% trifluoroacetic acid in acetonitrile, and the aliquot of the resulting peptide mixture was desalted using a GELoader microcolumn (Eppendorf, Prague, Czech Republic) packed with a Poros Oligo R3 material.<sup>23</sup> The purified and concentrated peptides were eluted from the microcolumn in several droplets directly onto MALDI plate using 1  $\mu$ L of  $\alpha$ -cyano-4-hydroxycinnamic acid matrix solution (5 mg/mL in 50% acetonitrile and 0.1% trifluoroacetic acid).

#### Protein Identification by MALDI-TOF/TOF Mass Spectrometry

MALDI mass spectra were measured on an Ultraflex III MALDI-TOF/TOF instrument (Bruker Daltonics, Bremen, Germany) equipped with a smartbeam solid state laser and LIFT technology for MS/MS analysis. PMF spectra were acquired in the mass range of 700–4000 Da and calibrated internally using the monoisotopic  $[M + H]^+$  ions of trypsin autoproteolytic fragments (842.5 and 2211.1 Da). For PMF database searching, peak lists in XML data format were created using the flexAnalysis 3.0 program with SNAP peak detection algorithm. No smoothing was applied, and a maximal number of assigned peaks was set to 50. After peak labeling, all known contaminant signals were removed.

The peak lists were searched using in-house MASCOT search engine against the Swiss-Prot 2011\_09 database subset of human proteins with the following search settings: peptide tolerance of 30 ppm, missed cleavage site value set to one, variable carbamidomethylation of cysteine, oxidation of methionine, and protein N-terminal acetylation. No restrictions on protein molecular weight and pI value were applied. Proteins with a Mascot score over the threshold 56 calculated for the used settings were considered as identified. If the score was lower or only slightly higher than the threshold value, the identity of protein candidate was confirmed by MS/MS analysis. In addition to the above mentioned MASCOT settings, a fragment mass tolerance of 0.6 Da and instrument type MALDI-TOF/TOF were applied for MS/MS spectra searching.

#### Classification of Protein Changes in HCT116 Resistant Cells and Computer Modeling of Interaction Networks

To assign the roles in biological processes, differentially expressed proteins were searched against the PANTHER 7.0 (<http://www.pantherdb.org/>).<sup>24</sup> Stringent criteria were further applied to select protein changes overlapping among resistant clones and alterations present exclusively in all four clones resistant to CYC116 or in all four clones resistant to ZM447439, irrespective of p53, as well as those present in all four p53<sup>+/+</sup> clones or in all four p53<sup>-/-</sup> clones resistant to both AURK inhibitors were searched. In addition, protein changes present in two clones either p53<sup>+/+</sup> or p53<sup>-/-</sup> and typical for CYC116 or ZM447439 were also evaluated. Furthermore, selection of candidate biomarkers of resistance to AURK inhibitors was performed according to the presence of significant protein

C

dx.doi.org/10.1021/pr300819m | J. Proteome Res. XXXX, XXX, XXX–XXX

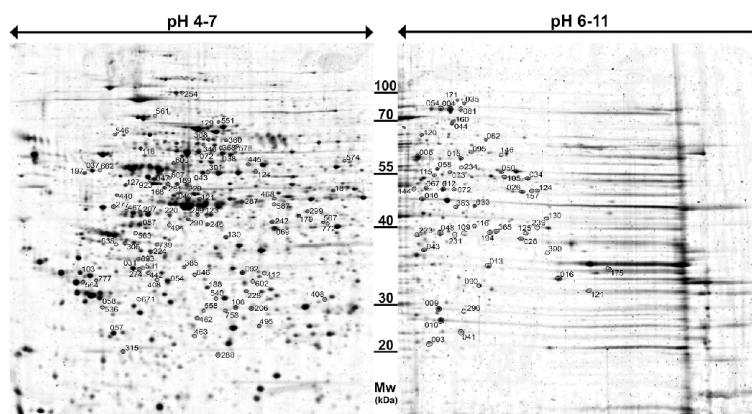


**Figure 2.** Significantly regulated protein spots in HCT116 cells resistant to AURK inhibitors. Representative maps of 2-DE gels in pH 4–7 and 6–11 show the protein spots significantly regulated in resistant cells ( $p < 0.05$ ) with numbers generated by REDFIN software. Spot numbers of pH 4–7 and 6–11 are in tables marked with N (neutral) and B (basic), respectively.

changes in at least five out of eight HCT116 resistant clones irrespective of inhibitor used and p53 phenotype.

To enhance observed proteomic data, selected identified proteins were introduced into the Interologous Interaction Database 1.95 of known and predicted mammalian and eukaryotic protein–protein interactions (<http://ophid.utoronto.ca/ophidv2.201/index.jsp>).<sup>25</sup> Protein–protein interaction networks were visualized using NAVIGaTOR 2.2.1 (<http://ophid.utoronto.ca/navigator/>).

#### Western Blot Analysis

Cell lysates were dissolved in SDS sample buffer, and 5  $\mu$ g of the protein extracts was separated in 12% SDS-PAGE gels using Mini Protean II Cell (Bio-Rad). Proteins were then transferred to Immobilon-P membranes (Merck Millipore) using a semidry blotting system (Biometra, Gottingen, Germany) and transfer buffer containing 48 mM Tris, pH 9.2, 39 mM glycine (Carl Roth GmbH), and 20% methanol (Lach-Ner, Neratovice, Czech Republic). The membranes were blocked for 1 h with 5% non-fat dry milk in TBS, pH 7.4, with 0.05% Tween 20 and incubated overnight with primary antibodies directed against  $\beta$ -tubulin (anti- $\beta$ -tubulin, 1:20000, Sigma, St. Louis, MO); platelet-activating factor acetylhydrolase IB subunit  $\beta$  (anti-PAFAH1B2, 1:1000, Abcam, Cambridge, United Kingdom); GTP-binding nuclear protein Ran (anti-Ran, 1:4000, Abcam); serine hydroxymethyltransferase (anti-SHMT2, 1:6000, Sigma Prestige Antibodies, St. Louis, MO); serpin B5 (anti-SERPINB5, 1:1000, Aviva Systems Biology, San Diego, CA); calretinin (anti-CALB2, 1:6000, Sigma Prestige Antibodies); and voltage-dependent anion-selective channel protein 2 (anti-VDAC2, 1:3000, Aviva Systems Biology). Peroxidase-conjugated secondary antibodies were diluted in 5% non-fat dry milk/TBS, pH 7.4, with 0.05% Tween 20 and applied as appropriate. Anti-mouse IgG antibody (Jackson ImmunoResearch, Suffolk, UK) and anti-rabbit IgG antibody (Jackson ImmunoResearch, Suffolk, UK) were diluted 1:10000, and anti-chicken IgY (Abcam) was diluted 1:100000. The ECL+ chemiluminescence detection system (GE Healthcare) was used to detect specific protein bands on Western blot, and membranes were then exposed to CL-XPosure films

(Thermo Scientific, Rockford, IL) in three independent experiments.

## RESULTS

### Overview of Proteome Changes in p53<sup>+/+</sup> and p53<sup>-/-</sup> HCT116 Cells Resistant to AURK Inhibitors

To characterize changes in protein expression involved in the development of drug resistance to AURK inhibitors, sensitive and resistant HCT116 cells with or without p53 were lysed, extracted proteins were separated by 2-DE in pH gradients 4–7 and 6–11, and protein spots were visualized by fluorescent SYPRO Ruby protein gel stain. Using REDFIN software, 984 and 390 protein spots in pH 4–7 and pH 6–11, respectively, were detected and matched in all gels of all analyzed samples (eight resistant clones, two sensitive parental cells, and four biological replicates of each sample). As shown in Figure 1, gels corresponding to the clones R1.2 and R1.3 resistant to CYC116 and carrying p53<sup>+/+</sup> were compared to sensitive HCT116 p53<sup>+/+</sup> counterparts, and CYC116 resistant clones R2.1 and R2.2 carrying p53<sup>-/-</sup> alleles were compared to sensitive HCT116 p53<sup>-/-</sup> cells. Similarly, the gels corresponding to cells resistant to ZM447439 (R3.1, R3.2, R4.2, and R4.3) were analyzed.

A statistical comparison revealed 144 significantly different protein spots with minimal fold-change  $\pm 1.20$  and present in at least one of all eight resistant clones (Figure 2 and Supplementary Table 1 in the Supporting Information). Among these proteins, 51 (35%) were up-regulated and 63 (44%) were down-regulated in cells resistant to AURK inhibitors. The remaining 30 proteins (21%) showed distinct regulation among resistant clones. Identified proteins from 144 spots represented 127 unique proteins, and 82 and 45 proteins were found in pH ranges 4–7 and 6–11, respectively. Fifteen proteins were present in two spots (031N, 274N; 037N, 662N; 129N, 467N; 168N, 281N; 197N, 495N; 290N, 739N; 305N, 638N; 360N, 095B; 564N, 777N; 012B, 067B; 028B, 125B; 034B, 105B; 035B, 171B; 044B, 160B; and 124B, 157B), two proteins were present in three spots (043N, 124N, 391N; and 004B, 054B, 081B), and there were only two spots each

D

dx.doi.org/10.1021/pr300819m | J. Proteome Res. XXXX, XXX, XXX–XXX

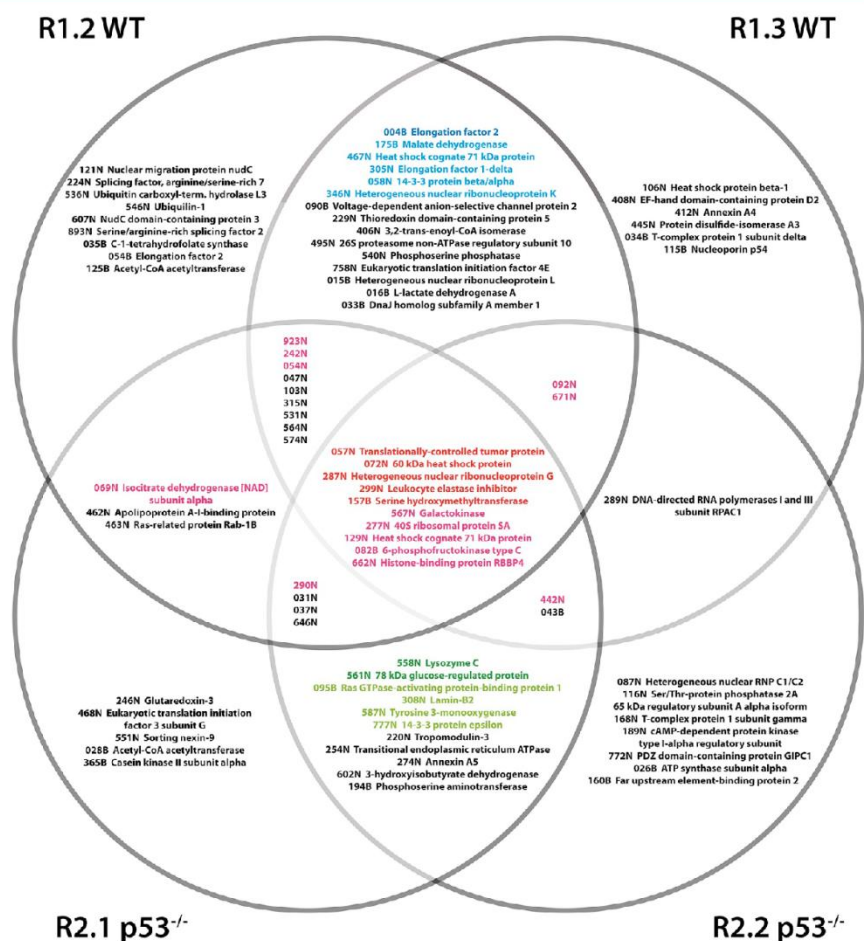


**Figure 3.** Venn diagram of proteins differentially expressed in HCT116 cells resistant to CYC116 and the overlap between cell types. In the diagram, the proteins in red color highlight p53-independent changes specific for CYC116 resistance (Table 1). The changes related to p53 phenotype are indicated in blue (WT) and green (p53<sup>-/-</sup>) colors where the light shade represents CYC116 specific changes (Table 3), while the dark shade further indicates the protein(s) also overlapping with the ZM447439 (Table 2). The black color indicates the proteins regulated in at least one resistant clone (Supplementary Table 1 in the Supporting Information). The magenta color displays the proteins regulated in at least five out of total eight resistant clones without any selectivity to a specific kind of AURK inhibitor or p53 phenotype (Figure 6).

containing two proteins (197N, 146B), thus indicating high resolution of protein fractionation applied in this study. Mass spectrometric data of all identified proteins are presented in Supplementary Table 2 in the Supporting Information.

Involvement of identified proteins in biological processes classified by PANTHER database 7.0 according to Gene Ontology is provided in the Supplementary Table 3 in the Supporting Information. The majority of identified proteins are involved in metabolic processes of proteins, lipids, carbohydrates, and nucleic acids; however, this study also revealed proteins participating in signal transduction, cell cycle, developmental processes, transport, and the immune system.

#### Overlap of Protein Alterations among HCT116 Resistant Cells

Figures 3 and 4 show Venn diagrams of proteins differentially expressed in individual HCT116 resistant cells and the overlap between the cell types. It was evident that the number of significant protein changes shared among HCT116 resistant cells was not too high. The highest overlap was observed between cells resistant to CYC116 carrying p53<sup>+/+</sup> (clones R1.2 and R1.3) and p53<sup>-/-</sup> (clones R2.1 and R2.2). These p53-independent changes specific for CYC116 resistant cells (Figure 3 and Table 1) included a decrease in translationally controlled tumor protein (spot 057N), 60 kDa heat shock protein (spot 072N), and heterogeneous nuclear ribonucleoprotein G (spot 287N) and an

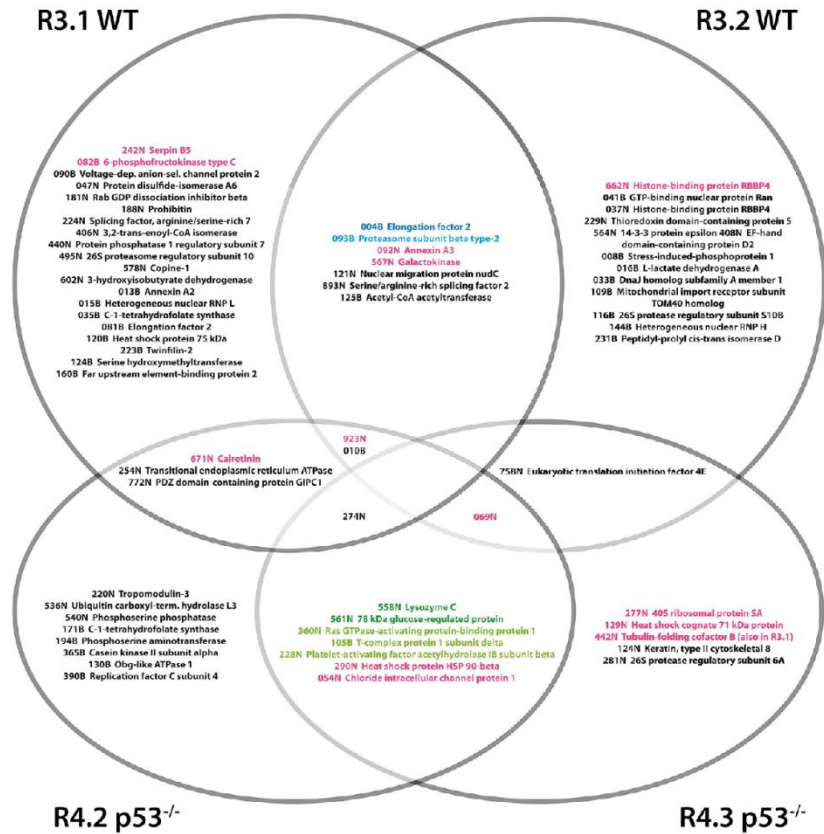


**Figure 4.** Venn diagram of proteins differentially expressed in HCT116 cells resistant to ZM447439 and the overlap between cell types. In this diagram, the changes related to p53 phenotype are indicated in blue (WT) and green (p53<sup>-/-</sup>) where the lighter shade of color represents ZM447439 specific changes (Table 3) and the dark shade further indicates the protein(s) also overlapping with the CYC116 (Table 2). The black color indicates the proteins regulated in at least one resistant clone (Supplementary Table 1 in the Supporting Information). The magenta color displays the proteins regulated in at least five out of total eight resistant clones without any selectivity to a specific kind of AURK inhibitor or p53 phenotype (Figure 6).

**Table 1. Protein Changes Typical for Individual AURK Inhibitors Irrespective of p53 Phenotype<sup>a</sup>**

spot no.	protein name	CYC116				ZM447439 <sup>b</sup>			
		p53 <sup>+/+</sup>		p53 <sup>-/-</sup>		p53 <sup>+/+</sup>		p53 <sup>-/-</sup>	
		R1.2	R1.3	R2.1	R2.2	R3.1	R3.2	R4.2	R4.3
057N	translationally controlled tumor protein	-1.86	-1.67	-2.82	-1.76				
072N	60 kDa heat shock protein	-1.63	-1.32	-1.57	-1.25				
287N	heterogeneous nuclear ribonucleoprotein G	-3.07	-2.23	-2.00	-1.90				
299N	leukocyte elastase inhibitor	1.89	1.91	2.98	2.50				
157B	serine hydroxymethyltransferase	1.46	1.82	1.43	1.31				

<sup>a</sup>Fold-change values for proteins significantly regulated in HCT116 resistant cells. <sup>b</sup>No p53-independent protein changes typical for ZM447439 resistant cells were found.

increase in leukocyte elastase inhibitor (spot 299N) and serine hydroxymethyltransferase (spot 157B). On the contrary, we did not find any overlap between cells resistant to ZM447439 carrying p53<sup>+/+</sup> (clones R3.1 and R3.2) and p53<sup>-/-</sup> (clones R4.2 and R4.3) (Figure 4 and Table 1).

We also observed that both CYC116 and ZM447439 resistant cells were characterized by differential expression of elongation factor 2 (spot 004B) exclusively in all four p53<sup>+/+</sup> clones (R1.2, R1.3, R3.1, and R3.2; Figures 3 and 4), while all four p53<sup>-/-</sup> clones (clones R2.1, R2.2, R4.2, and R4.3; Figures 3 and 4)

F

dx.doi.org/10.1021/pr300819m | J. Proteome Res. XXXX, XXX, XXX-XXX

**Table 2. Protein Changes Common to Both AURK Inhibitors Dependent on p53 Phenotype<sup>a</sup>**

spot no.	protein name	CYC116				ZM447439			
		p53 <sup>+/+</sup>		p53 <sup>-/-</sup>		p53 <sup>+/+</sup>		p53 <sup>-/-</sup>	
		R1.2	R1.3	R2.1	R2.2	R3.1	R3.2	R4.2	R4.3
004B	elongation factor 2	-1.72	-1.31			-1.93	-1.48		
558N	lysozyme C			1.33	1.43			1.63	1.33
561N	78 kDa glucose-regulated protein			-1.90	-1.80			-1.76	-2.10

<sup>a</sup>Fold-change values for proteins significantly regulated in HCT116 resistant cells.

**Table 3. Protein Changes Typical for Individual AURK Inhibitors Related to p53 Phenotype<sup>a</sup>**

spot no.	protein name	CYC116				ZM447439			
		p53 <sup>+/+</sup>		p53 <sup>-/-</sup>		p53 <sup>+/+</sup>		p53 <sup>-/-</sup>	
		R1.2	R1.3	R2.1	R2.2	R3.1	R3.2	R4.2	R4.3
175B	malate dehydrogenase	2.56	1.82						
467N	heat shock cognate 71 kDa protein	1.61	2.05						
305N	elongation factor 1- $\delta$	1.43	1.50						
058N	14-3-3 protein $\beta/\alpha$	-1.20	-1.67						
346N	heterogeneous nuclear ribonucleoprotein K	-1.33	-1.48						
095B	Ras GTPase-activating protein-binding protein 1			1.29	1.41				
308N	lamin-B2			-2.03	-4.60				
587N	tyrosine 3-monooxygenase			-1.38	-1.51				
777N	14-3-3 protein $\epsilon$			-1.83	-1.71				
093B	proteasome subunit $\beta$ type-2					1.84	2.08		
360N	Ras GTPase-activating protein-binding protein 1							1.93	1.82
105B	T-complex protein 1 subunit $\delta$							1.23	1.27
228N	platelet-activating factor acetylhydrolase IB subunit $\beta$							-2.13	-2.19

<sup>a</sup>Fold-change values for proteins significantly regulated in HCT116 resistant cells.

exhibited variant levels of lysozyme C (spot 558N) and 78 kDa glucose-regulated protein (spot 561N) (Table 2).

#### Protein Changes in HCT116 Resistant Cells Typical for Individual AURK Inhibitors Related to p53 Phenotype

As mentioned above, we selected the group of proteins significantly changed in p53-independent manner in cells resistant to CYC116 only. In addition to these, there were other proteins typical for cells resistant to CYC116 with protein alterations related to p53 phenotype. Three proteins, namely, malate dehydrogenase (spot 175B), heat shock cognate 71 kDa protein (spot 467N), and elongation factor 1- $\delta$  (spot 305N) were significantly increased as well as two proteins, 14-3-3 protein  $\beta/\alpha$  (spot 058N) and heterogeneous nuclear ribonucleoprotein K (spot 346N), were significantly decreased in two clones resistant to CYC116 carrying p53<sup>+/+</sup> (clones R1.2 and R1.3; Figure 3 and Table 3) but not in the clones carrying p53<sup>-/-</sup> (clones R2.1 and R2.2). Conversely, Ras GTPase-activating protein-binding protein 1 (spot 095N) was typically increased, while lamin-B2 (spot 308N), tyrosine 3-monooxygenase (spot 587N), and 14-3-3 protein epsilon (spot 777N) were decreased in HCT116 cells resistant to CYC116 carrying p53<sup>-/-</sup> (clones R2.1 and R2.2; Figure 3 and Table 3) but not in the clones p53<sup>+/+</sup> (clones R1.2 and R1.3).

As compared to what we could observe in cells resistant to CYC116, the number of protein alterations related to p53 phenotype typical for cells resistant to ZM447439 was limited to four proteins only. Proteasome subunit  $\beta$  type-2 (spot 93B) was significantly higher in p53<sup>+/+</sup> clones (clones R3.1 and R3.2; Figure 4 and Table 3) but not in the clones carrying p53<sup>-/-</sup> (clones R4.2 and R4.3), three proteins with an increased level of Ras GTPase-activating protein-binding protein 1 (spot 360N) and T-complex protein 1 subunit  $\delta$  (spot 105B) and decreased

level of platelet-activating factor (PAF) acetylhydrolase IB subunit  $\beta$  (spot 228N) were changed in p53<sup>-/-</sup> clones resistant to ZM447439 (clones R4.2 and R4.3; Figure 4 and Table 3) but not in the clones p53<sup>+/+</sup> (clones R3.1 and R3.2).

#### Computer Modeling of Possible Interaction Networks in HCT116 Resistant Cells

UniProtKB accessions of the proteins from Table 1 were introduced into Interologous Interaction Database to identify possible interaction partners, and Figure 5 depicts their interaction network generated by NAVIGATOR software. In total, 435 interactions were recognized for translationally controlled tumor protein (TCPT), 60 kDa heat shock protein (HSP60), heterogeneous nuclear ribonucleoprotein G (hnRNP G), leukocyte elastase inhibitor (LEI), and serine hydroxymethyltransferase (GLYM) (Supplementary Table 4 in the Supporting Information). Computer modeling highlighted a high number of mediated interactions among these proteins and revealed interconnectivity via autophagy protein 5 (AP5, ATG5\_HUMAN) and WD repeat domain phosphoinositide-interacting protein 2 (WPI2, WPI2\_HUMAN), indicating their possible role in resistance to CYC116.

#### Quest for Candidate Biomarkers of Resistance to AURK Inhibitors

In a quest for common candidate markers of resistance to AURK inhibitors, the proteins significantly changing their levels ( $p < 0.05$ ) in at least five out of total eight resistant clones without any selectivity to a specific kind of inhibitor or p53 phenotype were searched. On the basis of these criteria, 13 selected proteins (Figure 6) including 26S protease regulatory subunit 6B (PRS6B, spot 923N), serpin B5 (SPB5, spot 242N), annexin A3 (ANXA3, spot 092N), calretinin (CALB2, spot 671N), heat shock protein

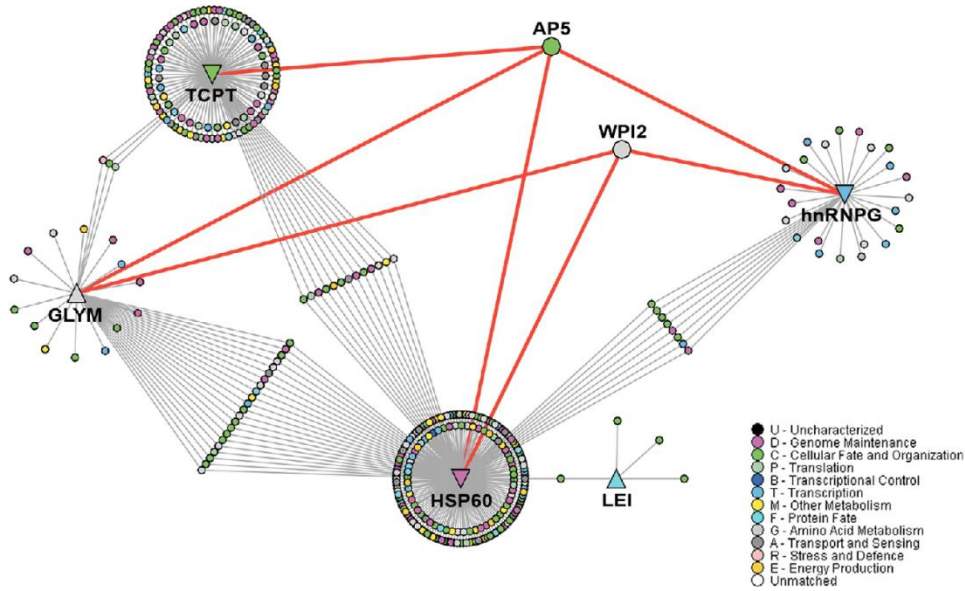


**Figure 5.** p53-independent interaction network in CYC116 resistant cells. Computer modeling of possible protein–protein interactions in HCT116 cells resistant to CYC116 depicts a high number of mediated interactions among proteins from Table 1 (translationally controlled tumor protein, TCPT; 60 kDa heat shock protein, HSP60; heterogeneous nuclear ribonucleoprotein G, hnRNPG; leukocyte elastase inhibitor, LEI; and serine hydroxymethyltransferase, GLYM) and highlighted by red link interconnections via autophagy protein 5 (AP5) and WD repeat domain phosphoinositide-interacting protein 2 (WPI2). The network generated by NAVIGaTOR software is best interpreted as follows: nodes represent proteins, and edges between nodes represent physical interactions between proteins. Proteins regulated specifically in all HCT116 clones resistant to CYC116 are indicated by a triangle (up- or down-regulated), and interacting proteins retrieved by Interologous Interaction Database and NAVIGaTOR software are indicated by an ellipse. The color of nodes represents Gene Ontology functionality.

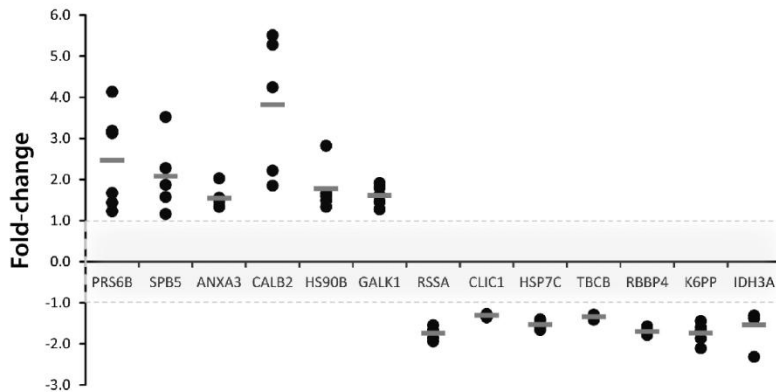


**Figure 6.** Biomarker candidates. Fold-change values for proteins significantly regulated in at least five out of eight resistant clones as compared to the corresponding control (fold-change  $> \pm 1.0$ ,  $p < 0.05$ ) are shown in the dot-plot graph. 26S protease regulatory subunit 6B (PRS6B,  $n = 6$ ), serpin B5 (SPB5,  $n = 5$ ), annexin A3 (ANXA3,  $n = 5$ ), calretinin (CALB2,  $n = 5$ ), heat shock protein HSP 90- $\beta$  (HSP90B,  $n = 5$ ), galactokinase (GALK1,  $n = 6$ ), 40S ribosomal protein SA (RSSA,  $n = 5$ ), chloride intracellular channel protein (CLIC1,  $n = 5$ ), heat shock cognate 71 kDa protein (HSP7C,  $n = 5$ ), tubulin-folding cofactor B (TBCB,  $n = 5$ ), histone-binding protein RBBP4 (RBBP4,  $n = 5$ ), 6-phosphofructokinase type C (K6PP,  $n = 5$ ), and isocitrate dehydrogenase [NAD] subunit  $\alpha$  (IDH3A,  $n = 5$ ).

HSP 90- $\beta$  (HSP90B, spot 290N), and galactokinase (GALK1, spot 567N) were found to represent the proteins that were up-

regulated in resistant clones; 40S ribosomal protein SA (RSSA, spot 277N), chloride intracellular channel protein (CLIC1, spot

H

[dx.doi.org/10.1021/pr300819m](https://doi.org/10.1021/pr300819m) | J. Proteome Res. XXXX, XXX, XXX–XXX

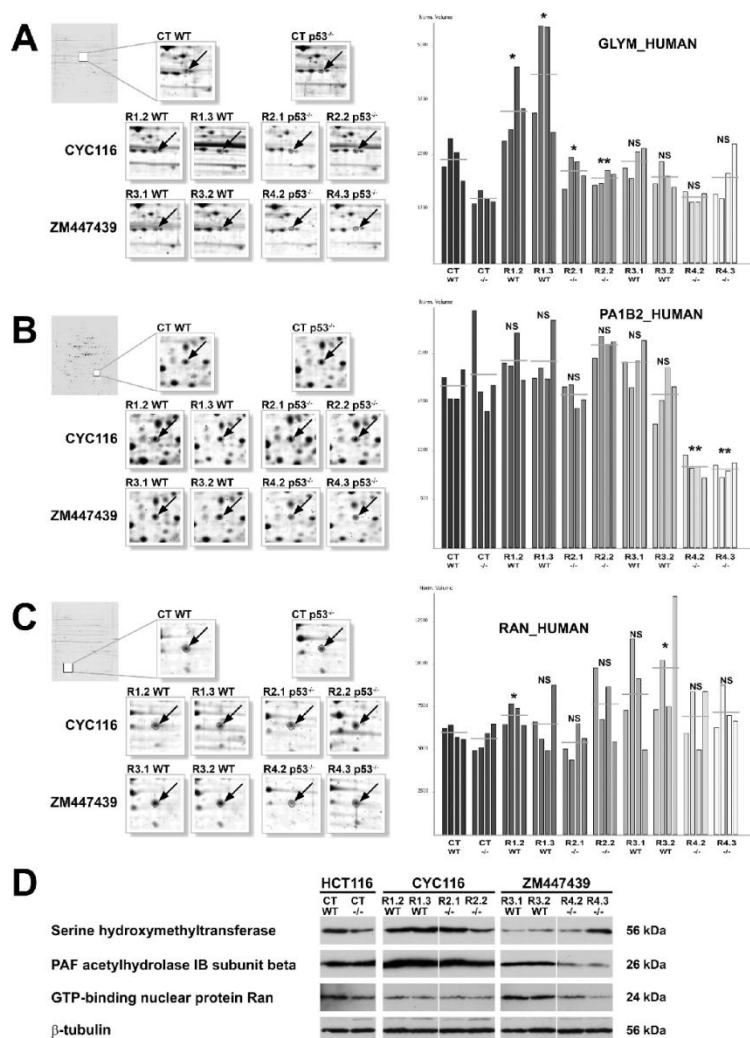


**Figure 7.** Protein changes in HCT116 resistant cells typical for individual AURK inhibitors. Significantly regulated protein spots between HCT116 sensitive (CT, control) cells and cells resistant to AURK inhibitors are indicated by arrows in the zoomed 2D gel images on the left with graphs on the right, generated by REDFIN software depicting normalized spot volumes in four individual gels. (A) Serine hydroxymethyltransferase, GLYM\_HUMAN; (B) PAF acetylhydrolase IB subunit  $\beta$ , PA1B2\_HUMAN; (C) GTP-binding nuclear protein Ran, RAN\_HUMAN (NS, not significant; \* $p < 0.05$ , \*\* $p < 0.01$ , and \*\*\* $p < 0.001$ , as compared to corresponding sensitive cell line HCT116 with wild-type p53<sup>+/+</sup> (WT) or mutated p53<sup>-/-</sup>). (D) Western blot analysis of serine hydroxymethyltransferase, PAF acetylhydrolase IB subunit  $\beta$ , and GTP-binding nuclear protein Ran. Sensitive and resistant cells were examined using specific antibodies, and  $\beta$ -tubulin was used as a loading control.

054N), heat shock cognate 71 kDa protein (HSP7C, spot 129N), tubulin-folding cofactor B (TFCB, spot 442N), histone-binding protein RBBP4 (RBBP4, spot 662N), 6-phosphofructokinase type C (K6PP, spot 082B), and isocitrate dehydrogenase [NAD] subunit  $\alpha$  (IDH3A, spot 069N) were the proteins down-regulated in resistant clones.

#### Verification of Selected Proteomic Data

Among significantly reproducible protein changes in HCT116 cells resistant to CYC116 and ZM447439 AURK inhibitors, 2-fold and higher changes were reached by translationally controlled tumor protein, heterogeneous nuclear ribonucleoprotein G, leukocyte elastase inhibitor, and 78 kDa glucose-regulated protein (Tables 1 and 2); malate dehydrogenase, heat

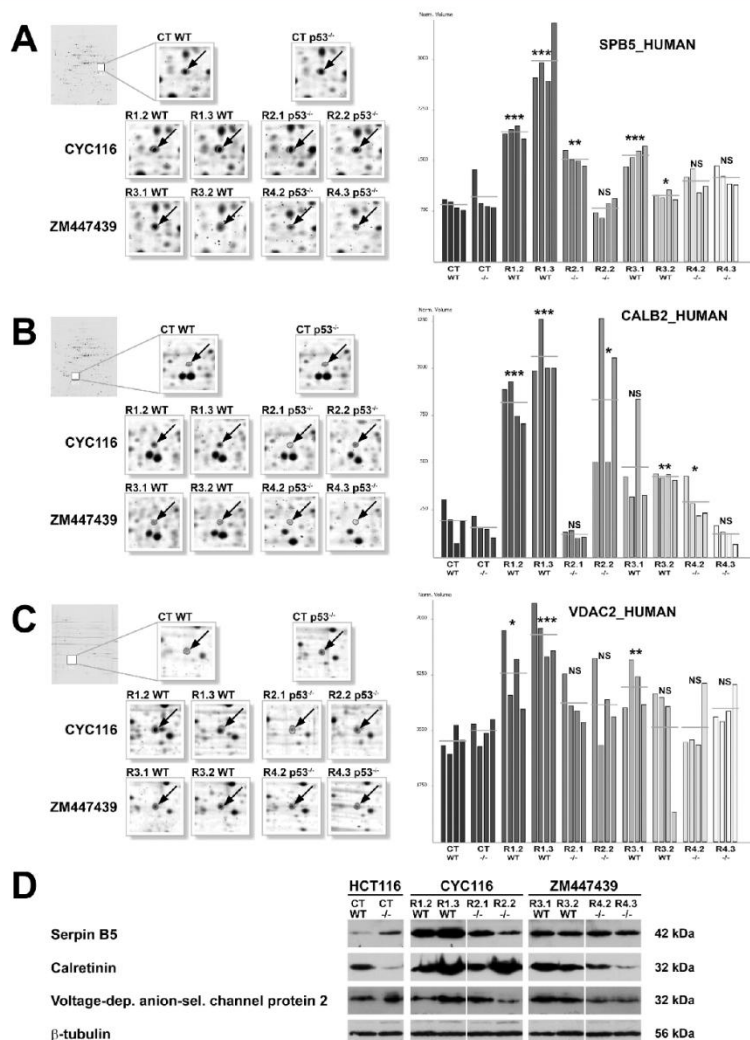


**Figure 8.** Apoptosis-related protein changes in HCT116 resistant cells. Significantly regulated protein spots between HCT116 sensitive (CT, control) cells and cells resistant to AURK inhibitors are indicated by arrows in the zoomed 2D gel images on the left with graphs on the right, generated by REDFIN software depicting normalized spot volumes in four individual gels. (A) Serpin B5, SPB5\_HUMAN; (B) Calretinin, CALB2\_HUMAN; (C) Voltage-dependent anion-selective channel protein 2, VDACC2\_HUMAN (NS, not significant; \* $p < 0.05$ , \*\* $p < 0.01$ , and \*\*\* $p < 0.001$ , as compared to corresponding sensitive cell line HCT116 with wild-type p53<sup>+/+</sup> (WT) or mutated p53<sup>-/-</sup>). (D) Western blot analysis of serpin B5, calretinin, and voltage-dependent anion-selective channel protein 2. Sensitive and resistant cells were examined using specific antibodies, and  $\beta$ -tubulin was used as a loading control.

shock cognate 71 kDa protein, lamin-B2, proteasome subunit  $\beta$  type-2, and PAF acetylhydrolase IB subunit  $\beta$  (Table 3); 26S protease regulatory subunit 6B, serpin B5, annexin A3, calretinin, heat shock protein HSP 90- $\beta$ , 6-phosphofructokinase type C, and isocitrate dehydrogenase [NAD] subunit  $\alpha$  (Figure 6). While this may reflect the importance of these proteins in the regulation of resistance development, the role of many other less prominent

protein alterations should not be ignored. To this end, we selected proteins representing some of the above mentioned groups for verification by Western blot analysis.

Leukocyte elastase inhibitor and serine hydroxymethyltransferase are the proteins whose expression was typically increased in cells resistant to CYC116 inhibitor. The level of serine hydroxymethyltransferase (spot 157B, GLYM\_HUMAN), a

J

dx.doi.org/10.1021/pr300819m | J. Proteome Res. XXXX, XXX, XXX–XXX



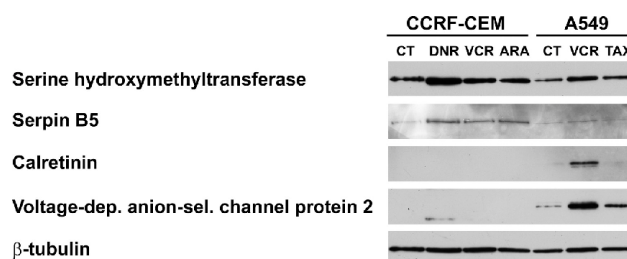


**Figure 9.** Protein changes in different cancer cells resistant to various anti-cancer drugs. The expression levels of serine hydroxymethyltransferase, serpin B5, calretinin, and voltage-dependent anion-selective channel protein 2 were measured by Western blotting in CCRF-CEM and A549 cells (CT, control) and cells resistant to daunorubicin (DNR), vincristine (VCR), cytarabine (ARA), and paclitaxel (TAX).  $\beta$ -tubulin was used as a loading control.

potential target enzyme for cancer therapy,<sup>26</sup> showed increase on 2-DE and Western blot in all clones resistant to CYC116 (Figure 7), confirming its independence on p53 phenotype. Interestingly, PAF acetylhydrolase IB subunit  $\beta$  (spot 228N, PA1B2\_HUMAN) was the typical down-regulated protein in p53<sup>-/-</sup> HCT116 cells resistant to ZM447439 only, and Western blotting allowed verification of this protein (Figure 7). Additionally, GTP-binding nuclear protein Ran (spot 041B, RAN\_HUMAN) typical for p53<sup>+/+</sup> HCT116 cells resistant to ZM447439 was included in the verification for its role in the translocation of p53 through the nuclear pore complex.<sup>27</sup> Despite the fact that significant up-regulation of this protein was observed in only one clone with 2-DE analysis, Western blotting confirmed up-regulation of the protein in both ZM447439 resistant HCT116 p53<sup>+/+</sup> clones (Figure 7).

Among significant protein changes in at least five out of total eight clones resistant to AURK inhibitors, serpin B5 and calretinin, previously described in regulating apoptosis,<sup>28,29</sup> showed visible overexpression in HCT116 cells. In seven out of eight resistant clones, considerable increase in serpin B5 (spot 242N, SPB5\_HUMAN) and calretinin (spot 671N, CALB2\_HUMAN) levels were observed, thus further detailing the information obtained using 2-DE (Figure 8). The changes in voltage-dependent anion-selective channel protein 2 (spot 090B, VDAC2\_HUMAN), a crucial component in mitochondrial apoptosis,<sup>30</sup> were less pronounced in 2-DE with significantly increased level in majority of p53<sup>+/+</sup> HCT116 resistant clones detected by Western blot in clones R3.1, R3.2, and R1.3 but not in R1.2 (Figure 8).

#### Involvement of Selected Proteins in Cancer Cell Resistance to Individual Anti-cancer Agents

To assess the role of selected proteins from this study in the development of resistance to different chemotherapeutics in different cancer cells, T-lymphoblastic leukemia CCRF-CEM cells carrying p53 mutations and A549 lung adenocarcinoma cells with p53 wild-type phenotype resistant to anti-cancer drugs with diverse structures and mechanistic targets<sup>20</sup> were examined. Using these cells, no changes in PAF acetylhydrolase and GTP-binding nuclear protein Ran were found (data not shown). However, the different levels of serine hydroxymethyltransferase, serpin B5, calretinin, and voltage-dependent anion-selective channel protein 2 in resistant cells as compared to corresponding controls were examined (Figure 9). Serine hydroxymethyltransferase and serpin B5 were up-regulated in CCRF-CEM cells resistant to daunorubicin, vincristine and cytarabine and in A549 cells resistant to vincristine. Calretinin and voltage-dependent

anion-selective channel protein 2 were detectable only in A549 cells showing a noticeable increase in cells resistant to vincristine.

#### DISCUSSION

The efficiency of specific regimens in cancer therapy can be improved by selective inhibition of AURKs.<sup>2</sup> Despite great expectations from such an approach, the development of resistance toward this type of cancer treatment has to be thoroughly investigated to avoid potential therapy failure. The published data demonstrate a variety of molecular mechanisms leading to the induction of resistance to anti-cancer drugs including the occurrence of drug-resistant Aurora B mutants after treatment by AURK inhibitors.<sup>5–9,31</sup> Nevertheless, there is a need to better describe such mechanisms and to translate these findings into clinical laboratory with predominant focus on expressed proteins that could be used as markers for therapy monitoring as well as targets for novel anti-cancer drugs.

In the present study, we considered CYC116 AURK inhibitor, which has been tested in phase I clinical evaluation,<sup>2</sup> and a model inhibitor ZM447439. By short-term culture in high doses of CYC116 and ZM447439, resistant cells were established, and 2D electrophoresis followed by MALDI-TOF/TOF was performed to comprehensively compare sensitive and resistant HCT116 colon cancer cells. The different levels of metabolic proteins such as isocitrate dehydrogenase, phosphoserine aminotransferase, and 40S ribosomal protein SA were identified, which have been already described in a number of proteomic studies of various drug-resistant cancer cell lines<sup>32</sup> and may reflect general response of cells to toxicity. The proteins directly involved in tumor progression and apoptosis were identified in our study, and important changes observed have become a focus of interest.

We identified several candidates; however, most protein changes were observed in individual resistant clones. Combining clones with the same p53 phenotype resistant to the single AURK inhibitor has led to the elimination of proteins expressed differently as a result of sporadic response to anti-cancer treatment. Because of the low overlap of expression changes between resistant cells, we hypothesize that colon cancer cells resort to different mechanisms to resist cell death induced by CYC116 and ZM447439. CYC116, which is highly effective at lower concentrations as compared to ZM447439,<sup>2,3</sup> was found to be a more specific and with amplified response in resistant cells.

Unlike ZM447439, CYC116 resistant cells expressed several proteins differently regardless of p53. Although these proteins are mainly involved in metabolism of proteins and nucleic acids, computer modeling revealed a high number of mediated interactions among these proteins, linking a variety of biological

processes. Interestingly, direct interconnections with autophagy protein 5 and WD repeat domain phosphoinositide-interacting protein 2 were observed, highlighting a possible role of autophagy process in p53-independent mechanisms of resistance to CYC116 AURK inhibitor. Autophagy, a lysosome-dependent degradation of cytoplasmic organelles and long-lived proteins, is frequently activated in cancer cells.<sup>33</sup> Recently, autophagy has been linked to drug resistance in cancer therapy, and, together with apoptosis, it has a critical role to play in determining cellular fate of tumor cells.<sup>34–37</sup> In HCT116 cells, regulation of translationally controlled tumor protein, 60 kDa heat shock protein, heterogeneous nuclear ribonucleoprotein G, leukocyte elastase inhibitor, and serine hydroxymethyltransferase and their direct interactions with two autophagy participating proteins appear to control the development of resistance to CYC116 AURK inhibitor.

Serine hydroxymethyltransferase plays a pivotal role in channelling metabolites between amino acid and nucleotide metabolism, as it reversibly catalyzes the conversion of serine into glycine while hydroxymethyl group is transferred to 5,6,7,8-tetrahydrofolate. The resultant compound is the sole precursor of purine biosynthesis, which is required for cell division. Hence, serine hydroxymethyltransferase have been indicated as a potential target enzyme for cancer therapy.<sup>26</sup> With regards to the revealed up-regulation of this enzyme in all HCT116 clones resistant to CYC116 and also in CCRF-CEM and A549 resistant cells with no apparent impact of p53 phenotype, we propose serine hydroxymethyltransferase as a target molecule that may resolve the problem of drug resistance to cancer therapy.

Recently, it was shown that inhibition of AURK was needed for efficient cell cycle arrest, which was mediated by induced p53 up-regulation via ATM/ATR protein kinases.<sup>38</sup> Other studies have indicated that inhibition of AURKs may provide a growth advantage to cells that have suffered from p53 loss.<sup>14</sup> Our study, using HCT116 colon cancer cells with and without p53, allowed us to characterize the impact of p53 phenotype on protein differences associated with resistance to AURK inhibitors. Elongation factor 2 was down-regulated specifically in p53<sup>+/+</sup> cells resistant to both CYC116 and ZM447439 AURK inhibitors. Yin et al. demonstrated that via association with elongation factor 2, p53 is involved in protein translation.<sup>39</sup> Accordingly, p53 might regulate translation in HCT116 cells and contribute to the development of resistance to AURK inhibitors. HCT116 cells with loss of p53 resistant to both CYC116 and ZM447439 AURK inhibitors were characterized by differential expression of lysozyme C and 78 kDa glucose-regulated protein. Lysozyme C, a protein specifically up-regulated in all p53<sup>-/-</sup> resistant cells, is known to protect cells against oxidative stress.<sup>40</sup> Therefore, such a protective mechanism may contribute to the resistance to AURK inhibitors in these cells. The second protein specifically regulated in all p53<sup>-/-</sup> resistant cells, 78 kDa glucose-regulated protein, has been previously associated with cancer and resistance to therapy.<sup>41–43</sup> Contrary to what was expected, the level of this anti-apoptotic protein was lower in HCT116 resistant cells.

Among the proteins specifically regulated in cells resistant to ZM447439, two proteins were associated with the development of drug resistance with respect to p53 background. While PAF acetylhydrolase was specifically down-regulated in p53<sup>-/-</sup> resistant cells, the increased level of GTP-binding nuclear protein Ran was observed only in p53<sup>+/+</sup> resistant cells. PAF (1-O-alkyl-2-acetyl-sn-glycerol-3-phosphorylcholine) deacetylation catalyzed by PAF acetylhydrolase induces the loss of PAF lipid

messenger activity.<sup>44</sup> Such an inactivation has been demonstrated to affect tumor growth, vascularization, and cell motility.<sup>45</sup> More interestingly, elevated PAF acetylhydrolase levels have been detected in the tumor tissues of patients with colorectal cancer as compared with healthy individuals.<sup>46</sup> These findings subsequently led us to hypothesize that in colon cancer cells, the decreased level of PAF acetylhydrolase may contribute to resistance development in cells that lack p53. Ran, a member of the ras oncogene family, is known to mediate nucleocytoplasmic transport of small RNAs and proteins, and its activity is essential for mitotic spindle assembly.<sup>47</sup> Previous studies suggested Ran as a promising molecular target for RNA interference-based therapeutics against a variety of tumors,<sup>48,49</sup> and these researchers proved that silencing of Ran induced colorectal cancer cells to undergo apoptosis. Our study extended the above mentioned observation showing that Ran-mediated regulation of apoptosis depends on p53 expression.

Mutated p53 can enhance resistance to anti-cancer drugs also by up-regulation of multi-drug resistance protein 1 (MDR1).<sup>50</sup> MDR1, also known as P-glycoprotein, is a member of ATP-binding cassette transporters located on cell membrane responsible for a tissue-specific excretion of cytotoxic agents out of tumor cells.<sup>51</sup> In the present study, resistant cell lines of different histogenetic origin and p53 phenotype were analyzed. Consistently with previous studies, CCRF-CEM resistant cells with p53 mutations show an increased expression and activity of MDR1 and p53 wild-type A549 cells highly express LRP (lung resistance-related protein), both manifesting a stable multi-drug resistance.<sup>20</sup> Further studies on such multi-drug resistance in HCT116 resistant cells would add to our findings.

Regulation of apoptosis plays a pivotal role in the development of drug resistance in cancer therapy.<sup>52</sup> In the present study, we found a higher level of proteins associated with apoptotic cell death, such as serpin B5, calretinin, and voltage-dependent anion-selective channel protein 2 in HCT116 cell resistant to AURK inhibitors. Serpin B5, the so-called maspin, has been proved to suppress the growth of various tumors including breast, prostatic, and cervical carcinomas,<sup>53–55</sup> while promoting the growth of tumors in the colon.<sup>28</sup> Previous studies also linked serpin B5 to resistance in cancer therapy, which suggested that the protein could be a target for novel anti-cancer drugs.<sup>56–58</sup> We found serpin B5 up-regulated in HCT116 cells resistant to AURK inhibitors and also in CCRF-CEM cells and A549 resistant cells, indicating its role in the development of resistance in a p53-independent manner.

Because of the unequivocal role of calcium in apoptosis, a relationship between calretinin and resistance to drug-induced cell death has been hypothesized.<sup>59</sup> This protein, which is expressed in poorly differentiated colon carcinomas,<sup>60</sup> plays a key role in processes such as message targeting and intracellular calcium buffering. The expression of calretinin in our study was substantially increased in cells resistant to AURK inhibitors and also in A549 cells resistant to vincristine but not in CCRF-CEM cells. Similar to calretinin, voltage-dependent anion-selective channel protein 2 was not detectable in CCRF-CEM cells; however, a higher level was demonstrated in p53<sup>+/+</sup> cells resistant to AURK inhibitors and in A549 cells resistant to vincristine. Voltage-dependent anion-selective channel protein 2 forms a channel through the mitochondrial outer membrane and acts as a crucial component in mitochondrial apoptosis.<sup>30</sup>

Options in cancer therapy are often limited to regimes based on statistical evaluation. Hence, there is a particular need for biomarkers to aid early detection of drug resistance. Taking into

L

dx.doi.org/10.1021/pr300819m | J. Proteome Res. XXXX, XXX, XXX–XXX

consideration that serpin B5 and calretinin were up-regulated with the highest fold-changes in almost all resistant cells used in our study, they ultimately represent the most promising molecules for cancer therapy monitoring. Moreover, serpin B5 with secreted annotation could be released by tumors into the bloodstream, where it can be non-invasively assessed during defined therapy, adding to signature of biomarkers useful in cancer treatment.

### CONCLUSIONS

Characterization of mechanisms leading to the development of drug resistance in cancer therapy is crucial to identifying targets for novel anti-cancer drugs, which may selectively eliminate resistant cells in specific disease stage. We have shown that serine hydroxymethyltransferase, PAF acetylhydrolase, GTP-binding nuclear protein Ran, serpin B5, calretinin, and voltage-dependent anion-selective channel protein 2 contribute to the development of drug resistance to AURK inhibitors. Following verification of observed protein changes, the overexpression of serine hydroxymethyltransferase, serpin B5, calretinin, and voltage-dependent anion-selective channel protein 2 was evident also in leukemia CCRF-CEM and lung adenocarcinoma A549 cells resistant to distinct anti-cancer drugs, suggesting that targeting these proteins may overcome the problem of drug resistance in cancer therapy. The study outlined here has been the key “stepping-stone” to current on-going studies on selected proteins and their levels in cancer patient samples with focus on their functionality as novel targets for cancer therapy. After further validation, monitoring of calretinin and serpin B5 levels may have a profound impact in cancer treatment in clinics. We believe that these in-depth studies will stimulate future research, ultimately leading to improved understanding of drug resistance in cancer therapy and, in particular, to the clarification of proteins functionality.

### ASSOCIATED CONTENT

#### Supporting Information

Supplementary Table 1, regulated proteins in HCT116 cells resistant to AURK inhibitors; Supplementary Table 2, mass spectrometric data of identified proteins; Supplementary Table 3, involvement of regulated proteins in biological processes; and Supplementary Table 4, I2D protein–protein interaction search results. This material is available free of charge via the Internet at <http://pubs.acs.org>.

### AUTHOR INFORMATION

#### Corresponding Author

\*Tel: +420 315 639 582. Fax: +420 315 639 510. E-mail: [kovarova@iapg.cas.cz](mailto:kovarova@iapg.cas.cz).

#### Author Contributions

The manuscript was written with contributions from all authors. All authors have given approval to the final version of the manuscript.

#### Notes

The authors declare no competing financial interest.

### ACKNOWLEDGMENTS

We greatly acknowledge Jaroslava Supolikova for skillful technical assistance. This work was supported in part by the Ministry of Education, Youth and Sports (Grant LC07017) and by Institutional Research Projects RVO67985904 (IAPG, AS

CR, v.v.i.) and RVO61388971 (IMIC, AS CR, v.v.i.). An infrastructural part of this project was supported from the Operational Program Research and Development for Innovations (CZ.1.05/2.1.00/01.0030).

### ABBREVIATIONS

AURK, Aurora kinase; PAF, platelet-activating factor; MDR1, multi-drug resistance protein 1

### REFERENCES

- (1) Kollareddy, M.; Dzubak, P.; Zheleva, D.; Hajdich, M. Aurora kinases: Structure, functions and their association with cancer. *Biomed. Pap. Med. Fac. Univ. Palacky Olomouc Czech Repub.* **2008**, *152* (1), 27–33.
- (2) Kollareddy, M.; Zheleva, D.; Dzubak, P.; Brahmshatriya, P. S.; Lepsik, M.; Hajdich, M. Aurora kinase inhibitors: Progress towards the clinic. *Invest. New Drugs* **2012**, *30*, 2411–2432.
- (3) Ditchfield, C.; Johnson, V. L.; Tighe, A.; Ellston, R.; Haworth, C.; Johnson, T.; Mortlock, A.; Keen, N.; Taylor, S. S. Aurora B couples chromosome alignment with anaphase by targeting BubR1, Mad2, and Cenp-E to kinetochores. *J. Cell Biol.* **2003**, *161* (2), 267–280.
- (4) Wang, S.; Midgley, C. A.; Scaerou, F.; Grabarek, J. B.; Griffiths, G.; Jackson, W.; Kontopidis, G.; McClue, S. J.; McInnes, C.; Meades, C.; Mezna, M.; Plater, A.; Stuart, I.; Thomas, M. P.; Wood, G.; Clarke, R. G.; Blake, D. G.; Zheleva, D. I.; Lane, D. P.; Jackson, R. C.; Glover, D. M.; Fischer, P. M. Discovery of N-phenyl-4-(thiazol-5-yl)pyrimidin-2-amine aurora kinase inhibitors. *J. Med. Chem.* **2010**, *53* (11), 4367–4378.
- (5) Gottesman, M. M.; Fojo, T.; Bates, S. E. Multidrug resistance in cancer: role of ATP-dependent transporters. *Nat. Rev. Cancer* **2002**, *2* (1), 48–58.
- (6) Elsaleh, H.; Powell, B.; McCaul, K.; Griew, F.; Grant, R.; Joseph, D.; Iacopetta, B. P53 alteration and microsatellite instability have predictive value for survival benefit from chemotherapy in stage III colorectal carcinoma. *Clin. Cancer Res.* **2001**, *7* (5), 1343–1349.
- (7) Youn, C. K.; Kim, M. H.; Cho, H. J.; Kim, H. B.; Chang, I. Y.; Chung, M. H.; You, H. J. Oncogenic H-Ras up-regulates expression of ERCC1 to protect cells from platinum-based anti-cancer agents. *Cancer Res.* **2004**, *64* (14), 4849–4857.
- (8) Dean, M. Cancer stem cells: Implications for cancer causation and therapy resistance. *Discovery Med* **2005**, *5* (27), 278–82.
- (9) Glasspool, R. M.; Teodoridis, J. M.; Brown, R. Epigenetics as a mechanism driving polygenic clinical drug resistance. *Br. J. Cancer* **2006**, *94* (8), 1087–92.
- (10) Hollstein, M.; Sidransky, D.; Vogelstein, B.; Harris, C. C. p53 mutations in human cancers. *Science* **1991**, *253* (5015), 49–53.
- (11) Gasco, M.; Crook, T. p53 family members and chemoresistance in cancer: what we know and what we need to know. *Drug Resist. Updates* **2003**, *6* (6), 323–328.
- (12) Vousden, K. H.; Lu, X. Live or let die: The cell's response to p53. *Nat. Rev. Cancer* **2002**, *2* (8), 594–604.
- (13) Moll, U. M.; Wolff, S.; Speidel, D.; Deppert, W. Transcription-independent pro-apoptotic functions of p53. *Curr. Opin. Cell Biol.* **2005**, *17* (6), 631–636.
- (14) Mao, J. H.; Wu, D.; Perez-Losada, J.; Jiang, T.; Li, Q.; Neve, R. M.; Gray, J. W.; Cai, W. W.; Balmain, A. Crosstalk between Aurora-A and p53: Frequent deletion or downregulation of Aurora-A in tumors from p53 null mice. *Cancer Cell* **2007**, *11* (2), 161–173.
- (15) Chen, S. S.; Chang, P. C.; Cheng, Y. W.; Tang, F. M.; Lin, Y. S. Suppression of the STK15 oncogenic activity requires a transactivation-independent p53 function. *EMBO J.* **2002**, *21* (17), 4491–4499.
- (16) Katayama, H.; Sasai, K.; Kawai, H.; Yuan, Z. M.; Bondaruk, J.; Suzuki, F.; Fujii, S.; Arlinghaus, R. B.; Czerniak, B. A.; Sen, S. Phosphorylation by aurora kinase A induces Mdm2-mediated destabilization and inhibition of p53. *Nat. Genet.* **2004**, *36* (1), 55–62.
- (17) Cheng, J.; Haas, M. Frequent mutations in the p53 tumor suppressor gene in human leukemia T-cell lines. *Mol. Cell. Biol.* **1990**, *10* (10), 5502–5509.

- (18) Zhang, L.; Zhang, J.; Hu, C.; Cao, J.; Zhou, X.; Hu, Y.; He, Q.; Yang, B. Efficient activation of p53 pathway in A549 cells exposed to L2, a novel compound targeting p53-MDM2 interaction. *Anticancer Drugs* **2009**, *20* (6), 416–424.
- (19) Dzubak, P.; Hajduch, M.; Gazak, R.; Svobodova, A.; Psotova, J.; Walterova, D.; Sedmera, P.; Kren, V. New derivatives of silybin and 2,3-dehydroisilybin and their cytotoxic and P-glycoprotein modulatory activity. *Bioorg. Med. Chem.* **2006**, *14* (11), 3793–3810.
- (20) Noskova, V.; Dzubak, P.; Kuzmina, G.; Ludkova, A.; Stehlik, D.; Trojanec, R.; Janostakova, A.; Korinkova, G.; Mihal, V.; Hajduch, M. In vitro chemoresistance profile and expression/function of MDR associated proteins in resistant cell lines derived from CCRF-CEM, K562, A549 and MDA MB 231 parental cells. *Neoplasma* **2002**, *49* (6), 418–425.
- (21) Hardy, E.; Castellanos-Serra, L. R. “Reverse-staining” of biomolecules in electrophoresis gels: analytical and micropreparative applications. *Anal. Biochem.* **2004**, *328* (1), 1–13.
- (22) Stastna, M.; Behrens, A.; McDonnell, P. J.; Van Eyk, J. E. Analysis of protein composition of rabbit aqueous humor following two different cataract surgery incision procedures using 2-DE and LC-MS/MS. *Proteome Sci.* **2011**, *9* (1), 8.
- (23) Gobom, J.; Nordhoff, E.; Mirgorodskaya, E.; Ekman, R.; Roepstorff, P. Sample purification and preparation technique based on nano-scale reversed-phase columns for the sensitive analysis of complex peptide mixtures by matrix-assisted laser desorption/ionization mass spectrometry. *J. Mass Spectrom.* **1999**, *34* (2), 105–116.
- (24) Thomas, P. D.; Campbell, M. J.; Kejarawal, A.; Mi, H.; Karlak, B.; Daverman, R.; Diemer, K.; Muruganujan, A.; Narechania, A. PANTHER: A library of protein families and subfamilies indexed by function. *Genome Res.* **2003**, *13* (9), 2129–2141.
- (25) Brown, K. R.; Jurisica, I. Online predicted human interaction database. *Bioinformatics* **2005**, *21* (9), 2076–2082.
- (26) Agrawal, S.; Kumar, A.; Srivastava, V.; Mishra, B. N. Cloning, expression, activity and folding studies of serine hydroxymethyltransferase: A target enzyme for cancer chemotherapy. *J. Mol. Microbiol. Biotechnol.* **2003**, *6* (2), 67–75.
- (27) Sorokin, A. V.; Kim, E. R.; Ovchinnikov, L. P. Nucleocytoplasmic transport of proteins. *Biochemistry (Moscow)* **2007**, *72* (13), 1439–1457.
- (28) Payne, C. M.; Holubec, H.; Crowley-Skillicorn, C.; Nguyen, H.; Bernstein, H.; Wilcox, G.; Bernstein, C. Maspin is a deoxycholate-inducible, anti-apoptotic stress-response protein differentially expressed during colon carcinogenesis. *Clin. Exp. Gastroenterol.* **2011**, *4*, 239–253.
- (29) Stevenson, L.; Allen, W. L.; Proutski, I.; Stewart, G.; Johnston, L.; McCloskey, K.; Wilson, P. M.; Longley, D. B.; Johnston, P. G. Calbindin 2 (CALB2) regulates 5-fluorouracil sensitivity in colorectal cancer by modulating the intrinsic apoptotic pathway. *PLoS One* **2011**, *6* (5), e20276.
- (30) Roy, S. S.; Ehrlich, A. M.; Craigen, W. J.; Hajnoczky, G. VDAC2 is required for truncated BID-induced mitochondrial apoptosis by recruiting BAK to the mitochondria. *EMBO Rep.* **2009**, *10* (12), 1341–1347.
- (31) Girdler, F.; Sessa, F.; Patercoli, S.; Villa, F.; Musacchio, A.; Taylor, S. Molecular basis of drug resistance in aurora kinases. *Chem. Biol.* **2008**, *15* (6), 552–562.
- (32) Zhang, J. T.; Liu, Y. Use of comparative proteomics to identify potential resistance mechanisms in cancer treatment. *Cancer Treat. Rev.* **2007**, *33* (8), 741–756.
- (33) Mizushima, N.; Klionsky, D. J. Protein turnover via autophagy: implications for metabolism. *Annu. Rev. Nutr.* **2007**, *27*, 19–40.
- (34) Han, W.; Sun, J.; Feng, L.; Wang, K.; Li, D.; Pan, Q.; Chen, Y.; Jin, W.; Wang, X.; Pan, H.; Jin, H. Autophagy inhibition enhances daunorubicin-induced apoptosis in K562 cells. *PLoS One* **2011**, *6* (12), e28491.
- (35) Ma, X. H.; Piao, S.; Wang, D.; McAfee, Q. W.; Nathanson, K. L.; Lum, J. J.; Li, L. Z.; Amaravadi, R. K. Measurements of tumor cell autophagy predict invasiveness, resistance to chemotherapy, and survival in melanoma. *Clin. Cancer Res.* **2011**, *17* (10), 3478–3489.
- (36) Qadir, M. A.; Kwok, B.; Dragowska, W. H.; Le, K. H.; Bally, D.; Gorski, M. B.; Macroautophagy, S. M. inhibition sensitizes tamoxifen-resistant breast cancer cells and enhances mitochondrial depolarization. *Breast Cancer Res. Treat.* **2008**, *112* (3), 389–403.
- (37) Yoon, J. H.; Ahn, S. G.; Lee, B. H.; Jung, S. H.; Oh, S. H. Role of autophagy in chemoresistance: regulation of the ATM-mediated DNA-damage signaling pathway through activation of DNA-PKcs and PARP-1. *Biochem. Pharmacol.* **2012**, *83* (6), 747–757.
- (38) Dreier, M. R.; Grabovich, A. Z.; Katusin, J. D.; Taylor, W. R. Short and long-term tumor cell responses to Aurora kinase inhibitors. *Exp. Cell Res.* **2009**, *315* (7), 1085–1099.
- (39) Yin, X.; Fontoura, B. M.; Morimoto, T.; Carroll, R. B. Cytoplasmic complex of p53 and eEF2. *J. Cell Physiol.* **2003**, *196* (3), 474–482.
- (40) Liu, H.; Zheng, F.; Cao, Q.; Ren, B.; Zhu, L.; Striker, G.; Vlassara, H. Amelioration of oxidant stress by the defensin lysozyme. *Am. J. Physiol. Endocrinol. Metab.* **2006**, *290* (5), E824–E832.
- (41) Chang, Y. J.; Huang, Y. P.; Li, Z. L.; Chen, C. H. GRP78 Knockdown Enhances Apoptosis via the Down-Regulation of Oxidative Stress and Akt Pathway after Epirubicin Treatment in Colon Cancer DLD-1 Cells. *PLoS One* **2012**, *7* (4), e35123.
- (42) Zhang, L. H.; Zhang, X. Roles of GRP78 in physiology and cancer. *J. Cell Biochem.* **2010**, *110* (6), 1299–1305.
- (43) Zhou, H.; Zhang, Y.; Fu, Y.; Chan, L.; Lee, A. S. Novel mechanism of anti-apoptotic function of 78-kDa glucose-regulated protein (GRP78): Endocrine resistance factor in breast cancer, through release of B-cell lymphoma 2 (BCL-2) from BCL-2-interacting killer (BIK). *J. Biol. Chem.* **2011**, *286* (29), 25687–25696.
- (44) Tjoelker, L. W.; Stafforini, D. M. Platelet-activating factor acetylhydrolases in health and disease. *Biochim. Biophys. Acta* **2000**, *1488* (1–2), 102–123.
- (45) Biancone, L.; Cantaluppi, V.; Del Sorbo, L.; Russo, S.; Tjoelker, L. W.; Camussi, G. Platelet-activating factor inactivation by local expression of platelet-activating factor acetyl-hydrolase modifies tumor vascularization and growth. *Clin. Cancer Res.* **2003**, *9* (11), 4214–4220.
- (46) Denizot, Y.; Truffinet, V.; Bouvier, S.; Gainant, A.; Cubertafond, P.; Mathonnet, M. Elevated plasma phospholipase A2 and platelet-activating factor acetylhydrolase activity in colorectal cancer. *Mediators Inflammation* **2004**, *13* (1), 53–54.
- (47) Clarke, P. R.; Zhang, C. Spatial and temporal coordination of mitosis by Ran GTPase. *Nat. Rev. Mol. Cell Biol.* **2008**, *9* (6), 464–477.
- (48) Honma, K.; Takemasa, I.; Matoba, R.; Yamamoto, Y.; Takeshita, F.; Mori, M.; Monden, M.; Matsubara, K.; Ochiya, T. Screening of potential molecular targets for colorectal cancer therapy. *Int. J. Gen. Med.* **2009**, *2*, 243–257.
- (49) Xia, F.; Lee, C. W.; Altieri, D. C. Tumor cell dependence on Ran-GTP-directed mitosis. *Cancer Res.* **2008**, *68* (6), 1826–1833.
- (50) Thottassery, J. V.; Zambetti, G. P.; Arimori, K.; Schuetz, E. G.; Schuetz, J. D. p53-dependent regulation of MDR1 gene expression causes selective resistance to chemotherapeutic agents. *Proc. Natl. Acad. Sci. U.S.A.* **1997**, *94* (20), 11037–11042.
- (51) Bush, J. A.; Li, G. Regulation of the Mdr1 isoforms in a p53-deficient mouse model. *Carcinogenesis* **2002**, *23* (10), 1603–1607.
- (52) Pommier, Y.; Sordet, O.; Antony, S.; Hayward, R. L.; Kohn, K. W. Apoptosis defects and chemotherapy resistance: molecular interaction maps and networks. *Oncogene* **2004**, *23* (16), 2934–2949.
- (53) Lovric, E.; Gatalica, Z.; Eyzaguirre, E.; Kruslin, B. Expression of maspin and glutathione-S-transferase-pi in normal human prostate and prostatic carcinomas. *Appl. Immunohistochem. Mol. Morphol.* **2010**, *18* (5), 429–432.
- (54) Yeom, S. Y.; Jang, H. L.; Lee, S. J.; Kim, E.; Son, H. J.; Kim, B. G.; Park, C. Interaction of testisin with maspin and its impact on invasion and cell death resistance of cervical cancer cells. *FEBS Lett.* **2010**, *584* (8), 1469–1475.
- (55) Zou, Z.; Anisowicz, A.; Hendrix, M. J.; Thor, A.; Neveu, M.; Sheng, S.; Rafidi, K.; Seftor, E.; Sager, R. Maspin, a serpin with tumor-suppressing activity in human mammary epithelial cells. *Science* **1994**, *263* (5146), 526–529.
- (56) Ben Shachar, B.; Feldstein, O.; Hacohen, D.; Ginsberg, D. The tumor suppressor maspin mediates E2F1-induced sensitivity of cancer cells to chemotherapy. *Mol. Cancer Res.* **2010**, *8* (3), 363–372.

(57) Feng, X. P.; Yi, H.; Li, M. Y.; Li, X. H.; Yi, B.; Zhang, P. F.; Li, C.; Peng, F.; Tang, C. E.; Li, J. L.; Chen, Z. C.; Xiao, Z. Q. Identification of biomarkers for predicting nasopharyngeal carcinoma response to radiotherapy by proteomics. *Cancer Res.* **2010**, *70* (9), 3450–3462.

(58) Nam, E.; Park, C. Maspin suppresses survival of lung cancer cells through modulation of Akt pathway. *Cancer Res. Treat.* **2010**, *42* (1), 42–47.

(59) Boyer, J.; Allen, W. L.; McLean, E. G.; Wilson, P. M.; McCulla, A.; Moore, S.; Longley, D. B.; Caldas, C.; Johnston, P. G. Pharmacogenomic identification of novel determinants of response to chemotherapy in colon cancer. *Cancer Res.* **2006**, *66* (5), 2765–2777.

(60) Haner, K.; Henzi, T.; Pfefferli, M.; Haner, K.; Salicio, V.; Schwaller, B. A bipartite butyrate-responsive element in the human calretinin (CALB2) promoter acts as a repressor in colon carcinoma cells but not in mesothelioma cells. *J. Cell Biochem.* **2010**, *109* (3), 519–531.

## 4. SUMMARY

This PhD thesis is focused on the identification of potential tumor cell resistance mechanisms to a novel Aurora kinase inhibitor CYC116, which has been tested in a Phase I clinical study. Alongside CYC116, we also included an experimental Aurora kinase inhibitor, ZM447439 to generate resistant HCT116 clones.

Discovery of a particular drug and its development process is highly expensive due to high expenditures of R&D and human clinical trials. On the other hand the typical development time of a drug until it is approvable for routine clinical use is 10-15 years (Figure 30). Evolution of induced resistance in cancer cells to a particular drug may result in treatment failure. Appearance of drug resistance in the clinic is very frustrating given the fact that its development consumed incredible amount of money and time. Hence predicting potential drug resistance mechanisms in the preclinical studies itself is very much necessary. Now the pharmaceutical and biotech companies are focusing to identify potential cancer cell line resistance mechanisms in preclinical studies using cell line models. Such studies may yield significant information related to molecular basis of drug resistance. Availability of reliable gene expression and functional genomics tools made possible to evaluate differentially expressed genes in resistant cell lines in comparison to parent sensitive cell lines. Such genes can be used as biomarkers to predict sensitivity of the response to the therapy. Deduced gene expression signatures and related pathways of resistant cell lines also aid in selecting appropriate anticancer agents for combination treatment along with the candidate drug. Based on the molecular basis of resistance one can select the combination agent relatively easy. Preliminary multidrug resistance characterization studies also help in selecting the combination agent. Moreover initial characterization studies also help for not choosing the agent for combination based on the cross-resistance profiles. Combination treatments after dose optimization may even prevent the emergence of resistance.

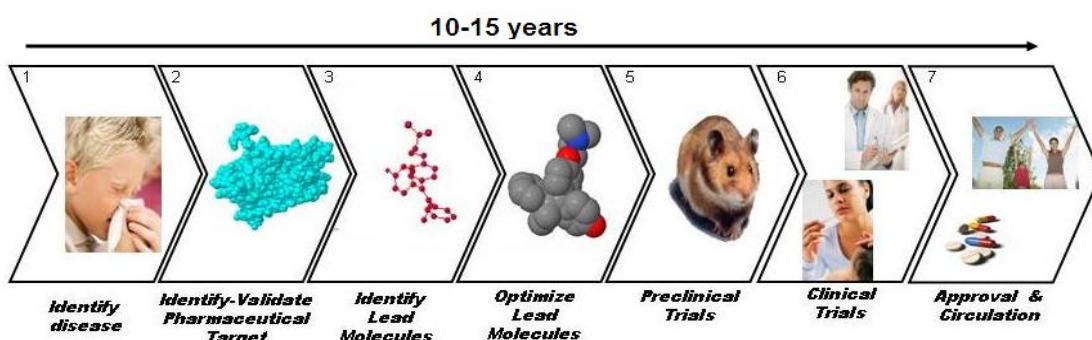


**Figure 30.** Typical drug development process  
(Taken from: [http://www.noesisinformatics.com/?page\\_id=8](http://www.noesisinformatics.com/?page_id=8))

The genes identified in drug resistance studies can be used to predict response to treatment in clinical setting and to stratify patients according to the expression of the genes. By the use of predictive biomarkers of sensitivity, the therapy can be administered only to those patients for whom it is beneficial, thereby decreasing the overall costs of cancer therapy and side effects. Those patients for whom the particular drug would not bring any benefit, can be quickly selected for another therapy with medicaments which are more suitable for them and do not need to undergo an unnecessary and ineffective treatment.

We initiated our study to understand cancer cell drug resistance mechanisms towards CYC116 at the late preclinical Phase. As with other targeted drugs, drug resistance to CYC116 in the clinic is possible. Since CYC116 is still in initial Phase I clinical trial studies, until now significant information on drug resistance in the clinical setting is not available. Hence our beforehand wealth of information aids in predicting sensitivity towards CYC116 therapy. Some of our key findings that may help in the development of CYC116 are discussed here. Generated CYC116 resistant clones are highly cross-resistant to well-known Aurora kinase inhibitors including VX-680, AZD1152, and MLN8054. This clearly suggests that common resistance mechanisms are possible. Hence combining CYC116 with other Aurora kinase inhibitors may not be useful in overcoming the resistance. Secondly, CYC116 resistant clones are highly cross-resistant to etoposide, gemcitabine, daunorubicin, topotecan, paclitaxel, and cisplatin. These approved anticancer agents should be avoided as combination agents. However, CYC116 resistant clones are sensitive to few anticancer agents including ABT-263, 5-Fluorouracil, bortezomib, oxaloplatin, and doxorubicin compared to parent cell lines. These agents in combination with CYC116 have potential to circumvent the resistance. However additional combination studies in cancer cell lines models are necessary to determine synergistic, additive, and antagonistic effects of combination agents. HCT116 is a near diploid cell line and has been also confirmed from our flowcytometry based cell cycle analysis. All CYC116 resistant clones became tetraploid or near tetraploid under *in vitro* conditions. Tetraploid which is a kind of chromosomal instability may provide additional survival advantage to cancer cells. Predicting the evolution of tetraploid stable phenotype of tumor in response to long-term treatment of CYC116 in the clinic is difficult. Nevertheless this beforehand information predicts the possibility of aneuploidy in the clinic. Treatment of P388 leukemia model of mice with CYC116 did not result in the evolution of stable tetraploid cells (data not shown), indicating that resistance mechanisms may be different under *in vivo* conditions. Moreover tetraploidy G1 check point may be compromised in HCT116 cell line even before the emergence of drug resistance to CYC116 given the fact that HCT116 cell line is highly prone to mutations due to defect in the recombinational DNA repair system. Cancer cell lines have different genetic backgrounds and resistance mechanisms may differ towards CYC116 depending on the cell line. Altogether, emergence of tetraploidy in response to CYC116 may be specific for some type of tumors.

Gene expression studies revealed several differentially expressed genes in CYC116 resistant. These genes are involved in several diverse functions including drug metabolism, cell survival, cell signaling, cell cycle regulation, transcriptional regulation, and transport. Some are structural and cell membrane genes and several other are not well characterized. Particularly CYP450 family members CYP1A1, CYP1B1 (cytochrome P450, family 1, subfamily B, polypeptide 1), CYP4F3 (cytochrome P450, family 4, subfamily F, polypeptide 3), and CYP4F12 (cytochrome P450, family 4, subfamily F, polypeptide 12) were found to be up-regulated in CYC116 resistant clones. Our data is in agreement with previously published data by Wang and co-workers (**Wang et al., 2010**), where they reported at least induction of CYP1A in human hepatocytes at 1  $\mu$ M CYC116 concentration. Hence possible induction of CYP1A1 in response to CYC116 is expected in the clinic. However the mechanism CYP450 interaction with CYC116 and mode of action are not known. Among the many survival genes upregulated, we found that antiapoptotic Bcl-xL overexpression can

modulate the cancer cell lines sensitivity to CYC116. We confirmed the profound role of Bcl-xL expression in CYC116-induced resistance by knocking it down by siRNA (small interfering RNA) mediated technology. Depletion of Bcl-xL expression genetically partially restored the sensitivity of resistant clones towards CYC116. On the other hand Bcl-xL overexpressing CYC116 clones are highly susceptible to ABT-263, a potent Bcl-2 inhibitor compared to parent cell lines. Hence ABT-263 could be potentially used to overcome the clinical resistance.

Resistance mechanisms seem to be different to ZM447439. There is no stable induction of polyploidy, no induction of CYP450 members, and Bcl-xL was not up-regulated. Instead ZM447439 induced three novel Aurora B mutations in resistant clones. Induction of Aurora B mutations under the ZM447439 selection pressure clearly confirms the specificity of ZM447439 towards Aurora kinases. Some of the mutations particularly L152S significantly affected ZM447439 binding, but not CYC116. The cell lines with Aurora B mutations are significantly less cross-resistant to CYC116, indicating that these mutations have no major effect on CYC116 binding. Moreover, our modeling studies showed that CYC116 can potentially inhibit the oncogenic activity of other resistant Aurora B mutants (**Girdler et al., 2008**) induced by ZM447439. These ZM447439 Aurora B mutations are highly likely to arise in the clinic, as majority of the Aurora kinase inhibitors have somewhat similar binding modes. In this situation CYC116 can be used to potentially overcome the resistance. Interestingly CYC116 did not induce any Aurora mutations. Drug target mutations represent most aggressive type of resistance mechanisms compared to other mechanisms. Since CYC116 did not induce drug target mutations, the resistance to CYC116 can be overcome relatively easily by rationally combining with other anticancer drugs based on the gene expression changes. As CYC116-induced upregulation of Bcl-xL, family of Bcl-2 inhibitors can potentially overcome the resistance.

Our data cumulatively provide a genetic basis of resistance to Aurora kinase inhibitors, which could be used to predict clinical response and also to select patients who might benefit from Aurora kinase inhibition. Moreover, our study suggest a role of Bcl-2 protein family inhibitors for reversal of drug resistance against Aurora kinase inhibitors and their possible significance for therapy of tumors primarily or secondary resistant to these drugs.



## 5. REFERENCES

1. Borst P, Evers R, Kool M, Wijnholds J (2000) A family of drug transporters: the multidrug resistance-associated proteins. *Journal of National Cancer Institute* 92;1295-302.
2. Huang Y, Ibrado AM, Reed JC, Bullock G, Ray S, Tang C, Bhalla K (1997) Co-expression of several molecular mechanisms of multidrug resistance and their significance for paclitaxel cytotoxicity in human AML HL-60. *Leukemia* 11;253-257.
3. Kovalchuk O, Filkowski J, Meservy J, Ilnytsky Y, Tryndyak VP, Chekhun VF, Pogribny IP (2008) Involvement of microRNA-451 in resistance of the MCF-7 breast cancer cells to chemotherapeutic drug doxorubicin. *Molecular Cancer Therapeutics* 7;2152-2159.
4. Pinedo HM. (2007), *Drug resistance in the treatment of cancer*, Cambridge University press, New York.
5. Aas T, Borresen AL, Geisler S, Smith-Sorensen B, Johnsen H, Varhaug JE, Akslen LA, Lonning PE (1996) Specific p53 mutations are associated with de novo resistance to doxorubicin in breast cancer patients. *Nature Medicine* 2;811-814.
6. Lou H, Dean M (2007) Targeted therapy for cancer stem cells: the patched pathway and ABC transporters. *Oncogene* 26;1357-1360.
7. Jia P, Wu S, Li F, Xu Q, Wu M, Chen G, et al. (2005) Breast cancer resistance protein-mediated topotecan resistance in ovarian cancer cells. *International Journal of Gynecological Cancer* 15;1042-1048.
8. Lord RV, Brabender J, Gandhara D, Alberola V, Camps C, Domine M, et al. (2002) Low ERCC1 expression correlates with prolonged survival after cisplatin plus gemcitabine chemotherapy in non-small cell lung cancer. *Clinical Cancer Research* 8;2286-2291.
9. Wong PR, Tsang WP, Chau PY, Co NN, Tsnag TY, Kwok TT, et al. (2007) p53-R273H gains new function in induction of drug resistance through down-regulation of procaspase-3. *Molecular Cancer Therapeutics* 6;1054-1061.
10. Goker E, Waltham M, Kheradpour A, Trippett T, Mazumdar M, Elisseyeff Y, et al. (1995) Amplification of the dihydrofolate reductase gene is a mechanism of acquired resistance to methotrexate in patients with acute lymphoblastic leukemia is correlated with p53 gene mutations. *Blood* 86;677-684.
11. Sartorius UA, Krammer PH (2002) Upregulation of Bcl-2 is involved in the mediation of chemotherapy resistance in human small cell lung cancer cell lines. *International Journal of Cancer* 97;584-592.
12. Gorre ME, Mohammed M, Ellwood K, Hsu N, Paquette R, Rao PN, Sawyers CL (2001) Clinical resistance to STI-571 cancer therapy caused by BCR-ABL gene mutation or amplification. *Science* 293;876-880.
13. Nazarian R, Shi H, Wang Q, Kong X, Koya RC, Lee H, et al (2010) Melanomas acquire resistance to B-RAF(V600E) inhibition by RTK or N-RAS upregulation. *Nature* 468;973-977.
14. Cree IA, Glaysher S, Harvey Al. (2010) Efficacy of anti-cancer agents in cell lines versus human primary tumor tissue. *Current Opinion in Pharmacology* 10;375-379.
15. Masters JRW (1991) *Human cancer in primary culture, A handbook*. Dodrecht: Kluwer academic publishers.

16. Pfragner R, Freshney RIJ (2004) Culture of human tumor cells. Hoboken, New Jersey: Wiley-Liss.
17. Bosanquet AG, Richards SM, Wade R, Else M, Matutes E, Dyer MJ, et al. (2009) Drug-cross resistance and therapy-induced resistance in chronic lymphocytic leukaemia by an enhanced method of individualized tumor response testing. *British Journal of Haematology* 146;384-395.
18. Dong X, Guan J, English JC, Flint J, Yee J, Evans K, et al. (2010) Patient-derived first generation xenografts of non-small cell lung cancers: promising tools for predicting drug responses for personalized chemotherapy. *Clinical Cancer Research* 16;1442-1451.
19. Larson SM, Schwartz LH (2006) 18F-FDG as a candidate for “qualified biomarker”: functional assessment of treatment response in oncology. *Journal of Nuclear Medicine* 47;901-903.
20. Hicks RJ (2009) Role of 18F-FDG PET in assessment of response in non-small cell lung cancer. *Journal of Nuclear Medicine* 50;31S-42S.
21. Wahl RL, Jacene H, Kasamon Y, Lodge MA (2009) From RECIST to PERSIST: Evolving consideration for PET response criteria in solid tumors. *Journal of Nuclear Medicine* 2009;122s-152s.
22. Calcagno AM, Salcido CD, Gillet JP, Wu CP, Fostel JM, Mumau MD et al. (2010) Prolonged drug selection of breast cancer cells and enrichment of cancer stem cell characteristics. *Journal of the National Cancer Institute* 102;1637-1652.
23. Girdler F, Sessa F, Patercoli S, Villa F, Musacchio A, Taylor S (2008) Molecular basis of drug resistance in aurora kinases. *Chemistry and Biology*;15:552-62.
24. Hurley LH (2002) DNA and its associated processes as targets for cancer therapy. *Nature Reviews Cancer* 2;188-200.
25. O’Shaughnessy J, Miles D, Vukelja S, Moiseyenko V, Ayoub JP, Cervantes J et al. (2002) Superior survival with capecitabine plus docetaxel combination therapy in anthracycline-pretreated patients with advanced breast cancer: phase III clinical results. *Journal of Clinical Oncology* 20;2812-2823.
26. Slamon DJ, Leyland-Jones B, Shak S, Fuchs H, Paton V, Bajamonde A et al. (2001) Use of chemotherapy plus a monoclonal antibody against HER2 for metastatic breast cancer that overexpresses HER2. *The New England Journal of Medicine* 344;783-792.
27. Doherty L, Gigas DC, Kesari S, Drappatz J, Kim R, Zimmerman J et al. (2006) Pilot study of the combination of EGFR and mTOR inhibitors in recurrent malignant gliomas. *Neurology* 67;156-158.
28. Siu LL, Awada A, Takimoto CH, Piccart M, Schwartz B, Giannaris T et al. (2006) Phase I trial of sorafenib and gemcitabine in advanced solid tumors with an expanded cohort in advanced pancreatic cancer. *Clinical Cancer Research* 12;144-151.
29. Joensuu H, Holli K, Heikkinen M, Suonio E, Aro AR, Hietanen P et al. (1998) Combination chemotherapy versus single-agent therapy as first- and second-line treatment in metastatic breast cancer: a prospective randomized trial. *Journal of Clinical Oncology* 16;3720-3730.
30. Borowski E, Bontemps-Gracz MM, Piwskowka A (2005) Strategies to overcome ABC-transporters-mediated multidrug resistance (MDR) of tumor cells. *Acta Biochimica Polonica* 52;609-627.

31. Thomas H, Coley HM (2003) Overcoming drug resistance in cancer: an update on the clinical strategy of inhibiting p-glycoprotein. *Cancer Control* 10;159-165.
32. Nurse P (2000) A long twentieth century of the cell cycle and beyond. *Cell* 100;71-78.
33. Lewin B. (1997), *Genes VI*, 6<sup>th</sup> edition, Oxford University press, New York.
34. Sherr CJ, McCormick F (2002) The RB and p53 pathways in cancer, *Cancer Cell* 2;103-112.
35. Lundberg AS, Weinberg RA (1998) Functional inactivation of Rb protein requires sequential modification by at least two distinct cyclin-CDK complexes. *Molecular and Cell biology* 18;753-761.
36. Pietenpol JA, Stewart ZA et al. (2002) Cell cycle checkpoint signalling: cell cycle arrest versus apoptosis. *Toxicology* 181-182;475-481.
37. Anichini A, Mortarini R, Sensi M, Zanon M (2005) APAF-1 signalling in human melanoma, *Cancer letters* 238;168-179.
38. Bayacscas JR, Yuste VJ, Sole C, Sanchez-Lopez I, Sequra MF, Perera R, Comella JX (2004) Characterization of splice variants of human-activated DNase with CIDE-N structure and function. *FEBS letters* 566;230-240.
39. Sclafain RA (2002) CDC7p-Dbf4p becomes famous in cell cycle. *Journal of Cell Science* 113;2111-2117.
40. Stillman B (1996) Cell cycle control of DNA replication. *Science* 274;1659-1664.
41. Lodish H et al.. (1995) *Molecular Cell Biology*, 2<sup>nd</sup> edition, Scientific American Books Inc. New York.
42. Djordjevic S, Driscoll PC (2002) Structural insight of phosphoinositide 3-kinases. *Trends in Biochemical Sciences* 27;426-432.
43. Pauklin S et al. (2005) ARF and ATR/ATM cooperate in p53-mediated apoptosis upon oncogenic stress. *Biochemical and Biophysical communications* 334;386-394.
44. Ferrara L, Kmiec EB (2006) Targeted repair activates CHK1 and CHK2 and stalls replication in corrected cells, *DNA repair* 5;422-31.
45. Hirano T (2005) Condensin: organizing and segregating the genome. *Current Biology* 15;65-275.
46. Nigg EA (2001) Mitotic kinases as Regulators of cell division and its checkpoints. *Nature Reviews: Molecular Cell Biology* 2;21-32.
47. Kollareddy M, Dzubak P, Zheleva D, Hajduch M (2008) Aurora Kinases: structure, functions, and their association with cancer. *Biomedical Papers* 152;27-33.
48. Garcia-Saez I (2004) Crystal structure of the motor domain of the human kinetochore protein CENP-E. *Journal of Molecular biology* 340;1107-1116.
49. Millband DN, Hardwick KG (2002) Fission yeast Mad3p is required for Mad2p to inhibit the anaphase-promoting complex and localizes to kinetochores in a Bub1p, Bub3p and Mph1p-dependent a manner. *Molecular and Cell Biology* 22;2728-2742.
50. Schmit TL, Ahmad N (2007) Regulation of mitosis via mitotic kinases: new opportunities for cancer management. *Molecular cancer therapeutics* 6;1920-1931.
51. Horing NC, Knowles PP, McDonald NQ, Uhlmann F (2002) The dual mechanism of separase regulation by securin. *Current Biology* 12;973-982.
52. Osouda, S. et al (2005), Null mutants of drosophila B-type lamin DM(0) show aberrant tissue differentiation rather than obvious nuclear shape distortion or specific defects during cell proliferation, *Developmental Biology*;284,219-232.

53. Wei G, Lonardo F, Ueda T, Kim T, Huvos Ag, Healey JH, Ladayni M (1999) CDK4 amplification in osteosarcoma: reciprocal relationship with INK4 gene alterations and mapping of 12q13 amplicons. *International Journal of Cancer* 80;199-204.
54. Kitahara K, Yasui W, Kuniyasu H, Yokozaki H, Akama Y, Yunotani S, et al. (1995) Cocurrent amplification of cyclin E and CDK2 genes in colorectal carcinomas. *International Journal of Cancer* 62;25-28.
55. Eggers JP, Grandgenett PM, Collission EC, Lewallen ME, Tremayne J, Singh PK, (2011) Cyclin-dependent kinase is amplified and overexpressed in pancreatic cancer and activated by mutant K-ras. *Clinical Cancer Research* 17;6140-6150.
56. Bartkova J, Zemanova M, Bartek J (1996) Expression of CDK7/CAK in normal and tumor cells of diverse histogenesis, cell cycle position and differentiation. *International Journal of Cancer* 66;732-737.
57. Hansel DE, Dhara S, Huang RC, Ashfaq R, Deasel M, Shimada Y, et al. (2005) CDC2/CDK1 expression in esophageal adenocarcinoma and precursor lesions serves a diagnostic and cancer progression marker and potential novel drug target. *American Journal of Surgical Pathology* 29;390-399.
58. Takai N, Hamanaka R, Yoshimatsu N, Miyakawa I (2005) Polo-like kinases (Plks) and cancer. *Oncogene* 24;287-291.
59. Lens SM, Voest EE, Medema RH (2010) Shared and separate functions of polo-like kinases and Aurora kinases in cancer. *Nature Reviews Cancer* 10;825-841.
60. Wolf G, Elez R, Doermer A, Holtrich U, Ackermann H, Stutte HJ et al.. (1997) Prognostic significance of polo-like kinase expression in non-small cell lung cancer. *Oncogene* 14; 543-549.
61. Li B, Ouyang B, Pan H, Reissmann PT, Slamon DJ, Arceci R, et al. (1996) Prk, a cytokine-inducible human protein serine/threonine kinase whose expression appears to be down-regulated in lung carcinomas. *Journal of Biological Chemistry* 271;19402-19408.
62. Park MT, Lee SJ (2003) Cell cycle and cancer. *Journal of Biochemistry and Molecular Biology* 36;60-65.
63. Petitjean A, Mathe E, Kato S, Ishioka C, Tavtigean SV, Hainaut P, Olivier M (2007) Impact of mutant p53 properties on TP53 mutant patterns and tumor phenotype: Lessons from the recent development in the IARC TP53 database. *Human Mutation* 28;622-629.
64. Willis A, Jung EJ, Wakefield T, Chen X (2004) Mutant p53 exerts a dominant genitive effect by preventing wild-type p53 from binding to the promoter of the target genes. *Oncogene* 23;2330-2338.
65. McClue SJ, Blake D, Clarke R, Cowan R, Cummings L, Fischer PM, et al. (2002) In vitro and in vivo tumor properties of the cyclin dependent kinase inhibitor CYC202 (R-Roscovitrine). *International Journal of Cancer* 102;463-468.
66. Benson C, White J, De Bono J, O'Donell A, Raynaud F, Cruickshank C, et al. (2007) A Phase I trial of the selective oral cyclin-dependent kinase inhibitor seliciclib (CYC202; R-Roscovitrine), administered twice daily for 7 days every 21 days. *British Journal of Cancer* 96;29-37.
67. Le Tourneau C, Faivre S, Laurence V, Delbaldo C, Vera K, Girre V, et al. (2010) Phase I evaluation of seliciclib (R-roscovitrine), a novel oral cyclin-dependent kinase inhibitor, in patients with advanced malignancies. *European Journal of Cancer* 46;3243-3250.

68. Rudolph D, Steegmaier M, Hoffmann M, Grauert M, Baum A, Quant J, et al. (2009) BI 6727, a polo-like kinase inhibitor with improved pharmacokinetic profile and broad antitumor activity. *Clinical Cancer Research* 15;3094-3102.
69. Schoffski P, Awada A, Dumez H, Gil T, Bartholomeus S, Wolter P, et al. (2012) A phase I dose-escalation study of the novel polo-like kinase inhibitor volasertib (BI 6727) in patients with advanced solid tumors. *European Journal of Cancer* 48;179-186.
70. Bischoff JR, Anderson L, Zhu Y, Mossie K, Ng L, Souza B, et al. (1998) A homologue of *Drosophila* Aurora kinase is oncogenic and amplified in human colorectal cancers. *EMBO Journal* 17;3052-3065.
71. Katayama H, Ota T, Jisaki F, Ueda Y, Tanaka T, Odashima S, et al. (1999) Mitotic kinase expression and colorectal cancer progression. *Journal of National Cancer Institute* 91;1160-1162.
72. Kollareddy M, Zheleva D, Dzubak P, Brahmakshatriya PS, Lepsik M, Hajduch M (2012) Aurora kinase inhibitors: Progress towards the clinic. *Investigational New Drugs* 30,2411-2432.
73. Wang S, Midgley CA, Scaerou F, Grabarek JB, Griffiths G, Jackson W, et al. (2010) Discovery of N-phenyl-4-(thiazol-5-yl)pyrimidin-2-amine aurora kinase inhibitors. *Journal of Medicinal Chemistry* 53;4367-4378.
74. Griffiths G, Scaerou F, Sorrell D, Duckmanton A, Tosh C, Lewis S, et al. (2008) Antitumor activity of CYC116, a novel small molecule inhibitor of aurora kinases and VEGFR2. *AACR Annual Meeting*; 12-16 April, San Diego, CA, USA, Abstract 651.
75. Hajduch M, Vydra D, Dzubak P, Stuart I, Zheleva D (2008) In vivo mode of action of CYC116, a novel small molecule inhibitor of Aurora kinases and VEGFR2. *AACR Annual Meeting*; 12-16 April, San Diego, CA, USA, Abstract 5645.
76. Ditchfield C, Johnson VL, Tighe A, Ellston R, Haworth C, Johnson T, et al. (2003) Aurora B couples chromosome alignment with anaphase by targeting BubR1, Mad2, and Cenp-E to kinetochores. *Journal of Cell Biology* 161;267-280.
77. Gadea BB, Ruderman JV (2005) Aurora kinase inhibitor ZM447439 blocks chromosome induced spindle assembly, the completion of chromosome condensation, and the establishment of the spindle integrity checkpoint in *Xenopus* egg extracts. *Molecular biology of the Cell* 16;1305-1318.
78. Wiseman LR, Spencer CM (1998) Paclitaxel. An update of its use in the treatment of metastatic breast cancer and ovarian and other gynaecological cancers. *Drugs aging* 12;305-34.
79. Tarlaci S (2008) Vincristine-induced fatal neuropathy in non-Hodgkin's lymphoma. *Neurotoxicity* 29;748-749.
80. Chatterjee K, Zhang J, Honbo N, Karliner JS (2010) Doxorubicin cardiomyopathy. *Cardiology* 115;155-162
81. Barlesi F, Villani P, Doddoli C, Gimenez C, Kleisbauer JP (2004) Gemcitabine-induced severe pulmonary toxicity. *Fundamental and Clinical Pharmacology* 18;85-91.
82. Sheikh Hamad D, Timmins K, Jalai Z (1997) Cisplatin-induced renal toxicity: possible reversal by N-acetyl treatment. *Journal of American Society of Nephrology* 8;1640-1644.
83. Kanwar VS, Gajjar A, Ribeiro RC, Bowman L, Parham DM, Jenkins JJ (1995) Unusual cutaneous toxicity following treatment with dactinomycin: a report of two cases. *Medical and Pediatric Oncology* 24;329-333.

84. Kantarjian HM, Cortes J, O'Brien S, Giles FJ, Albitar M, Rios MB, Shan J, Faderl S, Garcia-Manero G, Thomas DA, Resta D, Talpaz M (2002) Imatinib mesylate (STI571) therapy for Philadelphia chromosome–positive chronic myelogenous leukemia in blast Phase. *Blood* 99;3547-3553.
85. Abbott BL (2012) Dasatinib: From treatment of imatinib-resistant or -intolerant patients with chronic myeloid leukemia to treatment of patients with newly diagnosed chronic Phase chronic myeloid leukemia. *Clinical Therapeutics*; 34;272-281.
86. Ie Coutre PD, Giles FJ, Hochhaus A, Apperley JF, Ossenkoppele GJ, Blackesley R, Shou Y, Gallagher NJ, Baccarani M, Cortes J, Kantarjian HM (2011), Nilotinib in patients with Ph+ chronic myeloid leukemia in accelerated Phase following imatinib resistance or intolerance: 24-month follow-up results. *Leukemia* 26;1189-1194.
87. Flaherty KT, Puzanov I, Kim K.B, Ribas A, McArthur GA, Sosman JA, O'Dwyer PJ, Lee RJ, Grippo JF, Nolop K, Chapman PB (2010) Inhibition of Mutated, Activated BRAF in Metastatic Melanoma. *The New England Journal of Medicine* 363;809-819.
88. Maemondo M, Inoue A, Kobayashi K, Sugawara S, Oizumi S, Isobe H, et al. (2010) Gefitinib or chemotherapy for non-small-cell lung cancer with mutated EGFR. *The New England Journal of Medicine* 362;2380-2388.
89. Shepherd FA, Pereira JD, Ciuleanu T, Tan EH, Hirsh V, Thongprasert S (2005) Erlotinib in previously treated non-small-cell lung cancer. *The New England Journal of Medicine* 353;123-132.
90. Burris HA (2004) Dual Kinase Inhibition in the Treatment of Breast Cancer: Initial Experience with the EGFR/ErbB-2 Inhibitor Lapatinib. *The Oncologist* 9; 10-15.
91. Vogel CL, Cobleigh MA, Tripathy D, Gutheil JC, Harris LN, Fehrenbacher LN et al. (2002) Efficacy and safety of trastuzumab as a single agent in first-line treatment of HER2-overexpressing metastatic breast cancer. *Journal of Clinical Oncology* 20; 719-726.
92. Escudier B, Eisen T, Stadler WM, Szczylik C, Oudard S, Siebels M, et al. (2007) Sorafenib in advanced clear-cell renal-cell carcinoma. *The New England Journal of Medicine* 356;125-134.
93. Llovet JM, Ricci S, Mazzaferro V, Hilgard P, Gane E, Blanc JF, et al. (2008) Sorafenib in advanced hepatocellular carcinoma. *The New England Journal of Medicine* 359;378-390.
94. Disel U, Oztuzcu S, Besen AA, Karadeniz C, Kose F, Sumbul AT, et al. (2011) Promising efficacy of sorafenib In a relapsed thymic carcinoma with C-KIT exon 11 deletion mutation. *Lung Cancer* 71;109-112.
95. Gore ME, Szczylik C, Porta C, Bracarda S, Bjarnason GA, Oudard S, et al. (2009) Safety and efficacy of sunitinib for metastatic renal-cell carcinoma: an expanded-access trial. *The Lancet Oncology* 10;757-763.
96. Camidge DR, Bang Y, Kwak EL, Shaw T, Iafrate AJ, Maki RG, Solomon BJ, et al. (2011) Progression-free survival (PFS) from a Phase I study of crizotinib (PF-02341066) in patients with ALK-positive non-small cell lung cancer (NSCLC). *Proceedings of the American Society of Clinical Oncology*, 29 (2011); p. 2501 (abstr).
97. Fong PC, Boss DS, Yap TA, Tutt A, Wu P, Mergui-Roelvink, et al. (2009) Inhibition of poly(ADP-ribose) polymerase in tumors from BRCA mutation carriers. *The New England Journal of Medicine* 9;123-134.

- 98.** Eder JP, Shapiro GI, Appleman LJ, Zhu AX, Miles D, Keer H et al. (2010) A Phase I study of foretinib, a multi-targeted inhibitor of c-Met and vascular growth factor endothelial receptor 2. *Clinical Cancer Research* 16;3507-3516.

## 6. BIBLIOGRAPHY

Articles related to PhD thesis are labeled \*

### A. Review Articles

\***Kollareddy M**, Dzubak P, Zheleva D, Hajduch M (2008) Aurora Kinases: structure, functions, and their association with cancer. *Biomedical Papers* 152,27-33.

\***Kollareddy M**, Zheleva D, Dzubak P, Brahmshatriya PS, Lepsik M, Hajduch M (2012) Aurora kinase inhibitors: Progress towards the clinic. *Investigational New Drugs* 30, 2411-2432

### B. Original research articles

Brulikova L, Dzubak P, Hajduch M, Lachnitova L, **Kollareddy M**, Kolar M, Bogdanova K, Hlavac J. (2010) Synthesis of 5-[alkoxy-(4-nitro-phenyl)-methyl]-uridines and study of their cytotoxic activity. *European Journal of Medicinal Chemistry* 45;3588-94.

\* Hrabakova R, **Kollareddy M**, Tyleckova J, Halada P, Hajduch M, Gadher SJ, Kovarova H (2013) Cancer cell resistance to Aurora kinase inhibitors: Identification of novel targets for cancer therapy. *Journal of Proteome Research* 12;455-469

### C. Poster presentations

Posters related to PhD thesis are labeled \*

\***Kollareddy M**, Zheleva D, Dzubak P, Srovnal J, Radova L, Koudelakova V, Dolezal D, Dzubak P, Brahmshatriya PS, Lepsik M, Hobza P, Hajduch M (2012) Colorectal cancer CT116 cells resistant towards a novel Aurora kinase inhibitor CYC116: Molecular hallmarks of drug resistance and pharmacologic interventions restoring drug sensitivity. CYC116. AACR: Molecularly targeted therapy: Mechanisms of resistance conference; 9-12 May, San Diego, California, USA, Session B, Poster no. 30.

\***Kollareddy M**, Zheleva D, Dzubak P, Srovnal J, Radova L, Hajduch M (2011) Identification and characterization of potential tumor cell resistance mechanisms towards a novel Aurora kinase inhibitor, CYC116. American Association for Cancer Research Meeting; 2-6 April, Orlando, Florida, USA, Abstract 735.

\***Kollareddy M**, Zheleva D, Dzubak P, Hajduch M (2010) Tumor cell resistance mechanisms to Aurora kinase inhibitors. American Association for Cancer Research Meeting; 17-21 April, Washington DC, USA, Abstract 633.

**Kollareddy M**, Dzubak P, Hajduch M (2007) IMMUNO-MADLI: A powerful tool in proteomics. 3<sup>rd</sup> Czech Proteomic conference; 29-31 October, Prague, Czech Republic.



## D. Oral presentations

Oral presentations related to PhD thesis are marked as \*

\***Kollareddy M**, Zheleva, Dzubak P, Hrabakova R, Kovarova H, Martinkova J, Halada P, Srovnal J, Radova L, Hajduch M (2011). Characterization and identification of potential tumor resistance mechanisms towards CYC116, a novel Aurora kinase inhibitor. Proteomics & Life II Sigma conference; 22 March 2011, Academy of Sciences, Prague, Czech Republic

\***Kollareddy M**, Zheleva, Dzubak P, Hajduch M (2010). Characterization and identification of potential tumor resistance mechanisms towards CYC116, a novel Aurora kinase inhibitor. Conference dedicated to Průběžná zpráva projektu 303/09/H048; 22-23 October, Czech Republic

\***Kollareddy M**, Zheleva, Dzubak P, Hajduch M (2010). Characterization and identification of potential tumor resistance mechanisms towards CYC116, a novel Aurora kinase inhibitor. VI. Dny diagnostické, prediktivní a experimentální onkologie conference; 1-3 December, Olomouc, Czech Republic

\***Kollareddy M**, Zheleva, Dzubak P, Hajduch M (2009). Tumor cell resistance mechanisms to Aurora kinase inhibitors. Student conference dedicated to PhD students; 8-9 September, LF UP a FN, Olomouc, Czech Republic.

\***Kollareddy M**, Zheleva, Dzubak P, Hajduch M (2009). Tumor cell resistance mechanisms to Aurora kinase inhibitors. V. Dny diagnostické, prediktivní a experimentální onkologie conference; 25-27 November, Olomouc, Czech Republic

**Kollareddy M**, Dzubak P, Hajduch M (2008). Immuno-MALDI: A reliable tool in proteomics. Student conference dedicated to PhD students; 3-4 September, LF UP a FN, Olomouc, Czech Republic.

**Kollareddy M**, Dzubak P, Hajduch M (2008). Differential pRb cleavage upon exposure of different class of apoptosis inducing cytotoxic agents. IV. Dny diagnostické, prediktivní a experimentální onkologie conference; 26-28 November, Olomouc, Czech Republic.

## E. Patents

\***Kollareddy M**, Dzubak P, Srovnal J, Hrabakova R, Kovarova H, Hajduch M. Methods of determination of cancer cell drug sensitivity towards Aurora kinase inhibitors and overcoming their resistance. European Patent Office 2011; Application no. 1192330.6: Patent no. 2402.